

# Sheffield Hallam University

*Structural studies on some bivalent metal complexes.*

DEE, Terry.

Available from the Sheffield Hallam University Research Archive (SHURA) at:

<http://shura.shu.ac.uk/19547/>

## A Sheffield Hallam University thesis

This thesis is protected by copyright which belongs to the author.

The content must not be changed in any way or sold commercially in any format or medium without the formal permission of the author.

When referring to this work, full bibliographic details including the author, title, awarding institution and date of the thesis must be given.

Please visit <http://shura.shu.ac.uk/19547/> and <http://shura.shu.ac.uk/information.html> for further details about copyright and re-use permissions.

Structural Studies on some Bivalent  
Metal Complexes

Terry Dee

A thesis submitted to the Council for National Academic Awards  
in partial fulfilment for the Degree of Doctor of Philosophy

Sponsoring establishment: Sheffield City Polytechnic

Collaborating establishment: Rothamsted Experimental Station

Date: December 1981

ProQuest Number: 10694428

All rights reserved

INFORMATION TO ALL USERS

The quality of this reproduction is dependent upon the quality of the copy submitted.

In the unlikely event that the author did not send a complete manuscript and there are missing pages, these will be noted. Also, if material had to be removed, a note will indicate the deletion.



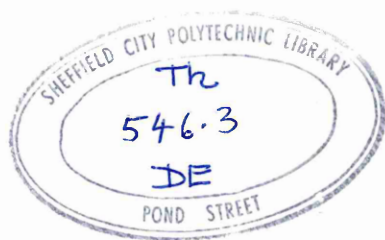
ProQuest 10694428

Published by ProQuest LLC (2017). Copyright of the Dissertation is held by the Author.

All rights reserved.

This work is protected against unauthorized copying under Title 17, United States Code  
Microform Edition © ProQuest LLC.

ProQuest LLC.  
789 East Eisenhower Parkway  
P.O. Box 1346  
Ann Arbor, MI 48106 – 1346



7908341-01

### Acknowledgements

The author would like to thank his supervisors, Drs M. Goldstein, I. W. Nowell and N. A. Bell for their help and interest shown during my three year study.

I would also like to thank the staff of the Science Faculty at Sheffield City Polytechnic for all their help over the last seven years.

Thanks and appreciation to Drs D. L. Hughes and M. Truter (Rothamsted Experimental Station, Harpenden) for use of an Enraf-Nonius CAD-4 diffractometer, Drs P. L. Goggin and R. J. Goodfellow (Department of Chemistry, University of Bristol) for the use of their n.m.r. and Raman facilities and the SERC for financial support for the past three years.

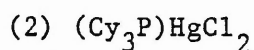
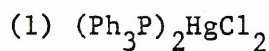
I would also like to thank Mrs Sue Lomas for typing this thesis.

## Contents

	<u>Page</u>
Abstract	3
Abbreviations	5
Chapter 1: Introduction	7
Chapter 2: Crystallographic and spectroscopic studies of some $(R_3P)_nHgX_2$ complexes [X = Cl, Br or I; n = 1 or 2]	43
Chapter 3: Crystallographic studies of selected cadmium (II) halide complexes $(R_3P)CdX_2$ [ $R_3P = Et_3P, Cy_3P, Me_2PhP;$ X = Cl, Br or I].	68
Chapter 4: Spectroscopic studies of some $(R_3P)CdX_2$ complexes	97
Chapter 5: Discussion of factors influencing the structures of some $(R_3P)_nMX_2$ complexes [M = Hg, Cd or Zn; n = 1 or 2; X = Cl, Br or I].	136
Summary and suggestions for future work	174
Appendices	179
References	246
Details of postgraduate study	250
Current publications	252

Structural Studies on Some  
Bivalent Metal ComplexesAbstract

Previous investigations of the solid-state structures of  $(R_3P)_2HgX_2$  and  $(R_3P)HgX_2$  complexes have been extended by the determination of the following crystal structures:



The structure of  $(Ph_3P)_2HgCl_2$  is that of a discrete monomer with a distorted tetrahedral geometry. In comparison with the structures of the  $(R_3P)_2HgX_2$  complexes previously determined, the degree of distortion can be related to the donor strengths of the phosphine and halogen ligands.

$(Cy_3P)HgCl_2$  forms a structure that contains two independent chlorine bridged dimer units in each unit cell. The structure of this complex, compared with other  $(R_3P)HgX_2$  complexes is determined by the donor strength and steric properties of the donor ligands.

The related  $(R_3P)CdX_2$  complexes have been crystallographically and spectroscopically investigated. The following crystal structures have been determined:

- |  |   |                   |
|--|---|-------------------|
| (3) $(Et_3P)CdI_2$                         | - | discrete dimer    |
| (4) $\alpha - (Cy_3P)CdCl_2$               | - | discrete tetramer |
| (5-7) $(Me_2PhP)CdX_2$ [ X = Cl, Br or I ] | - | polymers          |

The solid-state vibrational spectra of several  $(R_3P)CdX_2$  complexes have been studied using the crystal structures (3-7) as a basis for interpretation. The structure/spectra correlations so determined have then been applied to a number of related complexes of unknown structure. The indication from these studies is that the less extended

structures are formed with the stronger donating  $R_3P$  and X ligands.

The solid-state structures of  $(R_3P)MX_2$  complexes [ $M = Hg, Cd$  or  $Zn$ ] have been rationalised in terms of the donor strengths of the  $R_3P$  and X ligands, and the acceptor strengths of the metal atoms.

In general, the less associated structures are favoured by:

- (1) stronger  $\sigma$ -donor properties (e.g.  $Et_3P > Ph_3P$ );
- (2) stronger covalent M-X bonding (i.e.  $M-I > M-Br > M-Cl$ );
- (3) stronger acceptor strength of M (i.e.  $Hg > Cd > Zn$ ).

## Abbreviations

### General

TPP - 1,2,5 - triphenylphosphole	$\Theta$ - cone angle
Me - methyl	$\sum \sigma^*$ - Taft constant
Et - ethyl	$\Delta H_L$ - enthalpy of ligation
Bu - normal butyl	$M_r$ - relative molecular mass
Bu <sup>t</sup> - tertiary butyl	M - metal atom
Ph - phenyl	X - halogen (Cl, Br or I)
Cy - cyclohexyl	py - pyridine
R - alkyl- or aryl-	Im - imidazole
L - neutral unidentate ligand	tu - thiourea

### Crystallographic

$\text{\AA}$ - Angstrom	$F_{(000)}$ - number of electrons
$F_o$ - observed structure factor	R - refinement factor
$F_c$ - calculated structure factor	$\mu(\text{Mo-K}\alpha)$ - absorption coefficient
$D_m$ - measured density	I - intensity, of a reflection
$D_c$ - calculated density	
Z - number of molecules per unit cell	
w - weighting function	

## Spectroscopic

$\nu(\text{Cd-X})_t$	- cadmium-halogen stretching mode (terminal)		
$\nu(\text{Cd-X})_b$	- cadmium-halogen stretching mode (bridging)		
$\nu(\text{Cd-P})$	- cadmium-phosphine stretching mode		
$\nu(\text{Hg-X})_t$	- mercury-halogen stretching mode (terminal)		
$\nu(\text{Hg-X})_b$	- mercury-halogen stretching mode (bridging)		
$\nu(\text{Hg-P})$	- mercury-phosphorus stretching mode		
$\nu(\text{Cd-L})$	- cadmium-ligand stretching mode		
$\nu_{as}(\text{Hg-X})$	- antisymmetric mercury-halogen stretching mode		
$\nu_s(\text{Hg-X})$	- symmetric mercury-halogen stretching mode		
n.m.r.	- nuclear magnetic resonance		
$^1J(\text{Hg-P})$	- mercury-phosphorus coupling constant		
$^1J(\text{Cd-P})$	- cadmium-phosphorus coupling constant		
t	- terminal	m	- medium
b	- bridging	w	- weak
g	- gerade	I.R.	- infrared
u	- ungerade	Ra	- Raman
sh	- shoulder		
s	- strong		

## Contents

	<u>Page</u>
1.1 Background and objectives.	9
1.2 Structure/spectra correlation technique.	12
1.3 A survey of structural studies of $(R_3P)_n HgX_2$ complexes in the solid-state.	14
1.3.1 Introduction.	14
1.3.2 Crystallographic studies of $(R_3P)HgX_2$ complexes.	15
1.3.3 Crystallographic studies of $(R_3P)_2HgX_2$ complexes.	20
1.3.4 Spectroscopic studies of some $(R_3P)HgX_2$ complexes.	23
1.3.5 Spectroscopic studies of some $(R_3P)_2HgX_2$ complexes.	27
1.4 Survey of stereochemistry of $CdX_2$ complexes of neutral unidentate ligands.	29
1.4.1 Introduction.	29
1.4.2 Crystallographic studies of $LCdX_2$ complexes.	30
1.4.3 Crystallographic studies of $L_2CdX_2$ complexes.	34
1.4.4 Spectroscopic studies of $L_n CdX_2$ complexes. (n=1,2)	37

## 1.1 Background and objectives

For the last twenty years the far-infrared region of the electromagnetic spectrum ( $50-450\text{cm}^{-1}$ ) has been used by inorganic and co-ordination chemists as a structural tool. By considering positions and numbers of metal-ligand modes which appear in the far-infrared region, information about the structures of compounds can be obtained.

Many misinterpretations of spectroscopic data have been given in the past, mainly due to the lack of a sound basis for the spectroscopic interpretation. One method of obtaining a useful basis for more reliable spectroscopic interpretations is to examine crystallographically various 'model' compounds and then correlate the crystallographic and spectroscopic data. Examples of compounds that have previously been studied by this technique are the mercury (II) halide addition complexes formed with neutral unidentate phosphine ligands [1-8],  $(\text{R}_3\text{P})\text{HgX}_2$  and  $(\text{R}_3\text{P})_2\text{HgX}_2$ . A range of structures were found to exist in the solid-state for the  $(\text{R}_3\text{P})\text{HgX}_2$  complexes, in which the co-ordination numbers were increased beyond that of a monomer unit via varying extents of halogen bridging: halogen-bridged dimers,  $(\text{TPP})\text{HgCl}_2^*$  [1],  $(\text{Ph}_3\text{P})\text{HgCl}_2$  [1,2] and  $\beta$ - $(\text{Bu}_3\text{P})\text{HgCl}_2$  [1,3]; halogen-bridged tetramer,  $\alpha$ - $(\text{Bu}_3\text{P})\text{HgCl}_2$  [1,4]; and extended polymeric structures  $(\text{Et}_3\text{P})\text{HgCl}_2$  [2,5] and  $(\text{Me}_3\text{P})\text{HgCl}_2$  [2,5].

---

\* TPP = 1,2,5 - triphenylphosphole

In the  $(R_3P)_2HgX_2$  complexes, discrete monomers were found [6,7,8], with varying degrees of distortion from a regular tetrahedral geometry. These structures were rationalised in terms of the relative donor strength and size of the  $R_3P$  ligands. Chapter 2 contains further experimental work on these mercury complexes with the essential objectives of the work being a determination of:

- (i) the role the halogen plays in structures adopted;
- (ii) the effect that varying the steric and electronic nature of the  $R_3P$  ligand has on the solid-state structures.

From a survey of the literature [9], it seems that structural variations such as those found in mercury (II) complexes are likely to be of much wider significance.

A major part of the present work is concerned with investigating factors which influence the structures of cadmium dihalide addition complexes, mainly of the type  $(R_3P)CdX_2$ . As was the case with mercury (II) systems, there is a lack of systematic crystallographic data and inadequate spectroscopic data; thus one of the aims of the  $(R_3P)CdX_2$  study was to establish a firm crystallographic basis for the interpretation of far-infrared spectra of compounds of this type. The factors influencing the structure and geometry of  $(R_3P)CdX_2$  complexes are discussed in Chapter 5 in terms of:

- (i) the role of the halogen;
- (ii) the effect of varying the donor strength of the  $R_3P$  ligand;
- (iii) the steric importance of the  $R_3P$  ligand.

Finally, the results of the mercury and cadmium investigations are discussed in relation to each other and to the other Group II B element, zinc.

## 1.2 Structure/spectra correlation technique

From the low-frequency infrared and Raman spectroscopic techniques, an indication of the presence of metal-ligand vibrations for a complex can be obtained. The number, activity, symmetry and wavenumber positions of these vibrational modes are characteristic of the compound's structure.

Using group theory one can predict the theoretical number, activity and symmetry of the expected modes for a structure of a certain symmetry. Thus if the predicted vibrational modes and the experimentally observed modes correspond, then the spectral pattern can be considered diagnostic of the structure and hence can be used for more reliable interpretation of other spectral data.

There are three methods which have been used to predict these modes.

- (i) Point group analysis [10] - where the molecular symmetry (point group) is used to predict internal modes of vibration of essentially molecular units.
- (ii) Line group analysis [11] - the organic ligands are usually taken as point masses (as in the present work) to make the line group isomorphous with the point group.
- (iii) Factor group analysis [12] - the symmetry properties of the primitive unit cell of a crystalline substance are used to obtain information about both internal and external (lattice) modes.

These group theoretical approaches are very useful, but it must be remembered that in practice they give no information on the intensities and wavenumber positions of the predicted vibrational modes.

The methods used in the various group theoretical approaches in the present work are found in Appendix A.4 along with individual analyses.

### 1.3 A survey of structural studies of $(R_3P)_n HgX_2$ complexes in the solid-state

#### 1.3.1 Introduction

The majority of previous structural data on addition complexes of mercury halides and neutral unidentate ligands with the 1:1 and 2:1 stoichiometries ( $R_3P:HgX_2$ ) indicate a tendency for halogen-bridged structures for the 1:1 complexes to be formed [9,13] and tetrahedral monomers for the 2:1 complexes with varying degrees of distortion from a regular tetrahedral geometry [6-8]. In the case of the 1:1 complexes, the complexes have the ability to increase their co-ordination numbers beyond that of a monomer unit via halogen-bridges.

### 1.3.2 Crystallographic studies of $(R_3P)HgX_2$ complexes

As stated before, (Section 1.3.1) mercury (II) halide complexes in the solid-state have the ability to increase the mercury co-ordination number beyond that of the monomer unit by halogen-bridging. In the  $(R_3P)HgCl_2$  series of complexes [ $R_3P = Me_3P, Et_3P, Bu_3P, Ph_3P$  or  $TPP$ ] varying degrees of this halogen bridging were found [1-5], as shown in Figures 1.1 to 1.5.

$(Ph_3P)HgCl_2$  (Figure 1.1) consists [1] of discrete chlorine-bridged dimers in which mercury lies in a distorted tetrahedral environment with angles about mercury ranging from  $85.3(3)^\circ$  [ $Cl(2) - Hg - Cl(2')$ ] to  $128.7(4)^\circ$  [ $Cl(1) - Hg - P$ ]. There is a centre of symmetry at the centre of the four-membered ring [ $Hg', Cl(2), Cl(2'), Hg$ ] with the Hg-Cl bridge distances being almost equal [ $2.62(1)$  for Hg - Cl(2') and  $2.66\text{\AA}$  for Hg - Cl(2)]. Preliminary photographic studies indicated the analogous bromo and iodo complexes to be isomorphous and isostructural with  $(Ph_3P)HgCl_2$  [1].

The  $(TPP)HgCl_2$  structure [1], Figure 1.2, is very similar to that of  $(Ph_3P)HgCl_2$  but the Hg - Cl bridges are very asymmetrical with Hg - Cl bond distances of  $2.54(1)$  [ $Hg - Cl(2)$ ] and  $2.75(1)\text{\AA}$  [ $Hg - Cl(2')$ ]. Preliminary photographs [1] indicate  $(TPP)HgBr_2$  to be isomorphous and isostructural with  $(TPP)HgCl_2$ .

The previous two structures do not extend beyond the dimer stage but  $\alpha$ - $(Bu_3P)HgCl_2$  shows further extension to form a halogen-bridged tetramer [1]. Figure 1.3 shows the tetrameric

Figure 1.1

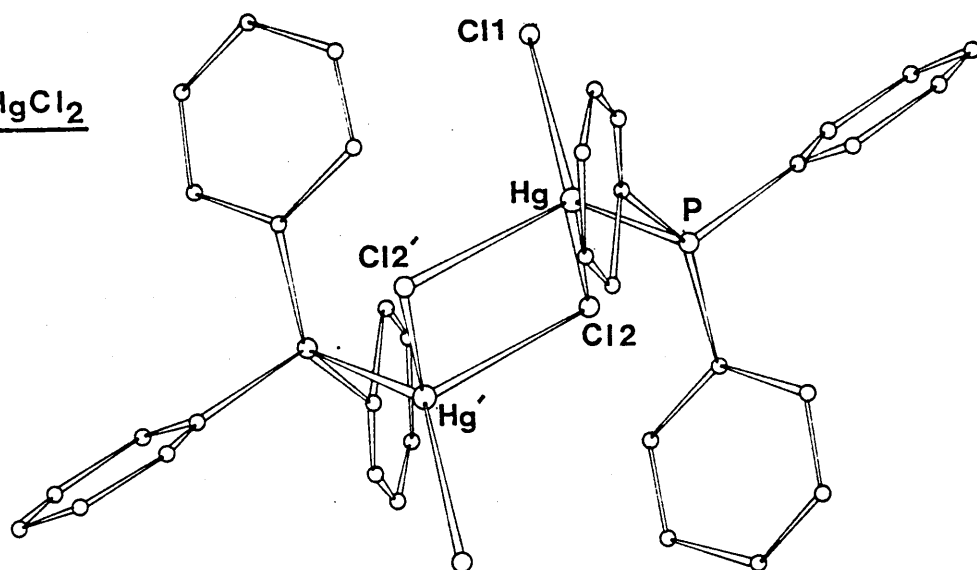
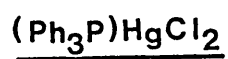


Figure 1.2

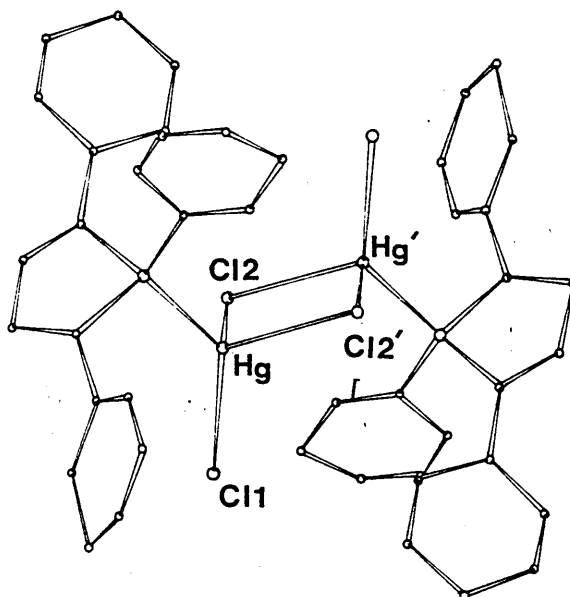
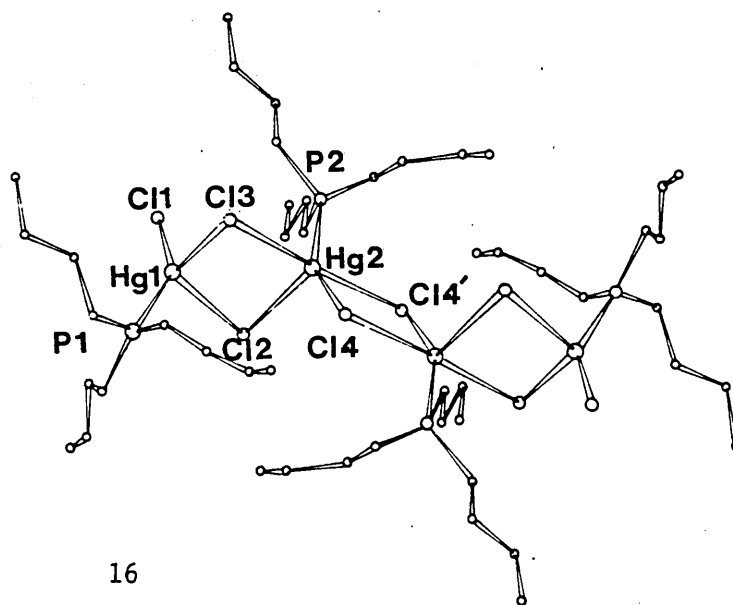
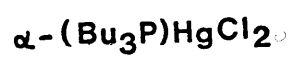


Figure 1.3



unit containing mercury in both tetra- and pentaco-ordinate environments. The tetramer comprises of two unsymmetrical chlorine-bridged dimers linked by longer chlorine bridges. Within the dimeric fragments, Hg1 and Hg2 are 3.793 $\overset{\circ}{\text{Å}}$  apart, with Hg-Cl bridge distances of 2.63(2), 2.71(2), 2.67(2) and 2.90(2) $\overset{\circ}{\text{Å}}$  for Hg1 - Cl(3), Hg1 - Cl(2), Hg2 - Cl(2) and Hg2 - Cl(3) respectively. The two dimers are related by a centre of symmetry and joined by relatively long contacts of 3.38(3) $\overset{\circ}{\text{Å}}$  between Hg2' - Cl(4) and Hg2 - Cl(4'). The terminal mercury (Hg1) is in a very distorted tetrahedral environment [ angles ranging from 92.6(7) to 147.8(7) $^\circ$  ] whereas Hg2 is in a distorted trigonal bipyramidal environment. The equatorial plane contains P2, Cl(2), Cl(4) and bond angles range from 98.6(7) [ Cl(4) - Hg2 - Cl(2) ] to 150.6(7) $^\circ$  [ P2 - Hg2 - Cl(4) ]. The axial positions are occupied by Cl(3) and Cl(4') such that the Cl(3) - Hg - Cl(4') arrangement is almost linear [ 177.0(1) $^\circ$  ].

The crystal structure of  $\beta$ -(Bu<sub>3</sub>P)HgCl<sub>2</sub> has been elucidated [ 3 ] and found to contain halogen-bridged dimers similar to those found in (Ph<sub>3</sub>P)HgCl<sub>2</sub>. The principal difference between the structures of the Ph<sub>3</sub>P and  $\beta$ -Bu<sub>3</sub>P complexes is in the relative magnitudes of the P - Hg - Cl<sub>terminal</sub> angle, viz. 128.7 $^\circ$  in (Ph<sub>3</sub>P)HgCl<sub>2</sub> compared with 150.9 $^\circ$  in  $\beta$ -(Bu<sub>3</sub>P)HgCl<sub>2</sub>. The latter value is similar to the P - Hg - Cl<sub>terminal</sub> angle found in  $\beta$ -(Bu<sub>3</sub>P)HgCl<sub>2</sub> [ 147.8, 150.6 $^\circ$  ]. The chlorine-bridge is found to be symmetrical in the  $\beta$ -Bu<sub>3</sub>P complex, with the Hg - Cl<sub>bridge</sub> distances being significantly longer than those found in (Ph<sub>3</sub>P)HgCl<sub>2</sub> [ 2.720, 2.736 $\overset{\circ}{\text{Å}}$  compared with 2.62, 2.66 $\overset{\circ}{\text{Å}}$  for (Ph<sub>3</sub>P)HgCl<sub>2</sub> ].

The complex  $(Et_3P)HgCl_2$ , Figure 1.4, shows even further extension via halogen-bridging and has been described as a chlorine-bridged polymer with mercury in a distorted trigonal bipyramidal environment [ 5 ]. There are two short Hg - Cl bonds at 2.42(1) and 2.56(1) $\overset{\circ}{\text{Å}}$ , Hg - Cl(2) and Hg - Cl(1), and a short Hg - P bond at 2.35(1) $\overset{\circ}{\text{Å}}$  lying in the equatorial positions around mercury, and two longer apical Hg - Cl contacts at 3.04(1) and 3.21(1) $\overset{\circ}{\text{Å}}$ , Hg - Cl(1') and Hg - Cl(2') . The angles within the equatorial  $PHgCl_2$  unit range from 98.7(3) [ Cl(1) - Hg - Cl(2) ] to 145.4(4) $^\circ$  [ Cl(2) - Hg - P ], while the angle between the two longer apical contacts Cl(1') - Hg - Cl(2') is close to linearity at 170.8(3) $^\circ$ .

$(Me_3P)HgCl_2$  is found to have a polymeric arrangement [ 5 ], which can be envisaged as being 'ionic', containing [ Cl - Hg -  $PMe_3$  ] $^+$  and  $Cl^-$  ions arranged alternatively in a zig-zag chain [ Figure 1.5 ]. The [ Cl - Hg -  $PMe_3$  ] $^+$  cation is almost linear [ Cl - Hg - P angle , 162.1(1) $^\circ$  ]. The co-ordination number of mercury is increased to five by three further Hg - Cl contacts: Hg-Cl(1), Hg - Cl(1') and Hg - Cl(1'') at 2.782(4), 2.94(4) and 3.489(4) $\overset{\circ}{\text{Å}}$  respectively. The 'chain-like' arrangement is different to that found in  $(Et_3P)HgCl_2$ , as the bridging involves only one of the chlorine atoms of the ' $Cl_2HgPMe_3$ ' unit. Preliminary photographs [ 5 ] indicate the bromo-analogue to be isostructural.

**Figure 1.4**

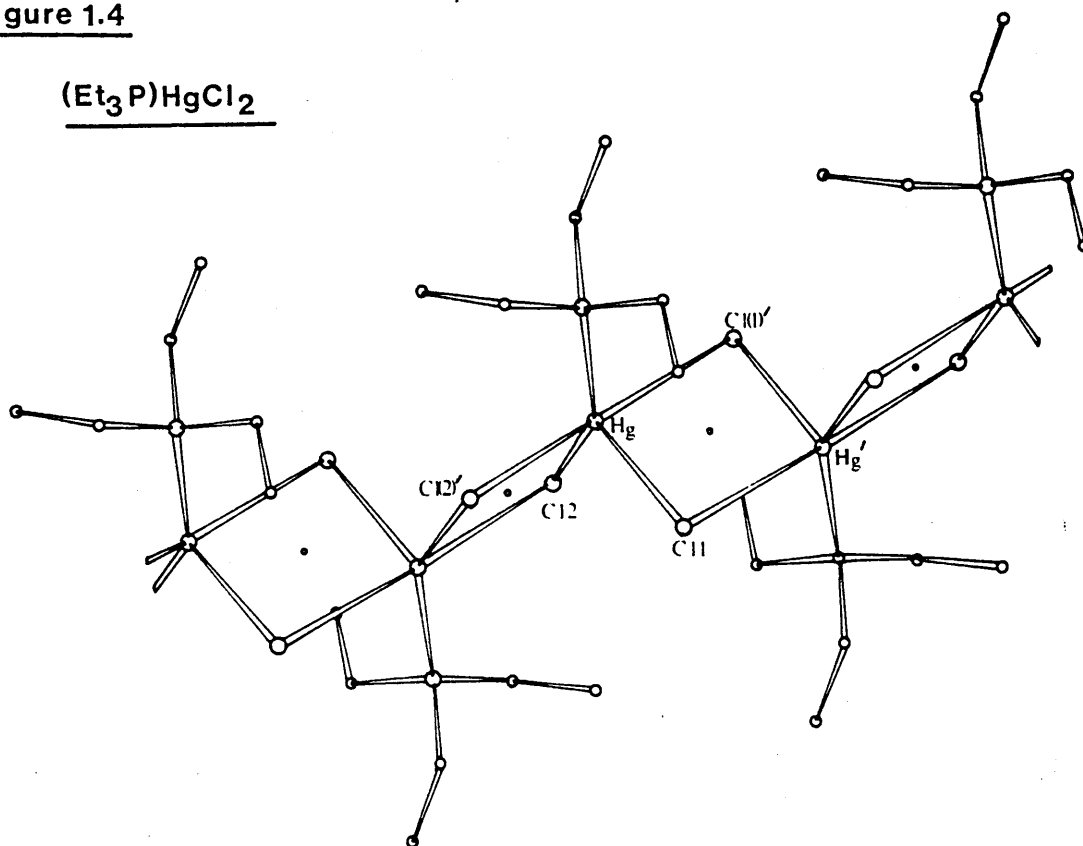
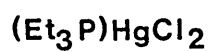
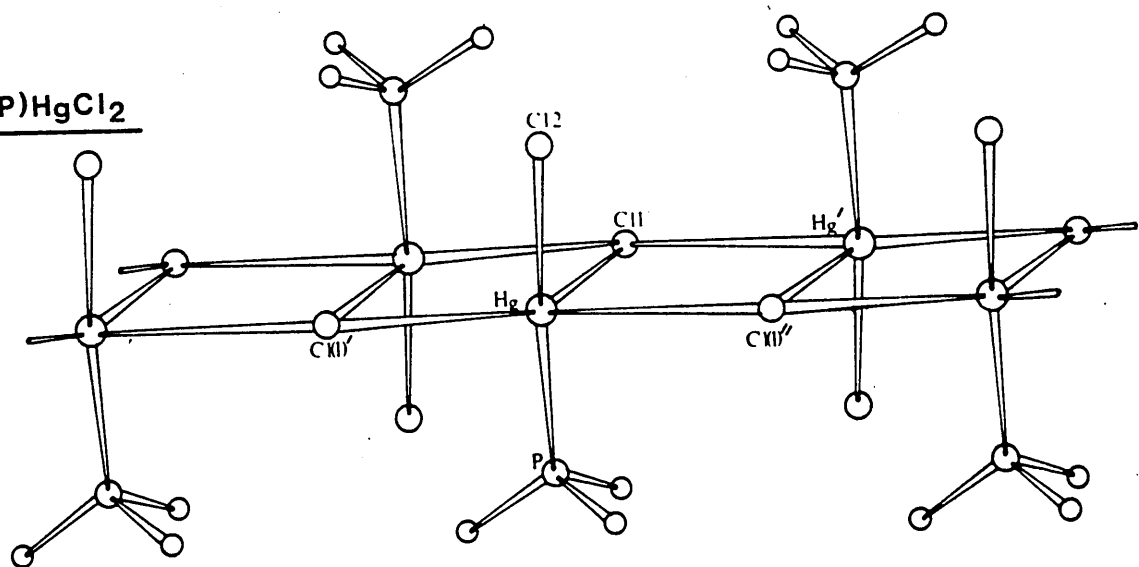
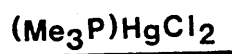


**Figure 1.5**



### 1.3.3 Crystallographic studies of $(R_3P)_2HgX_2$ complexes

The  $(R_3P)_2HgX_2$  complexes fully characterised so far [6,7,8,14] are all tetraco-ordinate monomers with varying degrees of distortion from a regular tetrahedral geometry (Figure 1.6). Of the structures reported,  $(Ph_3P)_2HgI_2$  [6] has an almost regular tetrahedral geometry around the mercury, as is evident from the I - Hg - I and P - Hg - P angles [110.43(9) $^\circ$  and 108.95(4) $^\circ$  respectively, Table 1.1].

$(Bu_3P)_2HgCl_2$  [8] is more distorted, the P - Hg - P [139(2) $^\circ$ ] and Cl - Hg - Cl angles [105(2) $^\circ$ ] being quite different. The structure of  $(EtMe_2P)_2HgBr_2$  [14] contains two independent monomer units in the unit cell (Figure 1.7), each having mercury in a distorted tetrahedral environment, with P - Hg - P angles of 147(2) and 150(2) $^\circ$  for P1 - Hg1 - P2 and P3 - Hg2 - P4 respectively (Table 1.1).

The remaining structure previously reported [7] is  $(Et_3P)_2HgCl_2$ , which is also a distorted tetrahedral species with a P - Hg - P angle of 158.5(5) $^\circ$  [Table 1.1].

Figure 1.6

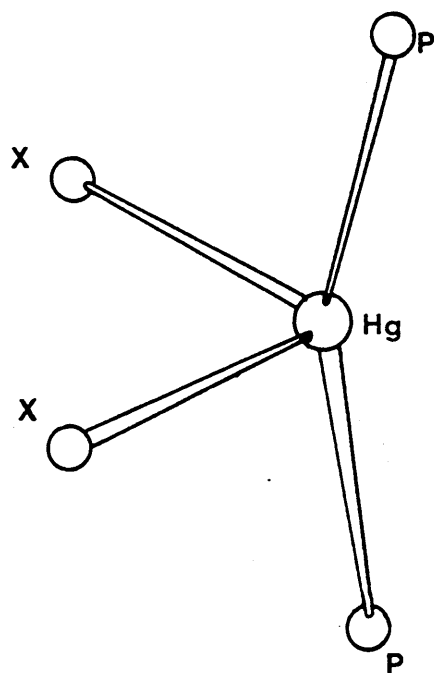


Figure 1.7

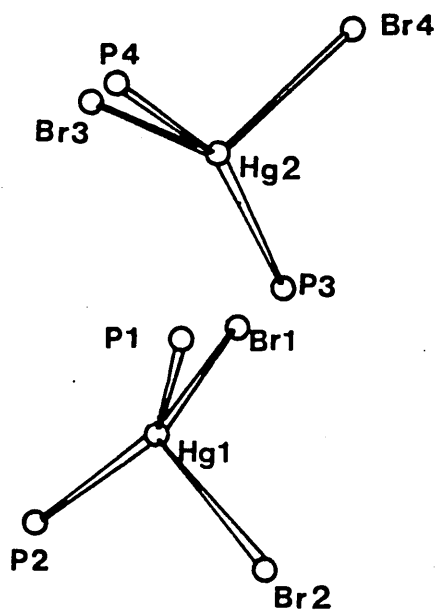
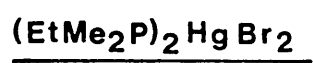


Table 1.1

Crystal data for  $(R_3P)_2HgX_2$  complexes

Compound	X - Hg - X /°	P - Hg - P /°	Ref
$(Ph_3P)_2HgI_2$	110.43(9)	108.95(4)	6
$(Bu_3P)_2HgCl_2$	105(2)	139(2)	8,14
$(EtMe_2P)_2HgBr_2$	102(1) 107(1)	147(2) 150(2)	14
$(Et_3P)_2HgCl_2$	105.5(5)	158.5(5)	7

#### 1.3.4 Spectroscopic studies of some $(R_3P)HgX_2$ complexes

The solid-state vibrational spectra of the complexes mentioned in Section 1.3.2 and those of their bromo- and iodo-analogues have been previously examined [ 14 ]. Using the structure/spectra correlation technique (Section 1.2), various correlations were put forward between  $\nu(Hg - Cl)$  spectral patterns and structural features.

Tables 1.2 and 1.3 show the  $\nu(Hg-Cl)$  assignments made [ 14 ]. The following is a summary of detailed structure/spectra correlations given by Jones [ 14 ], who was able to characterise spectroscopically (especially via infrared spectra) the five separate structures described in Section 1.3.2: an asymmetric dimer, an almost symmetric dimer, a chain polymer, a tetramer and an ionic chain.

- (a) In the structures of  $(R_3P)HgCl_2$  [  $R_3P = TPP, Ph_3P, Bu_3P, Et_3P$  or  $Me_3P$  ], the common structural feature of one short Hg - Cl bond is characterised by a band around  $280 - 300 \text{ cm}^{-1}$  in the infrared and Raman spectra, assigned to  $\nu(Hg - Cl)_t^*$  (Table 1.2).
- (b) The differentiation between each structural type was indicated by examination of the lower wavenumber regions ( $140 - 280 \text{ cm}^{-1}$ ) where the  $\nu(Hg - Cl)_b^*$  modes are expected to appear. It was shown [ 14. ] that the wavenumber positions of these  $\nu(Hg - Cl)_b$  modes varied in a manner dependent on the type and extent of chlorine-bridging.

---

\* t indicates a terminal chlorine in the dimeric cases and the nearest chlorine to mercury in the polymeric cases.

\* b represents bridging associated with the longer Hg - Cl contacts.

- (c) The  $(\text{Me}_3\text{P})\text{HgCl}_2$  'ionic' chain structure was distinguished from the other structures by the lack of  $\nu(\text{Hg} - \text{Cl})_b$  modes in the infrared between  $140 - 300 \text{ cm}^{-1}$ .
- (d) Differentiation between the polymeric  $(\text{Et}_3\text{P})\text{HgCl}_2$  complex and the dimeric  $(\text{Ph}_3\text{P})\text{HgCl}_2$  and  $(\text{TPP})\text{HgCl}_2$  complexes is by observation of strong bands in the infrared spectrum of the  $\text{Et}_3\text{P}$  complex at  $117 \text{ cm}^{-1}$  and  $90 \text{ cm}^{-1}$  (Table 1.3) in addition to the bands found in all three spectra around  $150 - 220 \text{ cm}^{-1}$ .
- (e) The more complicated nature of the spectrum of  $\alpha - (\text{Bu}_3\text{P})\text{HgCl}_2$  did not give rise to any information which would enable a definite identification of that particular 'tetramer' structure.

Table 1.2

$\nu(\text{Hg} - \text{X})$  modes associated with 'short' Hg - X bonds [14].

Complex	$d(\text{Hg} - \text{X}) / \overset{\circ}{\text{A}}$	IR active $\nu(\text{Hg} - \text{X})_t / \text{cm}^{-1}$	Ra active $\nu(\text{Hg} - \text{X})_t / \text{cm}^{-1}$
(TPP)HgCl <sub>2</sub>	2.41(3)	283	282
(Ph <sub>3</sub> P)HgCl <sub>2</sub>	2.37(1)	290	286
(Et <sub>3</sub> P)HgCl <sub>2</sub>	2.40(1)	286	270
(Me <sub>3</sub> P)HgCl <sub>2</sub>	2.36(1)	300	291
$\alpha$ -(Bu <sub>3</sub> P)HgCl <sub>2</sub>	2.28(3)	278	280
$\beta$ -(Bu <sub>3</sub> P)HgCl <sub>2</sub>	2.348(8)	295	n.r.
(TPP)HgBr <sub>2</sub>		195	195
(Ph <sub>3</sub> P)HgBr <sub>2</sub>		203	200
(Et <sub>3</sub> P)HgBr <sub>2</sub>		190	185
(Me <sub>3</sub> P)HgBr <sub>2</sub>		216	193
(Bu <sub>3</sub> P)HgBr <sub>2</sub>		188	186
(Ph <sub>3</sub> P)HgI <sub>2</sub>		163	160
(Bu <sub>3</sub> P)HgI <sub>2</sub>		151	150

n.r. = not recorded

Table 1.3

IR - active  $\nu$  (Hg - X)<sub>b</sub> modes associated with Hg - X<sub>bridge</sub> bonds [ 14 ] .

Complex	Structure	d(Hg - X) <sup>o</sup> /Å	$\nu$ (Hg - X) <sub>b</sub> /cm <sup>-1</sup>	
(TPP)HgCl <sub>2</sub>	asymmetric dimer	2.54(1),2.75(1)	219	156
(Ph <sub>3</sub> P)HgCl <sub>2</sub>	symmetric dimer	2.623(8),2.658(8)	188	183
(Et <sub>3</sub> P)HgCl <sub>2</sub>	polymeric chain	2.56(1),3.04(1),3.21(1)	203,198sh,117,105	
(Me <sub>3</sub> P)HgCl <sub>2</sub>	'ionic' chain	2.941(4),3.489(4),2.782(4)	141 and below	
$\alpha$ -(Bu <sub>3</sub> P)HgCl <sub>2</sub>	tetramer	2.67(2),2.90(2),3.38(3)	252,218,179	
$\beta$ -(Bu <sub>3</sub> P)HgCl <sub>2</sub>	symmetric dimer	2.720(6),2.736(6)	181	173
(TPP)HgBr <sub>2</sub>			151	117
(Ph <sub>3</sub> P)HgBr <sub>2</sub>			137	117
(Et <sub>3</sub> P)HgBr <sub>2</sub>			144,91,84,72	
(Me <sub>3</sub> P)HgBr <sub>2</sub>			166	
(Ph <sub>3</sub> P)HgI <sub>2</sub>			117	89

### 1.3.5 Spectroscopic studies of $(R_3P)_2HgX_2$ complexes

These complexes have also been studied [14] with the use of infrared and Raman spectra, in terms of  $C_{2v}$  symmetry, for which two  $\nu(Hg - X)$  modes are predicted in the infrared and Raman spectra (point group analysis).

The vibrational assignments of 2:1 complexes are given in Table 1.4, together with the magnitudes of the Hg - X bond lengths and the P - Hg - P angles. The magnitude of the Hg - X bond lengths and the P - Hg - P angles were shown [14] to influence the position of the  $\nu(Hg - X)$  bonds. Thus the  $\nu(Hg - X)$  modes were found to be in the ranges 160-240, 110-166 and 90-140  $cm^{-1}$  for the chloro-, bromo- and iodo- complexes respectively, with the lower wavenumber bands in each series characteristic of compounds having the larger P - Hg - P angles and longer Hg - X bonds.

This correlation between  $\nu(Hg - X)$  and molecular parameters can thus be used in the study of other  $(R_3P)_2HgX_2$  complexes to indicate the degree of distortion from a regular tetrahedral structure (Chapter 2).

Table 1.4

Relationship between the structures and spectra of some

$(R_3P)_2HgX_2$  complexes [14] .

Parameter	$(R_3P)_2HgCl_2$				$(R_3P)_2HgBr_2$				$(R_3P)_2HgI_2$			
	Ph <sub>3</sub> P	Bu <sub>3</sub> P	EtMe <sub>2</sub> P	Et <sub>3</sub> P	Ph <sub>3</sub> P	Bu <sub>3</sub> P	EtMe <sub>2</sub> P	Et <sub>3</sub> P	Ph <sub>3</sub> P	Bu <sub>3</sub> P	EtMe <sub>2</sub> P	Et <sub>3</sub> P
P-Hg-P angle/°		139		158.5			148.5		108.95			
av.Hg-X <sub>o</sub> Length/Å		2.60		2.68			2.79		2.75			
$\nu_{as}(Hg-X)$ /cm <sup>-1</sup>	223	205	181-169	176	155	127	112	132	129	107	94	109

## 1.4 Survey of stereochemistry of $\text{CdX}_2$ complexes of neutral unidentate ligands

### 1.4.1 Introduction

In the solid-state it is known that cadmium (II) halide addition complexes of the type  $\text{L}_n\text{CdX}_2$  [ L = neutral unidentate ligand; n = 1 or 2 ] generally pack together in such a way that extension from the monomer units is obtained by cadmium-halogen bridging interactions [18-34]. These interactions are usually longer than the sum of the covalent radii (Cd - Cl = 2.40; Cd - Br = 2.55; Cd - I = 2.74 $\overset{\circ}{\text{A}}$ ), but within the sum of the van der Waals' radii (Cd - Cl = 3.21; Cd - Br = 3.36; Cd - I = 3.56 $\overset{\circ}{\text{A}}$ ).

The structures of the complexes,  $(\text{R}_3\text{P})_n\text{HgX}_2$  (n = 1 or 2)

have been discussed in Section 1.3.2 and it was thought that similar structural variations might occur in the analogous cadmium complexes. However, despite the fairly close relationships found [15-17] between some trihalogeno salts of the two metals,  $[\text{MX}_3]^-$ , the mercury structures (Section 1.3.2) showed no relationship to the double-chained structures reported in the literature for  $\text{LCdX}_2$  type complexes (Section 1.4.2). Similarly, the halogen-bridged chain structure of  $\text{L}_2\text{MX}_2$  systems appears common for Cd [18-20] complexes but is rare for Hg.

It was thus decided to extend the work on mercury to  $\text{L}_n\text{CdX}_2$  systems (n = 1 or 2).

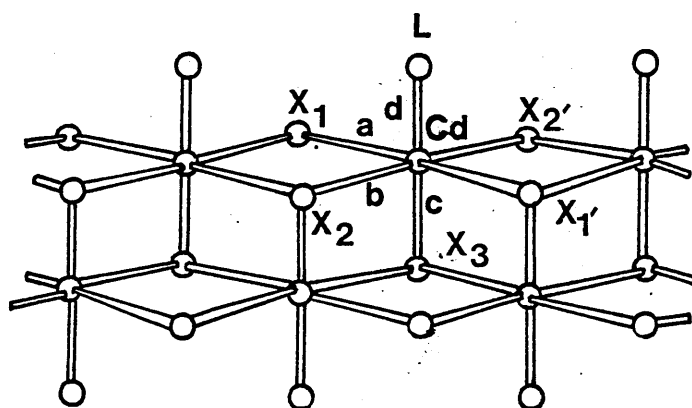
#### 1.4.2 Crystallographic studies of $\text{LCdX}_2$ complexes

At the start of the present project the structures of a number of complexes had been reported, three of which are of a similar structural type (Figure 1.8). They are  $(\text{MeNHCONH}_2)\text{CdCl}_2$  [18],  $(\text{imidazole})\text{CdCl}_2$  [19] and  $(\text{MeCSNH}_2)\text{CdCl}_2$  [20], where the donor atom of the ligand is oxygen, nitrogen and sulphur, respectively. The structure is that of a double-chain arrangement, in which two chains of cadmium atoms are linked by halogen bridges. The bridging units are not perfectly symmetrical. The two polymeric chains are linked together by further Cd - X interactions ('c' in Figure 1.8), with the ligand occupying the sixth co-ordination position on the cadmium atoms.

While the structures mentioned above have their ligands acting as neutral unidentate ligands, in the following two 1:1 complexes the ligands are bidentate. The pyridine-N-oxide complex  $(\text{C}_5\text{H}_5\text{NO})\text{CdI}_2$  [21] contains 'monomer' units which are linked together to form a polymeric chain, alternately bridged through pairs of iodine and oxygen atoms. The environment of the pentaco-ordinate Cd atom is distorted trigonal bipyramidal (Figure 1.9).

The structure of dichloro(dicyandiamide) cadmium (II) (Figure 1.10) [22] contains cadmium atoms surrounded by four chlorine and two nitrogen atoms, giving rise to a slightly distorted octahedral environment about the metal atoms. The chlorine atoms form bridges between adjacent metal atoms to form polymeric chains running parallel to each other. These chains are linked together by dicyandiamide bridges.

Figure 1.8 Structure of some LCdX<sub>2</sub> complexes



Bond lengths / Å

<u>L</u>	<u>X</u>	<u>a/Å</u>	<u>b/Å</u>	<u>c/Å</u>	<u>d/Å</u>
MeNHCONH <sub>2</sub>	Cl	2.67	2.62	2.60	2.18
C <sub>3</sub> H <sub>4</sub> N <sub>2</sub>	Cl	2.729(3)	2.604(2)	2.676(3)	2.243(5)
MeCSNH <sub>2</sub>	Cl	2.760(2)	2.570(2)	2.630(2)	2.55(1)

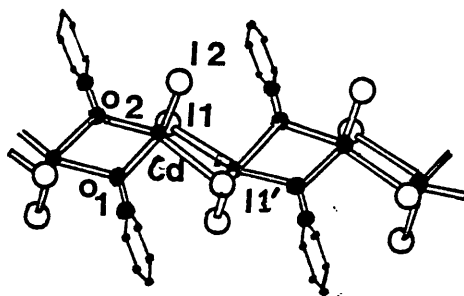
Bond angles (°)

<u>L</u>	<u>L-Cd-X<sub>1</sub></u>	<u>L-Cd-X<sub>2</sub></u>	<u>L-Cd-X<sub>3</sub></u>	<u>X<sub>2</sub>-Cd-X<sub>3</sub></u>	<u>X<sub>1</sub>-Cd-X<sub>3</sub></u>
MeCSNH <sub>2</sub>	98.2(7)	81.7(6)	158.6(4)	79.5(4)	90.6(4)
C <sub>3</sub> H <sub>4</sub> N <sub>2</sub>	90.5(2)	94.1(2)		87.5	90.8
MeNHCONH <sub>2</sub>	99.0	88.0			

<u>L</u>	<u>X<sub>1</sub>-Cd-X<sub>1</sub>'</u>	<u>X<sub>2</sub>-Cd-X<sub>2</sub>'</u>
MeCSNH <sub>2</sub>	171.4(4)	172.2(4)
C <sub>3</sub> H <sub>4</sub> N <sub>2</sub>	173.5(1)	—

Figure 1.9    Structure of  $(C_5H_5NO)CdI_2$



Bond lengths/Å

$$Cd - I(1) = 2.834(7)$$

$$Cd - I(1') = 2.963(9)$$

$$Cd - I(2) = 2.724(5)$$

$$Cd - O_2 = 2.383(64)$$

$$Cd - O_1 = 2.275(54)$$

Bond angles/°

$$I(1) - Cd - O_1 = 157.8(11)$$

$$I(2) - Cd - O_2 = 129.2(13)$$

$$I(1) - Cd - I(2) = 118.5(3)$$

$$I(1) - Cd - O_2 = 108.0(11)$$

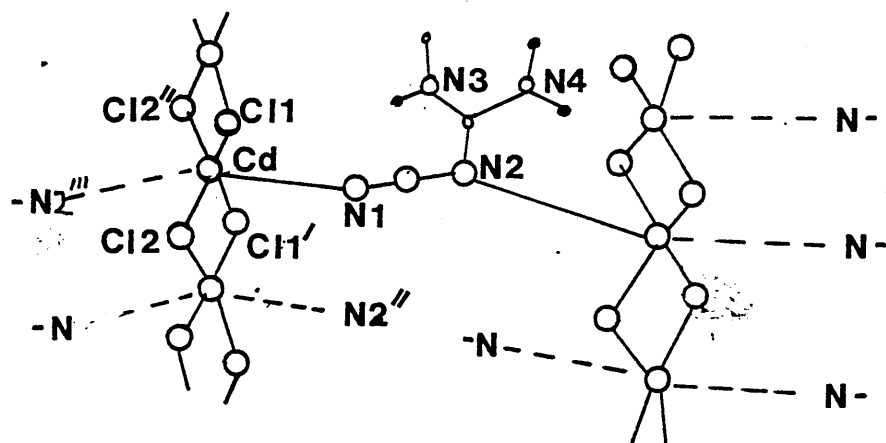
$$I(1) - Cd - I(1') = 93.2(3)$$

$$I(2) - Cd - I(3) = 104.0(3)$$

$$O_2 - Cd - O_1 = 66.0(20)$$

Figure 1.10

Structure of dichloro(dicyandiamide) Cd(II)



Bond lengths/ Å

Cd - Cl(1)	= 2.607(3)	Cd - Cl(2'')	= 2.630(3)
Cd - Cl(2)	= 2.647(3)	Cd - N(1)	= 2.358(4)
Cd - Cl(1')	= 2.572(3)	Cd - N(2''')	= 2.430(4)

Bond angles/ °

Cl(1) - Cd - N(1)	= 87.0(1)	Cl(2) - Cd - Cl(2'')	= 84.68(3)
Cl(1) - Cd - Cl(1')	= 85.03(4)	Cl(2) - Cd - N(2''')	= 80.6(1)
Cl(1) - Cd - Cl(2'')	= 97.36(4)	N(1) - Cd - Cl(2'')	= 84.9(1)
Cl(1) - Cd - N(2''')	= 97.6(1)	N(1) - Cd - N(2''')	= 98.7(1)
Cl(1') - Cd - N(1)	= 89.1(1)	Cl(1') - Cd - N(2'')	= 87.55(4)
Cl(2) - Cd - Cl(1')	= 99.25(25)	Cl(1') - Cd - N(2''')	= 91.0(1)

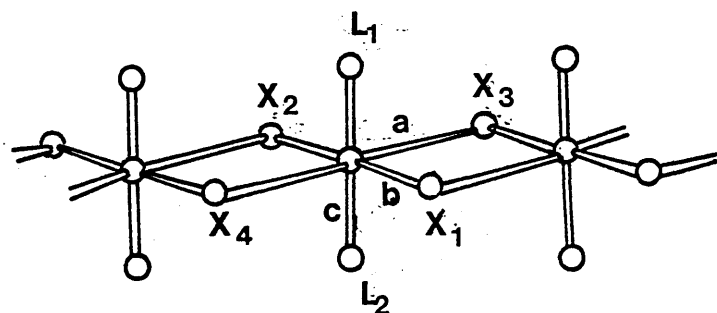
### 1.4.3 Crystallographic studies of $L_2CdX_2$ complexes

Two types of structure for these 2:1 complexes have been authenticated in the literature. The most common is that of a single chain polymeric structure having the cadmium atoms in an octahedral environment (Figure 1.11) formed by halide-bridges between cadmium atoms. The fifth and sixth co-ordination positions of the cadmium are taken up by the neutral monodentate ligand. This type of structure is observed in  $(Py)_2CdX_2$  [ X = Cl, or Br ] [ 23,24 ] ,  $(imidazole)_2 CdCl_2$  [ 25 ] and  $(NH_3)_2CdX_2$  [ X = Cl or Br ] [ 26 ] , which all have nitrogen-donor ligands, and by five complexes with oxygen as the donor atom, viz.  $(urea)_2CdCl_2$  [ 27 ] ,  $(methylurea)_2CdCl_2$  [ 28 ] ,  $(biuret)_2CdCl_2$  [ 29 ] ,  $(acetamide)_2 CdCl_2$  [ 30 ] and  $(HCONH_2)_2CdCl_2$  [ 31 ] .

The second structural type found for these 2:1 complexes is that of a tetrahedral monomer (Figure 1.12). Three complexes of this type have been reported previously, one involving a sulphur-donor ligand,  $(thiourea)_2CdCl_2$  [ 32 ] , one with phosphorus as the donor atom,  $(Ph_3P)_2CdCl_2$  [ 33 ] , and one of a nitrogen donor,  $(aniline)_2 - CdI_2$  [ 34 ] . In all cases the arrangement about cadmium is close to that of a regular tetrahedron.

Figure 1.11

Structure of some  $L_2CdX_2$  complexes



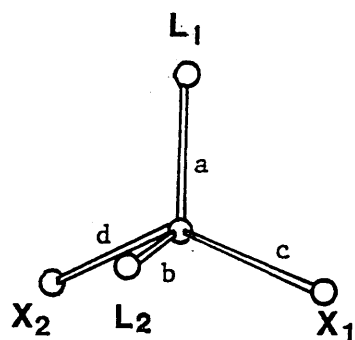
Bond lengths / Å

<u>L</u>	<u>X</u>	<u>a/Å</u>	<u>b/Å</u>	<u>c/Å</u>
Py	Cl	2.65	2.65	2.35
Im	Cl	2.731	2.706	2.248
NH <sub>3</sub>	Cl	2.71	2.71	2.10
NH <sub>3</sub>	Br	2.86	2.86	2.10
biuret	Cl	2.62	2.55	2.34
acetamide	Cl	2.58	2.58	2.23
HCONH <sub>2</sub>	Cl	2.383	2.912	2.34

Bond angles /°

<u>L</u>	<u>X</u>	<u>X<sub>1</sub> - Cd - X<sub>2</sub></u>	<u>L<sub>1</sub> - Cd - X<sub>1</sub></u>	<u>L<sub>1</sub> - Cd - X<sub>3</sub></u>
Py	Cl	88.1	90.5	89.0
Im	Cl	88.2	89.4	89.5
biuret	Cl	91.5(3)	87.9(5)	88.0(5)
HCONH <sub>2</sub>	Cl	89.8(3)	83(1)	—

Figure 1.12 Structure of  $(\text{Ph}_3\text{P})_2\text{CdCl}_2$   $(\text{tu})_2\text{CdCl}_2$



Bond lengths /Å

<u>Complex</u>	<u>a</u>	<u>b</u>	<u>c</u>	<u>d</u>
$(\text{Ph}_3\text{P})_2\text{CdCl}_2$	2.635(5)	2.632(6)	2.504(6)	2.440(6)
$(\text{tu})_2\text{CdCl}_2$	2.45	2.45	2.51	2.50

Bond angles /°

<u>Complex</u>	$\text{L}_1 - \text{Cd} - \text{L}_2$	$\text{L}_1 - \text{Cd} - \text{X}_1$	$\text{L}_1 - \text{Cd} - \text{X}_2$
$(\text{Ph}_3\text{P})_2\text{CdCl}_2$	107.6(2)	104.5(2)	105.7(2)
$(\text{tu})_2\text{CdCl}_2$	—	—	—
<u>Complex</u>	$\text{X}_1 - \text{Cd} - \text{X}_2$	$\text{X}_1 - \text{Cd} - \text{L}_2$	$\text{X}_2 - \text{Cd} - \text{L}_2$
$(\text{Ph}_3\text{P})_2\text{CdCl}_2$	113.9(2)	112.2(2)	112.1(2)
$(\text{tu})_2\text{CdCl}_2$	103	106	105

#### 1.4.4 Spectroscopic studies of $L_n CdX_2$ complexes

##### a) $LCdX_2$

(i) Double-stranded halogen-bridged chain: One of the best examples of spectral characterisation in terms of this structure is a study of (pyridine) $MX_2$  complexes [  $M = Cd; X = Cl$  or  $Br$  ] [ 35 ]. Line group analysis was used to predict

$$\overline{\nu}(M-X) = 3 A_g (Ra) + 2 B_g (Ra) + 2 A_u (I.R.) + 2 B_u (I.R.)$$

$$\overline{\nu}(M-N) = A_g (Ra) + B_u (I.R.)$$

The 3-4  $\nu(M-X)$  and one  $\nu(M-N)$  bands located in the infrared and Raman spectra (Table 1.5) were consistent with this line group analysis.

(ii)  $(R_3P)CdX_2$  complexes: These have all been suggested to have halogen-bridged dimeric structures [ 36,37 ] since the observed bands (Table 1.5) correlate with predictions for a halogen-bridged dimer from group theory i.e.

$$\overline{\nu}(Cd-X)_t = A_g (Ra) + B_u (I.R.)$$

$$\overline{\nu}(Cd-X)_b = A_g (Ra) + B_g (Ra) + A_u (I.R.) + B_u (I.R.)$$

$$\overline{\nu}(Cd-P) = A_g (Ra) + B_u (I.R.)$$

For example,  $(Bu^t_3P)CdX_2$  [ 36 ] complexes show  $\nu(Cd-X)_t$  at 285, 198 and 159  $cm^{-1}$  for  $X = Cl, Br$  or  $I$  respectively, and  $\nu(Cd-X)_b$  at 208, 148  $cm^{-1}$  for  $X = Cl, Br$  respectively.

A similar situation is found for  $(Cy_3P)CdX_2$  [ 37 ] .

b)  $L_2CdX_2$

- (i) Octahedral halogen-bridged chain structure: The spectral characterisations of  $(Py)_2CdX_2$  [ 38 ] and  $(aniline)_2CdX_2$  [ 39 ] have been reported. The line group theory prediction was ( $D_{2h}$ ):

$$\overline{\nu}(\text{Cd-X}) = A_g(\text{Ra}) + B_g(\text{Ra}) + B_{1u}(\text{I.R.}) + B_{3u}(\text{I.R.})$$

$$\overline{\nu}(\text{Cd-N}) = A_g(\text{Ra}) + B_{2u}(\text{I.R.})$$

However the observed number of bands (Table 1.6) was substantially in excess of the predicted number, indicating the need for a different group theory approach.

- (ii) Tetrahedral monomers: The  $(R_3P)_2CdX_2$  complexes which have been suggested to be tetrahedral monomers [ 37, 40, 41 ], show two  $\nu(M-X_2)$  modes in the infrared and Raman spectra (Table 1.6). This is consistent with a monomeric structure ( $C_{2v}$  point group). The  $\nu(Cd-X_2)$  modes are located in the ranges 260-270, 180-200, and 145-165  $\text{cm}^{-1}$  for the chloride, bromide and iodide complexes respectively. The  $\nu(Cd-P)$  modes were located around 130-140  $\text{cm}^{-1}$  in all the infrared and Raman spectra.

c) Summary of spectroscopic studies in  $L_nCdX_2$  complexes

The spectra of  $LCdX_2$  complexes show differentiation between the halide-bridged dimeric structure and the double-stranded halogen-bridged structure. Thus the halogen-bridged dimers give a  $\nu(Cd-X)_t$  band around 290, 200 and 165  $\text{cm}^{-1}$  for Cl, Br and I respectively and  $\nu(Cd-X)_b$  bands correspondingly

around 210, 150 and 100  $\text{cm}^{-1}$ . However the octahedral structure has 3-4 bands in the range of 170-240  $\text{cm}^{-1}$  for chloride and 128-179  $\text{cm}^{-1}$  for the bromide (all bands being in the infrared).

The 2:1 complexes are mainly tetrahedral monomers which give rise to two  $\nu(M-X_2)$  bands. The octahedral polymeric structures give rise to a more complex band pattern (Table 1.6).

Table 1.5

Assignments for some LCdX<sub>2</sub> complexes

L	X	$\nu(\text{Cd-X}) / \text{cm}^{-1}$		$\nu(\text{Cd-L}) / \text{cm}^{-1}$		Ref
		I.R.	Ra	I.R.	Ra	
Py	Cl	233,216, 188	221,180,158	150	110	35
		177	145			
Py	Br	179,173,128	175,140,127	147	110	
Bu <sup>t</sup> <sub>3</sub> P	Cl	285(t)	285(t)	n.o.	128	36
		208(b)	206(b)			
Bu <sup>t</sup> <sub>3</sub> P	Br	198(t)	200(t)	n.o.	118	
		148(b)	158(b)			
Bu <sup>t</sup> <sub>3</sub> P	I	159(t)	160(t)	n.o.	104	
$\beta$ -Cy <sub>3</sub> P*	Cl	294(t)	293(t)	n.o.	n.o.	
		210,202(b)	228,183(b)			
Cy <sub>3</sub> P	Br	206(t)	212(t)	n.o.	n.o.	37
		n.o.	183,172(b)			
Cy <sub>3</sub> P	I	n.o.	164(t)	n.o.	n.o.	

n.o. = not observed, t = terminal Cd-X, b = bridging Cd-X.

\* Another crystalline form ( $\alpha$ -) is known [37] : i.r. bands 273,249, 210-200 and Ra at 277, 273, 252, 248 cm<sup>-1</sup>.

Table 1.6

Assignments for some  $L_2CdX_2$  complexes

L	X	$\nu(Cd-X)/cm^{-1}$		$\nu(Cd-L)/cm^{-1}$		Ref
		I.R.	Ra	I.R.	Ra	
$Ph_3P$	Cl	268		136		40
		261				
	Br	195		134		
		176				
	I	166		133		
		145				
$(m-CH_3C_6H_4)_3P$	Cl	270	263	130	132	41
	Br	196		136	130	
		181	182			
	I	165	164	127	n.o.	
		133	133			
$(p-CH_3C_6H_4)_3P$	Cl	270	262	138	n.o.	41
	Br	198	199	136	n.o.	
		177	175			
	I	165	165	n.o.	n.o.	
		140	140			
$(p-CH_3OC_6H_4)_3P$	Cl	270	262	n.o.	n.o.	41
	Br	200	200	136	n.o.	
		180	181			
	I	159	n.o.	n.o.	n.o.	
		138				

Table 1.6 ctn

L	X	$\nu(\text{Cd-X})/\text{cm}^{-1}$		$\nu(\text{Cd-L})/\text{cm}^{-1}$		Ref
		I.R.	Ra	I.R.	Ra	
$(\text{p}-(\text{CH}_3)_2\text{NC}_6\text{H}_4)_3\text{P}$	Cl	266	250	n.o.	n.o.	41
		250				
	Br	187	190	n.o.	n.o.	
		175	174			
	I	154	155	n.o.	n.o.	
		139	137			
$\text{Cy}_3\text{P}$	Cl	260	n.o.	n.o.	n.o.	37
	Br	n.o.	n.o.	n.o.	n.o.	
	I	n.o.	n.o.	n.o.	n.o.	
$\text{C}_6\text{H}_5\text{NH}_2$	Cl	223		386,378	374	39
		208		328,311	324	
	Br	140	131	373	374	
		111	106	324	324	
Py	Cl	127-170		199		38
	Br	105		167,180		

n.o. = not observed

CHAPTER 2

CRYSTALLOGRAPHIC AND SPECTROSCOPIC STUDIES OF

SOME  $(R_3P)_nHgX_2$  COMPLEXES [ X = Cl, Br or I;

n = 1 or 2 ] .

## Contents

	Page
2.1 Introduction.	45
2.2 Crystallographic examination of $(\text{Ph}_3\text{P})_2\text{HgCl}_2$ .	46
2.3 Crystallographic examination of $(\text{Cy}_3\text{P})\text{HgCl}_2$ .	53
2.4 Spectroscopic studies of $(\text{Cy}_3\text{P})_n\text{HgX}_2$ .	
complexes ( $n = 1$ or $2$ ; $X = \text{Cl}, \text{Br}$ or $\text{I}$ ).	60
2.4.1 $(\text{Cy}_3\text{P})_2\text{HgX}_2$ .	60
2.4.2 $(\text{Cy}_3\text{P})\text{HgX}_2$ .	64

## 2.1 Introduction

Chapter 1 outlined the structural variations within the two series of complexes,  $(R_3P)_n HgX_2$  [ X = Cl, Br or I; n = 1 or 2 ]. A variety of structures was observed for the  $(R_3P)HgX_2$  complexes ranging from discrete dimers, to a loosely held tetramer, to polymeric chain structures. Discrete tetraco-ordinate monomers, with varying degrees of distortion from a regular tetrahedral geometry, were observed for the  $(R_3P)_2HgX_2$  complexes. It was suggested [ 14 ] that the degree of association in the  $(R_3P)HgX_2$  complexes and the extent of tetrahedral distortion of the  $(R_3P)_2HgX_2$  complexes could be related to the size and the donor strength of the phosphine ligand.

In order to investigate further the factors influencing the solid-state structures of  $(R_3P)_n HgX_2$  [ n = 1 or 2 ] complexes, the crystallographic and spectroscopic study reported in Chapter 1 has been extended. In particular the  $(Cy_3P)HgX_2$  [ X = Cl, Br or I ] and  $(Ph_3P)_2HgX_2$  complexes have been studied.

## 2.2 Crystallographic examination of $(\text{Ph}_3\text{P})_2\text{HgCl}_2$

### Crystal data

$\text{C}_{36}\text{H}_{30}\text{Cl}_2\text{HgP}_2$        $M_r = 796.08$ ,      Monoclinic

$a = 9.465(5)$ ,  $b = 17.525(6)$ ,  $c = 19.664(5)\text{\AA}$ ,

$U = 3261.60\text{\AA}^3$ ,  $\alpha = 90.00$ ,  $\beta = 90.10(6)$ ,

$\gamma = 90.00^\circ$ ,  $D_m = 1.60\text{g cm}^{-3}$  (by flotation using  $\text{CHCl}_3/\text{CHI}_3$ ),

$D_c = 1.62\text{g cm}^{-3}$        $Z = 4$ ,  $F(000) = 1560$ ,

$\mu(\text{Mo} - \text{K}\alpha) = 47.37\text{ cm}^{-1}$

### Systematic absences:

0k0 reflections are absent for  $k = 2n + 1$

h0l      "      "      "      "       $l = 2n + 1$

### Space group:

$P2_1/c$

### Data collection and structure refinement

A colourless crystal, approximate dimensions, 0.40 x 0.25 x 0.25 mm. was mounted with the <sup>a-axis coincident with the</sup> rotation ( $\omega$ ) - axis of a Stoe Stadi 2 two circle diffractometer. Data were collected using the background -  $\omega$  scan - background technique. Lorentz and polarisation corrections were applied. Those reflections having  $I/\sigma(I)$  greater than 3.0 were considered to be observed. [ The net intensity  $I = T - B$ , where  $T =$  scan count,  $B =$  mean background count over the scan width,  $\sigma(I) = (T - Bc/2t)^{1/2}$ , where  $c =$  scan time,  $t =$  time for background measurements at each end of the scan ] .

Thus out of 3824 unique reflections collected, 2763 had  $I/\sigma(I) \gg 3.0$  and were used for subsequent refinement. The positions of the mercury atoms were determined from the three-dimensional Patterson

function and the remaining non-hydrogen atoms were located from successive difference electron-density maps. Scattering factors were calculated [42] using an analytical approximation. The carbon atoms of the phenyl rings, after location from electron density maps, were fixed in ideal positions to give C-C bond lengths = 1.395 Å and C-C-C angles = 120.0°

The weighting scheme adopted was:

$$w = 1.3204 / [ \sigma^2(F_o) + 0.0015(F_o)^2 ] .$$

The structure was refined with full matrix refinement with anisotropic temperature factors of the form:

$$\exp [ - 2 \pi^2 (U_{11}h^2a^{*2} + U_{22}k^2b^{*2} + U_{33}l^2c^{*2} + 2U_{12}hka^{*}b^{*} + 2U_{13}hla^{*}c^{*} + 2U_{23}klb^{*}c^{*}) ] .$$

The function minimised in the refinement was  $\sum w ( |F_o| - |F_c| )^2$  and the final R value is given by:

$$R = \frac{\sum |F_o| - |F_c|}{\sum |F_o|}$$

The R' function is given by:

$$R' = \frac{\sum \sqrt{w} | |F_o| - |F_c| |}{\sum \sqrt{w} |F_o|}$$

[ w = weighting function ]

The final R value = 0.057 and R' = 0.063. The final atomic and thermal parameters are listed in Table A.1.1 and calculated and observed structure factors are contained in Appendix A.2. Bond angles and distances are given in Table 2.1.

Description of structure:

$(\text{Ph}_3\text{P})_2\text{HgCl}_2$  crystallises with four monomeric units in the unit cell. The geometry of these monomers is shown in Figure 2.1. The mercury is tetraco-ordinate, being bonded to two phosphorus atoms, at distances of 2.558(9) and 2.476(13) $\text{\AA}$  away. The co-ordination polyhedron about mercury is distorted with angles ranging from 135.2(4) $^\circ$  (P1-Hg-P2) to 99.3(4) $^\circ$  (Cl(2)-Hg-P1). Figure 2.2 shows the packing of the four monomers in the unit cell. The geometry of the complexed  $\text{Ph}_3\text{P}$  ligand is compatible with that observed for the free ligand [43]. The average P-C distance found (average = 1.79 $\text{\AA}$ ) is close to that observed for the free  $\text{Ph}_3\text{P}$  ligand (1.82 $\text{\AA}$ ). The average C-P-C angle in the present complex (106.5 $^\circ$ ) is less distorted from a regular tetrahedral geometry than that found in the free ligand (average = 103.0 $^\circ$ ). The C-P-Hg angles in this complex are slightly larger than that required for regular tetrahedral geometry (Table 2.1). Appendix A.3 contains relevant mean planes data for  $(\text{Ph}_3\text{P})_2\text{HgCl}_2$ . The angles between the phenyl rings are very similar to that found in the free ligand and in  $(\text{Ph}_3\text{P})\text{HgCl}_2$  (Table 2.2)

While both  $(\text{Ph}_3\text{P})_2\text{HgCl}_2$  and  $(\text{Ph}_3\text{P})_2\text{HgI}_2$  [6] adopt monomeric structures, there is a striking difference in the value of the P-Hg-P angle: 135.2(4) $^\circ$  for the chloride complex, 108.95(4) $^\circ$  for the iodide complex. This difference can be attributed to both the nature of the phosphine ligand and also of the halogen atom and will be discussed in Chapter 5.

Figure 2.1 The molecular structure of  $(\text{Ph}_3\text{P})_2\text{HgCl}_2$ .

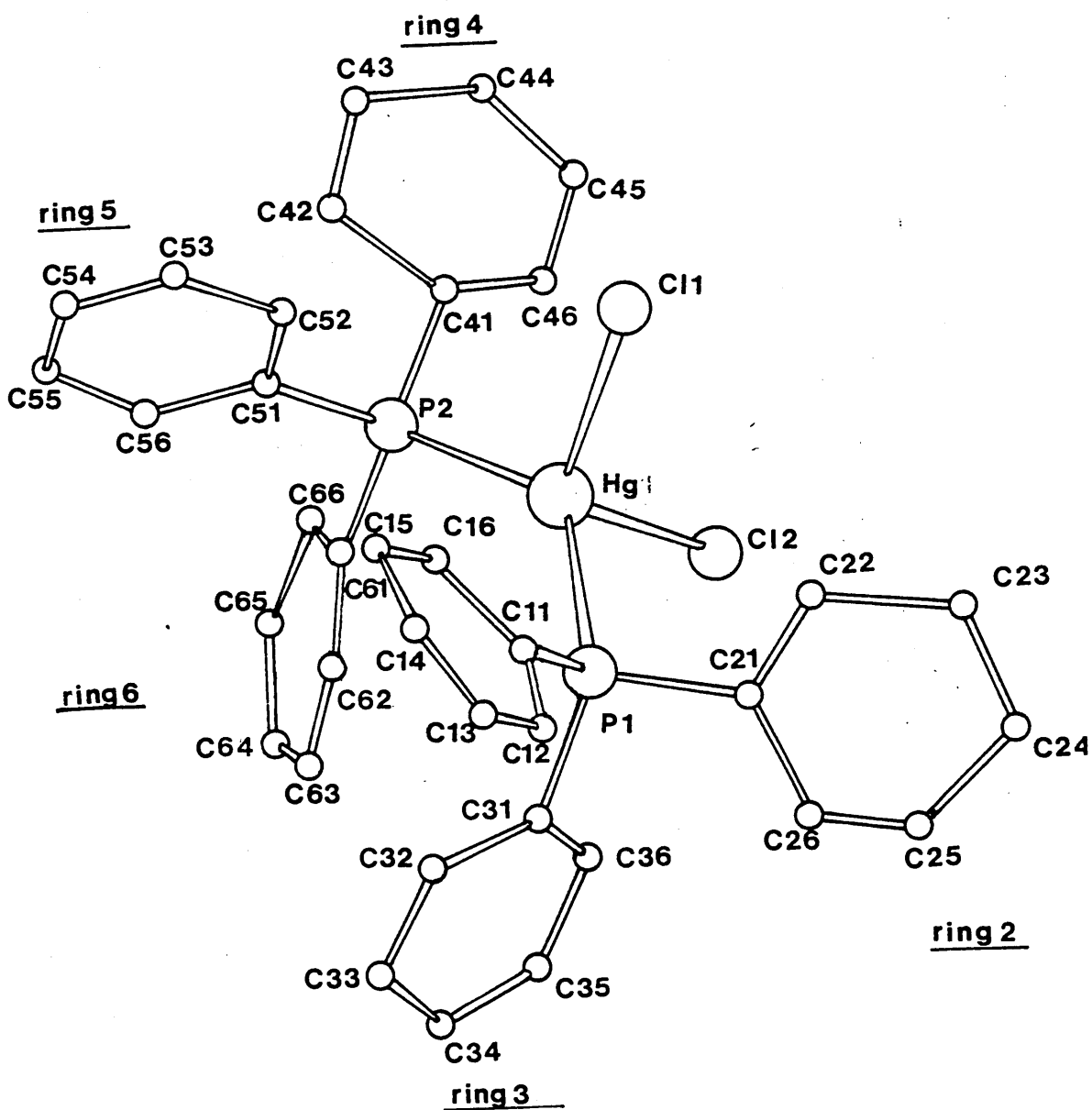


**Figure 2.2** The Crystal structure of  $(\text{Ph}_3\text{P})_2\text{HgCl}_2$

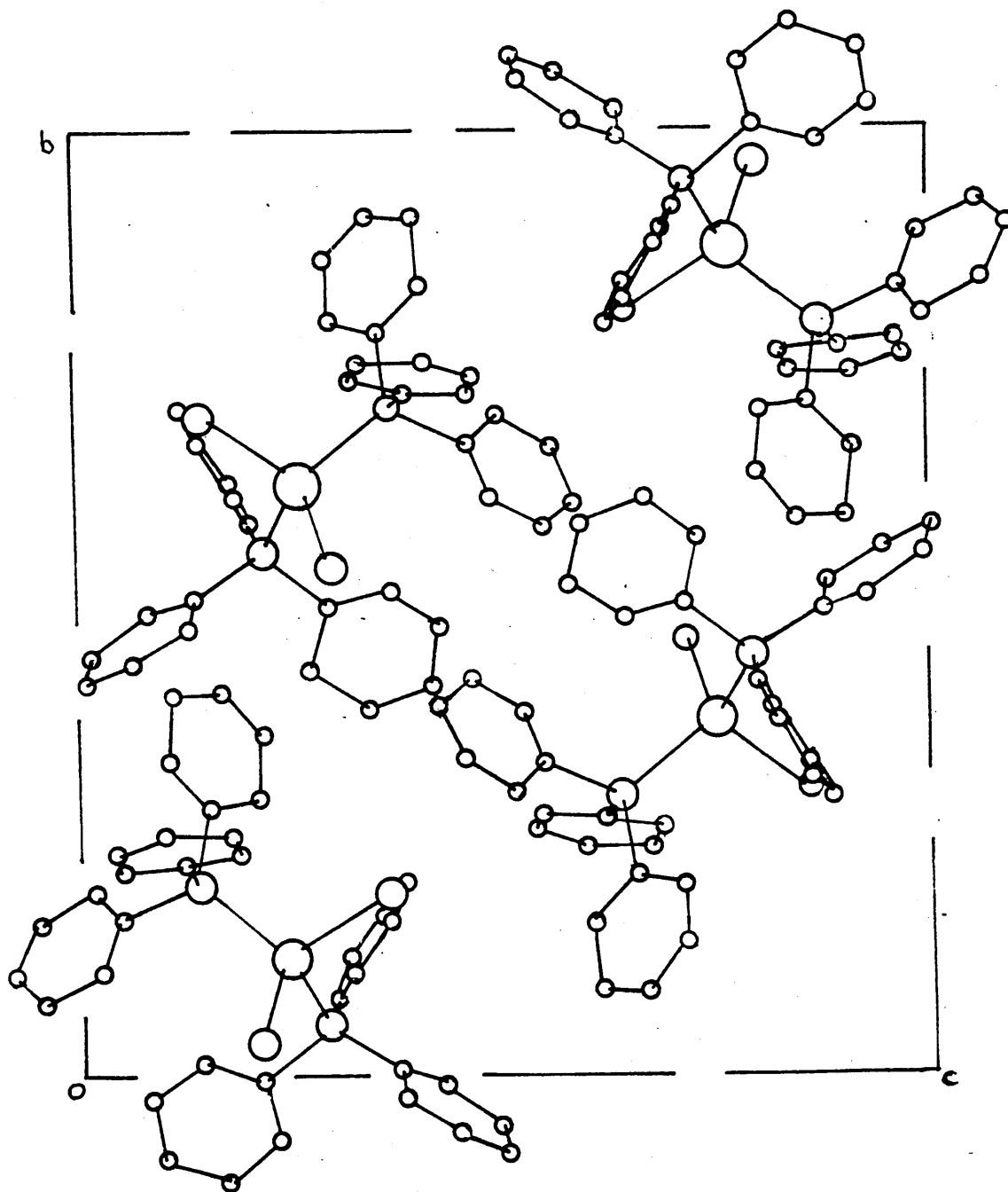


Table 2.1

Bond distances and angles for  $(\text{Ph}_3\text{P})_2\text{HgCl}_2$  with estimated standard deviations in parentheses.

---

a) Bond distances/ $\overset{\circ}{\text{Å}}$

Hg - Cl(1) = 2.558(9)	P1 - C21 = 1.726(39)
Hg - Cl(2) = 2.476(13)	P1 - C31 = 1.790(24)
Hg - P1 = 2.476(8)	P2 - C41 = 1.814(24)
Hg - P2 = 2.378(13)	P2 - C51 = 1.763(32)
P1 - C11 = 1.792(29)	P2 - C61 = 1.856(26)

All C-C bond lengths were fixed at  $1.395\overset{\circ}{\text{Å}}$ .

b) Bond angles/ $^\circ$

Cl(1) - Hg - Cl(2) = 113.3(4)	Hg - P2 - C51 = 105.1(14)
Cl(1) - Hg - P1 = 103.8(3)	Hg - P2 - C61 = 110.8(11)
Cl(1) - Hg - P2 = 104.0(4)	C11 - P1 - C21 = 104.2(15)
Cl(2) - Hg - P1 = 99.3(4)	C11 - P1 - C31 = 108.2(15)
Cl(2) - Hg - P2 = 100.9(4)	C21 - P1 - C31 = 106.0(13)
P1 - Hg - P2 = 135.2(4)	C41 - P2 - C51 = 105.1(14)
Hg - P1 - C11 = 113.7(11)	C41 - P2 - C61 = 106.8(11)
Hg - P1 - C21 = 112.3(10)	C51 - P2 - C61 = 108.9(17)
Hg - P1 - C31 = 111.8(9)	
Hg - P2 - C41 = 114.4(14)	

All C-C-C angles were fixed at 120.0

Table 2.2

<u>Mean planes</u> <sup>a</sup>	<u>Free ligand</u> [43]	<u>(Ph<sub>3</sub>P)HgCl<sub>2</sub></u> [6]	<u>(Ph<sub>3</sub>P)<sub>2</sub>HgCl<sub>2</sub></u>	
			<u>P1</u>	<u>P2</u>
A-B	84.0°	84.4°	86.4°	91.8°
B-C	78.1°	80.1°	60.7°	88.5°
C-A	76.5°	75.4°	77.8°	89.6°

a - mean planes equations are given in Appendix A.3 for (Ph<sub>3</sub>P)<sub>2</sub>HgCl<sub>2</sub>

### 2.3 Crystallographic examination of (Cy<sub>3</sub>P)HgCl<sub>2</sub>

#### Crystal data:

C<sub>18</sub>H<sub>33</sub>Cl<sub>2</sub>HgP: M<sub>r</sub> = 551.93, Triclinic,

a = 10.8431(5), b = 14.1183(4), c = 14.7919(3) Å.

U = 2088.80 Å<sup>3</sup>, α = 94.7630(6) β = 80.3793(5),

γ = 110.6223(6)°, D<sub>m</sub> = 1.70 g cm<sup>-3</sup> (by flotation using CHCl<sub>3</sub>/CHBr<sub>3</sub>)

D<sub>c</sub> = 1.75 g cm<sup>-3</sup>, Z = 4 F(000) = 1080

μ(Mo - Kα) = 73.97 cm<sup>-1</sup>.

#### Space group:

Preliminary photographs did not distinguish between P $\bar{1}$  and P1, but subsequent analysis showed the centrosymmetric space group, P $\bar{1}$ , to be correct.

#### Data collection and structure refinement:

The data set used for this structure was collected on an Enraf Nonius Cad-4 diffractometer\*. Details of the data collection are given in Appendix A.5.

A colourless crystal, approximate dimensions, 0.30 x 0.25 x 0.30 mm was used for intensity measurements. 5116 unique reflections were collected of which 3563 had I/σ(I) ≥ 3.0 and were used for refinement. Correction for absorption effects have been made to the data along with corrections for Lorentz and polarisation effects. Common isotropic temperature factors were applied to the hydrogen atoms and refined to a final value of U = 0.115(8) Å<sup>2</sup>.

---

\* In collaboration with D L Hughes - Rothamsted Experimental Station

The weighting scheme adopted was:

$$w = 1.5221 / [\sigma^2(F_o) + 0.00031(F_o)^2] .$$

The final R values were  $R = 0.039$  and  $R' = 0.040$ . Final atomic and thermal parameters are listed in Table A.1.2 (Appendix A.1) and calculated/observed structure factors are given in Appendix A.2. Bond angles and distances are given in Table 2.3. The relevant mean planes data are contained in Appendix A.3.

### Description of structure

The structure consists of two independent dimers within the unit cell (Figure 2.3). Figure 2.4 shows the arrangement of the two dimer units in the unit cell and the two  $\text{Hg}_2\text{Cl}_2$  bridging units are found to be almost  $90^\circ$  to each other. Both independent mercury atoms lie in distorted tetrahedral environments with angles about mercury ranging from  $85.9(1)$  to  $132.0(1)^\circ$ , Hg1, and  $84.1(2)$  to  $139.6(2)^\circ$ , Hg2. The  $\text{Cy}_3\text{P}$  ligands are arranged mutually trans and the four-membered  $\text{Hg}_2\text{Cl}_2$  ring is planar and contains a centre of symmetry.

One of the main differences between the two dimer units is shown by the Hg-Cl bridging distances. The Hg(2) dimer contains a very symmetric bridging arrangement with Hg(2) - Cl(22) and Hg(2) - Cl(22') equal to  $2.642(4)$  and  $2.665(5)\text{\AA}$  respectively. In contrast the dimer containing Hg(1) has very asymmetrical bridging with  $2.559(3)$  [ Hg1 - Cl(12') ] and  $2.778(3)\text{\AA}$  Hg1 - Cl(12) .

The P - Hg - Cl<sub>terminal</sub> angles also differ between the two dimers, with values of  $132.0(1)$  [ P1 - Hg1 - Cl(11) ] and  $139.6(1)^\circ$  [ P2 - Hg2 - Cl(21) ] being found.

The cyclohexyl rings adopt the preferred chair conformation with all C-C-C-C torsion angles lying close to  $60^\circ$  (Appendix A.3).

**Figure 2.3** Molecular structure of  $(\text{Cy}_3\text{P})\text{HgCl}_2$

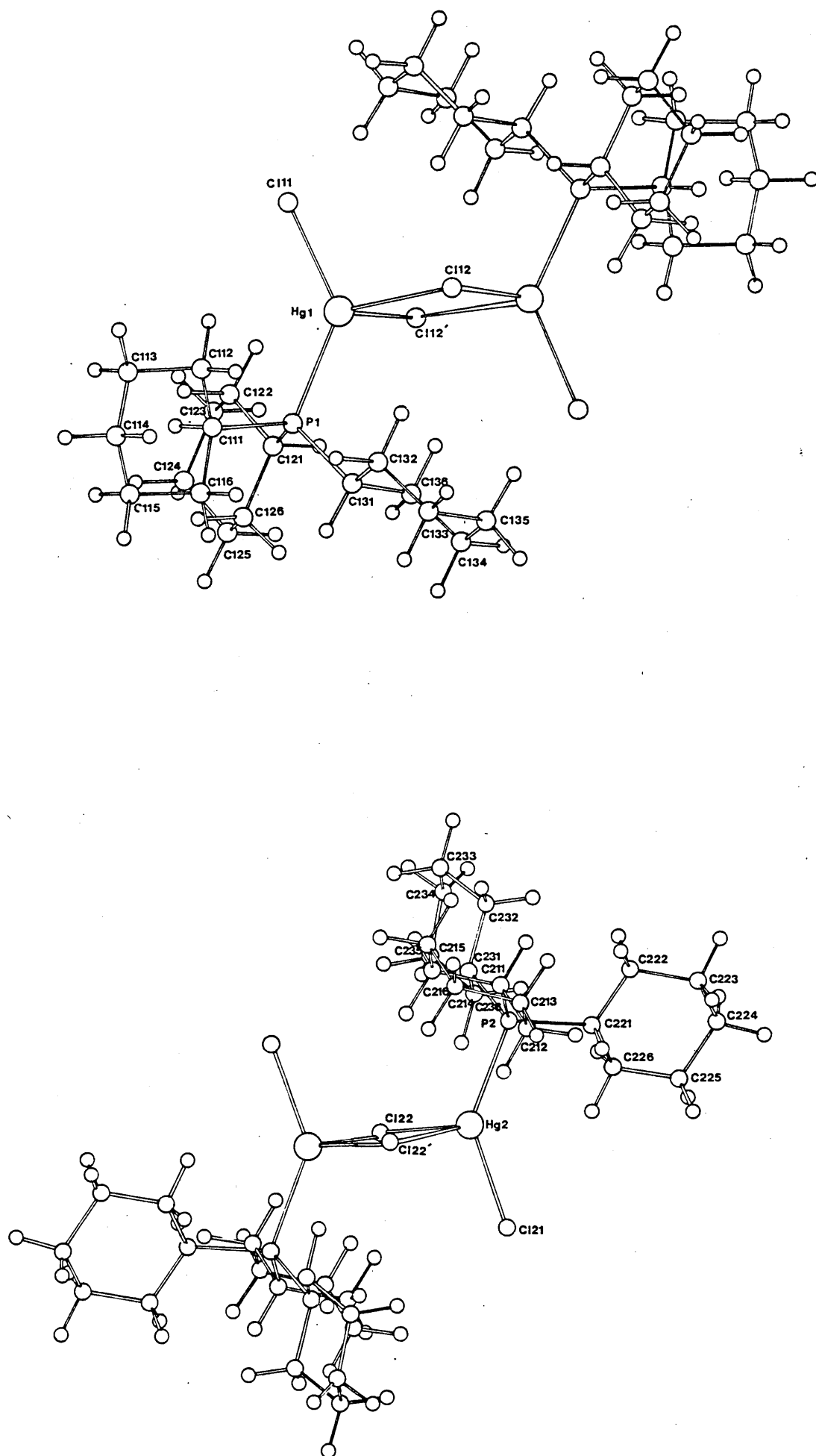


Figure 2.4  $(\text{Cy}_3\text{P})\text{HgCl}_2$  - arrangement of dimers in the unit cell

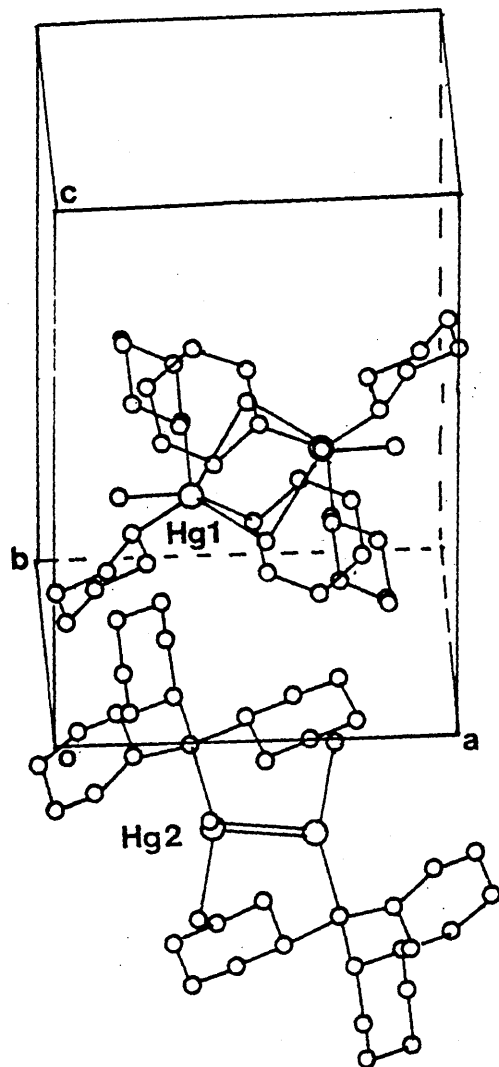


Table 2.3

Bond distances and angles for (Cy<sub>3</sub>P)HgCl<sub>2</sub> with estimated standard deviations

in parentheses

Symmetry code

none    x,    y,    z.

'        1-x, -y, 1-z.

"        1-x, -1-y, -z.

a) Bond lengths / Å

Hg1 - Cl(11) = 2.413(3)	Hg2 - Cl(21) = 2.391(5)
Hg1 - Cl(12) = 2.778(3)	Hg2 - Cl(22) = 2.642(4)
Hg1 - Cl(12') = 2.599(3)	Hg2 - Cl(22'') = 2.665(5)
Hg1 - P1 = 2.412(3)	Hg2 - P2 = 2.416(3)
P1 - C111 = 1.853(14)	P2 - C211 = 1.839(10)
P1 - C121 = 1.849(11)	P2 - C221 = 1.827(17)
P1 - C131 = 1.838(10)	P2 - C231 = 1.825(11)
C111- C112 = 1.537(15)	C211 - C212 = 1.559(16)
C112- C113 = 1.552(23)	C212 - C213 = 1.491(16)
C113- C114 = 1.508(22)	C213 - C214 = 1.480(24)
C114- C115 = 1.490(20)	C214 - C215 = 1.533(19)
C115- C116 = 1.513(22)	C215 - C216 = 1.530(16)
C116- C111 = 1.537(18)	C216 - C211 = 1.536(20)
C121- C122 = 1.494(15)	C221 - C222 = 1.481(20)
C122- C123 = 1.538(18)	C222 - C223 = 1.481(27)
C123- C124 = 1.492(23)	C223 - C224 = 1.412(23)
C124- C125 = 1.523(20)	C224 - C225 = 1.497(26)
C125- C126 = 1.519(18)	C225 - C226 = 1.464(30)
C126- C121 = 1.538(18)	C226 - C221 = 1.400(21)
C131- C132 = 1.491(18)	C231 - C232 = 1.521(17)
C132- C133 = 1.533(17)	C232 - C233 = 1.543(21)

C133 - C134 = 1.532(20)	C233 - C234 = 1.522(21)
C134 - C135 = 1.531(22)	C234 - C235 = 1.452(21)
C135 - C136 = 1.529(16)	C235 - C236 = 1.463(21)
C136 - C131 = 1.556(17)	C236 - C231 = 1.505(15)
Hg1 ---- Hg1' = 3.938(1)	Hg2 ---- Hg2'' = 3.774(1)

b) Bond angles /°

C1(11) - Hg1 - C1(12) = 106.1(1)	C1(21) - Hg2 - C1(22) = 95.2(2)
C1(11) - Hg1 - C1(12') = 101.5(1)	C1(21) - Hg2 - C1(22'') = 92.6(3)
C1(12) - Hg1 - C1(12') = 85.9(1)	C1(22) - Hg2 - C1(22'') = 84.1(2)
C1(11) - Hg1 - P1 = 132.0(1)	C1(21) - Hg2 - P2 = 139.6(2)
C1(12) - Hg1 - P1 = 99.8(1)	C1(22) - Hg2 - P2 = 111.8(1)
C1(12') - Hg1 - P1 = 120.3(1)	C1(22'') - Hg2 - P2 = 108.6(1)
Hg1' - C1(12) - Hg1 = 94.1(1)	Hg2'' - C1(22) - Hg2 = 95.9(1)
Hg1 - P1 - C111 = 112.2(4)	Hg2 - P2 - C211 = 110.2(4)
Hg1 - P1 - C121 = 108.0(4)	Hg2 - P2 - C221 = 107.4(5)
Hg1 - P1 - C131 = 111.0(5)	Hg2 - P2 - C231 = 112.1(4)
C111 - P1 - C121 = 105.5(6)	C211 - P2 - C221 = 107.5(6)
C111 - P1 - C131 = 110.9(5)	C211 - P2 - C231 = 107.8(5)
C121 - P1 - C131 = 108.7(5)	C221 - P2 - C231 = 111.8(6)
P1 - C111 - C112 = 112.9(10)	P2 - C211 - C212 = 110.1(8)
P1 - C111 - C116 = 115.0(8)	P2 - C211 - C216 = 112.7(8)
C111 - C112 - C113 = 108.5(12)	C211 - C212 - C213 = 111.8(10)
C112 - C113 - C114 = 110.5(11)	C212 - C213 - C214 = 113.6(12)
C113 - C114 - C115 = 111.7(12)	C213 - C214 - C215 = 111.1(12)
C114 - C115 - C116 = 113.0(14)	C214 - C215 - C216 = 111.7(11)
C115 - C116 - C111 = 110.6(22)	C215 - C216 - C211 = 110.5(11)
C116 - C111 - C112 = 109.3(10)	C216 - C211 - C212 = 109.6(9)

P1	-	C121	-	C122	=	110.8(7)	P2	-	C221	-	C222	=	119.5(11)
P1	-	C121	-	C126	=	111.7(8)	P2	-	C221	-	C226	=	119.6(13)
C121	-	C122	-	C123	=	111.6(9)	C221	-	C222	-	C223	=	114.3(13)
C122	-	C123	-	C124	=	111.5(11)	C222	-	C223	-	C224	=	117.9(15)
C123	-	C124	-	C125	=	112.0(16)	C223	-	C224	-	C225	=	115.4(17)
C124	-	C125	-	C126	=	112.0(10)	C224	-	C225	-	C226	=	113.5(15)
C125	-	C126	-	C121	=	109.5(14)	C225	-	C226	-	C221	=	120.4(16)
C126	-	C121	-	C122	=	112.9(11)	C226	-	C221	-	C222	=	116.4(14)

P1	-	C131	-	C132	=	110.9(7)	P2	-	C231	-	C232	=	114.5(9)
P1	-	C131	-	C136	=	109.6(7)	P2	-	C231	-	C236	=	113.4(9)
C131	-	C132	-	C133	=	111.2(1)	C231	-	C232	-	C233	=	109.4(13)
C132	-	C133	-	C134	=	111.7(11)	C232	-	C233	-	C234	=	111.6(14)
C133	-	C134	-	C135	=	108.5(14)	C233	-	C234	-	C235	=	111.4(13)
C134	-	C135	-	C136	=	113.3(11)	C234	-	C235	-	C236	=	112.6(14)
C135	-	C136	-	C131	=	109.1(10)	C235	-	C236	-	C231	=	109.6(11)
C136	-	C131	-	C132	=	111.5(12)	C236	-	C231	-	C232	=	110.4(10)

## 2.4 Spectroscopic studies of $(\text{Cy}_3\text{P})_n\text{HgX}_2$ complexes

(n = 1 or 2; X = Cl, Br or I).

### 2.4.1 $(\text{Cy}_3\text{P})_2\text{HgX}_2$

The structures of  $(\text{R}_3\text{P})_2\text{HgX}_2$  complexes are all tetrahedral monomers (Section 1.3.5), and the same structure is reasonably assumed for the  $\text{Cy}_3\text{P}$  complexes. On the basis of  $\text{C}_{2v}$  point group symmetry, the following modes are predicted:

$$\Gamma_{\text{int}} = 4A_1(\text{I.R.}, \text{Ra}) + A_2(\text{Ra}) + 2B_1(\text{I.R.}, \text{Ra}) + 2B_2(\text{I.R.}, \text{Ra})$$

$$\Gamma_{\text{Hg-X}} = A_1(\text{I.R.}, \text{Ra}) + B_1(\text{I.R.}, \text{Ra}).$$

$$\Gamma_{\text{Hg-P}} = A_1(\text{I.R.}, \text{Ra}) + B_2(\text{I.R.}, \text{Ra}).$$

The infrared spectrum is shown in Figure 2.5 while Table 2.4 contains the vibrational assignments. The infrared assignments for the chloride are in good agreement with previous suggestions [37], with the  $\text{Hg-Cl}$   $A_1$  and  $B_1$  modes located at 209 and 197  $\text{cm}^{-1}$ . These results are consistent with the Raman spectral assignments [37]. Raman spectra of the bromide and iodide complexes show [37]  $\text{Hg-X}$  at 144, 132  $\text{cm}^{-1}$  (bromide) and 103  $\text{cm}^{-1}$  (iodide).

The average position of the  $\text{Hg-Cl}$  modes can be correlated to the magnitude of the Hg-Cl bond lengths and the P-Hg-P angles as explained in Section 1.3.5. In the case of  $(\text{Cy}_3\text{P})_2\text{HgCl}_2$  the average position of the  $\text{Hg-Cl}$  infrared modes is close to that of  $(\text{Bu}^n_3\text{P})_2\text{HgCl}_2$  (Table 2.5). This implies that  $(\text{Cy}_3\text{P})_2\text{HgCl}_2$  has similar Hg-Cl bond lengths and P-Hg-P angle to  $(\text{Bu}^n_3\text{P})_2\text{HgCl}_2$ . This in turn suggests that the  $\text{Cy}_3\text{P-Hg}$  and  $\text{Bu}_3\text{P-Hg}$  interactions in these complexes are of similar magnitude.

Figure 2.5 Infrared spectrum of  $(\text{Cy}_3\text{P})_2\text{HgCl}_2$  ca. 300K.

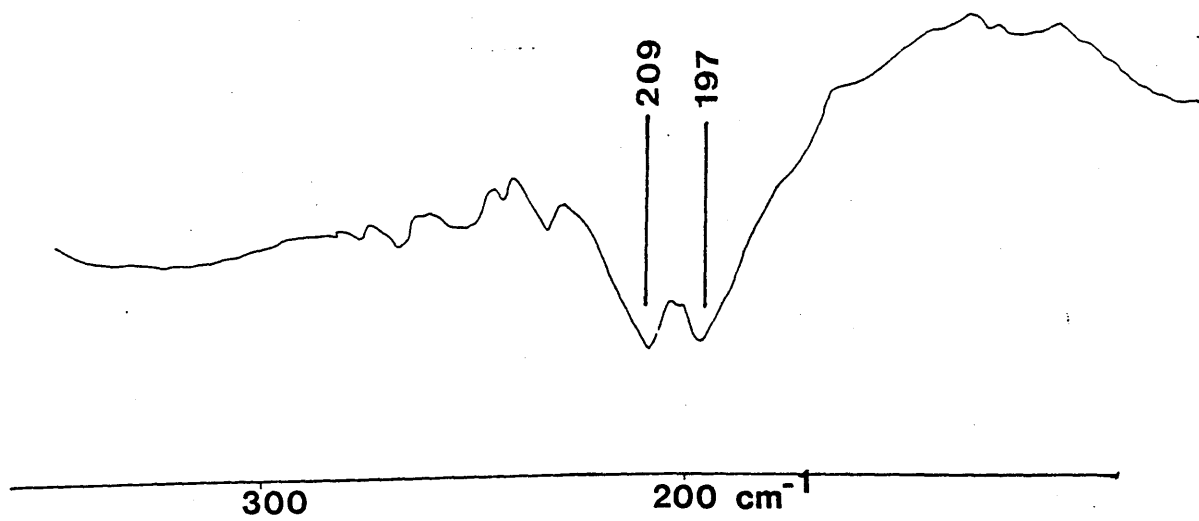


Figure 2.6 Infrared spectrum of  $(\text{Cy}_3\text{P})\text{HgCl}_2$  ca. 300K.

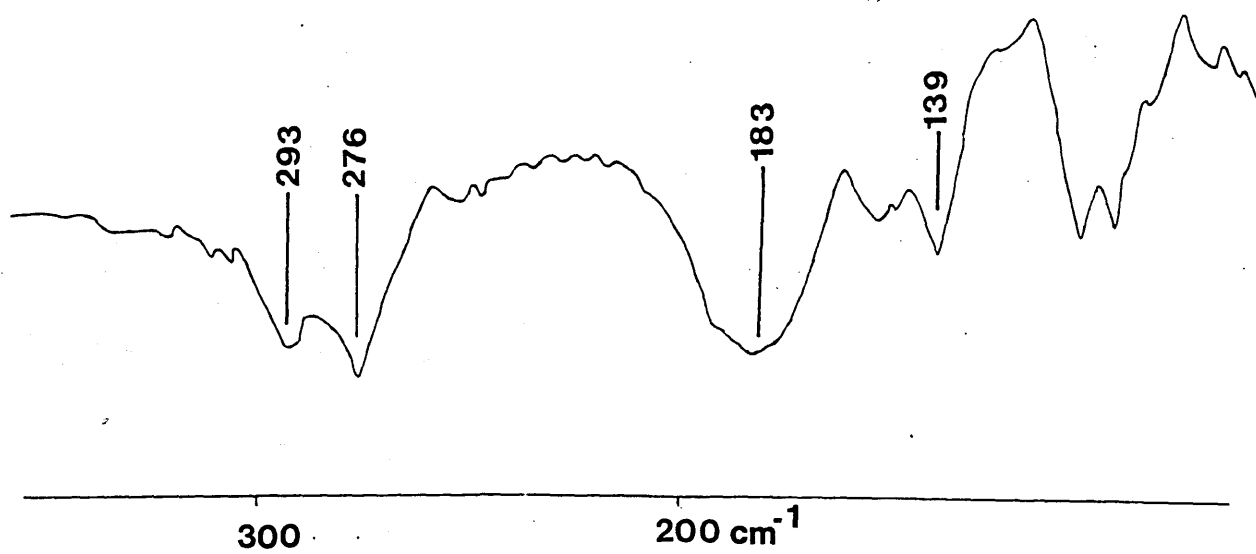


Table 2.4

Vibrational assignments for  $(\text{Cy}_3\text{P})_2\text{HgX}_2$  (X = Cl, Br or I) ( $\text{cm}^{-1}$ ).

Cl		Br		I		Assignments
I.R.	Ra	I.R.	Ra	I.R.	Ra	
209	208*		144*		103*	$\nu_s(\text{Hg-X})$
197	187*		132*			$\nu_a(\text{Hg-X})$
	134*				132*	$\nu_s(\text{Hg-P})$
					128*	$\nu_a(\text{Hg-P})$

\* Literature values

Table 2.5

Relationship between the Hg-Cl bond lengths and P-Hg-P angles  
of  $(R_3P)_2HgCl_2$  complexes with  $\tilde{\nu}(\text{Hg-Cl})$  mode band positions.

Complex	$\tilde{\nu}(\text{Hg-Cl})/\text{cm}^{-1}$ *	$d(\text{Hg-Cl})^*$ /Å	P-Hg-P angle/ $^\circ$
$(\text{Bu}_3\text{P})_2\text{HgCl}_2$	205	2.60	139
$(\text{Cy}_3\text{P})_2\text{HgCl}_2$	203	no structure obtained	
$(\text{Et}_3\text{P})_2\text{HgCl}_2$	176	2.68	158.5

\* Average values

### 2.4.2 $(\text{Cy}_3\text{P})\text{HgX}_2$

The structure of  $(\text{Cy}_3\text{P})\text{HgCl}_2$  consists of two independent centrosymmetric dimers per unit cell with no significant interaction between them (Section 2.3). A  $C_{2h}$  point group treatment can thus be applied as for  $(\text{Et}_3\text{P})\text{CdI}_2$  (Appendix A.4), and for each dimer the following modes are predicted:

$$\Gamma_{\text{tot}} = 7A_g + 5B_g + 4A_u + 8B_u$$

$$\Gamma_{\text{as}}(\text{Hg-Cl})_t = A_g(\text{Ra}) + B_u(\text{I.R.})$$

$$\Gamma_{\text{as}}(\text{Hg-P}) = A_g(\text{Ra}) + B_u(\text{I.R.})$$

$$\Gamma_{\text{as}}(\text{Hg-Cl})_b = A_g(\text{Ra}) + B_g(\text{Ra}) + A_u(\text{I.R.}) + B_u(\text{I.R.})$$

Thus  $1\Gamma_{\text{as}}(\text{Hg-Cl})_t$  band and two  $\Gamma_{\text{as}}(\text{Hg-Cl})_b$  bands in each of the infrared and Raman spectra (mutually exclusive) are predicted for each dimer unit. The spectra are shown in Figure 2.6 and Table 2.6 contains the vibrational assignments.

The two infrared bands in the spectrum of  $(\text{Cy}_3\text{P})\text{HgCl}_2$  at 293 and 276  $\text{cm}^{-1}$  are unquestionably both  $\Gamma_{\text{as}}(\text{Hg-Cl})_t$  modes, but since only one such mode is allowed for a simple dimer, they must each be due to one of the different dimers present. An analogous argument obtains for the two Raman bands observed at 282 and 272  $\text{cm}^{-1}$ . Evidently, the 293 and 282  $\text{cm}^{-1}$  bands are respectively the antisymmetric ( $B_u$ ) and symmetric ( $A_g$ )  $\Gamma_{\text{as}}(\text{Hg-Cl})_t$  modes of the dimer having the shorter Hg-Cl<sub>t</sub> bonds (2.391 $\text{\AA}$ ), while the 276  $\text{cm}^{-1}$  ( $B_u$ ) and 272  $\text{cm}^{-1}$  ( $A_g$ ) bands are  $\Gamma_{\text{as}}(\text{Hg-Cl})_t$  of the other dimer (Hg-Cl<sub>t</sub> bonds of 2.413 $\text{\AA}$ ). It is in many respects remarkable that the separate dimers can be observed from the spectra, but there is no other plausible alternative.

The  $\nu(\text{Hg-Cl})_b$  modes are more difficult to interpret in this way as they appear as very broad bands at ca.  $183 \text{ cm}^{-1}$  (I.R.) and 186 and  $147 \text{ cm}^{-1}$  (Ra). This failure to identify  $\nu(\text{Hg-Cl})_b$  bands characteristic of the individual dimers is somewhat surprising in view of the above, particularly because the bridging arrangements in the two dimers are distinctly different (see Section 2.3).

The previous interpretation of the spectra of  $(\text{Cy}_3\text{P})\text{HgCl}_2$  [ 37 ] was in terms of an assumed non-centrosymmetric dimeric structure; the four bands observed ( $283, 273 \text{ cm}^{-1}$  (I.R.) and  $282, 270 \text{ cm}^{-1}$  (Ra) ) were assigned as  $\nu(\text{Hg-Cl})_t$  modes from the same dimer unit. However with the knowledge of the true structure, it is now clear that this interpretation is erroneous. This demonstrates quite vividly the dangers of making structural deductions without a suitable crystallographically determined base.

The infrared spectrum of  $(\text{Cy}_3\text{P})\text{HgBr}_2$  contains one  $\nu(\text{Hg-Br})_t$  band at  $194 \text{ cm}^{-1}$  and a  $\nu(\text{Hg-Br})_b$  mode at  $139 \text{ cm}^{-1}$ . These are in the positions expected for a centrosymmetric dimeric structure as exemplified, for example, by  $(\text{Ph}_3\text{P})\text{HgBr}_2$  (corresponding bands at  $190$  and  $137 \text{ cm}^{-1}$ , [ 14 ] ). The Raman spectrum similarly is indicative of a simple centrosymmetric dimeric structure, with  $\nu(\text{Hg-Br})_t A_g$  at  $180$  and  $\nu(\text{Hg-Br})_b A_g$  at  $141 \text{ cm}^{-1}$  [ 37 ] .

The Raman bands for the iodide derivative have been reported [ 37 ] and are indicative of a structure analogous to the bromide complex. Assignment of  $\nu(\text{Hg-P})$  modes is not unambiguous but common bands appear to be found in the range  $137 - 146 \text{ cm}^{-1}$  in the Raman spectra (all three complexes) and at  $139 \text{ cm}^{-1}$  in the infrared spectra (Cl, Br).

In conclusion, the spectrum of  $(\text{Cy}_3\text{P})\text{HgCl}_2$  demonstrates the existence of two independent dimers in the unit cell whereas the spectra of the bromide and iodide complexes are readily interpreted in terms of a simple centrosymmetric dimeric structure.

Table 2.6

Vibrational assignments for  $(\text{Cy}_3\text{P})\text{HgX}_2$  complexes (X = Cl, Br or I)

$(\text{cm}^{-1})$

Cl		Br		I	Assignments
I.R.	*Ra	I.R.	*Ra	*Ra	
293 } 276 }		194			$\sim(\text{Hg-X})_{\text{t}} \text{B}_{\text{u}}$
	282 } 272 }		180	154	$\sim(\text{Hg-X})_{\text{t}} \text{A}_{\text{g}}$
183		139 <sup>**</sup>			$\sim(\text{Hg-X})_{\text{b}} \text{A}_{\text{u}}$ and $\text{B}_{\text{u}}$
	186 } 147 }		141 <sup>**</sup>	104	$\sim(\text{Hg-X})_{\text{b}} \text{A}_{\text{g}}$ and $\text{B}_{\text{g}}$
139		139 <sup>**</sup>			$\sim(\text{Hg-P}) \text{B}_{\text{u}}$
	146		141 <sup>**</sup>	137	$\sim(\text{Hg-P}) \text{A}_{\text{g}}$

\* Literature values [37], reassigned for the chloride in the present work

\*\* Accidental coincidence.

CHAPTER 3

CRYSTALLOGRAPHIC STUDIES OF SELECTED CADMIUM (II)

HALIDE COMPLEXES  $(R_3P)CdX_2$  [  $R_3P = Et_3P, Cy_3P, Me_2PhP;$

$X = Cl, Br \text{ or } I$  ]

## Contents

	<u>Page</u>
3.1 Introduction	70
3.2 Crystallographic examination of $(\text{Me}_2\text{PhP})\text{CdX}_2$ complexes (X = Cl, Br and I).	71
3.3 Crystallographic examination of $(\text{Et}_3\text{P})\text{CdI}_2$ .	81
3.4 Crystallographic examination of $\alpha - (\text{Cy}_3\text{P})\text{CdCl}_2$ .	88

### 3.1 Introduction

Crystallographic studies reported for  $(L)CdX_2$  [ L = neutral unidentate ligand and X = Cl, Br or I ], indicate that these complexes attain some degree of extension from the monomer unit by halogen-bridging. The ligands containing nitrogen-, oxygen- and sulphur- donor atoms all tend to give a double-chain arrangement (section 1.4.2), with the exception of (pyridine-N-oxide) $CdI_2$ , which forms a polymeric pentaco-ordinate cadmium structure (section 1.4.2, Figure 1.9). However the 1:1 stoichiometric complexes of the type  $(R_3P)CdX_2$  have not been structurally studied in a systematic manner.

The structural work reported has been mostly spectroscopic and suggests that the complexes are halogen-bridged dimers. It was decided systematically to study the crystal and molecular structures of selected  $(R_3P)CdX_2$  complexes in order to examine the factors influencing the types of structure adopted in the solid-state. In addition, it was hoped that these crystallographic studies would provide a sound basis for interpretation of spectroscopic data for such complexes.

### 3.2 Crystallographic examination of $(\text{Me}_2\text{PhP})\text{CdX}_2$ complexes

[ X = Cl, Br and I ]

#### Crystal data:

The three complexes are isostructural and the crystal data are summarised in Table 3.1.a.

#### Data collection and structure refinement:

The relevant parameters for data collection are listed in Table 3.1.b. The crystals for all three compounds were mounted with their a-axes coincident with the rotation ( $\omega$ )-axis of a Stoe Stadi 2 two-circle diffractometer. Data were collected using the background-  $\omega$  scan- background technique, Lorentz and polarisation corrections were applied and corrections were also made for absorption effects. Those reflections having  $I/\sigma(I)$  greater than the indicated value were considered to be observed. The relevant parameters concerned with structure refinement are listed in Table 3.1.c. The positions of the cadmium atoms were determined from the three-dimensional Patterson function for all three compounds. The remaining non-hydrogen atoms were located from successive difference electron-density maps. Scattering factors were calculated [ 42 ] using an analytical approximation. Hydrogen atoms were included in ideal positions calculated to give  $\text{C-H} = 1.08\text{\AA}$ . Common isotropic temperature factors were applied to methyl and phenyl hydrogen atoms and refined to the final values of  $U$  given in Table 3.1.c.

Table 3.1

Crystal data and details of data collection for  $(\text{Me}_2\text{PhP})\text{CdX}_2$

complexes [X = Cl, Br and I].

a) <u>Crystal data</u>	<u><math>(\text{Me}_2\text{PhP})\text{CdCl}_2</math></u>	<u><math>(\text{Me}_2\text{PhP})\text{CdBr}_2</math></u>	<u><math>(\text{Me}_2\text{PhP})\text{CdI}_2</math></u>
$M_r$	321.5	410.36	504.07
Crystal system	Monoclinic	Monoclinic	Monoclinic
$a/\text{\AA}$	7.057(5)	7.361(8)	7.839(8)
$b/\text{\AA}$	12.471(7)	12.599(7)	12.868(7)
$c/\text{\AA}$	12.905(8)	13.012(6)	13.526(8)
$\alpha/^\circ$	90.00	90.00	90.00
$\beta/^\circ$	93.08(5)	93.18(5)	94.17(6)
$\gamma/^\circ$	90.00	90.00	90.00
$U/\text{\AA}^3$	1134.17	1204.84	1360.83
$D_m/\text{g cm}^{-3}$	1.90	2.39	2.46
$D_c/\text{g cm}^{-3}$	1.88	2.26	2.46
Z	4	4	4
F(000)	624	768	912
$\mu(\text{Mo-K})/\text{cm}^{-1}$	23.0	82.7	57.0
Space group	$P2_1/n$	$P2_1/n$	$P2_1/n$
	(non standard settings of $P2_1/c$ )		

b) Collection of intensity data

size of crystal/mm	0.10x0.10x0.10	0.40x0.14x0.18	0.41x0.23x0.2
number of reflections collected	3314	3107	3651
number of reflections observed	2820	1783	2262
number of layers collected	10(0k1+9k1)	11(0k1+10k1)	11(0k1+10k1)
$I/\sigma(I)$	3.0	3.0	4.0

c) Refinement data

	<u>(Me<sub>2</sub>PhP)CdCl<sub>2</sub></u>	<u>(Me<sub>2</sub>PhP)CdBr<sub>2</sub></u>	<u>(Me<sub>2</sub>PhP)CdI<sub>2</sub></u>
U(methyl)/Å <sup>o2</sup>	0.170(30)	0.127(28)	0.154(60)
U(phenyl)/Å <sup>o2</sup>	0.157(10)	0.111(28)	0.125(50)

weighting scheme

values:-

<u>a</u>	1.0000	1.5319	1.0000
<u>b</u>	0.0086	0.0034	0.0180
R	0.037	0.067	0.098
R'	0.047	0.074	0.105

The weighting scheme adopted was:

$$w = \underline{a} / [ \sigma^2(F_o) + \underline{b}(F_o)^2 ]$$

The relevant a and b values are contained in Table 3.1.c.

The three structures were refined with full matrix refinement with anisotropic temperature factors for all non-hydrogen atoms.

The final R and R' values are listed in Table 3.1.c. The final atomic and thermal parameters are listed in Tables A.1.3 to A.1.5 (Appendix A.1) and calculated and observed structure factors are contained in Appendix A.2. Bond angles and distances are given in Table 3.2.

#### Description of the structures:

The three complexes have similar structures (Figure 3.1), consisting of a halogen-bridged polymeric arrangement, in which the cadmium atom is pentaco-ordinate. The cadmium atoms lie in distorted trigonal bipyramidal environments, with two relatively short Cd-X bonds [ X = Cl 2.481(1), 2.497(1); X = Br 2.569(2), 2.603(2); X = I 2.786(2), 2.759(2) Å ] and a short Cd-P bond [ 2.560(1) Å for X = Cl, 2.531(4) Å for X = Br and 2.553(4) Å for X = I ], lying in the equatorial positions. The two apical positions are taken up by two longer Cd-X contacts [ 2.745(1), 2.734(1) Å for X = Cl; 2.914(2), 2.918(2) Å for X = Br; 3.242(2), 3.201 Å for X = I ]. The cadmium atoms are essentially coplanar with P, X1 and X2; the deviations from the mean plane are listed in Appendix A.3, with the largest derivation being 0.019(10) Å. The trigonal arrangement around the central cadmium atom however, is distorted with angles ranging from 110.50(2), 111.3(1), 112.3(1)° [ X1 - Cd - X2 for X = Cl, Br and I respectively ] to 130.00(4), 126.9(1),

125.3(1)<sup>o</sup> [ X1 - Cd - P for X = Cl, Br and I respectively ] .

The angle between the two apical contacts X1' - Cd - X2'' is close to linearity at 178.60(4), 178.8(1) and 177.2(1)<sup>o</sup> for the chloride, bromide and iodide complexes respectively.

The phenyl rings are twisted out of the Cd, P, X1, X2 mean plane by 51.9<sup>o</sup>, 49.4<sup>o</sup> and 49.8<sup>o</sup> for the chloride, bromide and iodide complexes respectively, presumably to minimise steric interactions within the chain.

There are two polymeric chains per unit cell running parallel to the a-axis, (Figure 3.2). Similar packing arrangements are found in the bromide and iodide complexes.

The resulting crystal structures are quite different from the arrangements found in other (L)CdX<sub>2</sub> systems [ Figure 1.7, Section 1.4.2 ]. Although the pyridine-N-oxide complex [ 21 ] (Section 1.4.2, Figure 1.9) contains single chains, these involve both halogen and ligand atoms in the bridging unit.

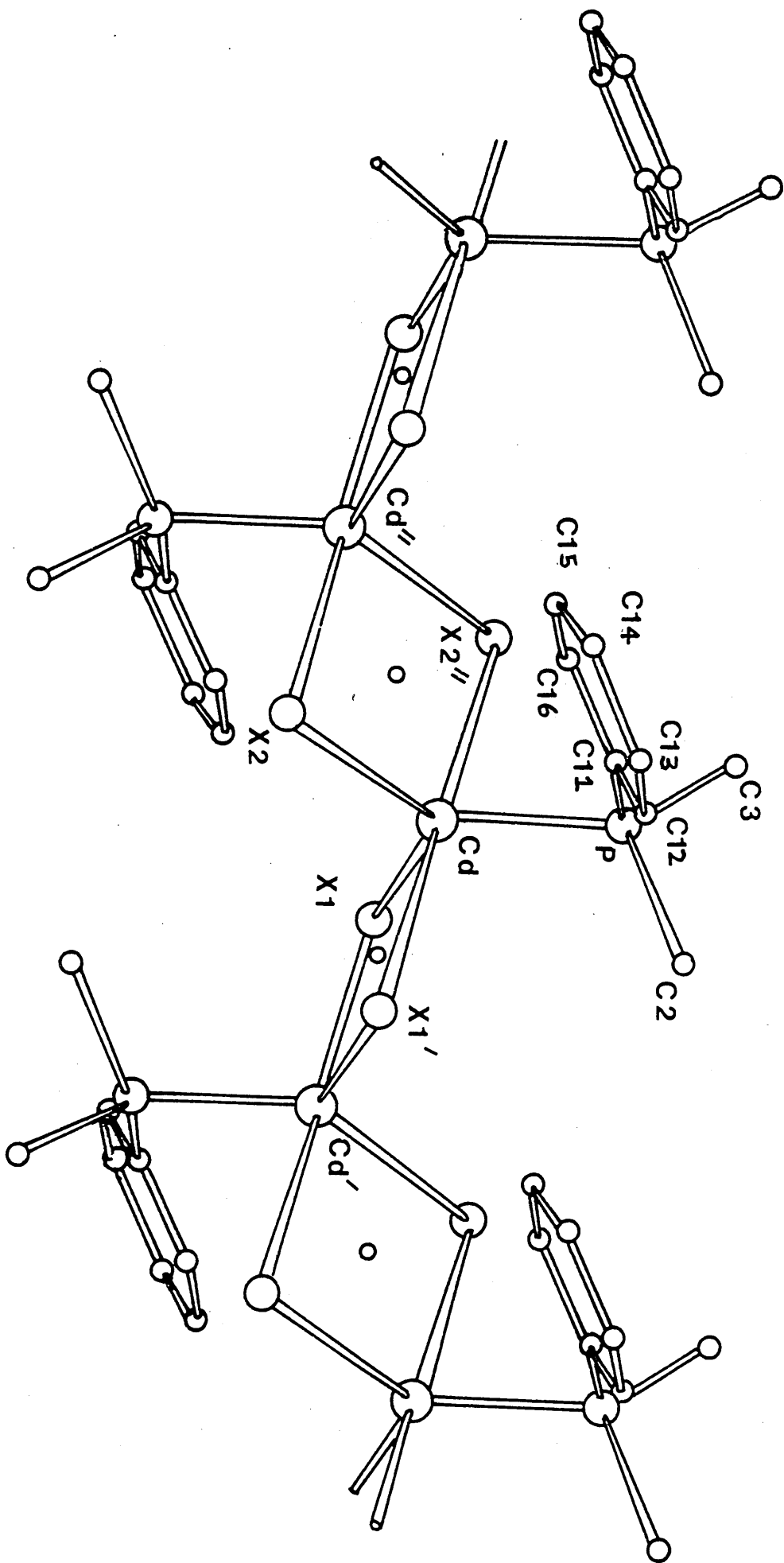


Figure 3.2 The Crystal structure of  $(\text{Me}_2\text{PhP})\text{CdCl}_2$

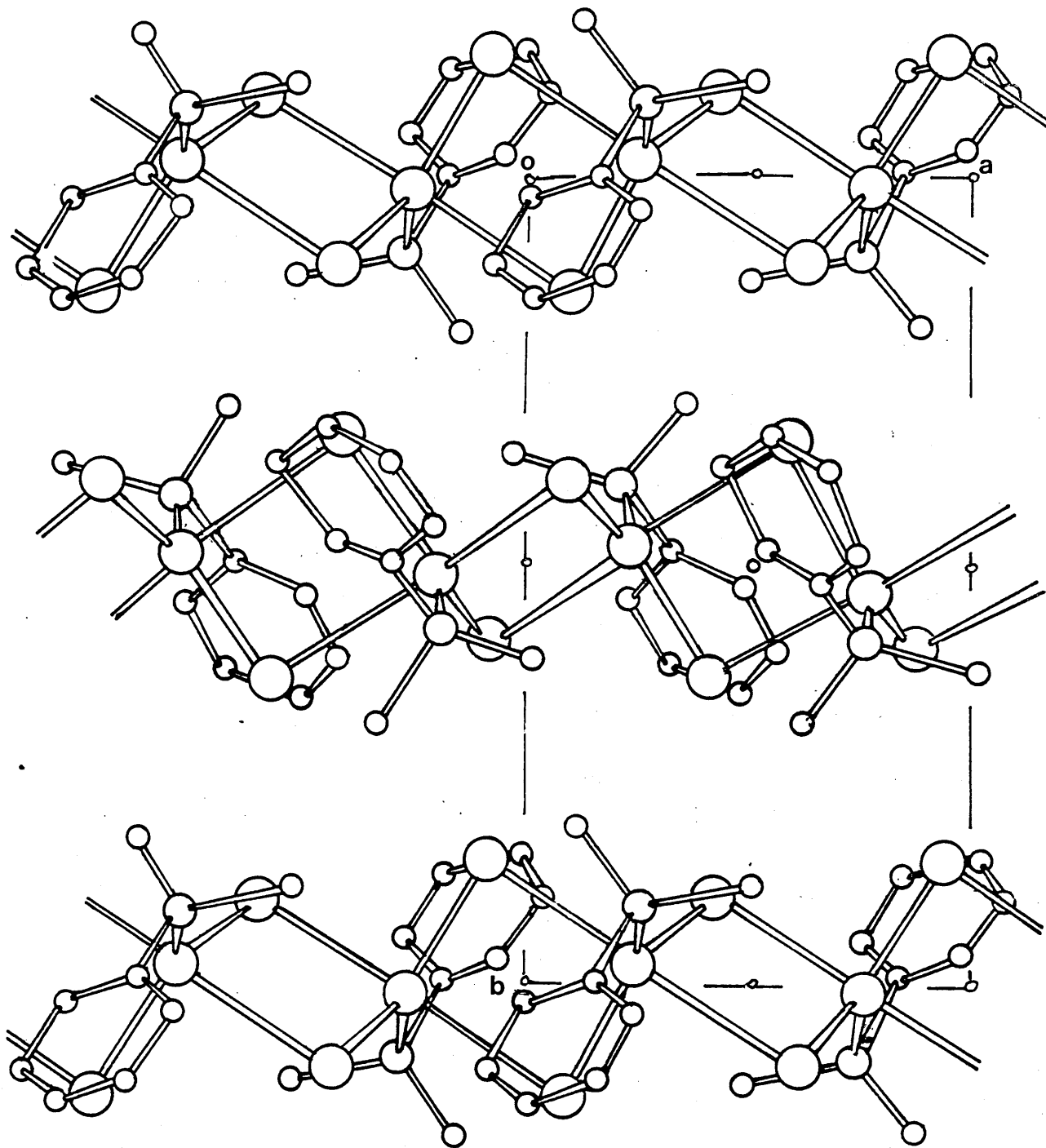


Table 3.2

Bond distances and angles for  $(Me_2PhP)CdX_2$  structures

[X = Cl, Br and I] with standard deviations in parentheses.

a) Symmetry code:

	<u>Cl</u>	<u>Br</u>	<u>I</u>
None	x, y, z	x, y, z	x, y, z
'	-x, -y, -z	2 <sup>o</sup> -x, -y, 1.0-z	-x, -y, 1.0-z
''	1.0-x, -y, -z	1.0-x, -y, 1.0-z	1.0-x, -y, 1.0-z

b) Metal co-ordination:

Bond lengths/Å :

<u>X</u>	<u>Cl</u>	<u>Br</u>	<u>I</u>
Cd - X1	2.481(1)	2.569(2)	2.768(2)
Cd - X2	2.497(1)	2.603(2)	2.759(2)
Cd- X1'	2.745(1)	2.914(2)	3.242(2)
Cd - X2''	2.734(1)	2.918(2)	3.201(2)
Cd - P	2.560(1)	2.531(4)	2.553(4)
Cd - Cd'	3.826(1)	3.952(1)	4.138(1)
Cd - Cd''	3.826(1)	4.868(1)	4.138(1)

Bond angles/ $^{\circ}$ 

<u>X</u>	<u>Cl</u>	<u>Br</u>	<u>I</u>
X1 - Cd - X2	110.50(2)	111.3(1)	112.3(1)
X1 - Cd - X1'	86.00(2)	88.0(1)	90.9(1)
X1 - Cd - X2''	92.60(2)	91.7(1)	114.4(1)
X1 - Cd - P	130.00(4)	126.9(1)	125.3(1)
X2 - Cd - X1'	93.40(2)	92.4(1)	89.6(1)
X2 - Cd - X2''	87.10(2)	88.8(1)	92.4(1)
X2 - Cd - P	119.50(3)	121.8(1)	122.5(1)
X1' - Cd - X2''	178.60(4)	178.8(1)	177.2(1)
X1' - Cd - P	88.70(2)	88.1(1)	89.2(1)
X2'' - Cd - P	92.20(1)	91.2(1)	77.9(1)
Cd - P - Cl1	108.90(10)	109.9(5)	110.4(6)
Cd - P - C2	115.50(20)	115.4(7)	116.4(6)
Cd - P - C3	115.70(30)	114.4(7)	116.2(10)
Cd - X1 - Cd'	94.0(1)	92.0(1)	89.1(1)
Cd - X2 - Cd''	92.9(1)	91.2(1)	87.6(1)

c) Ligand co-ordination:Bond lengths/Å

<u>X</u>	<u>Cl</u>	<u>Br</u>	<u>I</u>
P - Cl1	1.825(5)	1.811(15)	1.784(20)
P - C2	1.815(6)	1.787(20)	1.843(22)
P - C3	1.803(7)	1.808(16)	1.764(27)
Cl1 - Cl2	1.384(7)	1.390(21)	1.412(27)
Cl1 - Cl6	1.373(7)	1.361(22)	1.406(40)
Cl2 - Cl3	1.394(10)	1.399(30)	1.393(40)
Cl3 - Cl4	1.350(11)	1.311(32)	1.321(50)
Cl4 - Cl5	1.384(20)	1.407(26)	1.399(39)
Cl5 - Cl6	1.391(9)	1.392(25)	1.374(37)

## Bond angles/°

<u>X</u>	<u>C1</u>	<u>Br</u>	<u>I</u>
C11 - P - C2	105.8(3)	108.2(8)	104.1(10)
C11 - P - C3	106.8(3)	105.0(8)	106.4(12)
C2 - P - C3	103.7(4)	103.3(10)	102.0(14)
P - C11 - C12	123.3(5)	123.6(13)	128.2(21)
P - C11 - C16	117.4(4)	117.2(11)	119.2(13)
C12 - C11 - C16	119.2(5)	119.1(15)	112.7(22)
C11 - C12 - C13	119.1(6)	118.0(19)	124.2(30)
C12 - C13 - C14	122.4(6)	123.7(20)	119.3(22)
C13 - C14 - C15	119.8(6)	118.9(19)	120.8(27)
C14 - C15 - C16	119.1(6)	118.6(18)	119.4(32)
C15 - C16 - C11	121.1(5)	121.6(15)	123.6(23)

### 3.3 Crystallographic examination of (Et<sub>3</sub>P)CdI<sub>2</sub>

#### Crystal data:

C<sub>6</sub>H<sub>15</sub>CdI<sub>2</sub>P:                      M<sub>r</sub> = 484.37,                      Monoclinic,  
a = 8.462(4),                      b = 10.114(5),                      c = 15.563(8)Å.  
U = 1326.57Å<sup>3</sup>,                      α = 90.00,                      β = 95.20(5),  
γ = 90.00°                      D<sub>m</sub> = 2.39g cm<sup>-3</sup> (by flotation using CHCl<sub>3</sub>/CHI<sub>3</sub>),  
D<sub>c</sub> = 2.42g cm<sup>-3</sup>,                      Z = 4,                      F(000) = 1074  
μ(Mo - Kα) = 72.96cm<sup>-1</sup>.

#### Systematic absences:

0k0 reflections are absent for k = 2n + 1

h0l    "                      "                      "                      "                      l = 2n + 1

#### Space group:

P 2<sub>1</sub>/c

#### Data collection and structure refinement

A crystal of dimensions 0.50 x 0.32 x 0.24 mm was mounted about b and 15 layers h 0l — h 14 l were collected. A total of 3736 unique reflections were recorded of which 2941 had I/σ(I) > 3.0 and were used for structural analysis. The corrections for absorption effects have been made, along with corrections for Lorentz and polarisation effects. Common isotropic temperature factors were applied to the 'CH<sub>3</sub>' and 'CH<sub>2</sub>' hydrogens of the ethyl groups, refining to final values of U = 0.084(16) and 0.1474Å<sup>2</sup> respectively. The weighting scheme adopted was:

$$w = 1.000 / [\sigma^2(F_o) + 0.028446 (F_o)^2] .$$

The final R values were  $R = 0.0751$  and  $R' = 0.0824$ . Final atomic and thermal parameters are listed in Table A.1.4 (Appendix A.1) and calculated/observed structure factors are contained in Appendix A.2. Bond angles and distances are given in Table 3.3.

Description of structure:

The structure consists of discrete iodine-bridged dimers (Figure 3.3). Cadmium lies in a distorted tetrahedral environment with angles about cadmium ranging from  $97.3(1)$  to  $116.4(1)^\circ$ . The  $\text{Et}_3\text{P}$  ligands are arranged mutually trans to each other, and there is a centre of symmetry at the centre of the planar four-membered ring  $[\text{Cd}, \text{I}(1'), \text{Cd}', \text{I}(1)]$ . The Cd-I bridge distances are almost equal at  $2.862(1)$  and  $2.878(1)\text{\AA}$ . This is the first cadmium halogen-bridged dimer structure that has been fully authenticated by single crystal X-ray analysis. There is no further extension beyond the dimer stage (Figure 3.4) with the closest Cd-I distance being greater than  $4\text{\AA}$ .

The geometry of  $(\text{Et}_3\text{P})\text{CdI}_2$  is very similar to that of  $\text{Cd}_2\text{I}_6^{2-}$  anions in the salts  $\text{Cd}_2\text{N}(\text{CH}_2\text{CH}_2\text{NMe}_2)_3\text{I}_4$  (I) [44] and  $[\text{Sb}(\text{Bu}_2\text{dte})_2]^+$   $\text{Cd}_2\text{I}_6^{2-}$  [45]. The  $\text{Cd}_2\text{I}_6^{2-}$  anion forms an iodine-bridged dimer structure with Cd-I<sub>t</sub> bond lengths similar to those in  $(\text{Et}_3\text{P})\text{CdI}_2$  [  $2.704(1)$  and  $2.693(1)\text{\AA}$  for (I) compared with  $2.701(1)$  for  $(\text{Et}_3\text{P})\text{CdI}_2$  ]. The bridging distances are very similar [  $2.865(1)$ ,  $2.849(1)$  for (I);  $2.862(1)$ ,  $2.878(1)\text{\AA}$  for  $(\text{Et}_3\text{P})\text{CdI}_2$  ]. The angles around Cd in  $(\text{Et}_3\text{P})\text{CdI}_2$  and (I) are similar [ from  $97.3(1)$  for  $\text{I1} - \text{Cd} - \text{I1}'$  to  $116.4(1)^\circ$  for  $\text{I2} - \text{Cd} - \text{P}$  in the case of  $(\text{Et}_3\text{P})\text{CdI}_2$ , with the corresponding angles for (I) being  $98.9(4)$  to  $121.6(4)^\circ$  ].

The  $\text{Et}_3\text{P}$  ligand attains the conformation whereby the  $\beta$ - carbons of the ethyl groups are skew (C32), anti (C12), skew (C22) with respect to the cadmium atom (Figure 3.5), and is similar to that seen in other  $\text{Et}_3\text{P}$  metal complexes [46, 47, 48].

$(\text{Et}_3\text{P})\text{CdI}_2$  thus has a different type of structural arrangement to that found in  $(\text{Me}_2\text{PhP})\text{CdI}_2$ . The cadmium atoms attain tetra-coordinate and penta-coordinate environments in the  $\text{Et}_3\text{P}$  and the  $\text{Me}_2\text{PhP}$  complexes respectively. In  $(\text{Et}_3\text{P})\text{CdI}_2$  there is a short terminal Cd-I bond of  $2.701(1)\overset{\circ}{\text{A}}$  and two longer Cd-I distances of  $2.862(1)$  and  $2.878(1)\overset{\circ}{\text{A}}$ . In  $(\text{Me}_2\text{PhP})\text{CdI}_2$  there is strictly no 'terminal' Cd-I bond, two slightly longer Cd-I bond lengths of  $2.759(2)$  and  $2.768(2)\overset{\circ}{\text{A}}$  form a trigonal arrangement (with the phosphorus atom) around cadmium. In  $(\text{Me}_2\text{PhP})\text{CdI}_2$ , the  $\text{PCdI}_2$  units are joined together by two longer Cd-I interactions of  $3.201(2)$  and  $3.242(2)\overset{\circ}{\text{A}}$  which are longer than the bridging distances in the dimeric  $(\text{Et}_3\text{P})\text{CdI}_2$  structure.

Figure 3.3 The Molecular structure of  $(Et_3P)CdI_2$

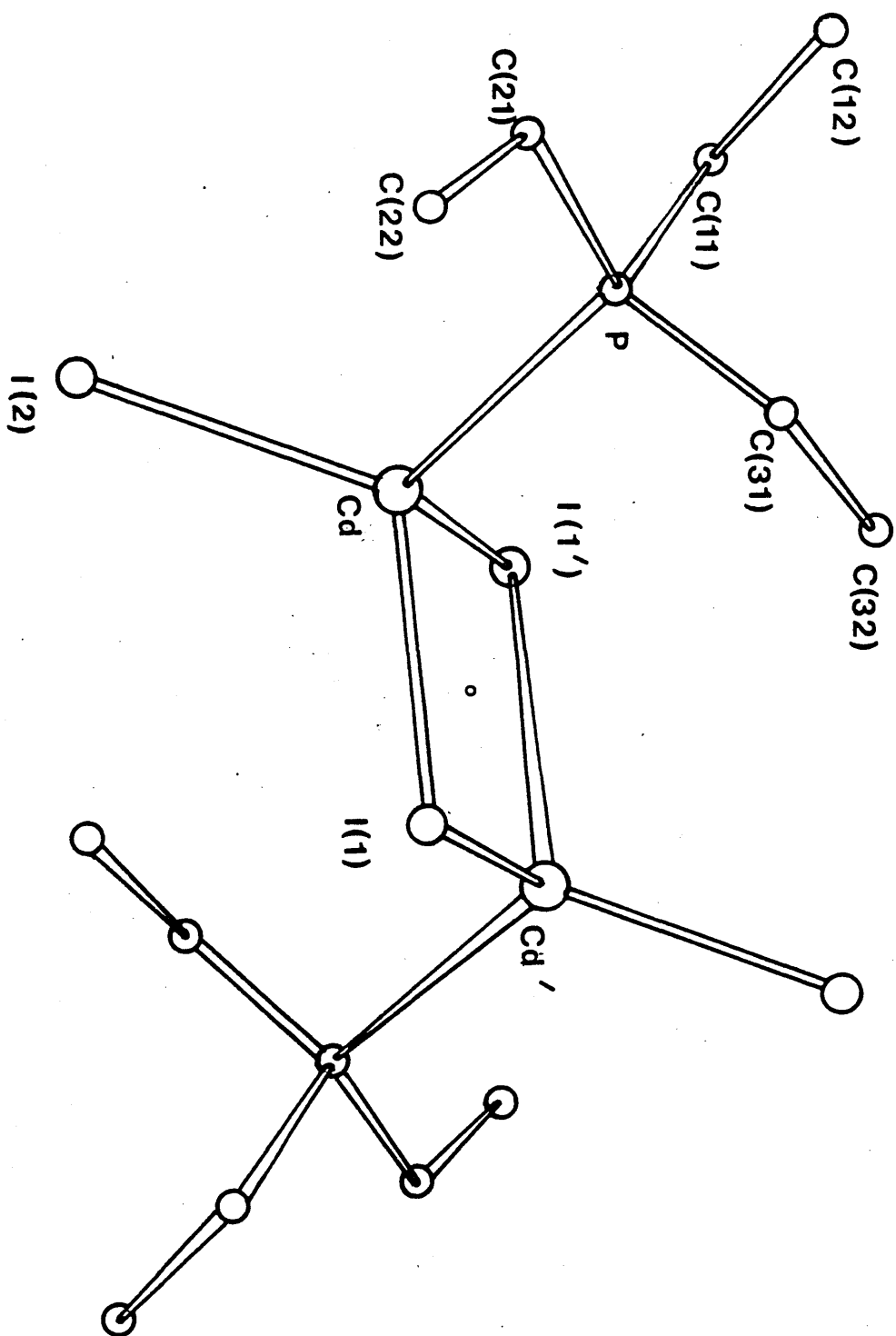


Figure 3.4   The Crystal structure of  $(Et_3P)CdI_2$

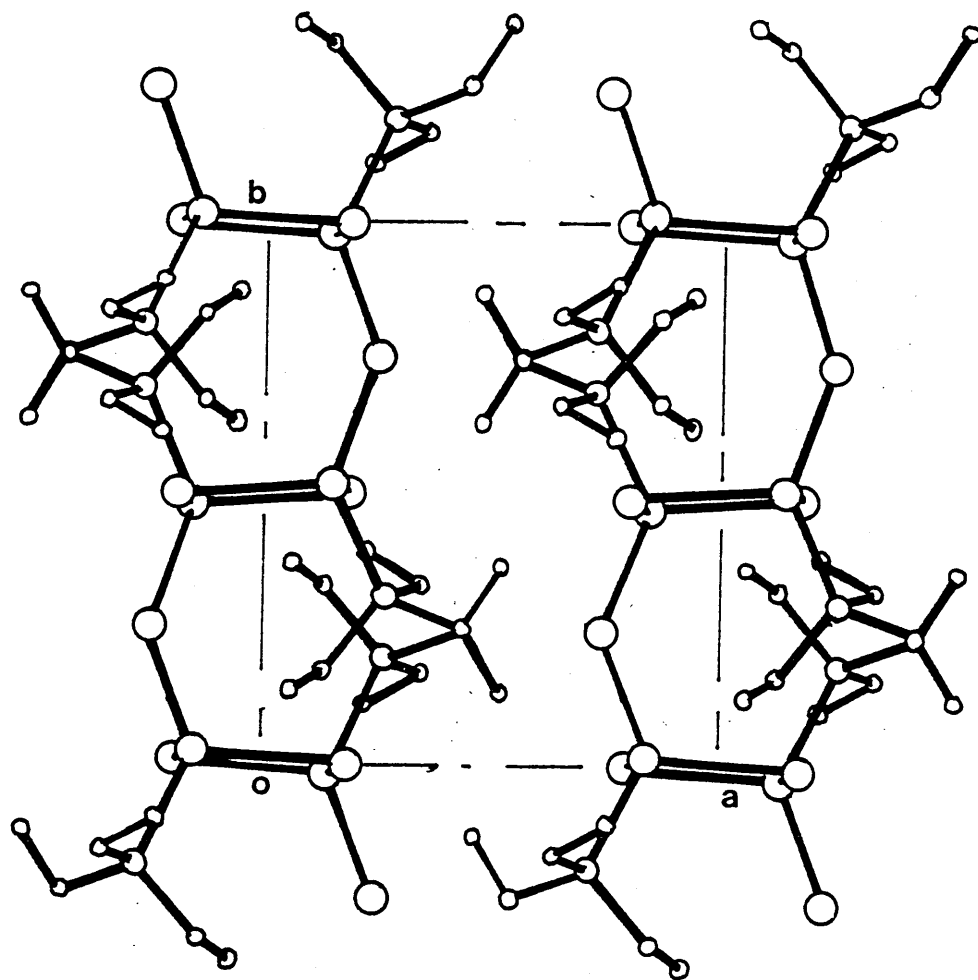


Figure 3.5 View along P1-Cd1 for  $(Et_3P)CdI_2$

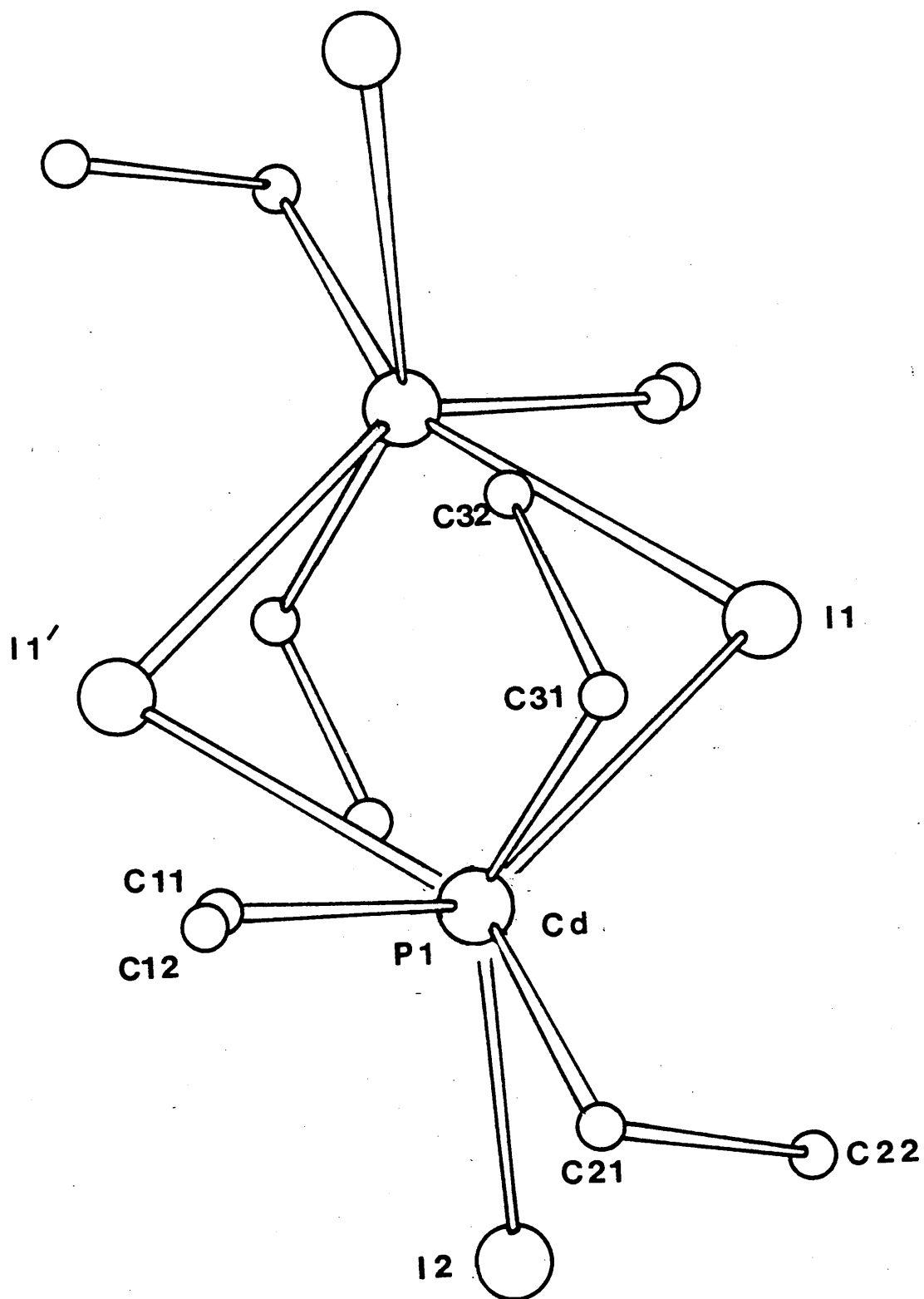


Table 3.3

Bond distances and angles for  $(Et_3P)CdI_2$  with standard deviations

in parentheses

a) Symmetry code:

None = x, y, z

' = 2.0-x, 1.0-y, -z.

b) Bond lengths/Å

Cd - I1 = 2.862(1)

P - C21 = 1.825(9)

Cd - I2 = 2.701(1)

P - C31 = 1.817(11)

Cd - I1' = 2.878(1)

C11 - C12 = 1.510(21)

Cd - Cd' = 3.791(1)

C21 - C22 = 1.523(19)

Cd - P = 2.542(2)

C31 - C32 = 1.540(15)

P - C11 = 1.820(12)

c) Bond angles/°

I1 - Cd - I2 = 112.3(1)

Cd - P - C31 = 114.6(4)

I1 - Cd - I1' = 97.3 (1)

P - C11 - C12 = 116.1(9)

I1 - Cd - P = 109.7(1)

P - C21 - C22 = 112.3(8)

I2 - Cd - P = 116.4(1)

P - C31 - C32 = 112.6(9)

I2 - Cd - I1' = 113.9(4)

C11 - P - C21 = 105.2(6)

I1' - Cd - P = 105.2(1)

C11 - P - C31 = 107.4(6)

Cd' - I1 - Cd = 82.7(1)

C21 - P - C31 = 105.1(5)

Cd - P - C11 = 111.6(4)

Cd - P - C21 = 112.3(5)

### 3.4 Crystallographic examination of $\alpha$ -(Cy<sub>3</sub>P)CdCl<sub>2</sub>

#### Crystal data:

$C_{18}H_{33}CdCl_2P$ :  $M_r = 463.74$ , Monoclinic,  
 $a = 14.127(8)$ ,  $b = 16.412(10)$ ,  $c = 19.833(12)\text{\AA}$   
 $U = 4228.11\text{\AA}^3$ ,  $\alpha = 90.00$ ,  $\beta = 113.14(20)$ ,  
 $\gamma = 90.00^\circ$ ,  $D_m = 1.50\text{g cm}^{-3}$  (by flotation  $CHCl_3/CHBr_3$ ),  
 $D_c = 1.46\text{g cm}^{-3}_m$   $Z = 8$ ,  $F(000) = 1904$   
 $\mu(\text{Mo} - K\alpha) = 12.43\text{cm}^{-1}$

#### Systematic absences:

0k0 reflections are absent for  $k = 2n + 1$

h0l " " " "  $l = 2n + 1$

#### Space group:

$P2_1/c$

#### Data collection and structure refinement:

A crystal, 0.48 x 0.20 x 0.20 mm, was mounted about  $a$  and 16 layers,  $0kl \rightarrow 15kl$ , were collected giving rise to 6996 reflections of which 4067 had  $I/\sigma(I) \geq 3.0$  and were used for refinement. Corrections for Lorentz and polarisation effects, and for absorption were made. A common isotropic temperature factor was applied to the cyclohexyl hydrogen atoms and refined to a final value of  $U = 0.064(11)\text{\AA}^2$ . The weighting scheme adopted was:

$$w = 0.7312 / [\sigma^2(F_o) + 0.001351(F_o)^2] .$$

Full matrix refinement and anisotropic temperature factors for all non-hydrogen atoms gave the final  $R = 0.042$  and  $R' = 0.045$ . Final atomic and thermal parameters are listed in Table A.1.5 (Appendix A.1) and calculated/observed structure factors are contained in Appendix A.2. Bond angles and distances are given in Table 3.4.

### Description of the structure

The structure consists of discrete tetrameric units (Figure 3.6), with the cadmium atoms in both penta- and tetraco- ordinate environments. Cd1 and Cd2 are arranged to give an unsymmetrical chlorine-bridged dimeric grouping [ Cd1 - Cl(11) = 2.484(2); Cd1 - Cl(21) = 2.538(1); Cd2 - Cl(11) = 2.803; Cd2 - Cl(21) = 2.522 $\overset{\circ}{\text{Å}}$  ]. The Cd1, Cl(11), Cl(21), Cd2, ring is almost planar (Appendix A.3), the deviations from the mean plane being 0.0355, -0.0322, -0.0351, and 0.0318 $\overset{\circ}{\text{Å}}$  for Cd1, Cl(11), Cl(21) and Cd2 respectively. These unsymmetrical dimeric units are linked in pairs by relatively long Cd-Cl contacts in a centrosymmetric manner. The resulting central Cd<sub>2</sub>Cl<sub>2</sub> ring which is required to be planar is very asymmetric [ Cd2 - Cl(22) and Cd2 - Cl(22') are 2.465(2) and 2.832(2) $\overset{\circ}{\text{Å}}$  respectively ]

The co-ordination polyhedron about each terminal cadmium atom (Cd1, Cd2) is a distorted tetrahedron with the Cl(11) - Cd1 - Cl(21) angle of 91.4(1) $^{\circ}$  and the Cl(11) - Cd1 - P1 angle of 118.2(1) $^{\circ}$ . The additional Cd-Cl interaction results in Cd2 having a distorted trigonal bipyramidal co-ordination. The atoms Cl(21), Cl(22), P2 form a trigonal plane around Cd2. Deviations from the mean plane (Appendix A.3) are Cd2, 0.0262; Cl(21), -0.0086; Cl(22), -0.0087; P2, -0.0090 $\overset{\circ}{\text{Å}}$ .

The angles between the bonds to these atoms in the trigonal plane range from  $116.0(1)$  [ C1(22) - Cd2 - C1(21) ] to  $122.2(1)^\circ$  [ C1(21) - Cd2 - P2 ]. The angle between the two apical bonds is close to linearity; i.e. angle C1(22') - Cd2 - C1(11) is  $173.0(1)^\circ$ . The bridge angles, Cd - Cl - Cd, in the two rings are close to  $90^\circ$ , viz. Cd2 - C1(11) - Cd1 is  $89.1(1)$  and Cd2 - C1(21) - Cd1 is  $94.6(1)^\circ$ .

The cyclohexyl rings adopt the preferred chair conformation such that all the C-C-C-C torsion angles lie close to the expected angle of  $60^\circ$  (Appendix A.3).

Figure 3.7 shows the arrangement of the tetramer units which run parallel to the a-axis in the unit cell.

Comparison of this tetrameric structure with that of  $(\text{Me}_2\text{PhP})\text{CdCl}_2$  complex shows the presence of pentaco-ordinate geometries in both structures. Thus all cadmium atoms in  $(\text{Me}_2\text{PhP})\text{CdCl}_2$  and the central two cadmium atoms in  $(\text{Cy}_3\text{P})\text{CdCl}_2$  are in distorted trigonal bipyramidal environments. The two geometries are compared below:

Bond lengths/ $\text{\AA}$

$(\text{Me}_2\text{PhP})\text{CdCl}_2$

Cd - C1(1)	=	2.481(2)
Cd - C1(2)	=	2.497(1)
Cd - C1(1')	=	2.745(1)
Cd - C1(2'')	=	2.734(1)
Cd - P	=	2.560(1)

$\alpha$ - $(\text{Cy}_3\text{P})\text{CdCl}_2$

Cd2 - C1(22)	=	2.465(2)
Cd2 - C1(21)	=	2.522(2)
Cd2 - C1(22')	=	2.832(2)
Cd2' - C1(22)	=	2.832(2)
Cd2 - P2	=	2.553(2)

While in  $(\text{Me}_2\text{PhP})\text{CdCl}_2$  polymeric chains are formed, in  $\alpha\text{-(Cy}_3\text{P)}\text{CdCl}_2$  only two cadmium atoms are pentaco-ordinate, the polymeric arrangement being terminated by two tetraco-ordinate cadmiums to give a tetrameric unit.

Figure 3.6 The Molecular structure of  $\alpha$ -(C<sub>3</sub>P)CdCl<sub>2</sub>.

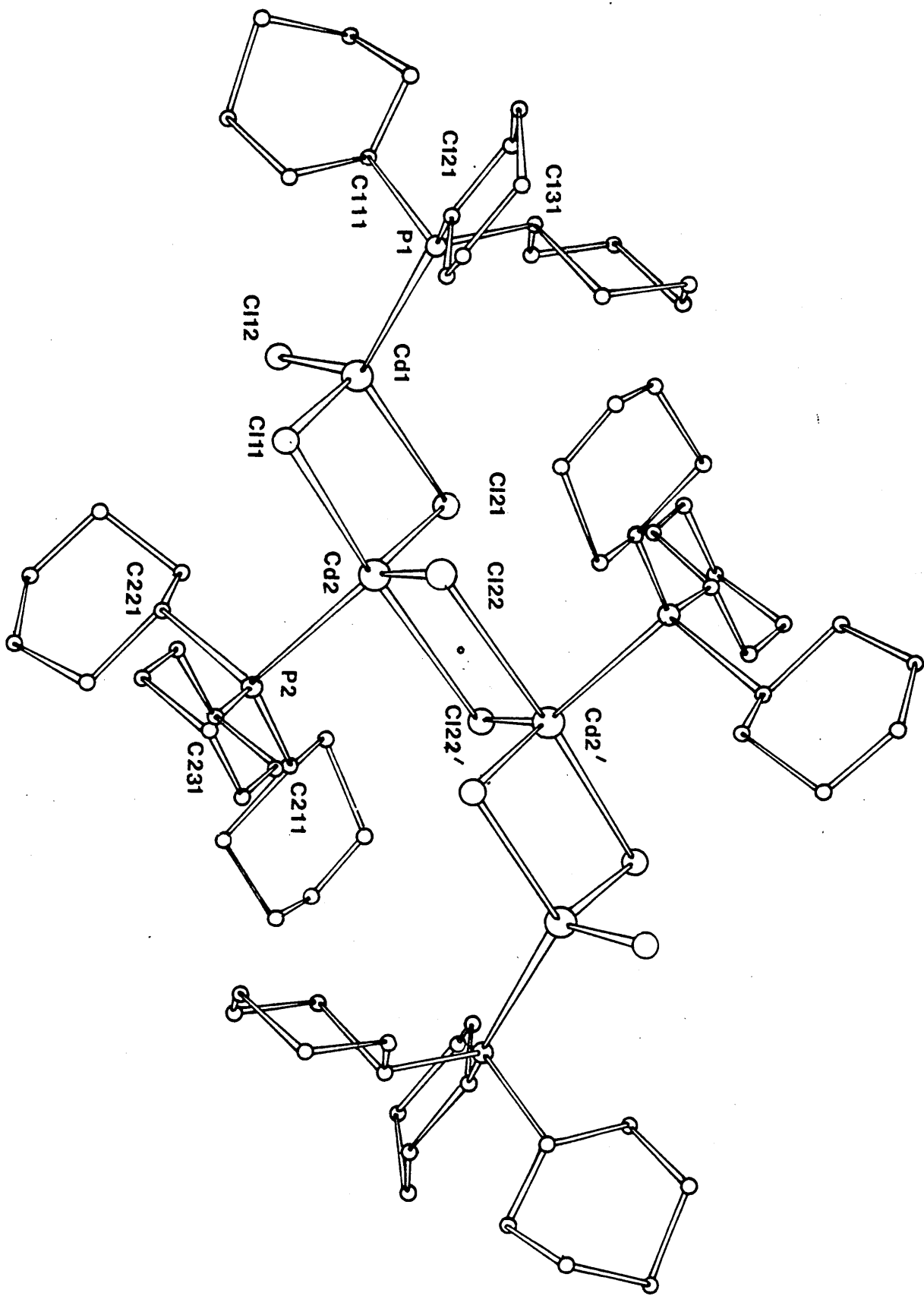


**Figure 3.7** The Crystal structure of  $d(Cy_3P)CdCl_2$

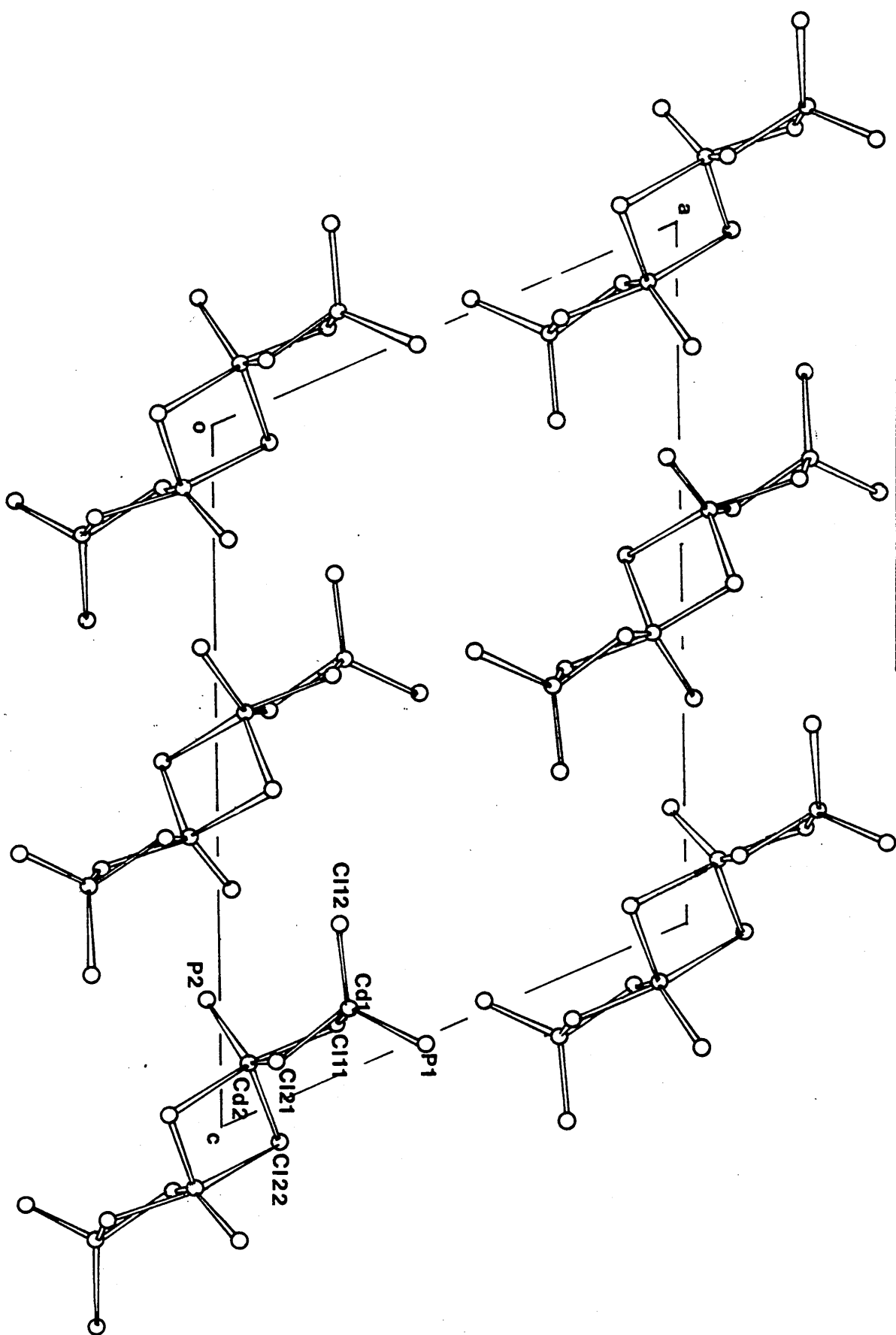


Table 3.4

Bond distances and angles for  $\alpha$ -(Cy<sub>3</sub>P)CdCl<sub>2</sub> with estimated standard

deviations in parentheses

a) Symmetry code

None = x, y, z

' = -x, -y, 2.0-z

b) Bond lengths/Å<sup>o</sup>

Cd1 - C1(11)	=	2.484(2)	Cd2 - C1(21)	=	2.522(2)
Cd1 - C1(12)	=	2.423(3)	Cd2 - C1(11)	=	2.803(3)
Cd1 - C1(21)	=	2.538(4)	Cd2 - C1(22)	=	2.465(2)
Cd1 - P1	=	2.569(2)	Cd2 - C1(22')	=	2.832(2)
Cd1 .... Cd2	=	3.717(1)	Cd2 .... Cd2'	=	3.958(2)
P1 - C111	=	1.851(13)	Cd2 - P2	=	2.553(2)
P1 - C121	=	1.839(9)	P2 - C211	=	1.849(11)
P1 - C131	=	1.841(10)	P2 - C221	=	1.836(13)
C111 - C112	=	1.523(16)	P2 - C231	=	1.828(9)
C112 - C113	=	1.521(26)	C211 - C212	=	1.526(16)
C113 - C114	=	1.499(22)	C212 - C213	=	1.561(29)
C114 - C115	=	1.497(22)	C213 - C214	=	1.510(28)
C115 - C116	=	1.541(20)	C214 - C215	=	1.523(35)
C111 - C116	=	1.505(14)	C215 - C216	=	1.549(24)
C121 - C122	=	1.528(18)	C211 - C216	=	1.476(16)
C122 - C123	=	1.530(15)	C221 - C222	=	1.514(13)
C123 - C124	=	1.506(16)	C222 - C223	=	1.521(23)
C124 - C125	=	1.512(22)	C223 - C224	=	1.420(22)
C125 - C126	=	1.515(15)	C224 - C225	=	1.509(17)

C121 - C126	= 1.545(12)	C225 - C226	= 1.531(21)
C131 - C132	= 1.526(12)	C221 - C226	= 1.460(15)
C132 - C133	= 1.535(16)	C231 - C232	= 1.531(17)
C133 - C134	= 1.513(24)	C232 - C233	= 1.519(14)
C134 - C135	= 1.506(15)	C233 - C234	= 1.513(18)
C135 - C136	= 1.524(15)	C234 - C235	= 1.524(22)
C131 - C126	= 1.527(18)	C235 - C236	= 1.524(14)
		C231 - C236	= 1.528(16)

c) Bond angles/°

C1(11) - Cd1 - C1(12)	= 113.1(1)	C1(22) - Cd2 - C1(21)	= 116.0(1)
C1(11) - Cd1 - C1(21)	= 91.4(1)	C1(22) - Cd2 - C1(22')	= 83.3(1)
C1(11) - Cd1 - P1	= 118.2(1)	C1(22) - Cd2 - C1(11)	= 92.4(1)
C1(12) - Cd1 - P1	= 107.4(1)	C1(22) - Cd2 - P2	= 121.7(1)
C1(21) - Cd1 - C1(12)	= 108.2(1)	C1(22') - Cd2 - P2	= 92.6(1)
C1(21) - Cd1 - P1	= 117.8(1)	C1(22') - Cd2 - C1(21)	= 91.2(1)
Cd2 - C1(11) - Cd1	= 89.1(1)	C1(22') - Cd2 - C1(11)	= 173.0(1)
Cd2 - C1(21) - Cd1	= 94.6(1)	C1(21) - Cd2 - P2	= 122.2(1)
Cd1 - P1 - C111	= 103.7(1)	C1(11) - Cd2 - C1(21)	= 84.8(1)
Cd1 - P1 - C121	= 116.8(3)	C1(11) - Cd2 - P2	= 95.0(1)
Cd1 - P1 - C131	= 113.5(3)	Cd2' - C1(22) - Cd2	= 96.7(1)
		Cd2 - P2 - C211	= 108.0(3)
C111 - P1 - C121	= 108.1(5)	Cd2 - P2 - C221	= 117.1(3)
C111 - P1 - C131	= 106.0(5)	Cd2 - P2 - C231	= 107.9(3)
C121 - P1 - C131	= 108.1(4)		
		C211 - P2 - C221	= 112.6(5)
P1 - C111 - C112	= 110.3(8)	C211 - P2 - C231	= 106.9(5)
P1 - C111 - C116	= 117.2(8)	C221 - P2 - C231	= 103.7(5)
C111 - C112 - C113	= 109.6(10)		

C112 - C113 - C114	= 112.5(12)	P2 - C211 - C212	= 109.9(8)
C113 - C114 - C115	= 110.5(15)	P2 - C211 - C216	= 118.4(9)
C114 - C115 - C116	= 112.2(9)	C211 - C212 - C213	= 108.1(13)
C115 - C116 - C111	= 110.2(9)	C212 - C213 - C214	= 112.4(18)
C116 - C111 - C112	= 111.0(10)	C213 - C214 - C215	= 111.7(14)
P1 - C121 - C122	= 112.3(7)	C214 - C215 - C216	= 109.1(16)
P1 - C121 - C126	= 114.5(6)	C215 - C216 - C211	= 109.5(13)
C121 - C122 - C123	= 110.5(11)	C216 - C211 - C212	= 112.8(9)
C122 - C123 - C124	= 111.1(9)	P2 - C221 - C222	= 116.2(9)
C123 - C124 - C125	= 111.6(11)	P2 - C221 - C226	= 116.1(8)
C124 - C125 - C126	= 110.4(11)	C221 - C222 - C223	= 111.5(11)
C125 - C126 - C121	= 111.0(9)	C222 - C223 - C224	= 114.9(13)
C126 - C121 - C122	= 111.8(9)	C223 - C224 - C225	= 114.3(12)
P1 - C131 - C132	= 110.5(7)	C224 - C225 - C226	= 111.4(12)
P1 - C131 - C136	= 112.9(6)	C225 - C226 - C221	= 112.6(10)
C131 - C132 - C133	= 110.9(8)	C226 - C221 - C222	= 113.7(9)
C132 - C133 - C134	= 111.0(10)	P1 - C231 - C232	= 110.8(7)
C133 - C134 - C135	= 111.8(12)	P1 - C231 - C236	= 110.2(7)
C134 - C135 - C136	= 111.7(9)	C231 - C232 - C233	= 111.1(9)
C135 - C136 - C131	= 110.7(9)	C232 - C233 - C234	= 111.4(10)
C136 - C131 - C132	= 109.0(9)	C233 - C234 - C235	= 109.8(9)
		C234 - C235 - C236	= 112.0(11)
		C235 - C236 - C231	= 110.6(10)
		C236 - C231 - C232	= 110.3(8)

CHAPTER 4

SPECTROSCOPIC STUDIES OF SOME  $(R_3P)CdX_2$

COMPLEXES

Contents

	<u>Page</u>
4.1 Introduction.	99
4.2 Complexes of known structure.	100
4.3 Summary of structure/spectra correlations.	118
4.4 Complexes of unknown structure.	119

#### 4.1 Introduction

A range of structures has been determined for  $(R_3P)CdX_2$  complexes ( $X = Cl, Br$  or  $I$ ), involving differing degrees of halide-bridging. These structures are described in Chapter 3, and range from a discrete dimer,  $(Et_3P)CdI_2$ , to an extended five co-ordinate arrangement,  $(Me_2PhP)CdX_2$  ( $X = Cl, Br$  or  $I$ ). Resulting from these structural differences one expects, and indeed finds, substantial differences in their far-infrared and Raman spectra ( $50 - 450\text{ cm}^{-1}$ ). These differences should enable one to characterise the various structural types in otherwise uncharacterised compounds.

For the most satisfactory interpretation of the spectra of these structurally known complexes, it was necessary to predict the number of metal-ligand vibrations using a group theoretical approach. In all cases the phosphine was taken as a point mass and the three approaches made were:-

- (i) point group analysis;
- (ii) line group analysis;
- (iii) factor group analysis.

These approaches are summarised in Section 1.2.

In the following sections the spectra of 'known' structures are first interpreted and then the structure/spectra correlations so obtained are applied to the structurally unknown complexes.

## 4.2 Complexes of known structure

### a) (Et<sub>3</sub>P)CdI<sub>2</sub>

The structure of this complex consists of discrete dimer units two of which crystallise in each monoclinic unit cell (P2<sub>1</sub>/c).

The various modes predicted by C<sub>i</sub> point group and C<sub>2h</sub><sup>5</sup> factor group analysis (Appendix A.4) are:-

#### Point Group

#### Factor Group

$$\Gamma_{\text{tot}} = 7A_g + 5B_g + 4A_u + 8B_u$$

$$12A_g + 12B_g + 12A_u + 12B_u$$

$$\Gamma(\text{Cd-I})_t = A_g(\text{Ra}) + B_u(\text{I.R.})$$

$$A_g(\text{Ra}) + B_g(\text{Ra}) + A_u(\text{I.R.}) + B_u(\text{I.R.})$$

$$\Gamma(\text{Cd-P}) = A_g(\text{Ra}) + B_u(\text{I.R.})$$

$$A_g(\text{Ra}) + B_g(\text{Ra}) + A_u(\text{I.R.}) + B_u(\text{I.R.})$$

$$\Gamma(\text{Cd-I})_b = A_g(\text{Ra}) + B_g(\text{Ra}) + A_u(\text{I.R.}) + B_u(\text{I.R.})$$

$$2A_g(\text{Ra}) + 2B_g(\text{Ra}) + 2A_u(\text{I.R.}) + 2B_u(\text{I.R.})$$

The vibrational spectra are shown in Figures 4.1 and 4.2, while Table 4.1 contains the wavenumber positions and vibrational assignments. The internal modes of the Et<sub>3</sub>P ligand may be eliminated by comparison of the spectra of the chloro-, bromo- and iodo- derivatives, Figures 4.1, 4.2, and by reference to the data reported for Et<sub>3</sub>P by Green [49]. This leaves the remaining bands due to  $\nu(\text{Cd-I})$ ,  $\nu(\text{Cd-P})$  and deformation modes.

$\nu(\text{Cd-I})_t$  have previously been located around 160 cm<sup>-1</sup> for similar iodine-bridged dimeric complexes (Table 4.2 [36, 37, 50]). Hence the band at 163 cm<sup>-1</sup> in the spectrum of (Et<sub>3</sub>P)CdI<sub>2</sub> is assigned as a  $\nu(\text{Cd-I})_t$  stretching mode. Symmetry B<sub>u</sub> is given by point group theory. There is no indication of the two dimer molecules in the unit cell giving rise to significant correlation splitting.

The  $\nu(\text{Cd-I})_t A_g$  counterpart is found at  $165 \text{ cm}^{-1}$  in the Raman spectrum, the infrared and Raman bands being mutually exclusive. The closeness of the  $A_u$  and  $A_g$  pair is not unexpected in view of the heavy  $[\text{CdI}_2\text{Cd}]$  unit which would decrease the vibrational coupling.

The bands arising from  $\nu(\text{Cd-I})_b$  modes are not as clearly assigned. From point group analysis two  $\nu(\text{Cd-I})_b$  bands are predicted in each of the infrared and Raman spectra. Of the likely candidates for  $\nu(\text{Cd-I})_b$ , namely the two bands at  $107$  and  $129 \text{ cm}^{-1}$ , the former is a very intense band and appears to be common to the spectra of all three complexes  $(\text{Et}_3\text{P})\text{CdX}_2$ , thus leaving the band at  $129 \text{ cm}^{-1}$  and its possible shoulder at  $132 \text{ cm}^{-1}$  to be due to the  $A_u$  and  $B_u$   $\nu(\text{Cd-I})_b$  modes. Only one Raman band is attributable to  $\nu(\text{Cd-I})_b$ , at  $122 \text{ cm}^{-1}$ , it thus being assumed that the  $A_g$  and  $B_g$  modes are coincident.

It is interesting to observe near (infrared) or actual (Raman) coincidence of each of the infrared and Raman pairs of  $\nu(\text{Cd-I})_b$  modes. Evidence to suggest the coincidence of these bands is shown by Baran [51], who studied a number of planar four membered ring systems and derived simple approximate equations relating the two infrared active  $\nu(\text{M-X})_b$  modes ( $\nu_s$  and  $\nu_a$ ) to the angle ( $\phi$ ) between the bridge bonds (Appendix A.4):

$$\cos \phi = \frac{[(\nu_s/\nu_a)^2 - 1]}{[(\nu_s/\nu_a)^2 + 1]}$$

Rearrangement gives the  $\nu_s/\nu_a$  ratio:

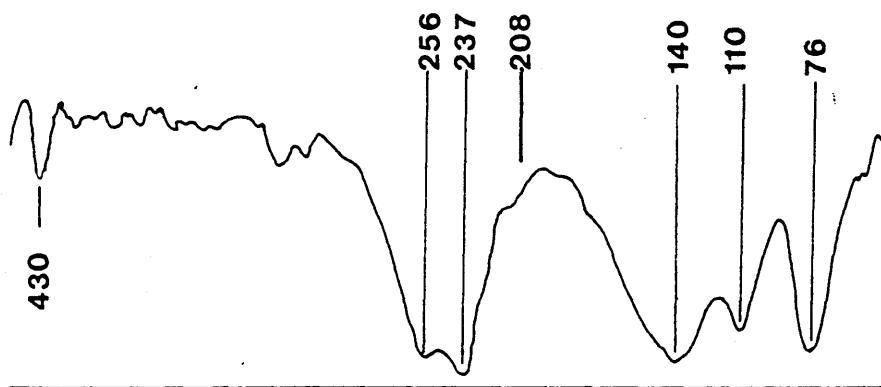
$$\nu_s/\nu_a = \frac{(1 - \cos \phi)}{(\cos \phi + 1)} \quad 101$$

Thus, knowing the angle  $\phi$  the ratio of  $\nu_s/\nu_a$  can be calculated; for  $\phi = 90^\circ$ , the two infrared-active  $\nu(M-X)_b$  modes should be coincident. The equation has been tested [14] by comparing a wide range of planar four membered ring systems using reliable far-infrared data with structural results (Table 4.3) [52, 53, 54]. The  $(Et_3P)CdI_2$  data have been included and indicate the correlation of the bridge angle  $\phi$  and the coincidence of the two  $\nu(Cd-I)_b$  modes to be upheld.

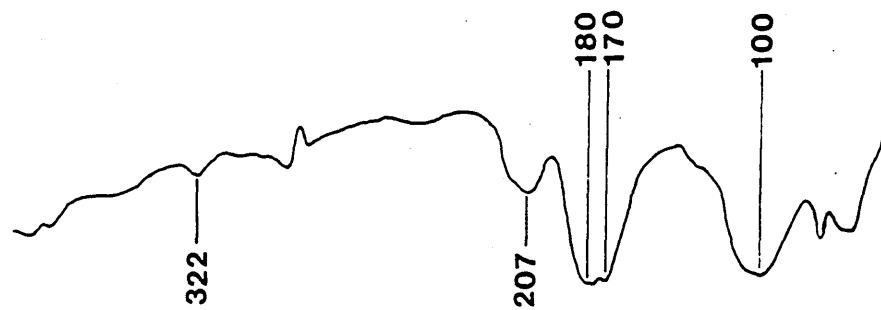
The assignment of the  $\nu(Cd-P)$  mode is difficult to confirm and is thus very tentative. Previous  $\nu(Cd-P)$  assignments for  $(R_3P)_2CdX_2$  and  $(R_3P)CdX_2$  complexes have been made around  $130\text{ cm}^{-1}$  and  $100\text{ cm}^{-1}$  respectively (Section 1.4.2; 1.4.3). Thus tentatively, the infrared band at 107 and Raman band at  $100\text{ cm}^{-1}$  are assigned as  $\nu(Cd-P)B_u$  and  $A_g$  respectively.

Figure 4.1 Far-infrared spectra of  $(Et_3P)CdX_2$  ( $X=Cl, Br$  or  $I.$ ), ca.30K.

X=Cl



X=Br



X=I

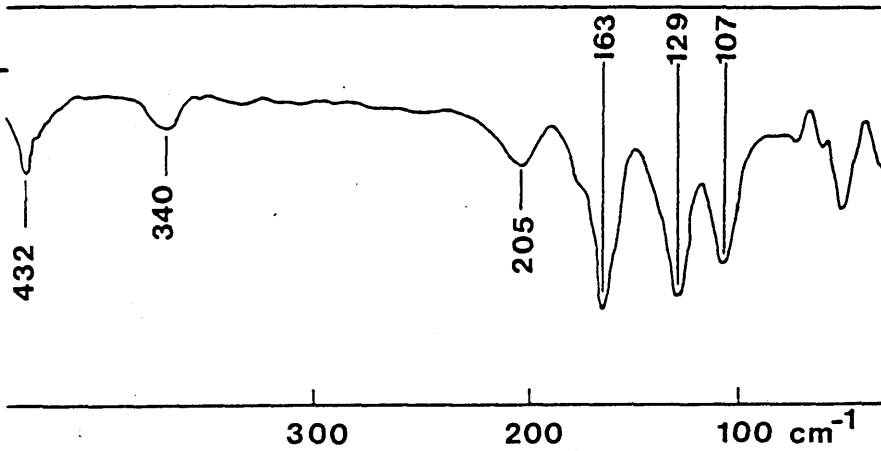
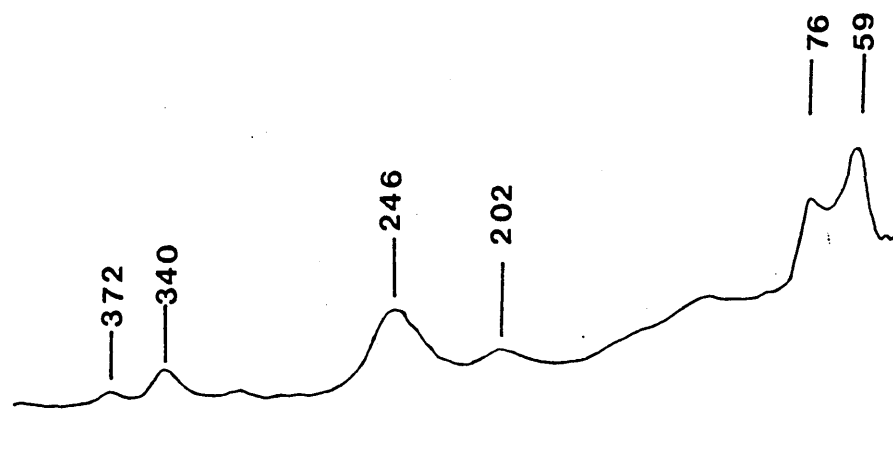
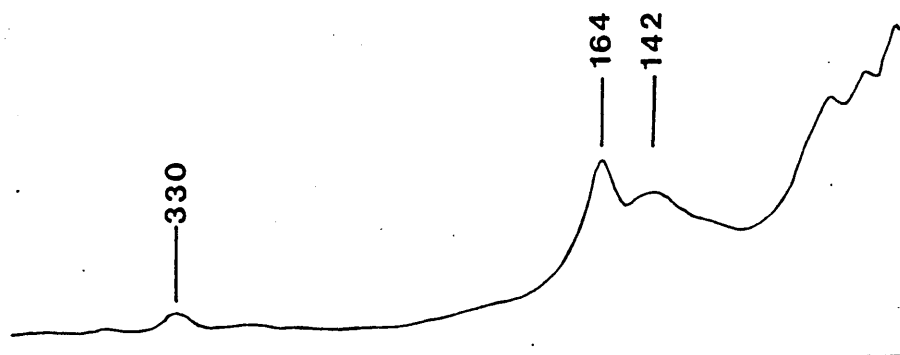


Figure 4.2 Raman spectra of  $(Et_3P)CdX_2$  ( $X=Cl, Br$  or  $I.$ ), c a. 70K.

X=Cl



X=Br



X=I

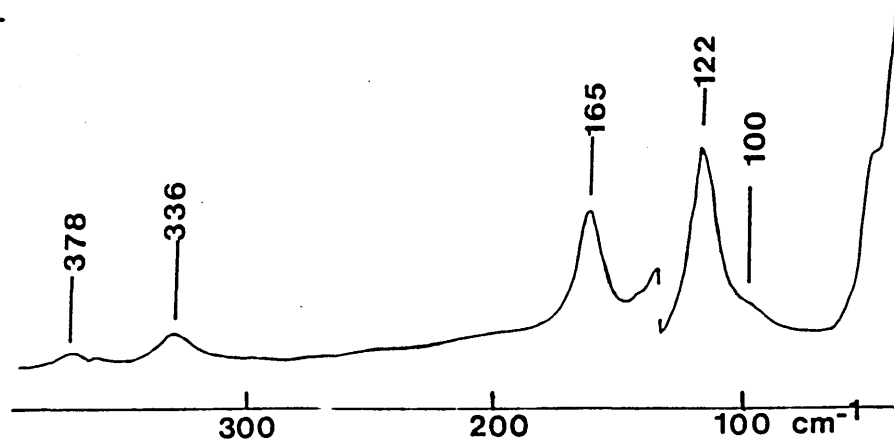


Table 4.1

Vibrational assignments for  $(Et_3P)CdI_2$  ( $cm^{-1}$ )

$(Et_3P)CdI_2$		Assignments
I.R.	Ra	
	165s	$\sphericalangle(Cd-I)_t$ $A_g$
163s		$\sphericalangle(Cd-I)_t$ $B_u$
132 } 129 }		$\sphericalangle(Cd-I)_b$ $A_u$ and $B_u$
	122	$\sphericalangle(Cd-I)_b$ $A_g$ and $B_g$
107		$\sphericalangle(Cd-P)$ $B_u$
	100	$\sphericalangle(Cd-P)$ $A_g$

Table 4.2

Infrared band positions of  $\nu(\text{Cd-I})$  modes for iodide-bridged dimeric structures

Complex	$\nu(\text{Cd-I})_t / \text{cm}^{-1}$	$\nu(\text{Cd-I})_b / \text{cm}^{-1}$	Ref.
$(\text{Bu}_3^t\text{P})\text{CdI}_2$	161	127	36
$(\text{Cy}_3\text{P})\text{CdI}_2$	172	121	37
* $\text{Cd}_2\text{I}_6^{2-}$	164, 140	127, 109	50
** $\text{Cd}_2\text{I}_6^{2-}$	170, 141	119, 107	50

\*  $\text{Cd}_2\text{I}_6^{2-}$  in complex  $[(n\text{-C}_6\text{H}_{13})_4\text{N}]_2[\text{Cd}_2\text{I}_6]$

\*\*  $\text{Cd}_2\text{I}_6^{2-}$  " "  $[\text{Pr}_4\text{N}]_2[\text{Cd}_2\text{I}_6]$  .

Table 4.3

Comparison of observed and calculated bridge angles for some  
four-membered ring systems [ 52 - 54 ] .

Compound	Bridge distance/Å	Source	$\phi$ obs/°	$\phi$ calc/°	$\nu(M-X)_b / \text{cm}^{-1}$
$\text{Au}_2\text{Cl}_6$	2 x 3.33(2), 2 x 2.34(2)	X-ray	94(2)	90.9	310, 305
$\text{I}_2\text{Cl}_6$	4 x 2.70	X-ray	96	100.7	205, 176
$\text{Ga}_2\text{Cl}_6$		*N.C.A.	86	86.5	305, 287
$(\text{Et}_4\text{N})_2\text{Hg}_2\text{Br}_6$	4 x 2.75	X-ray	91(2)	92.3	128, 123
$(\text{Et}_3\text{P})\text{CdI}_2$	2 x 2.862(2) 2 x 2.878(1)	X-ray	82.7(1)	89.56	132, 130

\* N.C.A. = Normal co-ordinate analysis

$\phi = M - \hat{X} - M$  bridge angle.

b)  $(\text{Me}_2\text{PhP})\text{CdX}_2$  [ X = Cl, Br or I ].

All three structures can be described as polymeric chains (Section 3.2). Cadmium lies in a distorted trigonal bipyramidal environment with two short Cd - X contacts, a short Cd - P contact and two longer Cd - X contacts which join the 'PCdX<sub>2</sub>' units into a chain.

Appendix A.4 shows that, as the structures crystallise in a monoclinic system (P2<sub>1</sub>/n) a simple C<sub>1</sub> line group treatment would be adequate for prediction of  $\mathcal{N}(\text{Cd-X})$  modes:

$$\left[ \text{chain} \right] = 9A_g(\text{Ra}) + 11A_u(\text{I.R.})$$

$$\left[ \mathcal{N}(\text{Cd-X}) \right] = 4A_g(\text{Ra}) + 4A_u(\text{I.R.})$$

$$\left[ \mathcal{N}(\text{Cd-P}) \right] = A_g(\text{Ra}) + A_u(\text{I.R.})$$

Thus there are four  $\mathcal{N}(\text{Cd-X})$  bands predicted in each of the infrared and Raman spectra (mutually exclusive). However, it can be envisaged that there could be two types of bridging  $\mathcal{N}(\text{Cd-X})$  modes, i.e. a higher wavenumber set of bands assigned to the modes associated with the movement of the shorter Cd-X bonds in the chain  $\left[ \mathcal{N}(\text{Cd-X})_g \right]$  and a lower wavenumber set of bands associated with the movement of the longer Cd-X contacts  $\left[ \mathcal{N}(\text{Cd-X})_1 \right]$ .

The vibrational spectra are shown in Figures 4.3 and 4.4; Table 4.4 contains the wavenumber positions and vibrational assignments. The internal modes of Me<sub>2</sub>PhP were eliminated by observation of similar bands at near constant positions in all three spectra.

The infrared spectrum of the chloride shows two prominent bands at 258 and 234 cm<sup>-1</sup>, assigned as  $\mathcal{N}(\text{Cd-Cl})_g$  modes, and a broad absorption band around 144 cm<sup>-1</sup> which is assigned as the  $\mathcal{N}(\text{Cd-Cl})_1$  mode.

A similar band pattern, showing expected halogen mass dependent shifts, is found for the bromide (two bands at 188 and 178  $\text{cm}^{-1}$  and a broad absorption around 98  $\text{cm}^{-1}$ ). The Raman bands expected for the short Cd-X bonds are at 259 and 240  $\text{cm}^{-1}$  (chloride) and 182 and 176  $\text{cm}^{-1}$  (bromide). Raman bands associated mainly with the longer Cd-X bonds could not be identified.

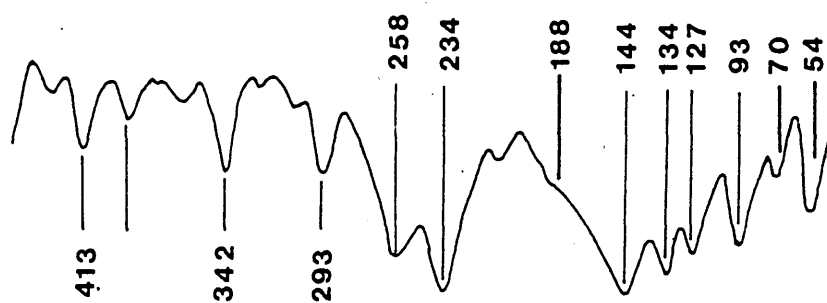
The iodide shows two intense absorptions in the infrared spectrum at 168 and 154  $\text{cm}^{-1}$  which appear in the positions expected for  $\nu(\text{Cd-I})_s$  of the shorter bonds on the basis of halogen mass dependence expected shifts. The  $\nu(\text{Cd-I})_s$  Raman bands are less obviously assigned. There is a band at 126  $\text{cm}^{-1}$ , which seems too low in wavenumber to be due to the Cd-I short bonds; also, it appears in the expected position for  $\nu(\text{Cd-P})$  (see later), but no alternative for  $\nu(\text{Cd-I})_s$  is available.

Indeed, the use of the Raman spectrum to detect  $\nu(\text{Cd-I})$  modes, which are all expected to appear below 150  $\text{cm}^{-1}$ , is not very satisfactory. The Raman bands in this range of the spectrum tend to be dominated by intense bands due to the phosphine ligand. Likewise, it is difficult to identify the  $\nu(\text{Cd-I})_l$  infrared bands (expected at c.a. 100  $\text{cm}^{-1}$ ).

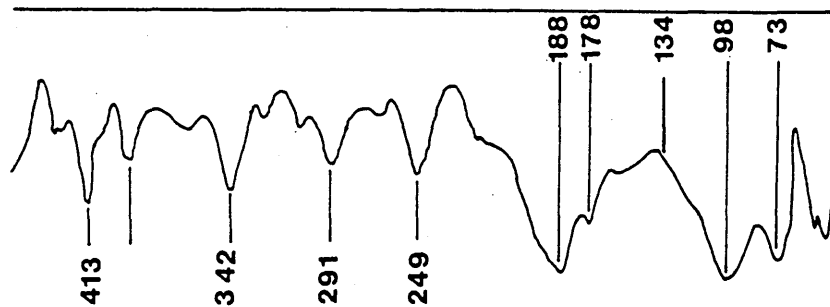
The  $\nu(\text{Cd-P})$  modes are again difficult to locate in the infrared spectrum. However, the Raman spectra of the chloride, bromide and iodide contain intense absorptions at 132, 133 and 126  $\text{cm}^{-1}$  respectively, in similar positions to the  $\nu(\text{Cd-P})$  modes for  $(\text{R}_3\text{P})_2\text{CdX}_2$  complexes (Section 1.4.3). Thus these bands are assigned as  $\nu(\text{Cd-P})A_g$ , with the  $A_u$  infrared counterparts at c.a. 134  $\text{cm}^{-1}$  in all three spectra.

**Figure 4.3** Far-infrared spectra of  $(\text{Me}_2\text{PhP})\text{CdX}_2$  ( $\text{X}=\text{Cl}, \text{Br}$  or  $\text{I}$ ), c a. 30K.

X=Cl



X=Br



X=I

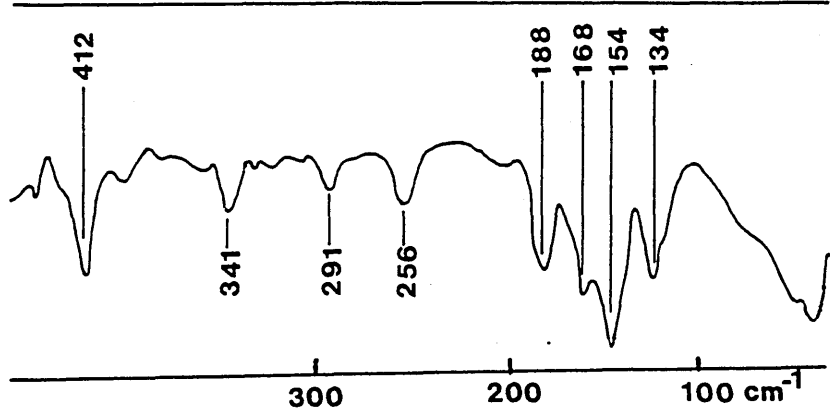
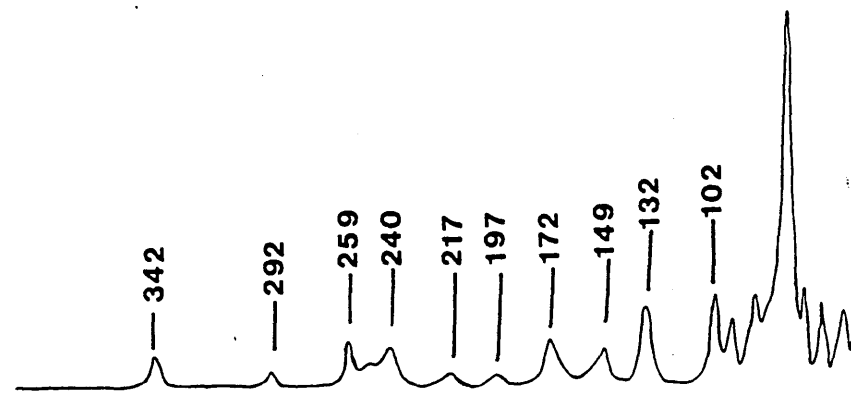


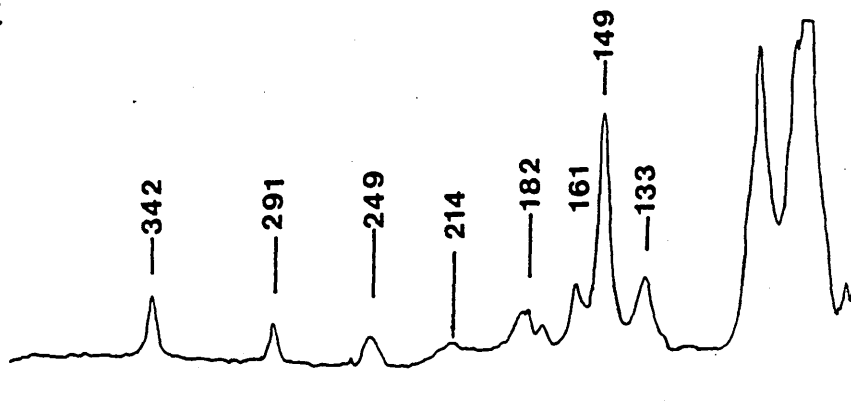
Figure 4.4

Raman spectra of  $(\text{Me}_2\text{PhP})\text{CdX}_2$  ( $\text{X}=\text{Cl}, \text{Br}$  or  $\text{I}$ ), c a. 70K.

X=Cl



X=Br



X=I

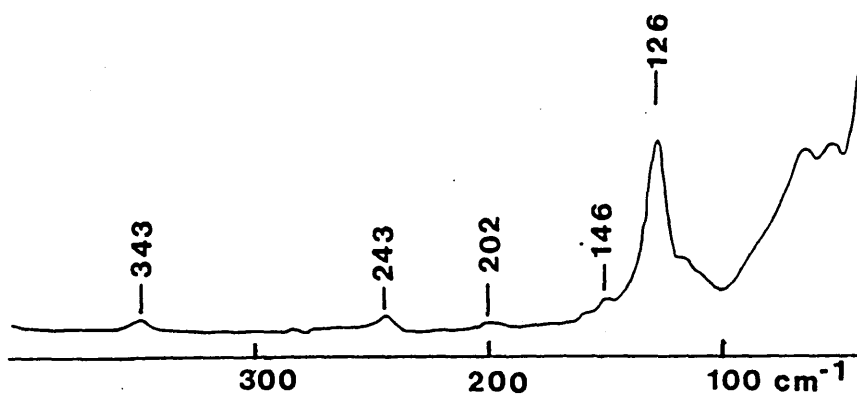


Table 4.4

Vibrational assignments for  $(\text{Me}_2\text{PhP})\text{CdX}_2$  complexes [ X = Cl, Br or I ].

$(\text{cm}^{-1})$

Cl		Br		I		Assignments .
I.R.	Ra	I.R.	Ra	I.R.	Ra	
258		188		168		$\nu(\text{Cd-X})_s A_u$
234		178		154		
	259		182		126	$\nu(\text{Cd-X})_s A_g$
	240		176		(tentative)	
144		98				$\nu(\text{Cd-X})_l A_u$
134		134		134		$\nu(\text{Cd-P}) A_u$
	132		133		126	$\nu(\text{Cd-P}) A_g$

c)  $\alpha$ -(Cy<sub>3</sub>P)CdCl<sub>2</sub>

The structure can be described as that of a chlorine-bridged tetramer, comprising two non-centrosymmetric dimers related by a centre of symmetry. The dimeric units are joined by very long Cd-Cl bonds (Section 3.4) forming links in which the cadmium atoms have a pentaco-ordinate environment.

A similar tetrameric structure is shown [ 3 ] by  $\alpha$ -(Bu<sup>n</sup><sub>3</sub>P)HgCl<sub>2</sub>, but in this case the central Hg-Cl contacts were considered to be very long and insignificant in assigning the vibrational spectra, so that a spectral interpretation was possible in terms of two identical distorted dimer units [ 3 ]. The asymmetry of the dimeric units (C<sub>1</sub>) gave rise to two  $\odot$ (Hg-Cl)<sub>t</sub>, four  $\odot$ (Hg-Cl)<sub>b</sub> and two  $\odot$ (Hg-P) modes in both the infrared and Raman spectra. The following assignments were made:

I.R./cm <sup>-1</sup>	Ra/cm <sup>-1</sup>	Assignments	
278	280	$\odot$ (Hg-Cl) <sub>t</sub>	
252	252	} $\odot$ (Hg-Cl) <sub>b</sub>	All of A symmetry
218	222		
190			
179	182		
149	156		

However in the case of the spectra of  $\alpha$ -(Cy<sub>3</sub>P)CdCl<sub>2</sub> the band patterns are more complex, and, in particular, there are more bands in the  $\odot$ (Cd-Cl) region than can be accommodated by a dimeric model. Consequently, the interpretation which must be applied is in terms of a tetrameric rather than a distorted dimeric structure.

In Appendix A.4 a simple  $C_i$  point group analysis is given to predict the number of modes associated with the tetrameric structure:-

$$\begin{aligned} \Gamma_{\text{tot}} &= 24 A_g + 24 A_u \\ \Gamma_{\text{vib}} &= 21 A_g (\text{Ra}) + 21 A_u (\text{I.R.}) \\ \Gamma(\text{Cd-P}) &= 2 A_g (\text{Ra}) + 2 A_u (\text{I.R.}) \\ \Gamma(\text{Cd-Cl})_t &= A_g (\text{Ra}) + A_u (\text{I.R.}) \\ \Gamma(\text{Cd-Cl})_b &= 6A_g (\text{Ra}) + 6A_u (\text{I.R.}) \end{aligned}$$

The vibrational spectra are shown in Figure 4.5 and the wavenumber positions and vibrational assignments in Table 4.5.

The internal modes of the ligand were eliminated by comparison of the spectra of the  $(\text{Cy}_3\text{P})\text{CdX}_2$  series. The halogen-mass dependence method for location of  $\nu(\text{Cd-Cl})$  modes could not be used since the bromide and iodide analogues appear to be of a different structural type. However, the  $\nu(\text{Cd-Cl})$  assignments suggested are in good agreement with those previously proposed [37]. The interpretation given (Table 4.5) identifies 11  $\nu(\text{Cd-Cl})$  modes, compared to the 14 predicted above. Considering the large number of bands and the spectral crowding, the agreement is good.

The  $\nu(\text{Cd-Cl})_t A_u$  and  $A_g$  modes are easily assigned to the bands at 278(I.R.) and 279(Ra)  $\text{cm}^{-1}$ . Their close positioning is easily understood since the two Cd-Cl terminal bonds are separated by a large and heavy skeletal framework. Consequently, there is very little vibrational coupling between them.

The number and positions of the  $\nu(\text{Cd-Cl})_b$  modes are quite different to those of  $\alpha - (\text{Bu}^n_3\text{P})\text{HgCl}_2$  exemplifying the subtle differences in structure.

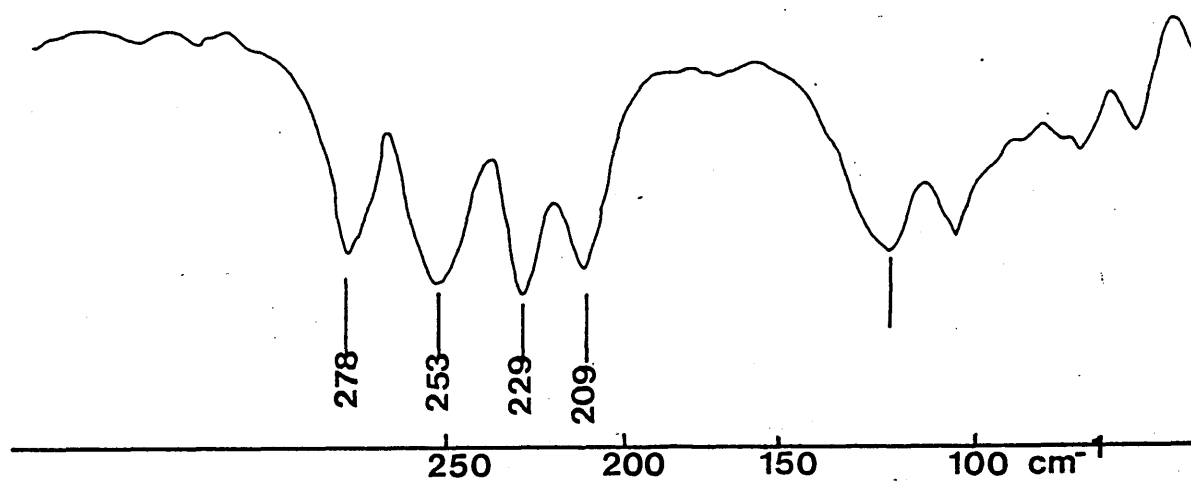
The wide wavenumber range of  $\nu(\text{Cd-Cl})_b A_g$  modes ( $172\text{-}272\text{ cm}^{-1}$ ) for  $\alpha - (\text{Cy}_3\text{P})\text{CdCl}_2$  can be explained by the very asymmetric nature of the dimer units, having bridging bond lengths of 2.484, 2.522, 2.538 and 2.803 $\overset{\circ}{\text{A}}$ . For example, the high position of the  $272\text{ cm}^{-1}$  band can be associated with a particularly short Cd-Cl bond of 2.484 $\overset{\circ}{\text{A}}$ , while the longer Cd-Cl bonds will give rise to the lower wavenumber bands. The corresponding bands in the infrared spectrum do not, apparently, cover so wide a range.

The  $\nu(\text{Cd-P})$  modes are difficult to locate. However the Raman band at  $152\text{ cm}^{-1}$  and the infrared band at  $124\text{ cm}^{-1}$  are possible candidates.

In conclusion, the spectra of  $\alpha - (\text{Cy}_3\text{P})\text{CdCl}_2$  are best interpreted in terms of a genuine tetrameric structure in contrast to those of  $\alpha - (\text{Bu}^n_3\text{P})\text{HgCl}_2$  which have been interpreted on the basis of a distorted dimeric structure.

**Figure 4.5** Far-infrared and Raman spectra of  $\alpha$ -(Cy<sub>3</sub>P)CdCl<sub>2</sub>

infrared (ca.300K)



Raman(ca.300K)

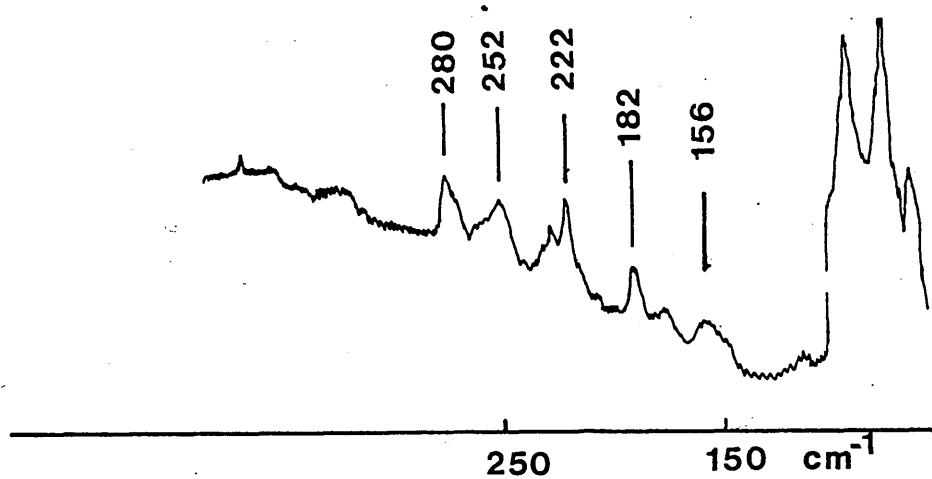


Table 4.5

Vibrational assignments for  $\alpha$ -(Cy<sub>3</sub>P)CdCl<sub>2</sub>

<u>Band position / cm<sup>-1</sup></u>		<u>Assignment</u>
<u>I.R.</u>	<u>Ra</u>	
	279	$\sim(\text{Cd-Cl})_t A_g$
278		$\sim(\text{Cd-Cl})_t A_u$
	272	$\sim(\text{Cd-Cl})_b A_g$
	259	
253		$\sim(\text{Cd-Cl})_b A_u$
	252	$\sim(\text{Cd-Cl})_b A_g$
229		$\sim(\text{Cd-Cl})_b A_u$
	228	$\sim(\text{Cd-Cl})_b A_g$
209		$\sim(\text{Cd-Cl})_b A_u$
	185	$\sim(\text{Cd-Cl})_b A_g$
	172	
	152	$\sim(\text{Cd-P}) A_g$
124		$\sim(\text{Cd-P}) A_u$

### 4.3 Summary of structure/spectra correlations

The infrared spectra (and to a lesser extent the Raman spectra) of  $(R_3P)CdX_2$  complexes show features which are considered characteristic of each of three structures shown, and these are summarized as follows.

The halogen-bridged dimer structure is exemplified by  $(Et_3P)CdI_2$ , which exhibits the expected  $\nu(Cd-I)_t$  mode around  $160\text{ cm}^{-1}$  and the  $\nu(Cd-I)_b$  modes around  $130\text{ cm}^{-1}$  in the infrared spectrum.

The pentaco-ordinate polymeric structure has two sets each of two bands in the infrared, which can be considered as due largely to the movement of the shorter Cd-X bonds (at higher  $\text{cm}^{-1}$ ) and the longer Cd-X bonds (at lower  $\text{cm}^{-1}$ ).

For example, in  $(Me_2PhP)CdX_2$ :

<u><math>(Cd-X)_S / \text{cm}^{-1}</math></u>	<u><math>(Cd-X)_L / \text{cm}^{-1}</math></u>	<u>X</u>
258, 234	144	Cl
188, 178	98	Br
168, 154	n.o.	I

The spectra of  $\alpha-(Cy_3P)CdCl_2$  can be interpreted on the basis of a halogen-bridged tetrameric structure, with  $\nu(Cd-Cl)_t$  around  $280\text{ cm}^{-1}$  and  $\nu(Cd-Cl)_b$  modes between  $272 - 150\text{ cm}^{-1}$ .

#### 4.4 Complexes of unknown structure

a)  $(\text{Bu}^t_3\text{P})\text{CdX}_2$  [ X = Cl, Br or I ] .

In all three infrared spectra (Figure 4.6) there are two groups of bands below  $400\text{ cm}^{-1}$  which progressively shift to lower frequencies as X is changed from Cl to Br to I, and are obviously metal-halogen stretching modes (bands below  $100\text{ cm}^{-1}$  for the chloride are clearly deformation modes). The higher wavenumber bands in all three spectra ( $290$ ,  $200$  and  $161\text{ cm}^{-1}$  for chloro-, bromo- and iodo- derivatives respectively), are clearly assigned to the  $\mathcal{D}(\text{Cd-X})_{\text{t}}\text{B}_{\text{u}}$  mode of a halogen-bridged dimer (Table 4.6). The corresponding Raman bands  $\mathcal{D}(\text{Cd-X})_{\text{t}}\text{A}_{\text{g}}$ , are located at  $281$ ,  $200$  and  $160\text{ cm}^{-1}$  for the chloro-, bromo- and iodo- complexes respectively).

The lower wavenumber infrared absorption in each case, at ca.  $202\text{ cm}^{-1}$  (broad),  $151$  and  $146\text{ cm}^{-1}$ , and  $127\text{ cm}^{-1}$  for the chloride, bromide and iodide respectively, are in the usual positions and show the expected shift for  $\mathcal{D}(\text{Cd-X})_{\text{b}}$  of a halogen-bridged dimer (c.f. Section 1.4.4). In the Raman spectrum, (Figure 4.7) bands at  $208$  (broad),  $160$  and  $136\text{ cm}^{-1}$  for the chloro-, bromo- and iodo- complexes respectively are similarly assigned as being due to the coincidence of  $\mathcal{D}(\text{Cd-X})_{\text{b}}\text{A}_{\text{g}}$  and  $\mathcal{D}(\text{Cd-X})_{\text{b}}\text{B}_{\text{g}}$  modes. These results obtained are in good accord with those of previous workers [ 36 ], except that the bands due to the the  $\mathcal{D}(\text{Cd-I})_{\text{b}}$  modes in the infrared were not previously observed.

The spectra are thus readily interpreted in terms of a halogen-bridged dimeric structure. Coincidence (or near coincidence) of  $\nu(\text{Cd-X})_b$  modes in the infrared and in the Raman spectra suggest near symmetrical bridging (c.f. Section 4.2).

As found in previous studies on  $(\text{R}_3\text{P})\text{CdX}_2$  complexes, the  $\nu(\text{Cd-P})$  modes are very difficult to assign with any great confidence.

Figure 4.6

Far-infrared spectra of  $(\text{Bu}_3\text{P})\text{CdX}_2$  ( $\text{X} = \text{Cl}, \text{Br}$  or  $\text{I}$ .) c.a. 30K.

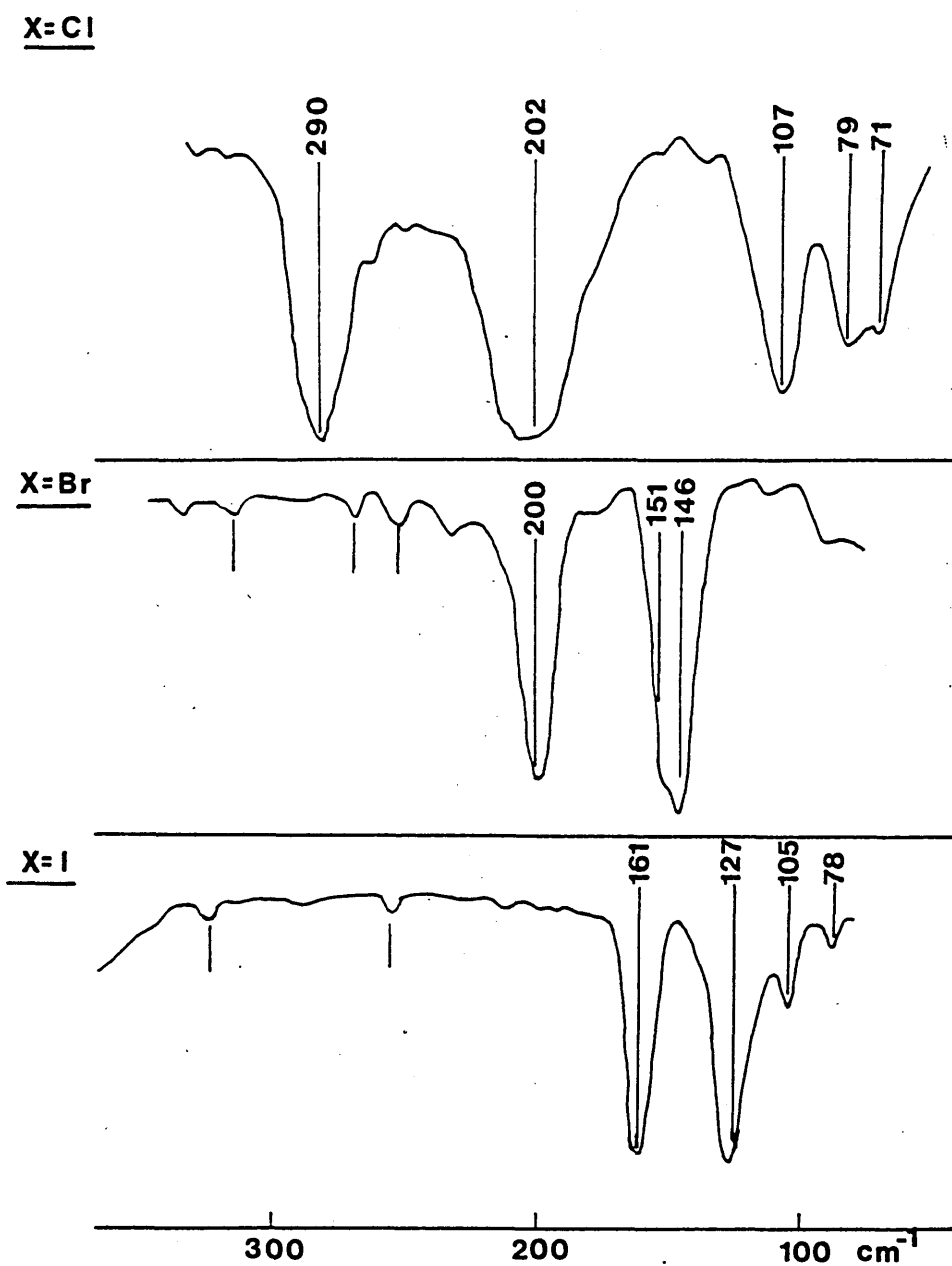


Figure 4.7

Raman spectra of  $(\text{Bu}_3^t\text{P})\text{CdX}_2$  ( $\text{X} = \text{Cl}, \text{Br}$  or  $\text{I}$ .) c a. 70 K.

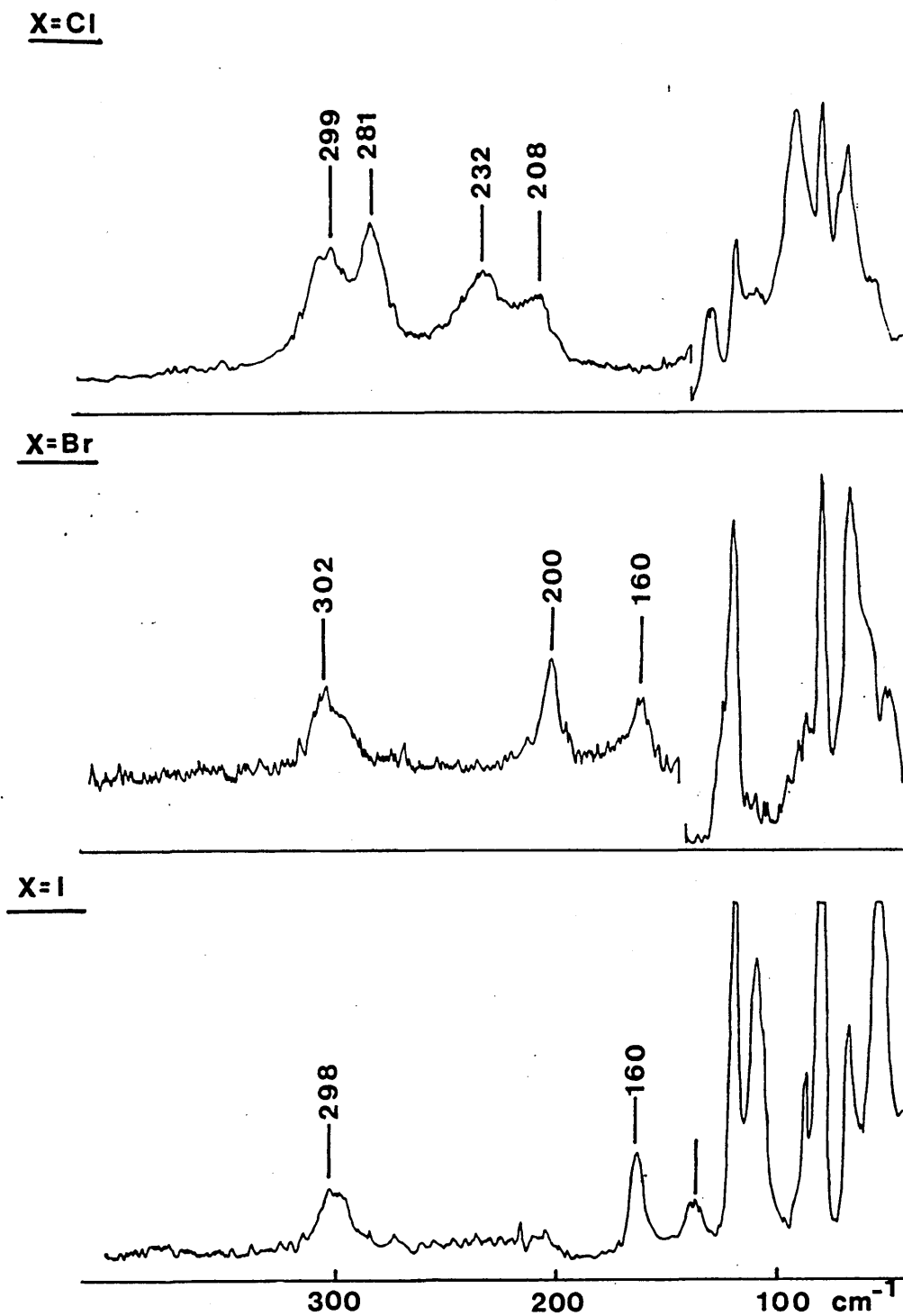


Table 4.6

Vibrational assignments for  $(\text{Bu}^t_3\text{P})\text{CdX}_2$  complexes [ X = Cl, Br or I ] .

( $\text{cm}^{-1}$ )

Cl		Br		I		Assignment
I.R.	Ra	I.R.	Ra	I.R.	Ra	
290		200		161		$\sim(\text{Cd-X})_t B_u$
	281		200		160	$\sim(\text{Cd-X})_t A_g$
202b		151		127		$\sim(\text{Cd-X})_b A_u$ and $B_u$
		146				
	208		160		136	$\sim(\text{Cd-X})_b A_g$ and $B_g$

b)  $(\text{Et}_3\text{P})\text{CdX}_2$  [ X = Cl or Br ].

The iodide derivative has been found crystallographically to be an iodine-bridged dimer and its spectrum has been discussed in an earlier Section (4.2.a).

The vibrational spectra of the chloride and bromide are shown in Figures 4.8 and 4.9 and Table 4.7 contains the wavenumber positions and vibrational assignments.

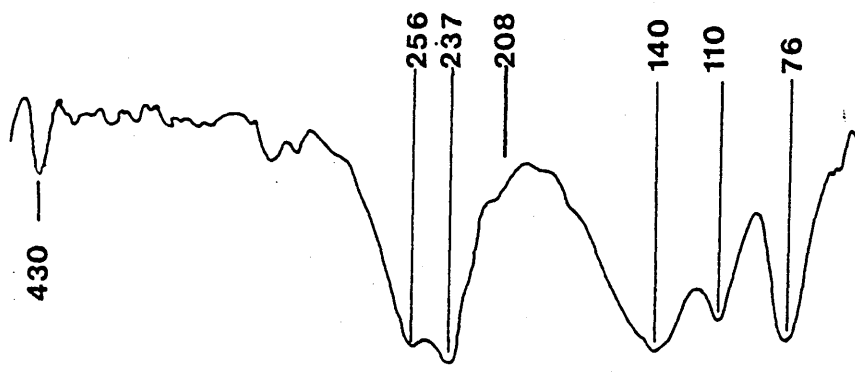
The spectra of the chloride and bromide analogues (Figures 4.8 and 4.9) contain two groups of bands which can be considered as  $\curvearrowright(\text{Cd-X})$  modes, as they show the expected halogen mass shifts, but the patterns of bands are quite different to that of the iodide. In fact, the positions of the bands are not compatible with dimeric structures, but are similar to those assigned for  $\curvearrowright(\text{Cd-X})$  in  $(\text{Me}_2\text{PhP})\text{CdX}_2$  [ X = Cl or Br ], and are hence indicative of similar polymeric structures. The close similarity between the spectra of  $(\text{Et}_3\text{P})\text{CdX}_2$  and  $(\text{Me}_2\text{PhP})\text{CdX}_2$  [ X = Cl or Br ] is illustrated in Table 4.7 (c.f. also Figures 4.3, 4.4, 4.8 and 4.9).

Thus in each case the two higher wavenumber bands are attributed to vibrational modes of the shorter Cd-X bonds of a pentaco-ordinate polymeric structure and the lower wavenumber bands due to the longer Cd-X bonds.

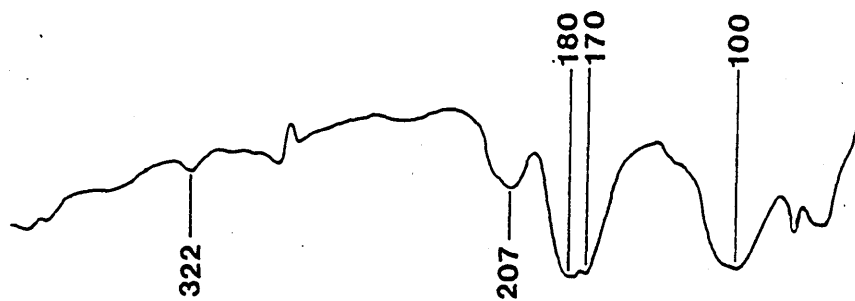
Similarly, in the Raman spectra, bands corresponding to those in the  $(\text{Me}_2\text{PhP})\text{CdX}_2$  for shorter Cd-X bonds are observed at 246 and  $100\text{ cm}^{-1}$  for the chloride and bromide respectively, but the lower  $\curvearrowright(\text{Cd-X})$  Raman bands were not distinguishable. Once again the  $\curvearrowright(\text{Cd-P})$  modes can be tentatively assigned and appear in the infrared spectra at  $110\text{ cm}^{-1}$  (chloride) and  $100\text{ cm}^{-1}$  (bromide).

Figure 4.8 Far-infrared spectra of  $(Et_3P)CdX_2$  ( $X=Cl, Br$  or  $I.$ ), ca.30K.

X=Cl



X=Br



X=I

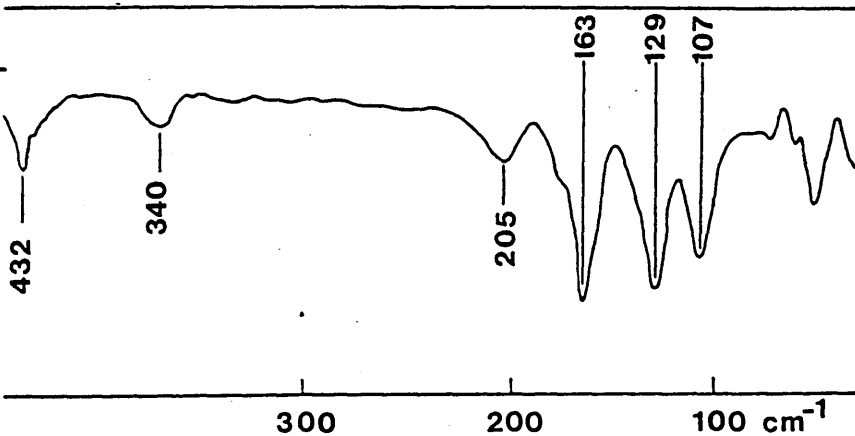
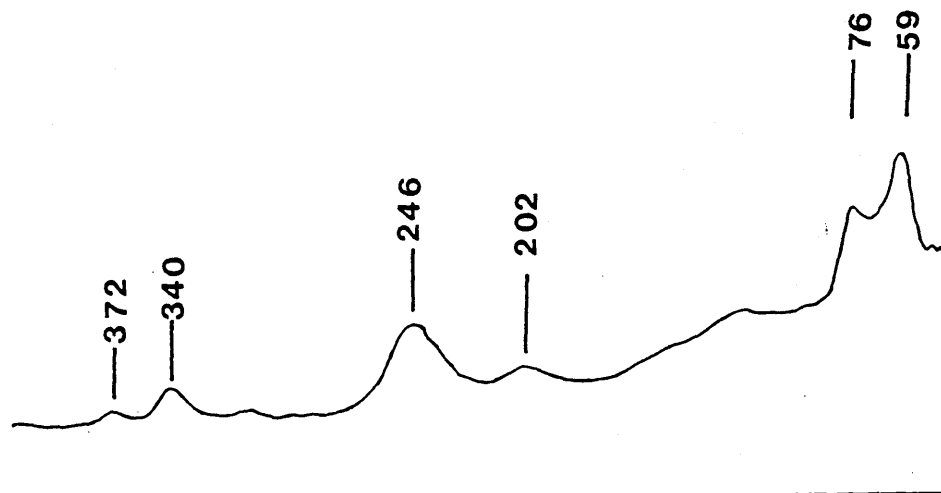


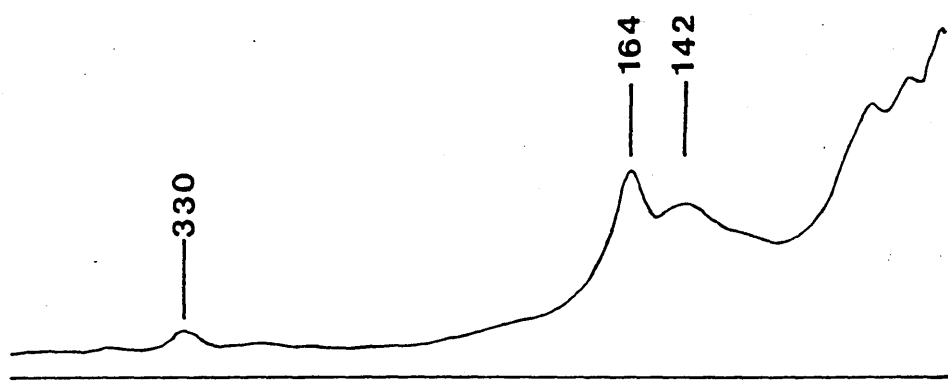
Figure 4.9

Raman spectra of  $(Et_3P)CdX_2$  ( $X=Cl, Br$  or  $I$ ), c a. 70K.

X=Cl



X=Br



X=I

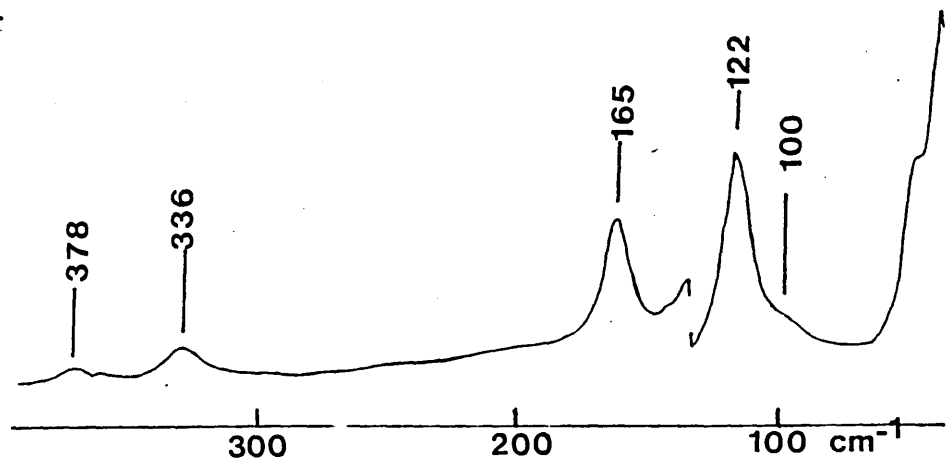


Table 4.7

Vibrational assignments for  $(Et_3P)CdX_2$  [ X = Cl or Br ]

in comparison with  $(Me_2PhP)CdX_2$  [ X = Cl or Br ] ( $cm^{-1}$ ).

$(Et_3P)CdCl_2$		$(Me_2PhP)CdCl_2$		$(Et_3P)CdBr_2$		$(Me_2PhP)CdBr_2$		Assignments
I.R.	Ra	I.R.	Ra	I.R.	Ra	I.R.	Ra	
256		258		180		188		$\sim (Cd-X)_{S_u}^A$
237		234		170		178		
	246		259		164		182	$\sim (Cd-X)_{S_g}^A$
			240				176	
140		144		100		98		$\sim (Cd-X)_1 A_u$
110		134		100		134		$\sim (Cd-P) A_u$
			133				133	$\sim (Cd-P) A_g$

c) (MePh<sub>2</sub>P)CdX<sub>2</sub> [ X = Cl or Br ]

The iodide derivative was not obtained as all attempts gave the 2:1 stoichiometric complex. Identification of internal modes of the ligand was facilitated by reference to an earlier study on (MePh<sub>2</sub>P)<sub>2</sub>PdCl<sub>2</sub> [ 55 ].

The infrared spectra (Figure 4.10) show a  $\nu$  (Cd-X) band pattern similar to that of (Et<sub>3</sub>P)CdX<sub>2</sub> [ X = Cl or Br ] (Figure 4.8) and (Me<sub>2</sub>PhP)CdX<sub>2</sub> [ X = Cl or Br ] (Figure 4.10), and hence are strongly indicative of a pentaco-ordinate cadmium polymeric structure.

Thus the chloride derivative has two strong absorption bands at 256 and 242 cm<sup>-1</sup> which are in the expected region of the spectrum where  $\nu$ (Cd-Cl) modes of the shorter Cd-Cl bonds appear, and are accordingly assigned  $\nu$ (Cd-Cl)<sub>s</sub>A<sub>u</sub> (Table 4.8). The spectrum of the bromide contains a broad absorption band around 183 cm<sup>-1</sup>, again in the approximate position for the  $\nu$ (Cd-Br)<sub>s</sub>A<sub>u</sub> modes of the shorter Cd-Br bonds and also showing the expected halogen-mass shift. On inspection of the Raman spectra (Figure 4.11) it is evident that the chloride derivative has two weak bands at 263 and 253 cm<sup>-1</sup> which appear to correspond to the 256 and 242 cm<sup>-1</sup> infrared bands. However, the Raman spectrum of the bromide shows two similar bands (264 and 255 cm<sup>-1</sup>), so the location of  $\nu$ (Cd-Cl)<sub>s</sub>A<sub>g</sub> is not clear. As there is no other plausible alternative, it is suggested that  $\nu$ (Cd-Cl)<sub>s</sub>A<sub>g</sub> is masked by internal ligand modes at 263 and 253 cm<sup>-1</sup>.

The  $\nu$ (Cd-X)<sub>g</sub>A<sub>g</sub> Raman band for the bromide is found at 180 cm<sup>-1</sup>, well clear of internal ligand modes.

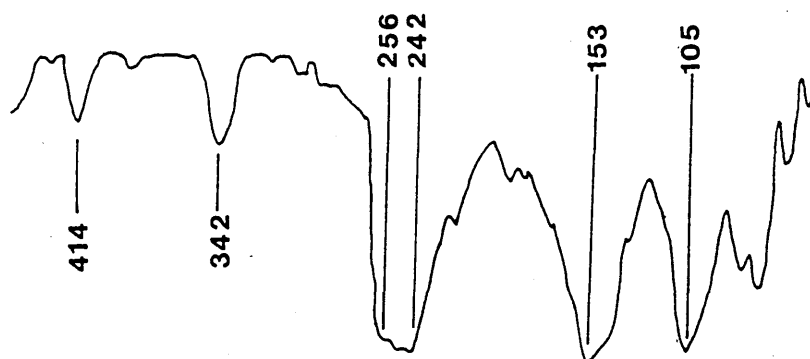
The infrared-active  $\nu$  (Cd-X) modes due to the longer Cd-X bonds of the polymeric structure are evident at  $153 \text{ cm}^{-1}$  (chloride) and c a.  $104 \text{ cm}^{-1}$  (bromide) and are assigned  $\nu$  (Cd-X)  $A_{1u}$ .

Raman bands at  $153$  (chloride) and  $115$  (bromide)  $\text{cm}^{-1}$  are similarly assigned (Table 4.8). The  $\nu$  (Cd-P) mode can be tentatively located at  $105 \text{ cm}^{-1}$  (chloride) and  $104 \text{ cm}^{-1}$  (bromide) in the infrared spectra.

**Figure 4.10**

**Far-infrared spectra of  $(\text{MePh}_2\text{P})\text{CdX}_2$  ( $\text{X}=\text{Cl}, \text{Br}$  or  $\text{I}$ ) c.a. 30 K.**

**X=Cl**



**X=Br**

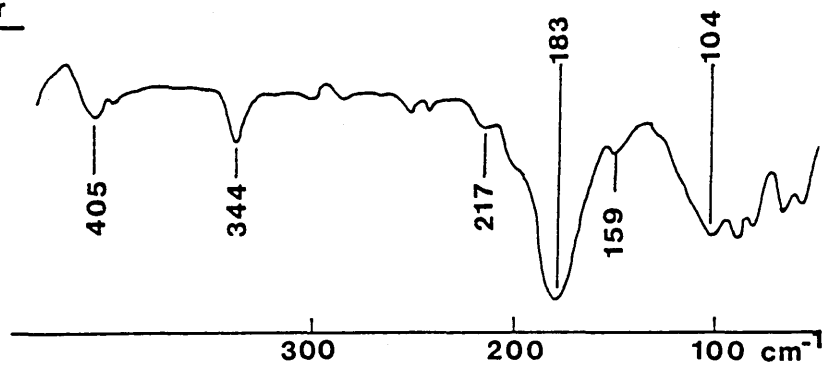
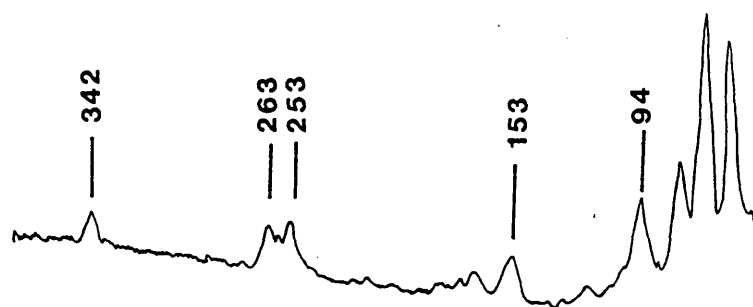


Figure 4.11

Raman spectra of  $(\text{MePh}_2\text{P})\text{CdX}_2$  ( $\text{X}=\text{Cl}, \text{Br}$  or  $\text{I}$ ) c a.70K.

X=Cl



X=Br

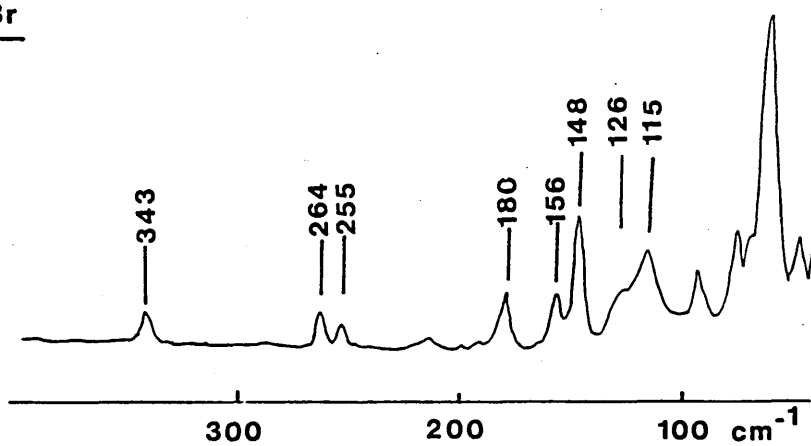


Table 4.8

Vibrational assignments ( $\text{cm}^{-1}$ ) for  $(\text{MePh}_2\text{P})\text{CdX}_2$  [X = Cl or Br].

Cl		Br		Assignments
I.R.	Ra	I.R.	Ra	
256		183		$\sim (\text{Cd-X})_s A_u$
242				
	263 253		180	$\sim (\text{Cd-X})_s A_g$
153		104*		$\sim (\text{Cd-X})_l A_u$
	153		115	$\sim (\text{Cd-X})_l A_g$
105		104*		$\sim (\text{Cd-P}) A_u$

\* Accidental coincidence.

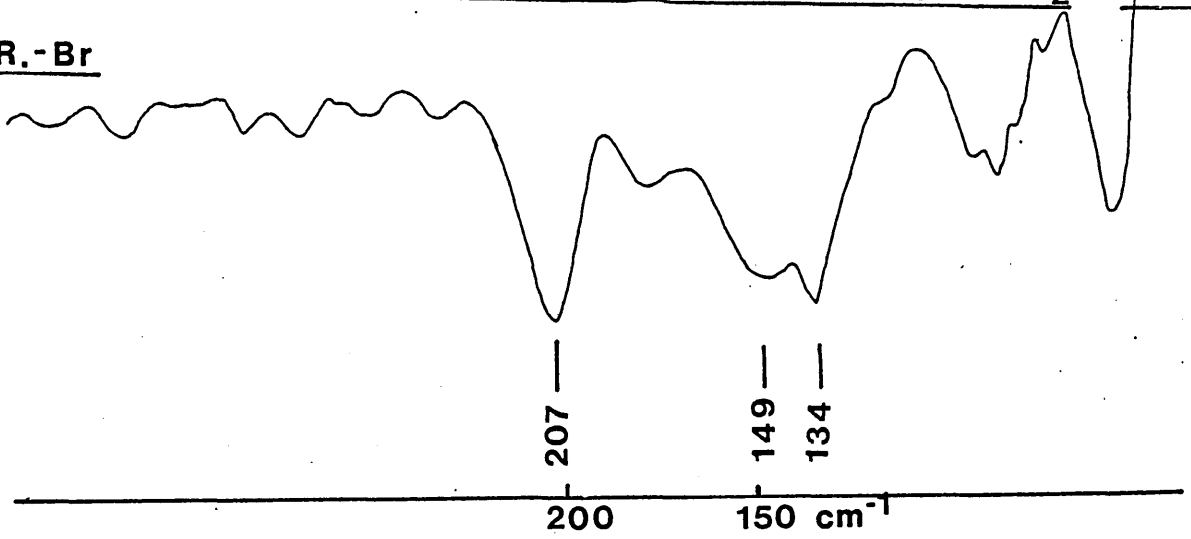
d)  $(\text{Cy}_3\text{P})\text{CdX}_2$  [ X = Cl ( $\beta$  - form), Br or I ].

An interpretation of the spectrum of  $\alpha$ - $(\text{Cy}_3\text{P})\text{CdCl}_2$  has already been given in Section 4.2.c. However a second form of  $(\text{Cy}_3\text{P})\text{CdCl}_2$  (designated the  $\beta$  - isomer) has been reported in the literature [37], its major peaks <sup>are reported (Table 4.9),</sup> along with spectra for the bromide and iodide reported in Figure 4.12.

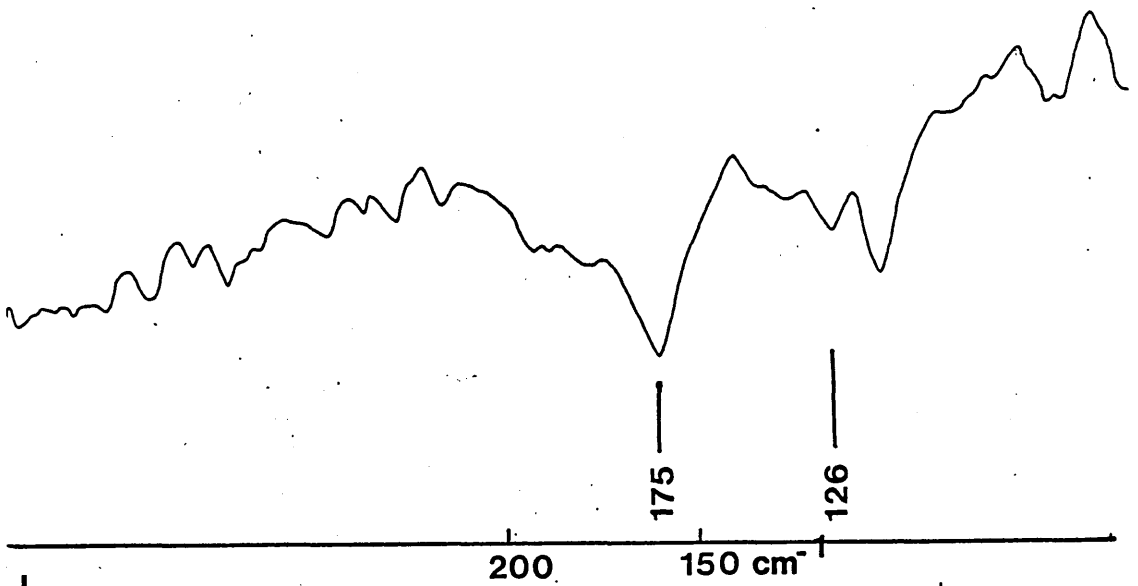
The  $\beta$ - $(\text{Cy}_3\text{P})\text{CdCl}_2$  and the bromide and iodide derivatives give rise to infrared and Raman spectra that contain  $\curvearrowright(\text{Cd-X})$  band patterns typical of a halide-bridged dimer. This is clearly evident by comparison of Figures 4.12 with Figures 4.1, 4.2 [ $(\text{Et}_3\text{P})\text{CdX}_2$ ] and 4.6, 4.7 [ $(\text{Bu}^t_3\text{P})\text{CdX}_2$ ; X = Cl, Br or I]. The assignments given in Table 4.9 have been made on this basis, and are in agreement with literature data [37].

Figure 4.12 Far-infrared and Raman spectra of  $(\text{Cy}_3\text{P})\text{CdX}_2$  ca30K

I.R.-Br



I.R.-I



Ra.-I

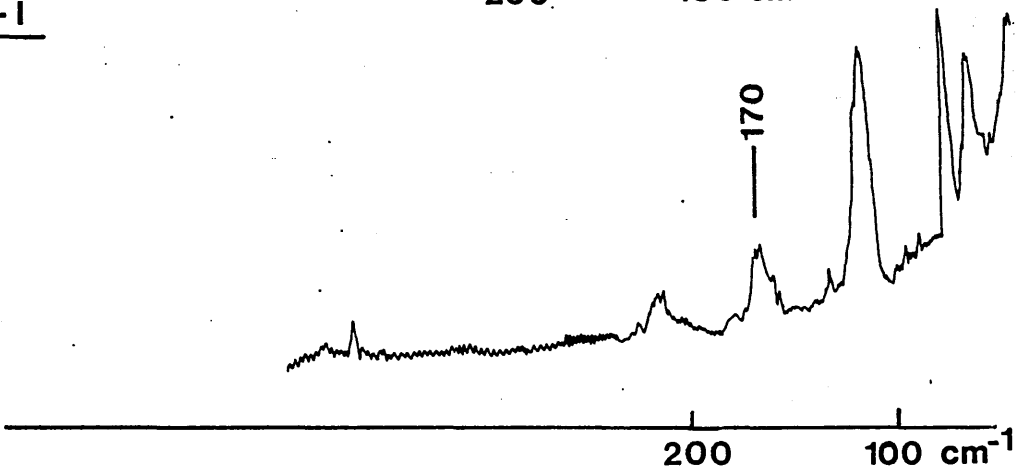


Table 4.9

Vibrational assignments ( $\text{cm}^{-1}$ ) for  $(\text{Cy}_3\text{P})\text{CdX}_2$  complexes

[X = Cl, Br or I]

* Cl ( $\beta$ -form).		Br		I		Assignment
I.R.	Ra	I.R.	Ra	I.R.	Ra	
294		207		175		$\sim(\text{Cd-X})_{\text{t}} \text{B}_{\text{u}}$
	293				170	$\sim(\text{Cd-X})_{\text{t}} \text{A}_{\text{g}}$
210 202		149		126		$\sim(\text{Cd-X})_{\text{b}} \text{A}_{\text{u}}$ and $\text{B}_{\text{u}}$
	183		*148		*121	$\sim(\text{Cd-X})_{\text{b}} \text{A}_{\text{g}}$ and $\text{B}_{\text{g}}$

\* Literature values

CHAPTER 5

DISCUSSION OF FACTORS INFLUENCING THE STRUCTURES

OF SOME  $(R_3P)_nMX_2$  COMPLEXES

[M = Hg, Cd or Zn; n = 1 or 2; X = Cl, Br or I].

## Contents

	<u>Page</u>
5.1 Introduction.	138
5.2 Donor properties of $R_3P$ ligands.	139
5.3 Solid-state structures of $(R_3P)_2HgX_2$ complexes.	143
5.3.1 Discussion of previous $(R_3P)_2HgX_2$ complexes.	143
5.3.2 Discussion of the molecular structure of $(Ph_3P)_2HgCl_2$ .	147
5.4 Solid-state structures of $(R_3P)HgX_2$ complexes.	149
5.4.1 Discussion of previous $(R_3P)HgX_2$ complexes.	149
5.4.2 Discussion of the structure of $\alpha$ - $(Cy_3P)HgCl_2$ .	150
5.5 Structural studies on some $(R_3P)_2CdX_2$ complexes.	159
5.6 Solid-state structures of $(R_3P)CdX_2$ complexes.	161
5.7 An overview of the solid-state structures of $(R_3P)MX_2$ complexes [ M = Cd, Hg or Zn; X = Cl, Br or I ] .	170

## 5.1 Introduction

Discussion of the factors influencing the final solid-state structures of the mercury and cadmium complexes will involve the following criteria:

- (i) the nature of the halogen atom;
- (ii) the nature of the metal;
- (iii) the nature of the  $R_3P$  ligand.

The nature of the halogen atom and the metal will be discussed at the appropriate part of the discussion, however it will be useful to discuss initially the donor properties of the  $R_3P$  ligands (Section 5.2).

## 5.2 Donor Properties of R<sub>3</sub>P ligands

Donor properties of R<sub>3</sub>P ligands are expected to be related to the following parameters:

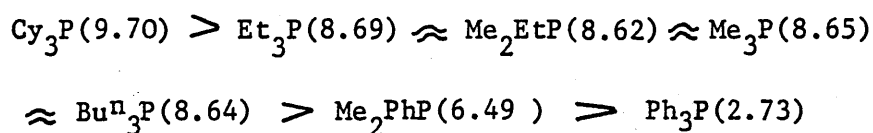
(i) Taft constants ( $\sum \sigma^*$ ) [ 56 ] - which are purely electronic in origin arising from the inductive effects of R- substituents.

(ii) Basicity values ( $\text{p}K_a$ ) [ 56 ] - experimentally determined values of the extent of interaction between R<sub>3</sub>P and a proton in aqueous solution.

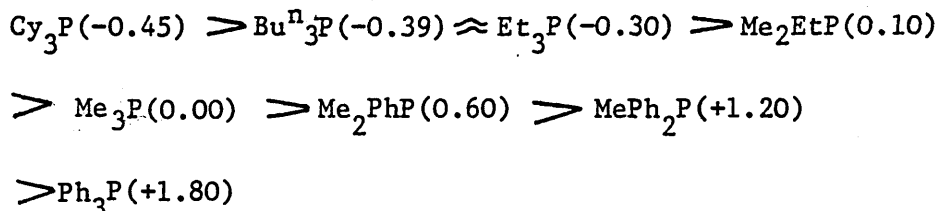
(iii) Cone angle ( $\Theta$ ) [ 57 ] - a steric parameter which is a measure of the degree of congestion around the bonding face of phosphorus.

The orders of donor strengths predicted for the R<sub>3</sub>P ligands under study from the various parameters are as follows:

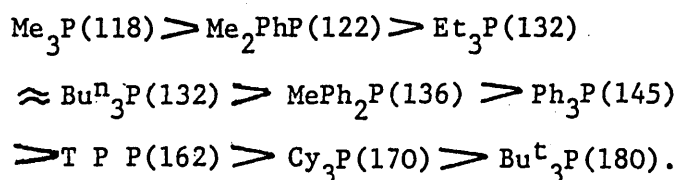
(i)  $\text{p}K_a$  values:



(ii) Taft constants:



(iii) Cone angle ( $^\circ$ ):



The  $pK_a$  values for a range of  $R_3P$  ligands have been obtained [56], and Figure 5.1 shows the values plotted against Taft constants. This plot shows that the donor strength of the  $R_3P$  ligands predicted from Taft constants and  $pK_a$  values correlate reasonably well.

Tolman [57] in relating structural, spectroscopic and equilibria data, and stressed that electronic and steric effects of these  $R_3P$  ligands are inter-related. In support of this, Mann [58] found that  $^{31}P$  chemical shifts of tertiary phosphines could not be correlated simply with the electronegativity of the substituents joined to the phosphorus. It was concluded that steric effects (as identified by variations in C-P-C angles) played a significant role.

Further information on the relative donor strengths of  $R_3P$  ligands has been afforded by a study of the enthalpies of ligation ( $\Delta H_L$ ) of phosphines with mercury (II) halides in benzene solution [59]. It was found that for a particular halide, the  $\Delta H_L$  values (determined at 20°C) correlated reasonably well with Taft constants (Figure 5.2), substantiating the relative donor strengths of these  $R_3P$  ligands as predicted by Taft constants.

Figure 5.1 Plot of pKa of R<sub>3</sub>P ligand in H<sub>2</sub>O vs Taft constant  $\Sigma\sigma^*$

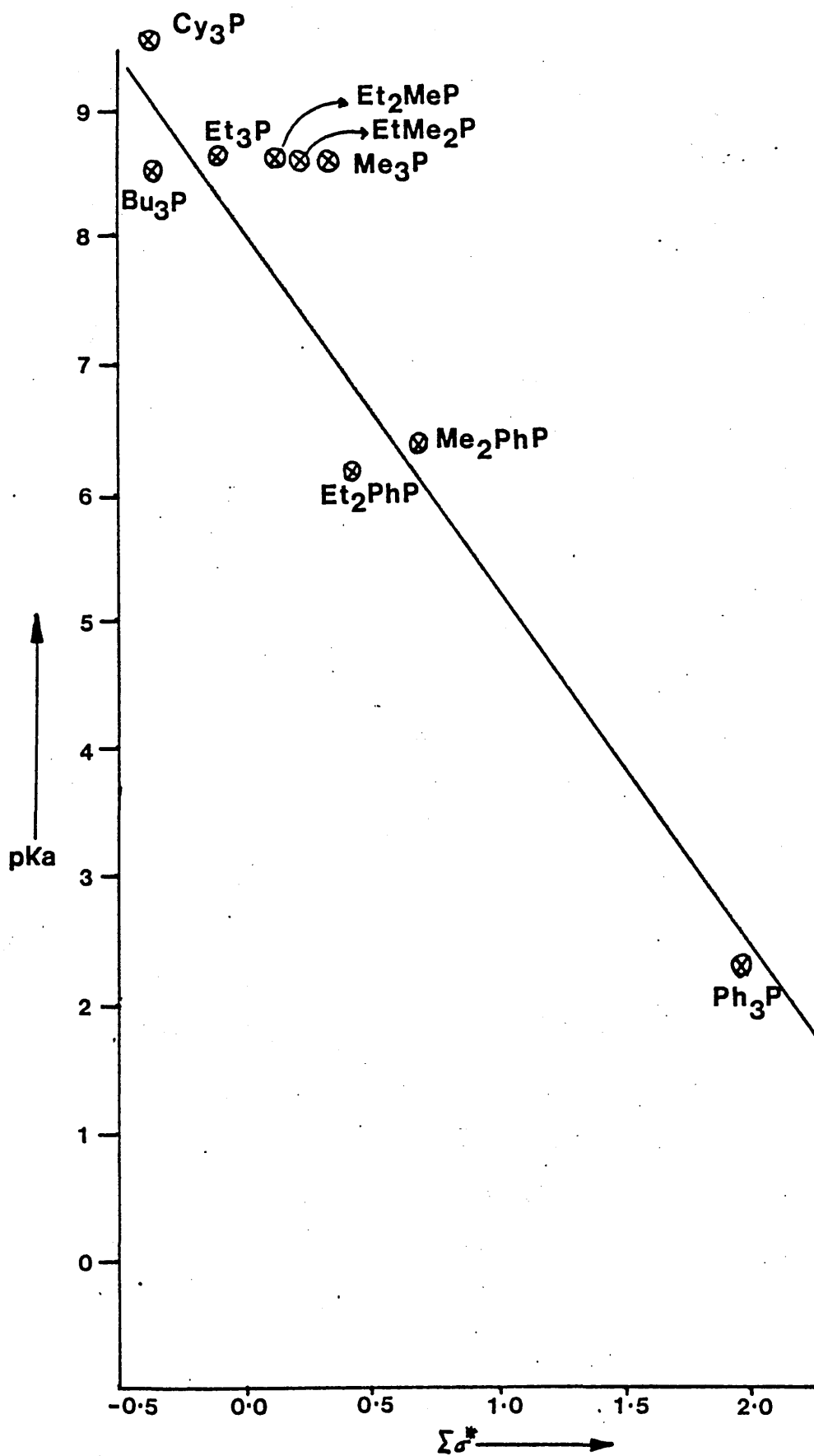
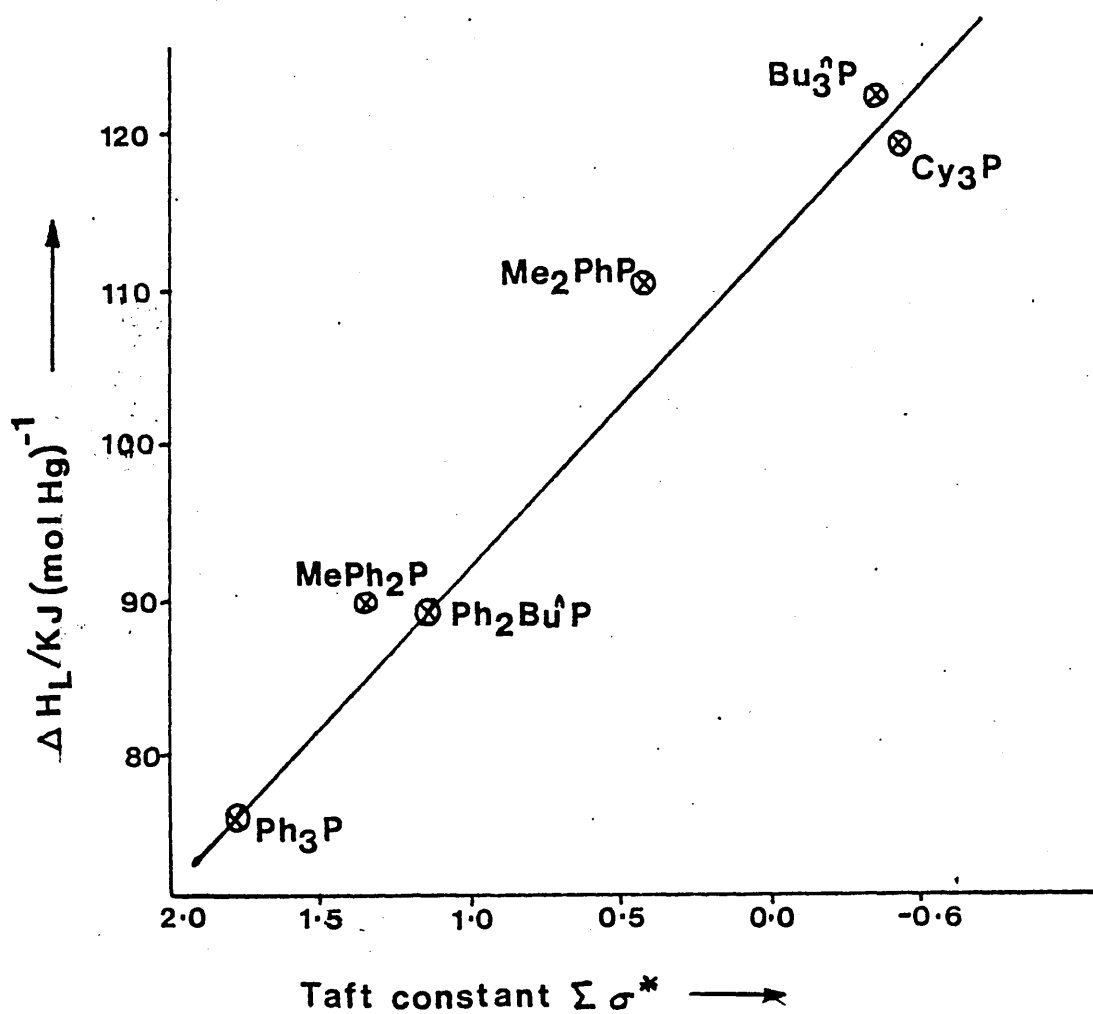


Figure 5.2 Correlation between  $\Delta H_L$  and  $\Sigma \sigma^*$



### 5.3 Solid-state structures of $(R_3P)_2HgX_2$ complexes

#### 5.3.1 Discussion of previous $(R_3P)_2HgX_2$ complexes

The crystal structures of the  $(R_3P)_2HgX_2$  complexes [X = Cl, Br or I], are all known to be monomeric but with varying degrees of distortion from regular tetrahedral geometry (Section 1.3.3). The structures have been rationalised in terms of a competition between the phosphines and halogens for bonding about mercury, and a tendency towards characteristic digonal co-ordination [ 14 ]. Nyholm [ 60 ] and Orgel [ 61 ] explained the latter characteristic in terms of the small  $5d^{10} \rightarrow 5d^96s$  separation of mercury, which allows  $d_{z^2}$  and s orbitals to mix to form ds hybrids which have strong z-directional character (i.e. linear). Two electrons can be placed into each ds hybrid orbital so formed and strong electron density will develop along the + z and - z directions hence favouring linear two co-ordination.

From a consideration of the structural parameters (Table 5.1), a competition of the ligands for the bonding around mercury is indicated. Thus in the complexes having the largest P-Hg-P angles, there is an accompanying percentage increase in the Hg-Cl bond lengths. The shorter Hg-P bond lengths in the  $Et_3P$  complex compared with the values observed in the  $Bu^*_3P$  complex is in accordance with the predicted stronger  $\sigma$ -donor strength of the former ligand. This has been rationalised [ 14 ] in terms of the stronger  $\sigma$ -donor ligand tending to achieve a more linear P-Hg-P arrangement at the expense of the halide.

Table 5.1

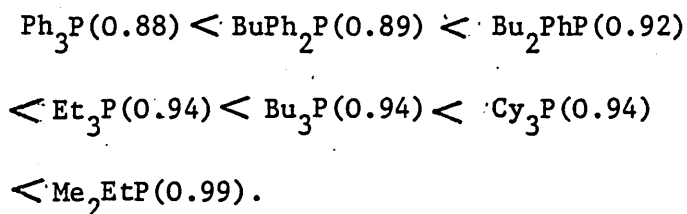
Summary of crystal structures of some  $(R_3P)_2HgX_2$  complexes

X	$R_3P$	Ref.	$d(Hg-X)$ /Å	$d(Hg-P)$ /Å	X-Hg-X /°	P-Hg-P /°	*Ave. % increase in Hg-X
Cl	$Ph_3P$	p.w.	2.558(8), 2.476(13)	2.476(8), 2.378(8)	113.3(4)	135.2(4)	11.0
I	$Ph_3P$	6	2.733(1), 2.763(1)	2.574(1), 2.574(1)	110.43(9)	108.95(4)	7.0
$CF_3$	$Ph_3P$	72	2.12(2)	2.91(2)	146.6(9)	94.8(1)	
CN	$Ph_3P$	73	2.19(1), 2.27(3)	2.43, 2.59	110.4	109(1)	
SCN	$Ph_3P$	73	2.57	2.49	96.7(1)	118.1(1)	
$ONO_2$	$Ph_3P$	73	2.51	2.45	70.0(1)	131.8	
Cl	$Bu^nP$	8	2.55(5), 2.66(5)	2.34(6), 2.64(6)	105(2)	139(2)	14.0
Cl	$Et_3P$	7	2.68(1), 2.68(1)	2.39(1), 2.39(1)	105.5(5)	158.5(5)	17.0
Br	$Me_2EtP$	14	2.72(2), 2.79(2)	2.44(6), 2.50(5)	102(1)	147(2)	16.0
			2.73(3), 2.88(2)	2.39(5), 2.48(6)	107(1)	150(2)	

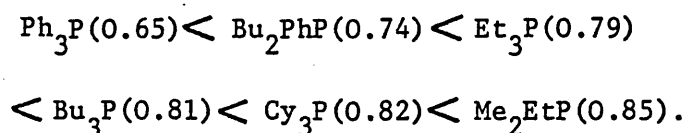
\* % increase in Hg-X is the % increase in the Hg-X bond as compared with the bond lengths found in the gas phase [ 74 ].

The larger P-Hg-P angle found in  $(\text{Et}_3\text{P})_2\text{HgCl}_2$  compared with that in  $(\text{Me}_2\text{EtP})_2\text{HgBr}_2$ , suggests that the nature of the halogen also has an influence on the geometry of these complexes. Table 5.1 contains structural data on a wide range of  $(\text{Ph}_3\text{P})_2\text{HgX}_2$  complexes ( $\text{X} = \text{Cl}, \text{I}, \text{CF}_3, \text{CN}, \text{SCN}, \text{ONO}_2$ ) which indicate that the X groups appear to compete with the phosphorus in bonding around the mercury. Thus when X is a strongly  $\sigma$ -bonding group (e.g.  $\text{CF}_3$ ) the X-Hg-X grouping tends towards a linear arrangement, with the Hg-P bond lengths being relatively long. However, when X is a weaker  $\sigma$ -donor (such as  $\text{ONO}_2$ ), the X-Hg-X angle decreases substantially and the Hg-P bonds become shorter.

Solution phase n.m.r. data [ 62-66 ] complement the solid-phase observations (Table 5.2). For similar  $\text{R}_3\text{P}$  ligands,  $^1\text{J}(\text{HgP})$  values for these  $(\text{R}_3\text{P})_2\text{HgX}_2$  complexes decrease in the sequence of X:  $\text{Cl} \rightarrow \text{Br} \rightarrow \text{I}$  and are higher for complexes involving the stronger P-Hg-P interactions. Expressing the  $^1\text{J}(\text{HgP})$  coupling constants for the  $(\text{R}_3\text{P})_2\text{HgBr}_2$  series as proportions of the values of the corresponding chlorides [ 14 ] , then the variation with  $\text{R}_3\text{P}$  is :



with the iodide derivatives:



These results indicate that as the  $\sigma$ -donor strength of the phosphine increases so it takes a more dominant role in the bonding about mercury at the expense of the halide.

Table 5.2     N.m.r. parameters for some  $(R_3P)_2HgX_2$  adducts [63].

Complex	Solvent	Temp/ $^{\circ}C$	$\delta(P)/Hz$	$\delta(Hg)/Hz$	$^1J(HgP)Hz$
$(Bu^i_3P)_2HgCl_2$	$CDCl_3$	20	28.9	-409	5125
" $HgBr_2$	$CDCl_3$	20	23.9	-476	4829
" $HgI_2$	$CDCl_3$	20	9.3	-722	4089
$(Et_3P)_2HgCl_2$	$CH_2Cl_2$	30	37.1	-409	5067
" $HgBr_2$	$CH_2Cl_2$	30	30.9	-470	4788
" $HgI_2$	$CH_2Cl_2$	30	16.8	-	4004
$(Me_2EtP)_2HgCl_2$	$CDCl_3$	-30	16.0	-497	5606
" $HgBr_2$	$CDCl_3$	-30	14.1	-504	5560
" $HgI_2$	$CDCl_3$	-30	3.2	-555	4778

### 5.3.2 Discussion of the molecular structure of $(\text{Ph}_3\text{P})_2\text{HgCl}_2$

$(\text{Ph}_3\text{P})_2\text{HgCl}_2$  is a monomer with a large P-Hg-P angle (Table 5.1). This angle is strikingly different to that in  $(\text{Ph}_3\text{P})_2\text{HgI}_2$  (135.2(4) compared to 108.95(4)<sup>o</sup>) illustrating the influence of the halogen upon the extent of the tetrahedral distortion. Of the two halogens, it appears that it is the sterically larger iodine, that forms the stronger  $\sigma$ -bonds with mercury, thereby giving rise to a smaller P-Hg-P bond angle. The stronger P-Hg-P interaction in  $(\text{Ph}_3\text{P})_2\text{HgI}_2$  is also indicated by the shorter Hg-P bond lengths.

Considering the  $(\text{R}_3\text{P})_2\text{HgX}_2$  structures in the general context of  $\text{L}_2\text{HgX}_2$  complexes two separate mercury-ligand interactions are evident:

(i) With the weaker interactions e.g. in  $(\text{Py})_2\text{HgCl}_2$  [ 67 ],  $(\text{Phenoxathiin})_2\text{HgCl}_2$  [ 68 ] and  $(\text{CH}_3\text{OH})_2\text{HgCl}_2$  [ 69 ], the complexes all contain virtually undistorted  $\text{HgCl}_2$  units which are weakly attached to two donor ligands. Additional Hg-Cl contacts between the monomers result in polymeric arrangements with the mercury atoms in distorted octahedral environments.

(ii) With the stronger interactions of sulphur- or phosphorus-donor ligands, the resulting monomeric structures range from the undistorted tetrahedral  $(\text{Ph}_3\text{P})_2\text{HgI}_2$  [ 6 ], through the distorted tetrahedral arrangements found in the stronger  $\text{R}_3\text{P}$  complexes [ 7,8,14 ], to an arrangement in which the donor-ligands appear to displace the halogen atoms and adopt digonal co-ordination about mercury e.g.  $(\text{thiosemicarbazide})_2\text{HgCl}_2$  [ 70 ]. In  $(\text{thiourea})_2\text{HgCl}_2$  [ 71 ] for example one chlorine atom has actually been displaced resulting in an ionic structure consisting of  $[(\text{tu})_2\text{HgCl}]^+$  and  $\text{Cl}^-$  ions.

Finally, it has been shown [ 14 ] (Section 1.3.5) that the wavenumber positions of  $\nu(\text{Hg-X})$  modes for the  $(\text{R}_3\text{P})_2\text{HgX}_2$  monomers reflect the stereochemistry, and  $\nu(\text{Hg-X})$  modes may be found within a range of wavenumbers viz. 160-240, 110-166 and 90 - 140  $\text{cm}^{-1}$  for chloro-, bromo- and iodo complexes, respectively. The  $\nu(\text{Hg-X})$  modes which occur at the lower wavenumber ends of these ranges indicate larger P-Hg-P angles and longer Hg-X bonds. Chapter 2 contains spectroscopic data for  $(\text{Cy}_3\text{P})_2\text{HgCl}_2$  which are re-interpreted with the knowledge of the above relationship. In view of the  $\nu(\text{Hg-X})$  positions (Section 2.4) the geometry of  $(\text{Cy}_3\text{P})_2\text{HgCl}_2$  can be considered similar to that of  $(\text{Bu}^n_3\text{P})_2\text{HgCl}_2$ , which in turn indicates similar P-Hg-P interactions.

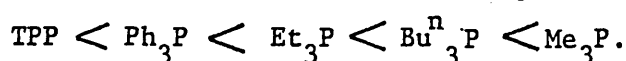
## 5.4 Solid-state structures of $(R_3P)HgX_2$ complexes

### 5.4.1 Discussion of previous $(R_3P)HgX_2$ complexes

The solid-state structures of  $(R_3P)HgX_2$  complexes (Section 1.3.2) range from a discrete dimer, through a loosely held tetramer to various polymeric structures, all formed by varied extents of halogen bridging. It has been suggested [ 14 ] that these results can be rationalised in terms of a reaction pathway involving the following steps:

- (i) An initial Hg-P interaction in solution, whereby the  $R_3P$  ligand approaches the  $HgX_2$  unit. The degree of Hg-P interaction may be related to the donor strength of  $R_3P$ .
- (ii) The formation of a stable solution-phase species which from limited data, [ 76-79 ], appears to be a halogen-bridged dimer.
- (iii) The final step of the pathway is crystallisation, and structural data for selected  $(R_3P)HgCl_2$  complexes are summarised in Table 5.3.

The feature most worthy of note is the variation of the  $Cl_s$ -Hg-P angle. The value of this angle varies from  $127.8(5)^\circ$  [  $(TPP)HgCl_2$  ] to  $162.1(1)^\circ$  [  $(Me_3P)HgCl_2$  ] and may be related to the nature of the initial Hg-P interaction. Thus as the donor strength of the phosphine increases so a more linear  $Cl_s$ -Hg-P arrangement is adopted, with the phosphine progressively replacing one of the two chlorine atoms. The increasing  $Cl_s$ -Hg-P angle given in Table 5.3 correlates well with the predicted order of donor strengths of the relevant  $R_3P$  ligands (Section 5.1):



However, the data can also be interpreted in terms of differing cone angles for the  $R_3P$  ligands. Thus the extent of association has been related to the size of the phosphine ligand [57] and to help resolve the relative importance of steric factors and donor strengths, the tricyclohexyl complex  $(Cy_3P)HgCl_2$  has been investigated.  $Cy_3P$  is a 'bulky' ligand (cone angle =  $170^\circ$ ) and is known from various data, including  $\Delta H_L$ ,  $^{31}P$  nmr to be a strong donor. In contrast to the small, strong  $\sigma$ -donating  $Et_3P$  and  $Me_3P$  ligands,  $Cy_3P$  is a bulky yet stronger  $\sigma$ -donor and this combination has led to the structural determination of  $\alpha-(Cy_3P)HgCl_2$ .

#### 5.4.2 Discussion of the structure of $\alpha-(Cy_3P)HgCl_2$

The crystal structure of  $\alpha-(Cy_3P)HgCl_2$  shows the presence of two independent chlorine-bridged dimers (Section 2.3). Relevant bond angles and distances for these dimers are given in Table 5.3.

If only donor strength were considered to be important, one would expect the  $Cl_s-Hg-P$  angle to lie in the range observed for the  $Bu^t_3P$  or  $Et_3P$  complexes ( $145-151^\circ$ ). It is surprising therefore to find that the two independent dimers have  $Cl_s-Hg-P$  angles of  $139.6(2)$  and  $132.0(1)^\circ$ . Not only are the values smaller than might be expected but the two angles are also very significantly different. To examine what factors may be important in the understanding of these differences, the two independent dimers have been more closely examined.

Figures 5.3 and 5.4 show parts of the two dimers including the nearest intra- and inter- dimer hydrogen contacts. The related bond distances and angles are summarised in Table 5.4. The nearest  $Cl---H$  contacts are those within the dimer molecules themselves,

Table 5.3 Summary of some structural data for  $(R_3P)_2HgCl_2$  complexes

Complex	Structure	$Cl_s - Hg - P$ / $^\circ$	$d(Hg-P)$ / $\text{\AA}$	$d(Hg-Cl)_s$ / $\text{\AA}$	$d(Hg-Cl)_b$ / $\text{\AA}$	Co-ordination polyhedron about mercury
$(TPP)_2HgCl_2$	asymmetric dimer	127.8(5)	2.44(1)	2.40	2.54, 2.75	Distorted tetrahedron
$(Ph_3P)_2HgCl_2$	Near symmetrical dimer	128.7(4)	2.406(7)	2.37	2.62, 2.66	"
$(Cy_3P)_2HgCl_2$	Two independent dimers					
	i) asymmetrical	132.0(1)	2.412(3)	2.413(3)	2.599(3), 2.778(3)	"
	ii) symmetrical	139.6(2)	2.416(3)	2.391(5)	2.665(5), 2.642(4)	"
$\alpha - (Bu^i)_3P)_2HgCl_2$	Tetramer	147.8(7)	2.35(2)	2.27	2.63, 2.71 2.67, 2.90	
		150.6(7)	2.34(2)	2.28	3.38	
$\beta - (Bu^i)_3P)_2HgCl_2$	Near symmetrical dimer	150.9(3)	2.377(6)	2.348(8)	2.72(6), 2.736(6)	Distorted tetrahedron
$(Et)_3P)_2HgCl_2$	Polymeric chain	145.4(3)	2.35(1)	2.42	2.56, 3.04 3.21	Distorted trigonal bipyramid
$(Me)_3P)_2HgCl_2$	'ionic chain'	162.1(1)	2.365(3)	2.355	2.78, 2.94 3.49	Distorted square- pyramid

Figure 5.3  $(C_7H_9P)HgCl_2$  - Diagram of half of the dimeric unit involving Hg1.

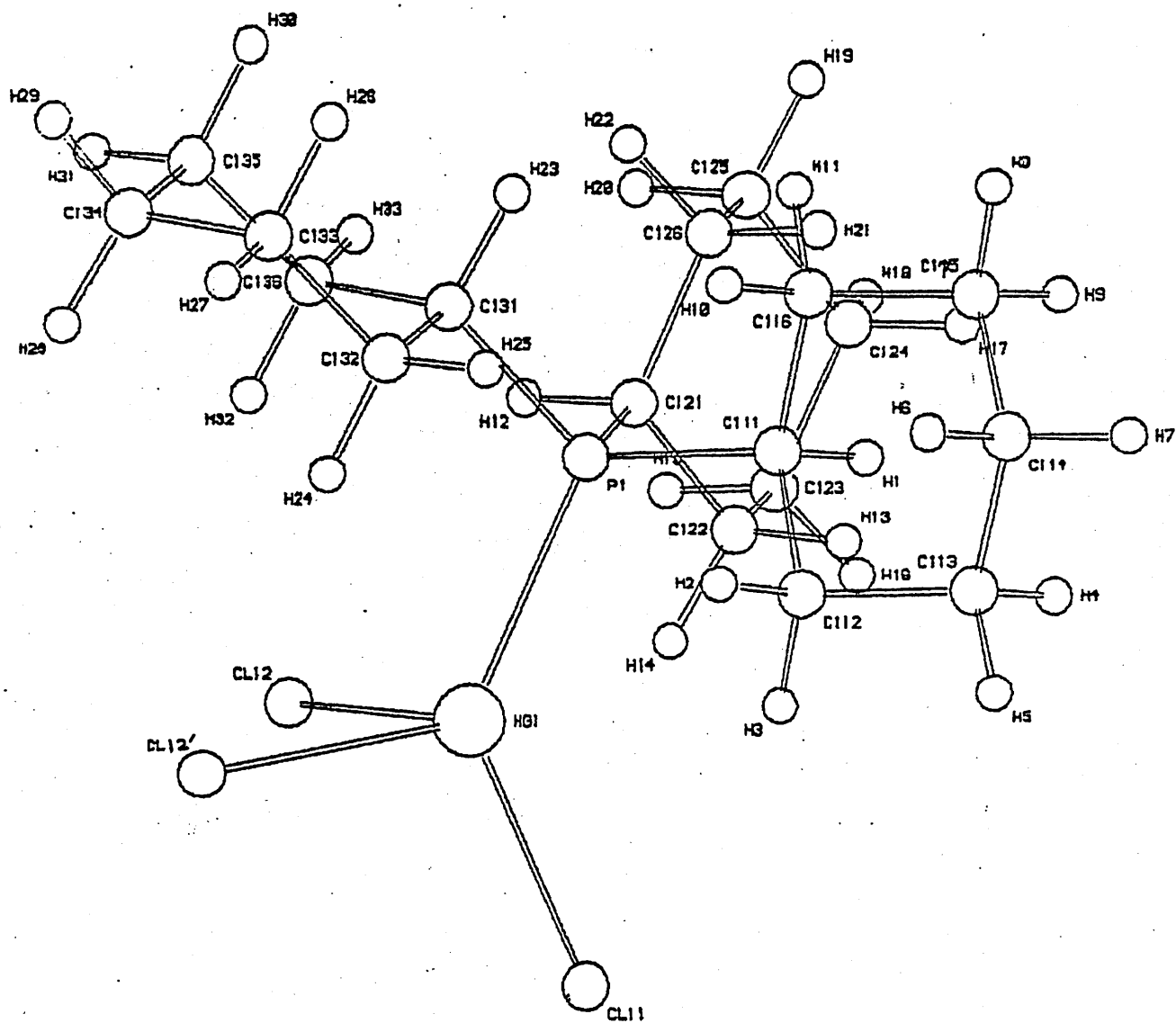


**Figure 5.4**  $(C_{y_3P})HgCl_2$  - Diagram of half of the dimeric unit involving Hg<sub>2</sub>.

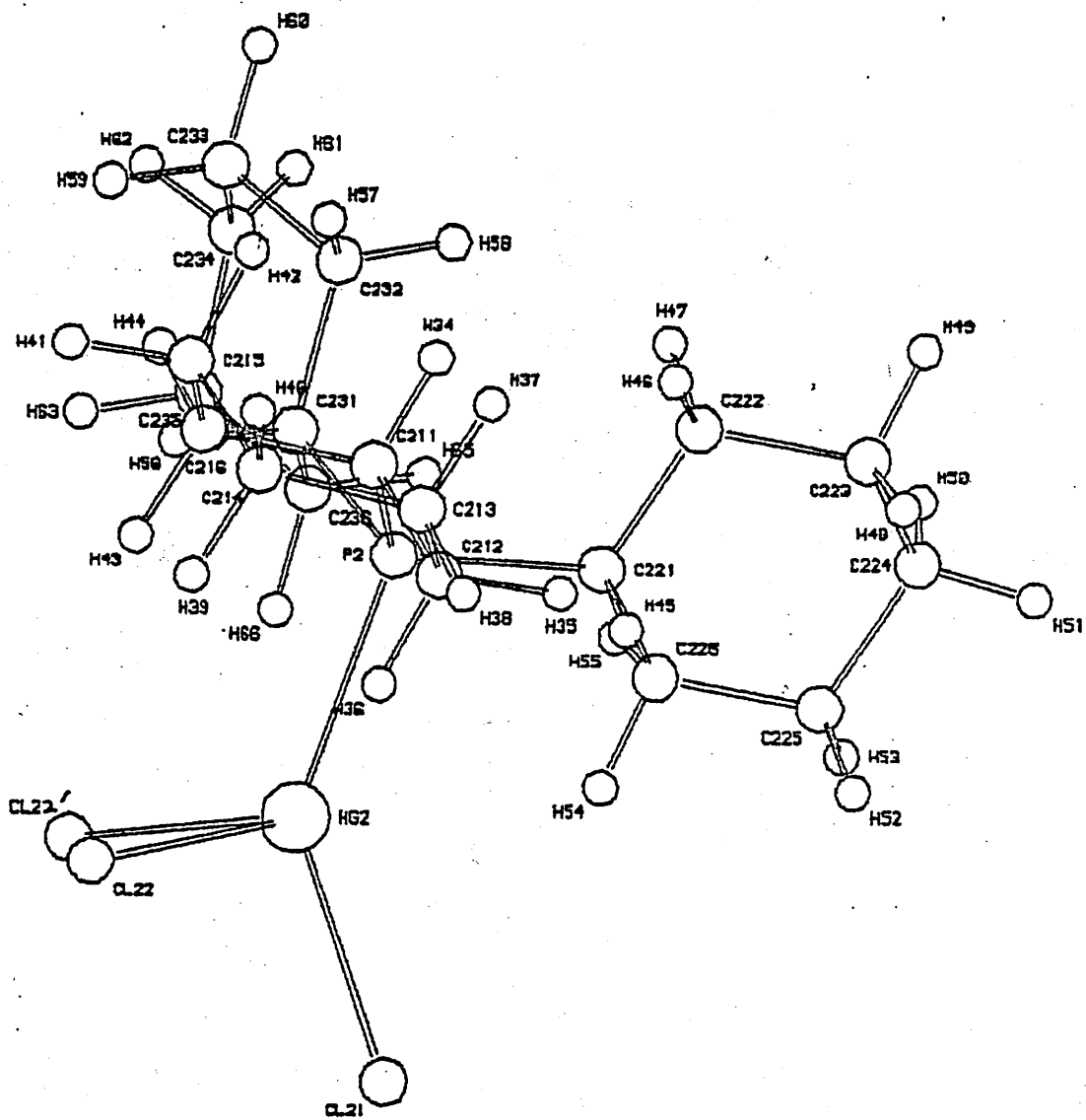


Table 5.4 Structural data for  $(\text{Cy}_3\text{P})\text{HgCl}_2$

a) Bond distances/Å

Hg1 - Cl(11) = 2.413(3)	Hg2 - Cl(21) = 2.391(5)
Hg1 - Cl(12) = 2.778(3)	Hg2 - Cl(22) = 2.642(4)
Hg1 - Cl(12') = 2.599(3)	Hg2 - Cl(22'') = 2.665(5)
Hg1 - P1 = 2.412(3)	Hg2 - P2 = 2.416(3)
P1 - C111 = 1.853(14)	P2 - C211 = 1.839(10)
P1 - C121 = 1.849(11)	P2 - C221 = 1.827(17)
P1 - C131 = 1.830(10)	P2 - C231 = 1.825(11)
*Cl(11)---H4 = 2.899	*Cl(21)---H18 = 2.850
*Cl(12)---H59 = 2.911	Cl(22)---H66' = 2.784
Cl(12')---H24 = 2.803	Cl(22'')---H66 = 2.784
	Cl(22)---H43 = 2.835

\* Intermolecular

b) Bond angles/°

Cl(11) - Hg1 - Cl(12) = 106.1(1)	Cl(21) - Hg2 - Cl(22) = 95.2(2)
Cl(11) - Hg1 - Cl(12') = 101.5(1)	Cl(21) - Hg2 - Cl(22'') = 92.6(3)
Cl(12) - Hg1 - Cl(12') = 85.9(1)	Cl(22) - Hg2 - Cl(22'') = 84.1(2)
Cl(11) - Hg1 - P1 = 132.0(1)	Cl(21) - Hg2 - P2 = 139.6(2)
Cl(12) - Hg1 - P1 = 99.8(1)	Cl(22) - Hg2 - P2 = 111.8(1)
Cl(12') - Hg1 - P1 = 120.3(1)	Cl(22'') - Hg2 - P2 = 108.6(1)
C111 - P1 - C121 = 105.5(6)	C211 - P2 - C221 = 107.5(6)
C111 - P1 - C131 = 110.9(5)	C211 - P2 - C231 = 107.8(5)
C121 - P1 - C131 = 108.7(5)	C221 - P2 - C231 = 111.8(6)

and these distances (Table 5.4) are within the sum of the van der Waals' radii for chlorine and hydrogen ( 2.8 - 3.0Å). It appears that the differing  $Cl_s$ -Hg-P angles can be attributed to differences in the Cl---H intradimer interactions in each of the two dimers. The fact that the Hg-P bond lengths in both dimers (2.412(3) and 2.416(3)Å) and the C-P-C angles of the ligands are similar (Table 5.4), indicates that the cyclohexylphosphine-mercury interactions are similar in the two dimers.

In the near symmetrical dimer (Figure 5.4), the  $Cl_b$ -Hg-P angles are very similar and lie close to a regular tetrahedral value [ 111.8(1) and 108.6(1) for Cl(22)-Hg-P2 and Cl(22')-Hg2-P2 ]. In contrast, the analogous angles in the unsymmetrical dimer (Figure 5.3), are very different to each other [ 99.8(1)° compared to 120.3(1)° for Cl(12)-Hg1-P1 and Cl(12')-Hg1-P1 ]. In both dimers the larger  $Cl_b$ -Hg-P angle is associated with the shorter of the two Hg- $Cl_b$  distances. It is possible therefore that both the  $Cl_b$ -Hg-P angle of 120.3(1)° and the smaller  $Cl_s$ -Hg-P angle found in the asymmetrical dimer, both reflect an attempt to relieve steric strain within the dimer. The origin of the differing strains in the two dimers can be seen by reference to Figures 5.5 and 5.6, which show projections down the respective Hg-P bonds. It can be seen that the nature of the short  $Cl_b$ ---H interactions are subtly different. In the case of the near symmetrical dimer the cyclohexyl groups are so arranged as to give rise to close  $Cl_b$ ---H interactions of (Cl(22')---H66, Cl(22)---H43). The reduction of these steric interactions can be achieved by rotation of the  $Cy_3P$  group about the P2-Hg2 bond. In the asymmetric dimer unit the

Figure 5.5 View down Hg1 - P1 for (Cy<sub>3</sub>P)HgCl<sub>2</sub>.

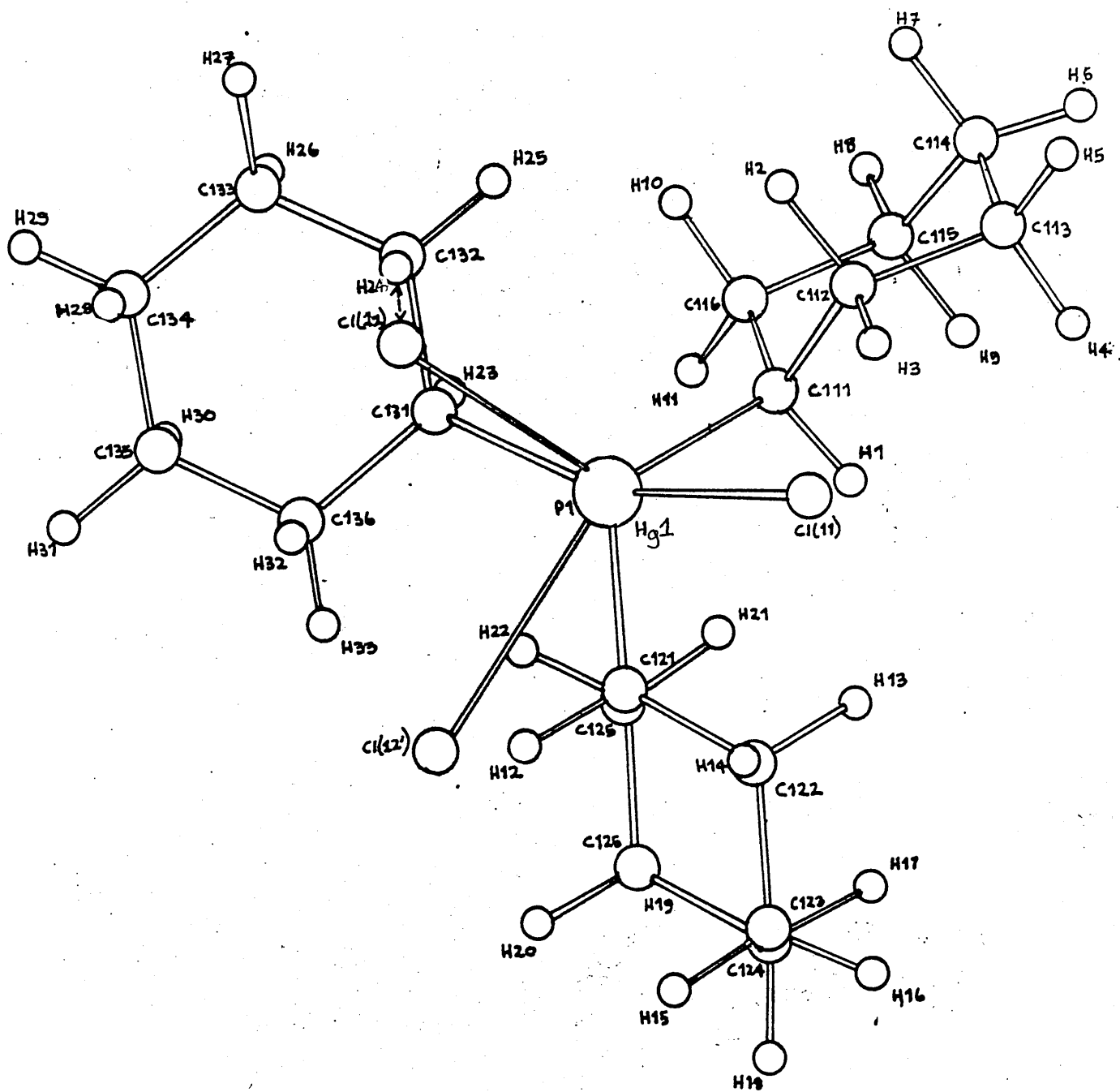
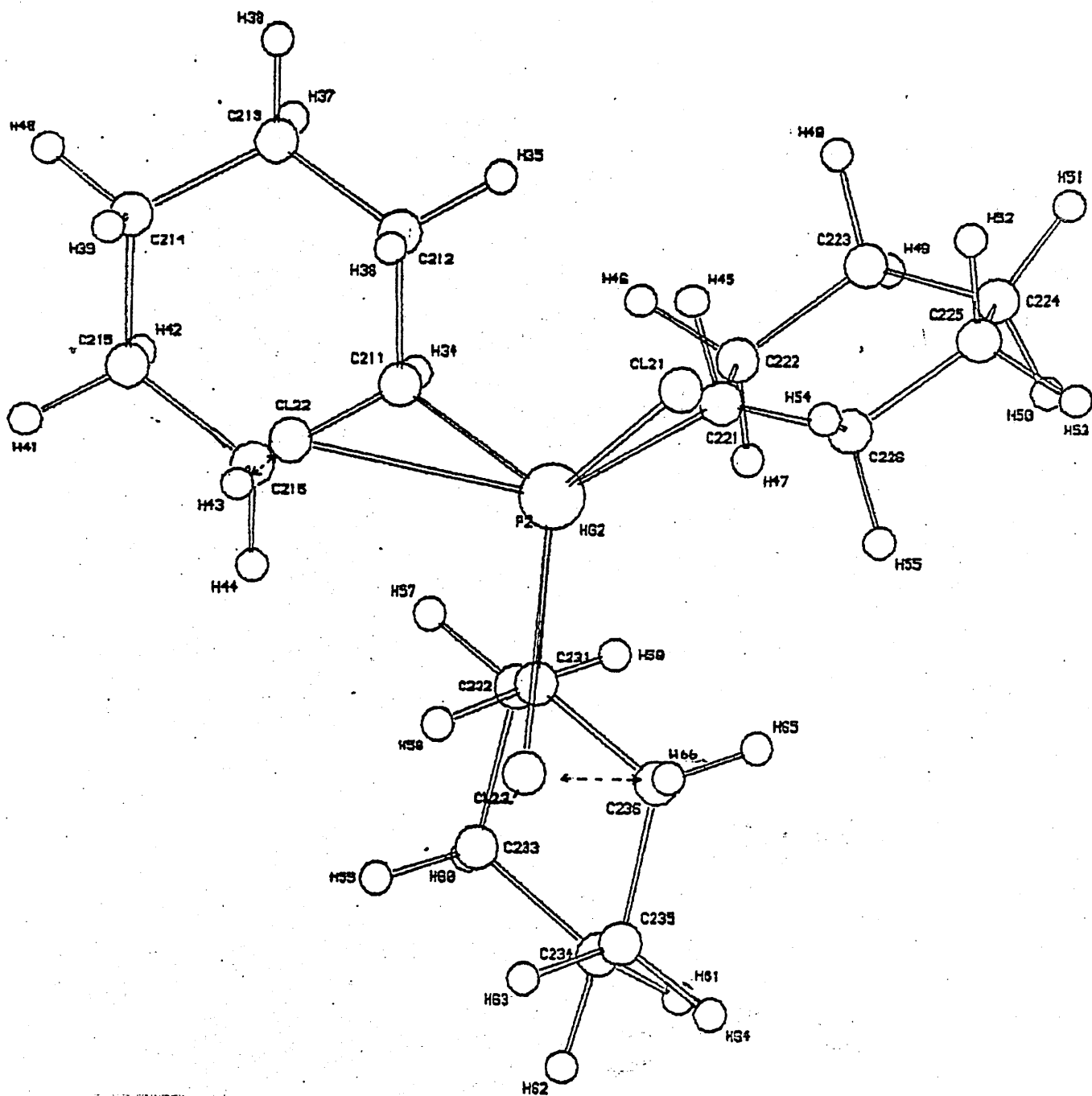


Figure 5.6 View down Hg2-P2 for (Cy<sub>3</sub>P)HgCl<sub>2</sub>.



orientation of the cyclohexyl rings gives rise to only one  $\text{Cl}_b$  --- H close contact ( $\text{Cl}(12')\text{---H}24$ ). The orientation of  $\text{Cl}(12')$  and H24 is such that a reduction in the steric interaction can be achieved by increase of the  $\text{Cl}(12')\text{-Hg1-P1}$  bond angle. Indeed the resulting angle is  $120.3(1)^\circ$ , and is accompanied by a small  $\text{Cl}(11)\text{-Hg1-P1}$  angle of  $132.0(1)^\circ$ . The  $\text{Cl}_s\text{-Hg-P}$  angle of  $139.6(2)^\circ$  found in the near symmetrical dimer can be envisaged as a more 'unstrained' value. While difference between the  $\text{Cl}_s\text{-Hg-P}$  angles in the two dimers has been discussed, both these angles are smaller than that expected for a strong donor ligand. It appears that the 'bulky' nature of the  $\text{Cy}_3\text{P}$  ligand and the inflexibility of the cyclohexyl rings, sterically inhibits the opening up of the  $\text{Cl}_s\text{-Hg-P}$  angle beyond  $139.6^\circ$ .

### 5.5 Structural studies on some $(R_3P)_2CdX_2$ complexes

Spectroscopic data (infrared) on the  $(R_3P)_2CdX_2$  complexes suggest that the structures are all tetrahedral monomers.  $(Ph_3P)_2CdCl_2$  adopts a monomeric tetrahedral structure [33] and the number of modes predicted from point group analysis ( $C_{2v}$ ) is as follows:

$$\nu(Cd-X) = A_1(I.R., Ra) + B_1(I.R., Ra)$$

$$\nu(Cd-P) = A_1(I.R., Ra) + B_2(I.R., Ra)$$

The assignments of bands found in the solid-state far-infrared spectra of various  $(R_3P)_2CdX_2$  complexes are tabulated in Table 5.5. (Analytical data are contained in Appendix A.5).

The positions of both the  $\nu(Cd-X)_s$  and  $\nu(Cd-X)_{as}$  stretching modes for the complexes  $(R_3P)_2CdX_2$  ( $R_3P = Ph_3P, MePh_2P$ ;  $X = Br, I$ ) differ by about  $10\text{ cm}^{-1}$  from the analogous  $(Et_3P)_2CdX_2$  complexes. In the comparable  $(R_3P)_2HgBr_2$  complexes the differences were about  $23\text{ cm}^{-1}$ , which in turn was related to the differing P-Hg-P angles and Hg-Br bond distances (Section 1.3.3). The more limited spectroscopic data within these  $(R_3P)_2CdX_2$  complexes do not afford definite evidence of similar structural variations.

Table 5.5

Far-infrared assignments for some  $(R_3P)_2CdX_2$  complexes

ca. room temperature

<u>Complex</u>	<u><math>(Cd-X)_s/cm^{-1}</math></u>	<u><math>(Cd-X)_{as}/cm^{-1}</math></u>
$(Ph_3P)_2CdCl_2$	268	261
$(Ph_3P)_2CdBr_2$	198	176
$(Ph_3P)_2CdI_2$	166	144
$(MePh_2P)_2CdBr_2$	200	183
$(MePh_2P)_2CdI_2$	163	146
$(Et_3P)_2CdBr_2$	186	168
$(Et_3P)_2CdI_2$	156	135
$(Cy_3P)_2CdCl_2$	* 260	* 260

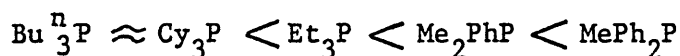
\* broad band

## 5.6 Solid-state structures of $(R_3P)CdX_2$ complexes

In order to rationalise the factors which influence the co-ordination behaviour and final structural arrangements adopted in the solid-state, the initial Cd-P interaction in solution and the stable solution-phase species need to be discussed:

### (i) The initial Cd-P interaction in solution

The extent of the initial Cd-P interaction in solution may be related to the donor properties of the  $R_3P$  ligands (Section 5.1). The order of donor strengths of the  $R_3P$  ligands studied in the  $(R_3P)CdX_2$  complexes is as follows:



Although data is limited, it seems reasonable to assume that the donor properties of  $Bu^{\text{t}}_3P$  are similar to that of  $Bu^{\text{n}}_3P$  and  $Cy_3P$  (Section 5.1).

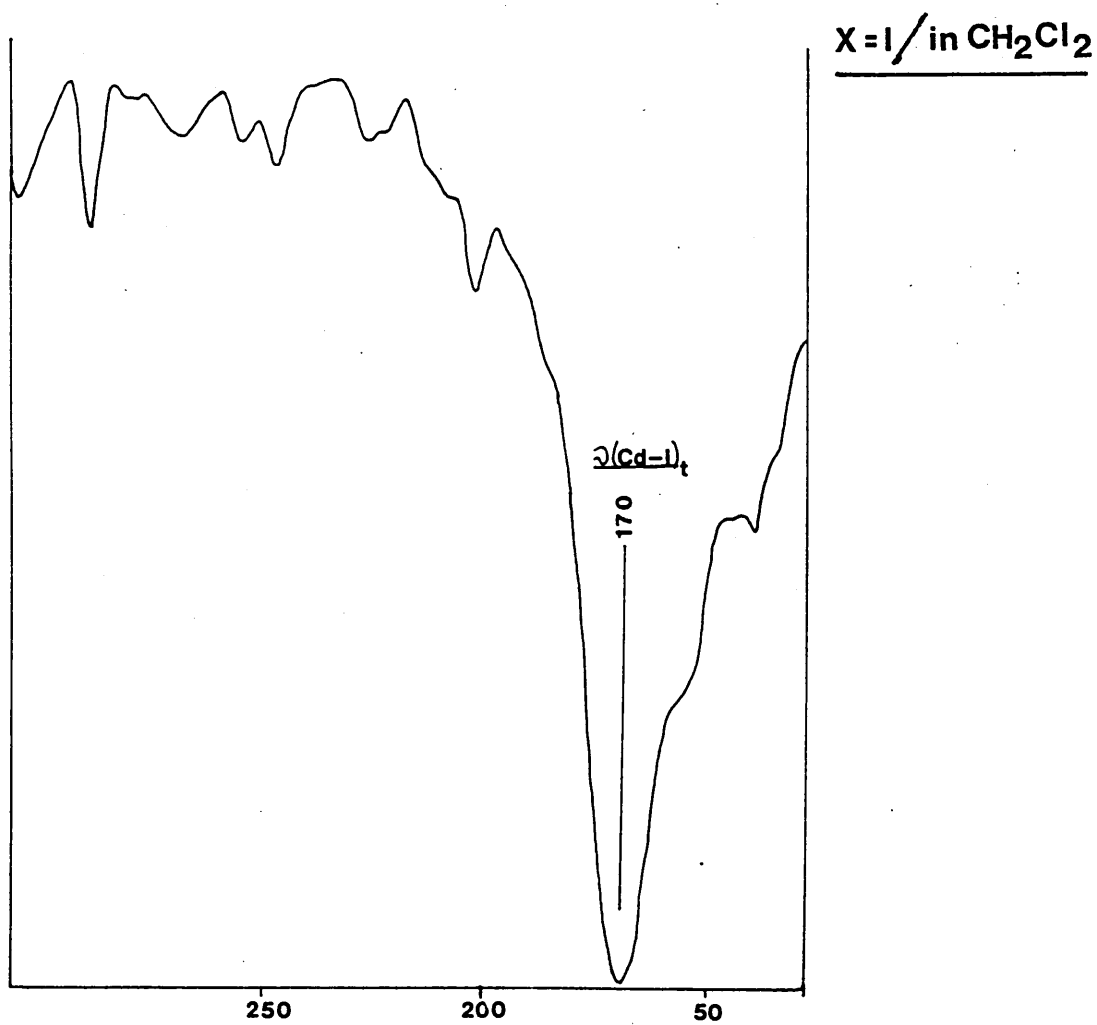
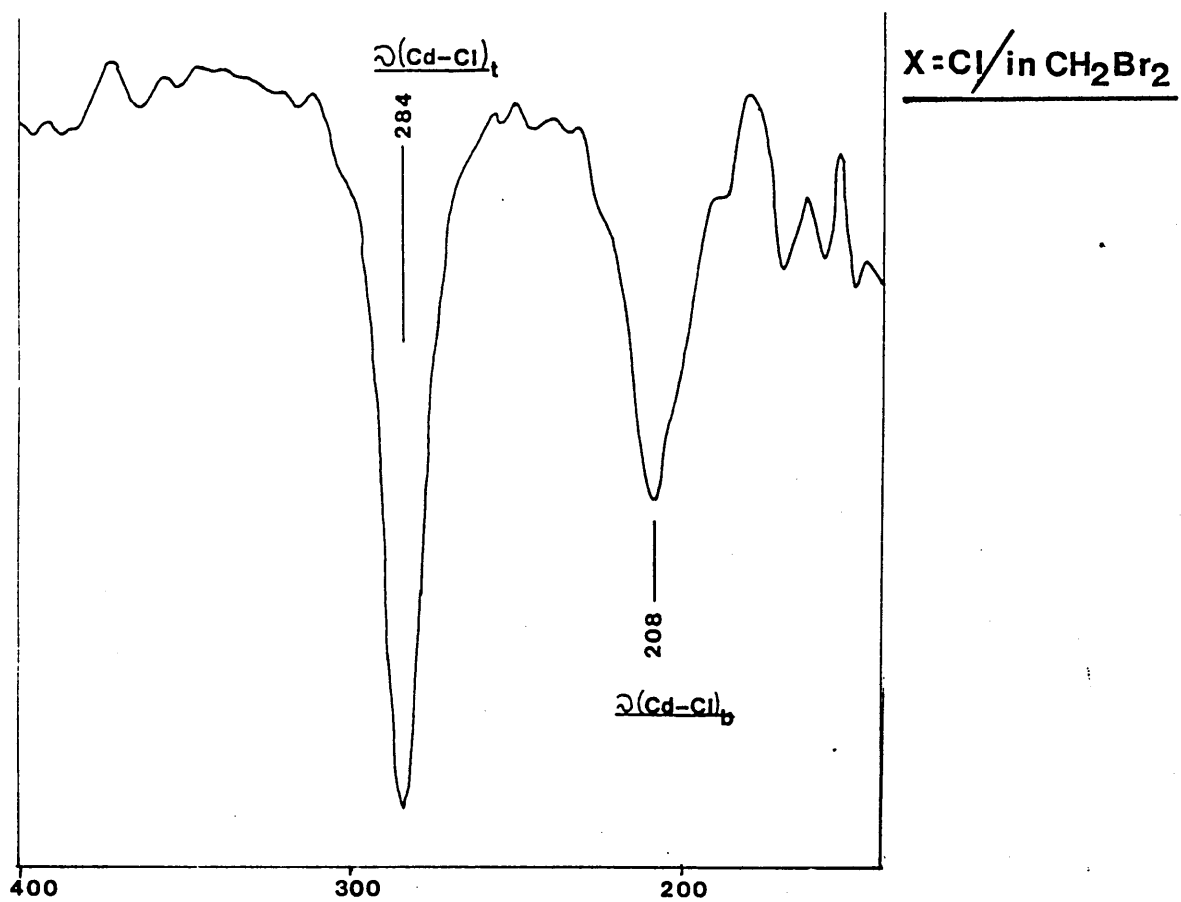
### (ii) Stable solution-phase species:-

Solution phase data on these  $(R_3P)CdX_2$  complexes is limited, reflecting their low solubility in solvents suitable for spectroscopic studies. However, the limited data available do suggest the stable solution phase to be dimeric.

#### a) Far-infrared spectra of $(Bu^{\text{t}}_3P)CdCl_2$ in dibromomethane and $(Me_2PhP)CdI_2$ in dichloromethane:-

The far-infrared spectra together with vibrational assignments are shown in Figure 5.7. By comparison with the solid-state assignments (Section 4.2.b and 4.4.a) the present spectra suggest the presence of halogen-bridged dimers. The  $\omega(Cd-X)_t$  mode is assigned to the bands at 284 and 170  $cm^{-1}$  for the chloride and iodide complexes

**Figure 5.7** Far-infrared spectra of  $(\text{Bu}_3^t\text{P})\text{CdX}_2$  complexes in solution



respectively. The two  $\nu(\text{Cd-Cl})_b$  modes appear at  $208 \text{ cm}^{-1}$  for  $(\text{Bu}^t_3\text{P})\text{CdCl}_2$ , however, the  $\nu(\text{Cd-I})_b$  modes of  $(\text{Me}_2\text{PhP})\text{CdI}_2$  are not observed due to the unsuitability of the solvent in the wavenumber range where the modes are expected.

b)  $^1\text{H}$  and  $^{31}\text{P}$  n.m.r. spectra of  $(\text{Bu}^t_3\text{P})\text{CdX}_2$  ( $\text{X} = \text{Cl}, \text{Br}$  or  $\text{I}$ ) complexes

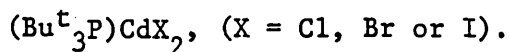
$^{31}\text{P}$  n.m.r. spectra have been recorded using  $\text{CH}_2\text{Cl}_2/\text{CD}_2\text{Cl}_2$  (80/20) as solvent. The chemical shift,  $\delta$  ( $^{31}\text{P}$ ), and coupling constants,  $^1\text{J}(^{111}\text{CdP})$ ,  $^1\text{J}(^{113}\text{CdP})$  and  $^1\text{J}(^{113}/^{111}\text{CdP})$ ,  $\delta$  ( $^1\text{H}$ ) and  $^3\text{J}(\text{P-H})$  were recorded at room temperature and are listed in Table 5.6. These results agree with those observed by Goel et al. [36] and the  $^1\text{J}(\text{CdP})$  values are those expected for a halogen-bridged dimeric arrangement.

Table 5.6

Various n.m.r. parameters for  $(\text{Bu}^t_3\text{P})\text{CdX}_2$  complexes

Complex	$^{31}\text{P}$ ppm	$^1\text{J}(^{111}\text{CdP})$ /Hz	$^1\text{J}(^{113}\text{CdP})$ /Hz	$^1\text{J}(^{113}/^{111}\text{CdP})$ /Hz	$^1\text{H}$ /ppm	$^3\text{J}(\text{P-H})$ /Hz
$(\text{Bu}^t_3\text{P})\text{CdCl}_2$	68.7	2170	2271	1.046	1.57	14.0
$(\text{Bu}^t_3\text{P})\text{CdBr}_2$	62.9	2012	2104	1.046	1.59	13.9
$(\text{Bu}^t_3\text{P})\text{CdI}_2$	48.3	1742	1821	1.046	1.63	13.7

c) Relative molecular mass determinations for



The relative molecular mass determinations obtained in  $\text{CH}_2\text{Cl}_2$  [36] indicate that each compound is essentially dimeric in solution.

(iii) Solid-state structures of  $(\text{R}_3\text{P})\text{CdX}_2$  complexes

The solid-state structures obtained have been given in Chapter 3 and are summarised in Table 5.7.

The latter contains structures obtained from X-ray analysis and also structures that have been inferred from spectroscopic studies. (far-infrared, Raman).

There appear to be two major factors which influence the structures adopted in the solid-state:

- a) the nature of the phosphine;
- b) the nature of the halogen.

a) Role of the tertiary phosphine:

It appears that the tertiary phosphines thought to be the weaker donors give rise to the more extended structures. The stronger donating phosphines give rise to less extended structures, with  $\alpha - (\text{Cy}_3\text{P})\text{CdCl}_2$  being tetrameric and  $(\text{Bu}^t_3\text{P})\text{CdCl}_2$  being a dimeric structure.

A similar trend is seen in the two iodide complexes studied, with  $(\text{Et}_3\text{P})\text{CdI}_2$  being found to be dimeric while  $(\text{Me}_2\text{PhP})\text{CdI}_2$  adopts a polymeric arrangement in the solid-state. The influence of the differing phosphines upon the structures adopted in the solid-state can be readily rationalised in terms of the "Pauling Electroneutrality Principle" [79]. Thus, in the case of those complexes which contain

Table 5.7 Table of structure/spectra correlations for some  $(R_3P)CdX_2$  complexes

← ——— Increasing donating strength of  $R_3P$  ligand

$R_3P$	$Bu_3P$	$Cy_3P$	$Et_3P$	$Me_2PhP$	$MePh_2P$
Cl	* Dimer	+ $\alpha$ -form tetramer	* Pentaco-ord. polymer	+ Pentaco-ord. polymer	* Pentaco-ord. polymer
Br	* Dimer	* Dimer	* Pentaco-ord. polymer	+ Pentaco-ord. polymer	* Pentaco-ord. polymer
I	* Dimer	* Dimer	+ Dimer	+ Pentaco-ord. polymer	-

~~$\beta$ -form Dimer~~

\* from far-infrared/Raman

+ from crystal structure analysis

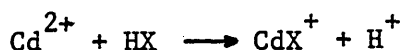
stronger donor-phosphine ligands (e.g.  $(\text{Bu}^t_3\text{P})\text{CdCl}_2$ ), sufficient electron density is donated to cadmium by the phosphine as to require only a tetraco-ordinate dimeric species to be formed.

If, however the amount of electron density donated by the phosphine is reduced (as for example in  $(\text{Et}_3\text{P})\text{CdCl}_2$  and  $(\text{Me}_2\text{PhP})\text{CdCl}_2$ ) the cadmium obtains the extra electron density required to neutralise its positive charge by forming pentaco-ordinate polymeric structures.

In  $\alpha-(\text{Cy}_3\text{P})\text{CdCl}_2$  a tetrameric arrangement is adopted with cadmium occupying both penta- and tetraco-ordinate environments. Such a structural arrangement can be easily correlated with the intermediate donor strength of  $\text{Cy}_3\text{P}$  compared with  $\text{Bu}^t_3\text{P}$ ,  $\text{Me}_2\text{PhP}$ , and  $\text{Et}_3\text{P}$ .

#### b) Role of the halogen

The relative donor strengths of the halogen atoms is indicated by comparison of the  $\log K_1$  values [80] for the following reaction:



$$K_1 = \frac{[\text{CdX}^+][\text{H}^+]}{[\text{Cd}^{2+}][\text{HX}]} \quad (K_1 = \text{stepwise stability constant})$$

<u><math>\log K_1</math></u>	<u>X</u>	<u>Temp/<math>^{\circ}\text{C}</math></u>
2.00	Cl	18
2.17	Br	18
2.42	I	18

Thus the donor strengths of the halogens increase from chlorine to bromine to iodine.

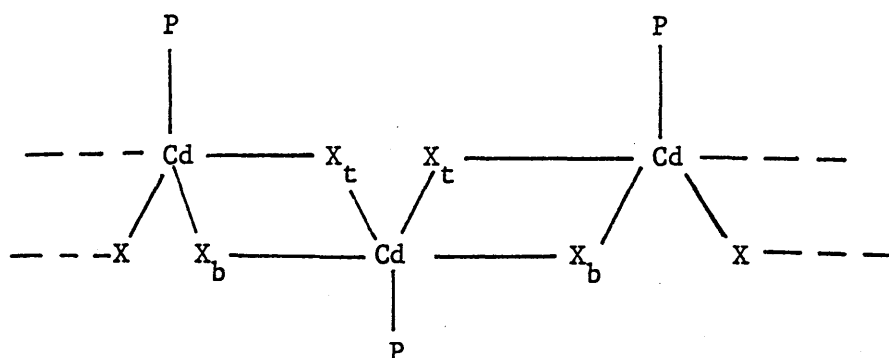
The order of donor strengths of the halogen atoms can be used to rationalise the influence of the halogen upon the structures of the  $(R_3P)CdX_2$  complexes in the solid state. The weaker donating halogens give rise to the more extended pentaco-ordinate structures e.g.  $(Et_3P)CdX_2$  [ X = Cl, Br ], whereas the stronger donating iodine gives rise to the less -extended iodine-bridged dimer. Similarly while  $\alpha$  -  $(Cy_3P)CdCl_2$  adopts a tetrameric structure, the bromide and iodide derivatives are dimeric. Thus the electron density donated by the stronger donor halogen is sufficient as to require only a tetraco-ordinate dimeric species to be formed. When the electron density donated by the halogen is decreased, a more-extended structure is formed.

Even in the complexes  $(Me_2PhP)CdX_2$  ( X = Cl, Br or I ) where all three complexes adopt a pentaco-ordinate polymeric arrangement, the influence of the relative donor strengths of the halogen can be seen.

Differences between the average  $Cd-X_t$  bond distance and the average  $Cd-X_b$  distance are given in Table 5.8. If the donor strengths of the three halogens were the same, the related  $(Cd-X_b)_{AV} - (Cd-X_t)_{AV}$  values would be expected to be similar. However, the values are found to increase from Cl to Br to I and in addition, the  $Cd-X_t$  values become closer to the sum of the covalent radii as the atomic number of X increases. These observations suggest that iodine is much more localised with one cadmium atom compared with the lighter halogens. Thus, of the halogens, it is chlorine that most readily facilitates bridging between  $R_3PCdX_2$  units.

Table 5.8 Comparison of geometries of  $(Me_2PhP)CdX_2$

complexes (X = Cl, Br or I)



<u>X</u>	$Cd-X_b / \overset{\circ}{\text{A}}$	$Cd-X_t / \overset{\circ}{\text{A}}$ A	$(Cd-X_b)_{AV.} / \overset{\circ}{\text{A}}$ $-(Cd-X_t)_{AV.} / \overset{\circ}{\text{A}}$	sum of covalent radii $Cd-X / \overset{\circ}{\text{A}}$ B	A - B
Cl	2.745	2.481	0.25	2.44	0.041, 0.057, <u>0.049</u>
	2.734	2.497			
Br	2.918	2.569	0.33	2.55	0.019, 0.053, <u>0.036</u>
	2.914	2.603			
I	3.242	2.768	0.459	2.74	0.028, 0.019, <u>0.023</u>
	3.201	2.759			

5.7 An overview of the solid-state structures of  $(R_3P)MX_2$  complexes [M = Cd, Hg or Zn; X = Cl, Br or I].

The solid-state structures for these complexes as determined by X-ray analysis and spectroscopic techniques are summarised in Table 5.9.

a)  $(R_3P)CdX_2$  complexes

When the  $(R_3P)CdX_2$  systems are considered in the general context of  $(L)CdX_2$  complexes, the following trends may be seen:

(i) Weaker ligands, for example those containing N- and O- donor atoms give rise to double-chain structures (Section 1.4.2). The small amount of electron density donated by these weaker donors requires cadmium to adopt an octahedral co-ordination.

(ii) With stronger donor ligands such as tertiary phosphine ligands, the co-ordination number about cadmium falls from six to five and/or four. The structures range from the pentaco-ordinate polymeric structures for the weaker donating  $Me_2PhP$  ligand to the tetraco-ordinate dimeric structures found in the stronger donor phosphine complexes (e.g.  $(Et_3P)CdI_2$ ).

b)  $(R_3P)HgX_2$  complexes

The range of structures adopted in the  $(R_3P)HgCl_2$  complexes may be rationalised in a similar way to that given above for the cadmium complexes. As with the  $(R_3P)CdX_2$  complexes, the stronger donating phosphines give rise to less-extended structures. The most extended structures are the dimeric arrangements as found for example in  $(TPP)HgCl_2$ ,  $(Ph_3P)HgCl_2$ ,  $(Cy_3P)HgCl_2$ ,  $(\beta-Bu^N_3P)HgCl_2$ .

Table 5.9 Table of structures for some (R<sub>3</sub>P)MX<sub>2</sub> complexes

(R <sub>3</sub> P)CdX <sub>2</sub>	Increasing donor strength										
	R <sub>3</sub> P X	Me <sub>3</sub> P	Me <sub>2</sub> EtP	Bu <sup>t</sup> <sub>3</sub> P	Cy <sub>3</sub> P	Bu <sup>n</sup> <sub>3</sub> P	Et <sub>3</sub> P	Me <sub>2</sub> PhP	MePh <sub>2</sub> P	Ph <sub>3</sub> P	TPP
	Cl	-	-	D	<del>α-T*</del> β-D	-	P	P*	P	-	-
	Br	-	-	D	D	-	P	P*	P	-	-
	I	-	-	D	D	-	D*	P*	-	-	-
(R <sub>3</sub> P)HgX <sub>2</sub>	Cl	I	I	D	D*	<del>α-D*</del> β-D*	D	D	D	D*	D*
	Br	I	I	D	D	D	D	D	D	D	D
	I	I	I	D	D	D	D	D	D	D	D
(R <sub>3</sub> P)ZnX <sub>2</sub>	Cl	-	-	D	-	-	-	-	-	-	-
	Br	-	-	D	-	-	-	-	-	-	-
	I	-	-	D	-	-	-	-	-	-	-

Key:- D = tetrahedral halogen-bridged dimer; P = Pentaco-ordinate polymer;  
 I = ionic e.g. [R<sub>3</sub>P-M-X]<sup>+</sup> X<sup>-</sup> ; - no complex prepared in the present work.  
 \* crystal structure obtained

Even the 'suggested polymeric'  $(Et_3P)HgCl_2$  and 'tetrameric'  $(\alpha-Bu^t_3P)HgCl_2$  structures can be described in terms of loosely linked dimers. With the strongest donating phosphines, the structures obtained are even less extended with an ionic structure found in  $(Me_3P)HgCl_2$  and suggested for  $(Me_2EtP)HgX_2$  complexes.

The influence of the differing phosphines upon the resulting  $(R_3P)HgX_2$  structures adopted in the solid-state can be rationalised in terms of the "Pauling Electroneutrality Principle". Thus, complexes which contain stronger-donor ligands (e.g.  $(Me_3P)HgCl_2$ ), have sufficient electron density donated to mercury by the phosphine and leads to the formation of an ionic structure,  $[Me_3P-Hg-Cl]^+ + Cl^-$ . However, when the amount of electron density is reduced the additional electron density required by mercury is obtained by forming the tetraco-ordinate dimeric structure.

#### c) $(R_3P)ZnX_2$ complexes

Very few  $(R_3P)ZnX_2$  complexes have been authenticated and most of the phosphine ligands form the 2:1 stoichiometric complexes. The only authenticated 1:1 zinc complexes reported are the  $(Bu^t_3P)ZnX_2$  complexes [36] ( $X = Cl, Br$  or  $I$ ). These have been inferred, from spectroscopic studies, to be halogen-bridged dimers in the solid-state. The difficulty in preparing 1:1  $(R_3P)ZnX_2$  complexes can be explained in terms of the electroneutrality principle. The only 1:1 zinc complexes reported are found by the reaction of zinc dihalides with the strongly donating  $Bu^t_3P$  ligand. The extensive donation of electron density onto the metal enables the formation of stable 1:1 complexes. However, with the weaker  $R_3P$  ligands (e.g.  $Ph_3P$ ) the positive charge on the zinc is not

satisfied by the presence of just one phosphine ligand; and the 2:1 complexes  $(R_3P)_2ZnX_2$  are preferentially formed.

### Summary and suggestions for future work

It has been shown that for the various  $(R_3P)MX_2$  complexes  $[M = Zn, Cd, Hg; X = Cl, Br \text{ or } I]$  a range of structures exists in the solid-state with varying extents of halogen bridging between the ' $(R_3P)MX_2$ ' units. The exact range of structures established depends on the nature of the metal:-

$(R_3P)HgX_2$  complexes: range from 'ionic' monomeric type structures, e.g.  $[Me_3PHgCl]^+Cl^-$ , to the tetraco-ordinate halogen-bridged dimers  $\alpha-(Cy_3P)HgCl_2$ ,  $(TPP)HgCl_2$  and  $(Ph_3P)HgCl_2$ .

$(R_3P)CdX_2$  complexes: range from a halogen-bridged dimeric structure,  $(Et_3P)CdI_2$ , through a halogen-bridged tetrameric structure,  $\alpha-(Cy_3P)CdCl_2$ , to pentaco-ordinate polymeric structures as in  $(Me_2PhP)CdX_2$  ( $X = Cl, Br \text{ or } I$ ).

$(R_3P)ZnX_2$  complexes: the only spectroscopically authenticated structure is the halogen-bridged dimeric complex,  $(Bu^t_3P)ZnX_2$ ;  $X = Cl, Br \text{ or } I$ .

The changes in structure for a given metal may be related to the donor properties of the ligands and the varying extents of the M-P interactions. A rationalisation of the structures found is that the stronger donating  $R_3P$  ligands give rise to the less extended structures and that for a given  $R_3P$  ligand the donor-acceptor interaction decreases in the sequence  $Hg > Cd > Zn$ .

Thus, complexes containing the stronger-donor ligands have sufficient electron density donated to the metal by the phosphine which leads to the formation of the less extended structures. However, when the amount of electron density donated by the phosphine is reduced, the

additional electron density "required" by the metal is obtained by forming the more extended structures through a greater extent of halogen-bridging. The less extended range of structures in the mercury series compared to the range found in the cadmium series, and the fact that the majority of the zinc complexes formed are of the 2:1 stoichiometry, is attributed to the decreased M-P interaction.

Although  $(\text{Me}_3\text{P})\text{HgCl}_2$  is an ionic type complex in the solid-state, there is no information on the equivalent  $(\text{Me}_3\text{P})\text{CdX}_2$  complexes. It would thus be particularly interesting to study the cadmium series, by spectroscopy initially and then the possibility of X-ray structural analysis, to investigate whether or not similar structures are formed.

The nature of the halogen atoms plays an important role in the adopted structures of these  $(\text{R}_3\text{P})\text{MX}_2$  complexes. The structural work on  $(\text{R}_3\text{P})\text{CdX}_2$  complexes, for example where  $\text{R}_3\text{P} = \text{Et}_3\text{P}$ , has shown that for a given phosphine, the more covalent Cd-I bonding gives rise to the less extended iodine-bridged dimer and the chloride gives rise to a more extended pentaco-ordinate structure.

However, no actual X-ray structural evidence has been obtained to suggest a similar structural variation with changing halogen for the  $(\text{R}_3\text{P})\text{HgX}_2$  complexes.

Thus a programme of crystallographic studies, especially of selected  $(\text{R}_3\text{P})\text{HgI}_2$  complexes needs to be carried out.

In the formation of the  $(\text{R}_3\text{P})\text{HgCl}_2$  complexes, the  $\text{Cl}_s\text{-Hg-P}$  angles vary significantly with the nature of the phosphine ligand. The

stronger donating phosphine ligands (e.g.  $\text{Me}_3\text{P}$  and  $\text{Et}_3\text{P}$ ) give rise to a more linear  $\text{Cl}_s\text{-Hg-P}$  angle, reflecting the characteristic linear two co-ordination found in many mercury complexes. For the  $(\text{Cy}_3\text{P})\text{HgCl}_2$  complex the resulting  $\text{Cl}_s\text{-Hg-P}$  of each of the two independent dimeric units present are significantly smaller than expected for a complex containing the strongly donating  $\text{Cy}_3\text{P}$  ligand. This may be attributed to the 'bulky' nature of  $\text{Cy}_3\text{P}$  and the inflexibility of the cyclohexyl rings, sterically inhibiting the opening up of the  $\text{Cl}_s\text{-Hg-P}$  angles.

The structure spectra correlations for the  $(\text{R}_3\text{P})\text{CdX}_2$  complexes has allowed structure/  $\sim(\text{Cd-X})$  mode position relationships to be applied to a number of related complexes of otherwise unknown structure:

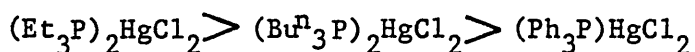
$(\text{Bu}^t_3\text{P})\text{CdX}_2$	$(\text{X} = \text{Cl, Br or I})$	}	discrete halogen-
$(\text{Cy}_3\text{P})\text{CdX}_2$	$(\text{X} = \beta \text{ form Cl, Br or I})$		bridged dimers
$(\text{Et}_3\text{P})\text{CdX}_2$	$(\text{X} = \text{Cl or Br})$	}	pentaco-ordinate
$(\text{MePh}_2\text{P})\text{CdX}_2$	$(\text{X} = \text{Cl or Br})$		polymers

The location of  $\sim(\text{Cd-P})$  modes has been difficult due to the interference of the internal ligand modes, and most assignments have been very tentative.

The structure/spectra correlations for the  $(\text{R}_3\text{P})\text{HgX}_2$  complexes have been extended. A particularly interesting case is that of  $(\text{Cy}_3\text{P})\text{HgCl}_2$  where the spectra, previously interpreted in terms of a distorted dimer structure, can only be properly interpreted on the basis of the presence of two separate dimers found in the solid-state structure. However, while the rationalisation of the structures of

the  $(R_3P)HgX_2$  complexes indicates that all of them, except for  $(Me_3P)HgCl_2$ , are some form of a halogen bridged dimer in the solid-state, their spectra are not very easily interpreted on this basis. Thus the whole question of whether some of these  $(R_3P)HgCl_2$  structures are actual polymers or just different forms of loosely held dimers needs thorough investigation. The spectra of these  $(R_3P)HgX_2$  complexes needs a major re-interpretation with particular attention being paid to the nature and position of the suggested  $\nu(Hg-X)_b$  modes.

In the 2:1 complexes,  $(R_3P)_2HgX_2$ , the X and  $R_3P$  groups compete for the bonding about mercury. A number of  $(R_3P)_2HgCl_2$  complexes consist of extremely distorted tetraco-ordinate monomers. The degree of distortion is shown by the large size of the P-Hg-P angle, which varies in the order:



The variation may be explained by the stronger donating  $R_3P$  ligand competing more effectively than the chlorine atoms for accommodation around mercury in a digonal arrangement. Comparison of the geometries of  $(Ph_3P)_2HgCl_2$  and  $(Ph_3P)_2HgI_2$  shows that the P-Hg-P angles are strikingly different. The larger angle  $135.2(4)^\circ$  is formed when the halogen is the smaller, weaker  $\sigma$ -donor bonding chlorine compared with the iodide  $108.95(4)^\circ$ . This again shows the importance of the linear  $\sigma$ -bonding at mercury.

The  $\nu(Hg-X)$  modes located in the infrared and Raman spectra of these  $(R_3P)_2HgX_2$  monomers show a dependence upon the Hg-X bond lengths. The  $\nu(Hg-X)$  modes are found within the ranges of wavenumbers viz 160-240, 110-166 and 90-140  $cm^{-1}$  for the chloro-, bromo- and iodo-complexes respectively, where the lower wavenumber ends of these ranges

correspond to the longer Hg-X bonds. It is also found that the longer Hg-X bonds are present in the  $(R_3P)_2HgX_2$  complexes that contain the larger P-Hg-P angles. From analysis of the  $\delta(Hg-Cl)$  mode positions for  $(Cy_3P)_2HgCl_2$  it is predicted that the geometry of the monomeric structure, suggested to be present in the solid-state, is similar to that of  $(Bu^{\text{n}}_3P)_2HgCl_2$ . This prediction needs to be confirmed by a determination of the structure of  $(Cy_3P)_2HgCl_2$ , and would further extend the structure/spectra correlations for  $(R_3P)_2HgX_2$  complexes.

A more detailed spectroscopic investigation is needed into the  $(R_3P)_2CdX_2$  complexes to firmly establish if the relationships found for the mercury analogues also apply for these complexes.

## Appendices

	Page	
Appendix A.1	Final positional and thermal parameters	180
Appendix A.2	Tables of observed and calculated structure factors	204
Appendix A.3	Equations of least squares planes	213
Appendix A.4	Point group, line group and factor group analysis	226
Appendix A.5	Experimental techniques	237

Appendix A.1

Final positional parameters ( $\times 10^4$ ) and thermal parameters ( $\times 10^4$ ).

(E.s.d's for non-hydrogen given in parentheses)

Anisotropic temperature factors are of the form:-

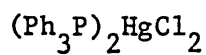
$$\exp \left[ -2\pi^2 (U_{11}h^2 a^{*2} + U_{22}k^2 b^{*2} + U_{33}l^2 c^{*2} + 2U_{12}hka^* b^* + 2U_{13}hla^* c^* + 2U_{23}klb^* c^*) \right]$$

Isotropic temperature factors are of the form:-

$$\exp -8\pi^2 U(\sin^2 \Theta) / \lambda^2$$

Table A.1.1

Final positional (a) and thermal (b) parameters for



(a)	<u>x</u>	<u>y</u>	<u>z</u>
Hg	- 694(3)	2425(1)	1251(1)
Cl(1)	10(16)	3597(4)	1949(4)
Cl(2)	1067(17)	2076(5)	375(5)
P1	- 340(17)	1347(4)	2048(4)
P2	- 2589(17)	2864(4)	559(4)
C11	- 1150(42)	1488(16)	2861(12)
C12	- 803(42)	990(16)	3389(12)
C13	- 1470(42)	1058(16)	4018(12)
C14	- 2485(42)	1625(16)	4119(12)
C15	- 2832(42)	2122(16)	3591(12)
C16	- 2165(42)	2054(16)	2962(12)
C21	1421(38)	1196(12)	2234(11)
C22	2260(38)	1826(12)	2393(11)
C23	3688(38)	1727(12)	2546(11)
C24	4276(38)	997(12)	2540(11)
C25	3437(38)	367(12)	2381(11)
C26	2010(38)	467(12)	2228(11)
C31	- 981(34)	467(11)	1702(12)
C32	- 2191(34)	125(11)	1967(12)
C33	- 2764(34)	- 519(11)	1653(12)
C34	- 2126(34)	- 820(11)	1074(12)
C35	- 915(34)	- 479(11)	808(12)
C36	- 343(34)	165(11)	1122(12)
C41	- 2164(44)	3685(11)	37(12)
C42	- 3227(44)	4211(11)	- 111(12)

	<u>x</u>	<u>y</u>	<u>z</u>
C43	- 2934(44)	4840(11)	- 523(12)
C44	- 1580(44)	4943(11)	- 786(12)
C45	- 517(44)	4417(11)	- 638(12)
C46	- 809(44)	3787(11)	- 226(12)
C51	- 4020(34)	3157(13)	1068(12)
C52	- 3819(34)	3563(13)	1671(12)
C53	- 4981(34)	3784(13)	2059(12)
C54	- 6345(34)	3600(13)	1844(12)
C55	- 6546(34)	3194(13)	1241(12)
C56	- 5384(34)	2973(13)	853(12)
C61	- 3199(46)	2101(11)	- 27(12)
C62	- 3168(46)	1348(11)	204(12)
C63	- 3499(46)	752(11)	- 238(12)
C64	- 3860(46)	909(11)	- 912(12)
C65	- 3890(46)	1661(11)	- 1143(12)
C66	- 3560(46)	2257(11)	- 701(12)

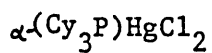
(b)

	$U_{11}$	$U_{22}$	$U_{33}$	$U_{12}$	$U_{13}$	$U_{23}$	
Hg	393(7)	374(6)	411(6)	- 41(12)	- 105(7)	2(7)	
C1(1)	536(25)	508(38)	564(47)	-143(57)	- 7(64)	- 135(34)	
C1(2)	589(26)	635(44)	543(49)	- 53(67)	14(67)	- 90(38)	
P1	409(22)	419(35)	399(41)	-126(58)	- 120(60)	- 30(32)	
P2	406(22)	429(36)	383(39)	- 83(56)	- 195(57)	8(30)	
	$U$	$U$	$U$	$U$	$U$	$U$	
C11	730(131)	C12	781(132)	C13	955(149)	C14	756(123)
C15	886(162)	C16	650(123)	C21	312(64)	C22	975(163)

	U		U		U		U
C23	1173(185)	C24	844(155)	C25	932(169)	C26	864(143)
C31	551(89)	C32	464(86)	C33	529(100)	C34	692(107)
C35	752(127)	C36	832(130)	C41	467(89)	C42	802(127)
C43	896(150)	C44	618(113)	C45	1219(181)	C46	826(144)
C51	517(90)	C52	630(110)	C53	513(98)	C54	797(150)
C55	817(130)	C56	673(119)	C61	482(100)	C62	771(114)
C63	754(131)	C64	1172(185)	C65	865(135)	C66	762(131)

Table A.1.2

Final positional (a) and thermal (b) parameters for



a)	<u>x</u>	<u>y</u>	<u>z</u>
Hg1	3371(1)	19(1)	4592(1)
C 1(11)	1539(4)	- 1482(3)	5110(3)
C 1(12)	5224(4)	- 731(2)	3940(2)
P1	3441(3)	1602(2)	4044(2)
C111	2031(12)	1442(8)	3419(7)
C112	1359(13)	341(9)	3103(9)
C113	63(14)	261(10)	2736(9)
C114	380(16)	960(12)	1946(10)
C115	1122(14)	2027(11)	2206(10)
C116	2367(13)	2142(9)	2603(9)
C121	3245(12)	2431(8)	5053(7)
C122	2019(13)	1910(9)	5702(8)
C123	1843(17)	2586(10)	6550(9)
C124	1877(18)	3592(11)	6284(10)
C125	3123(17)	4119(10)	5610(10)
C126	3280(13)	3465(8)	4769(8)
C131	5039(11)	2229(9)	3325(7)
C132	5333(14)	1530(10)	2577(8)
C133	6676(13)	2041(11)	1983(9)
C134	7819(14)	2409(13)	2555(9)
C135	7497(13)	3116(11)	3325(10)
C136	6167(12)	2624(10)	3935(8)
Hg2	3797(1)	- 4354(1)	- 158(1)
C1(21)	3336(8)	- 4930(4)	- 1672(3)
C1(22)	6400(4)	- 3922(3)	- 566(3)

	<u>x</u>	<u>y</u>	<u>z</u>
P2	3236(3)	- 3259(2)	1060(2)
C211	4653(11)	- 2074(8)	1124(8)
C212	5163(13)	- 1596(8)	159(8)
C213	6328(14)	- 640(9)	180(9)
C214	7444(15)	- 756(10)	561(10)
C215	6972(14)	- 1219(10)	1513(9)
C216	5808(13)	- 2221(9)	1501(8)
C221	1866(13)	- 2935(10)	764(10)
C222	1499(14)	- 2102(9)	1275(9)
C223	541(17)	- 1795(12)	871(12)
C224	- 499(18)	- 2562(12)	500(14)
C225	- 108(15)	- 3382(12)	- 43(11)
C226	867(18)	- 3667(12)	342(14)
C231	2807(13)	- 3844(8)	2177(7)
C232	2628(18)	- 3147(10)	2990(8)
C233	2510(21)	- 3691(13)	3880(10)
C234	1364(18)	- 4699(12)	3945(10)
C235	1487(17)	- 5347(11)	3145(10)
C236	1636(13)	- 4818(10)	2226(9)
H1	1346	1665	3933
H2	2028	124	2569
H3	1106	- 155	3674
H4	- 601	470	3277
H5	- 411	- 510	2500
H6	- 429	814	1736
H7	660	701	1475
H8	1397	2487	1607
H9	470	2209	2717
H10	3061	1940	2081

	<u>x</u>	<u>y</u>	<u>z</u>
H11	2813	2919	2826
H12	4085	2583	5412
H13	1160	1722	5354
H14	2096	1226	5923
H15	2643	2702	6942
H16	901	2212	6966
H17	1018	3480	5954
H18	1838	4064	6894
H19	3069	4819	5417
H20	3978	4280	5967
H21	2478	3350	4381
H22	4222	3838	4351
H23	4966	2866	3010
H24	5366	871	2800
H25	4556	1300	2149
H26	6628	2600	1654
H27	6870	1503	1467
H28	7921	1763	2845
H29	8737	2810	2125
H30	7470	3780	3027
H31	8279	3336	3748
H32	6210	1996	4282
H33	5969	3174	4435
H34	4311	- 1554	1586
H35	4366	- 1438	- 75
H36	5455	- 2135	- 307
H37	6006	- 81	598
H38	6679	- 378	- 513
H39	7846	- 1249	105
H40	209	- 23	611

	<u>x</u>	<u>y</u>	<u>z</u>
H41	7791	- 1352	1741
H42	6659	- 691	1983
H43	6131	- 2770	1068
H44	5464	- 2498	2190
H45	2448	- 2535	157
H46	2392	- 1451	1305
H47	1055	- 2357	1961
H48	1100	- 1295	317
H49	97	- 1387	1398
H50	- 1244	- 2911	1070
H51	- 923	- 2219	65
H52	320	- 3115	- 727
H53	- 991	- 4043	- 73
H54	1349	- 4027	- 206
H55	312	- 4270	865
H56	3665	- 4035	2252
H57	3475	- 2452	2940
H58	1731	- 2981	2984
H59	3429	- 3822	3897
H60	2330	- 3218	4463
H61	442	- 4558	3974
H62	1333	- 5085	4554
H63	2366	- 5540	3149
H64	622	- 6030	3182
H65	742	- 4655	2199
H66	1791	- 5309	1652

(b)	$U_{11}$	$U_{22}$	$U_{33}$	$U_{12}$	$U_{13}$	$U_{23}$
Hg1	544(4)	407(3)	526(3)	220(3)	- 107(3)	39(2)
C1.(11)	565(26)	575(22)	1001(30)	125(20)	- 95(22)	207(21)
C1 (12)	632(24)	592(20)	432(18)	377(19)	- 161(17)	- 144(15)
P1	323(19)	332(16)	369(17)	113(15)	- 77(15)	9(14)
C111	306(77)	395(64)	261(65)	70(59)	16(58)	0(53)
C112	439(90)	448(76)	593(83)	- 61(70)	- 197(73)	178(67)
C113	497(99)	559(84)	564(88)	- 41(76)	- 301(81)	- 98(73)
C114	518(101)	851(110)	560(92)	197(89)	- 306(78)	- 45(83)
C115	423(91)	701(95)	727(101)	181(79)	- 250(79)	80(79)
C116	414(90)	382(70)	777(97)	- 21(66)	- 359(76)	109(68)
C121	279(74)	418(67)	391(68)	227(60)	- 67(58)	- 76(56)
C122	495(92)	443(73)	593(82)	186(69)	60(71)	113(66)
C123	872(130)	655(88)	439(82)	274(89)	9(80)	21(71)
C124	1068(153)	767(107)	568(90)	565(111)	- 150(96)	- 212(82)
C125	833(125)	494(83)	665(102)	200(88)	- 116(94)	- 38(77)
C126	491(90)	395(67)	461(73)	247(66)	- 76(65)	- 118(58)
C131	351(75)	464(71)	350(66)	158(62)	- 94(57)	40(57)
C132	559(100)	680(91)	444(80)	293(81)	- 148(73)	- 47(72)
C133	347(87)	905(105)	412(76)	237(81)	57(66)	- 59(74)
C134	444(104)	1116(128)	549(90)	334(98)	145(79)	159(93)
C135	301(88)	828(108)	695(99)	26(82)	- 175(76)	167(88)
C136	250(77)	632(82)	423(72)	124(67)	- 75(61)	- 49(64)
Hg2	515(4)	543(3)	600(4)	- 153(3)	- 157(3)	273(3)
C1(21)	2309(76)	1124(38)	826(33)	- 245(29)	- 921(42)	446(45)
C1(22)	506(23)	541(20)	919(27)	208(19)	179(20)	221(18)
P2	355(20)	399(17)	478(19)	- 93(15)	- 198(16)	159(16)
C211	365(71)	312(61)	453(72)	- 83(55)	- 234(58)	44(55)
C212	462(89)	462(75)	552(83)	40(64)	- 196(69)	165(70)
C213	717(110)	507(84)	620(92)	134(71)	- 104(81)	161(80)

	$U_{11}$	$U_{22}$	$U_{33}$	$U_{12}$	$U_{13}$	$U_{23}$
C214	474(95)	559(86)	809(105)	60(74)	- 97(80)	214(78)
C215	534(15)	685(91)	653(91)	146(80)	- 311(76)	- 96(75)
C216	407(86)	597(81)	451(74)	117(70)	- 177(64)	10(63)
C221	449(87)	684(87)	799(100)	378(77)	- 286(78)	- 336(80)
C222	565(95)	538(81)	801(97)	239(75)	- 247(78)	- 321(73)
C223	817(130)	840(113)	1347(149)	629(100)	- 426(116)	- 302(108)
C224	978(150)	973(125)	1622(176)	692(123)	- 887(140)	- 515(124)
C225	614(106)	1107(123)	1007(117)	590(101)	- 586(93)	- 557(100)
C226	960(143)	980(125)	1907(188)	788(119)	- 1026(144)	- 934(130)
C231	488(86)	549(72)	388(72)	199(66)	- 74(60)	- 39(57)
C232	1173(159)	499(81)	416(73)	209(94)	- 167(85)	- 55(64)
C233	1487(196)	1086(141)	396(96)	538(140)	- 192(111)	- 12(97)
C234	984(146)	852(109)	667(102)	362(108)	85(96)	226(90)
C235	825(131)	600(92)	924(117)	125(91)	73(98)	176(91)
C236	406(89)	545(82)	763(98)	- 64(72)	21(74)	- 35(75)

Table A.1.3

Final positional (a) and thermal (b) parameters for  $(\text{Me}_2\text{PhP})\text{CdCl}_2$

(a) $(\text{Cd} \times 10^5)$	<u>x</u>	<u>y</u>	<u>z</u>
Cd	25383(1)	2221(2)	5148(2)
C1(1)	4219(2)	936(1)	- 978(1)
C1(2)	648(2)	- 1399(1)	- 13(1)
P	2623(2)	850(1)	2405(1)
C11	1522(10)	- 173(3)	3186(4)
C12	2384(10)	- 601(6)	4081(5)
C13	1447(12)	- 1397(6)	4612(5)
C14	- 331(12)	- 1707(6)	4313(5)
C15	-1202(10)	- 1293(6)	3414(5)
C16	- 263(8)	- 515(5)	2864(4)
C2	1336(12)	2079(5)	2639(5)
C3	4952(11)	1097(6)	3002(6)
H12	3765	- 321	4336
H13	2159	- 1774	5279
H14	- 1072	- 2278	4773
H15	2592	- 1569	3143
H16	- 948	- 176	2171
H21	- 96	2010	2306
H22	2038	2744	2286
H23	1299	2213	3465
H31	5838	402	2903
H32	4836	1252	3819
H33	5574	1784	2640

(b)	$U_{11}$	$U_{22}$	$U_{33}$	$U_{12}$	$U_{13}$	$U_{23}$
Cd	290(2)	411(2)	337(2)	- 23(1)	53(1)	29(1)
C1(1)	298(5)	450(5)	379(5)	24(4)	52(3)	82(4)
C 1(2)	310(5)	374(5)	675(7)	20(4)	- 56(5)	- 40(4)
P	375(6)	340(4)	337(5)	20(4)	29(4)	- 20(4)
C11	383(24)	402(20)	310(18)	21(15)	22(16)	- 35(14)
C12	504(33)	704(35)	457(26)	- 72(27)	155(24)	88(25)
C13	721(48)	695(37)	480(28)	- 96(33)	- 93(28)	97(26)
C14	638(42)	640(33)	553(31)	- 196(30)	92(27)	44(27)
C15	430(32)	750(37)	570(31)	- 175(28)	20(24)	14(27)
C16	374(26)	516(24)	467(24)	- 20(20)	- 23(19)	- 2(20)
C2	807(50)	440(25)	592(32)	191(28)	115(30)	- 132(23)
C3	490(36)	654(33)	646(35)	- 150(27)	- 115(27)	- 116(28)

Table A.1.4

Final positional (a) and thermal (b) parameters for

(Me<sub>2</sub>PhP)<sub>2</sub>CdBr<sub>2</sub>

(a)	<u>x</u>	<u>y</u>	<u>z</u>
Cd	7550(1)	209(1)	5516(1)
Br1	9157(2)	1018(1)	3998(1)
Br2	5707(2)	- 1477(1)	4956(1)
P	7723(5)	856(3)	7360(3)
C11	6650(20)	- 97(11)	8174(11)
C12	7487(29)	- 514(15)	9068(13)
C13	6522(37)	- 1260(16)	9619(18)
C14	4882(29)	- 1591(16)	9335(15)
C15	4019(28)	- 1175(14)	8430(16)
C16	4965(23)	- 450(13)	7854(13)
C2	9966(29)	1112(16)	7902(17)
C3	6541(30)	2091(13)	7558(15)
H12	8840	- 271	9333
H13	7146	- 1569	10328
H14	4224	- 2196	9769
H15	2646	- 1401	8189
H16	4356	- 159	7134
H21	10800	415	7819
H22	9906	1304	8708
H23	10548	1770	7502
H31	5150	2021	7257
H32	7204	2727	7167
H33	6562	2261	8372

(b)	$U_{11}$	$U_{22}$	$U_{33}$	$U_{12}$	$U_{13}$	$U_{23}$
Cd	544(6)	460(5)	586(6)	- 53(4)	34(4)	- 45(4)
Br1	537(8)	462(7)	649(8)	13(5)	29(6)	649(8)
Br2	546(8)	385(6)	897(11)	10(5)	- 130(7)	897(11)
P	601(20)	372(15)	614(21)	32(13)	- 24(15)	614(21)
C11	557(76)	454(63)	567(73)	60(63)	- 19(52)	561(73)
C12	958(128)	700(100)	569(89)	- 53(90)	- 207(80)	569(89)
C13	1171(194)	736(121)	873(143)	- 12(110)	- 133(124)	873(143)
C14	790(126)	744(109)	814(116)	- 44(87)	- 7(88)	814(116)
C15	771(117)	662(99)	796(114)	- 76(78)	- 26(84)	796(114)
C16	620(94)	575(81)	689(92)	33(64)	- 81(69)	689(92)
C2	880(134)	646(104)	872(129)	- 169(87)	- 34(99)	872(129)
C3	1025(136)	414(70)	833(111)	133(72)	71(93)	833(111)

Table A.1.5

Final positional (a) and thermal (b) parameters for the structure

(Me<sub>2</sub>PhP)CdI<sub>2</sub>

(a)	<u>x</u>	<u>y</u>	<u>z</u>
Cd	2595(2)	193(1)	5510(1)
I1	824(2)	- 1588(1)	4919(1)
I2	4040(2)	1161(1)	3953(1)
P	2894(7)	906(4)	7275(3)
C11	1951(29)	35(14)	8105(11)
C12	2686(52)	- 380(18)	9004(15)
C13	1854(53)	- 1068(22)	9602(16)
C14	251(58)	- 1329(21)	9352(18)
C15	- 567(42)	- 986(21)	8466(19)
C16	276(44)	- 322(20)	7872(15)
C2	1844(35)	2160(15)	7482(15)
C3	4999(40)	1139(26)	7778(20)
H12	3970	- 146	9250
H13	2499	- 1393	10265
H14	- 424	- 1816	9855
H15	- 1861	- 1235	8263
H16	- 383	- 71	7184
H21	520	2121	7202
H22	2481	2770	7103
H23	1915	2323	8268
H31	5761	449	7697
H32	4980	1331	8555
H33	5546	1777	7390

(b)	$U_{11}$	$U_{22}$	$U_{33}$	$U_{12}$	$U_{13}$	$U_{23}$
Cd	752(11)	858(10)	408(5)	- 185(7)	167(5)	- 140(5)
I1	568(8)	645(7)	621(6)	- 13(5)	- 56(5)	- 5(5)
I2	578(8)	709(7)	478(5)	- 12(5)	138(4)	41(4)
P	665(31)	655(23)	410(16)	87(20)	15(17)	- 170(15)
C11	730(128)	639(89)	405(59)	108(86)	0(65)	57(60)
C12	1594(308)	657(111)	587(94)	- 327(153)	- 197(136)	33(87)
C13	1466(321)	870(162)	540(91)	329(184)	- 66(135)	181(98)
C14	1483(320)	844(139)	611(109)	162(176)	336(153)	215(101)
C15	866(200)	911(153)	765(122)	18(107)	162(120)	189(138)
C16	1162(225)	894(139)	522(86)	80(141)	97(107)	104(90)
C2	969(165)	588(87)	614(88)	44(95)	- 65(95)	- 109(74)
C3	684(175)	1464(259)	704(120)	- 81(162)	- 132(113)	- 229(142)

Table A.1.6

Final positional (a) and thermal (b) parameters for the structure

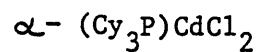
(E t<sub>3</sub>P)CdI<sub>2</sub>

(a)	<u>x</u>	<u>y</u>	<u>z</u>
Cd	8514(1)	4812(1)	833(4)
I1	11901(1)	5019(1)	1020(1)
I2	7484(1)	2516(1)	1471(1)
P	7297(2)	6919(2)	1372(1)
C11	5620(15)	7470(13)	645(7)
C12	4756(19)	8677(20)	929(11)
C21	6502(14)	6687(14)	2414(6)
C22	7717(17)	6089(15)	3085(7)
C31	8664(13)	8300(12)	1528(7)
C32	9400(20)	8693(17)	695(8)
H111	4779	6666	567
H112	6055	7696	31
H121	3790	8918	453
H122	5567	9502	1003
H123	4291	8471	1539
H211	5494	6031	2328
H212	6128	7634	2645
H221	7189	5970	3686
H222	8729	6740	3180
H223	8095	5138	2964
H311	9617	8022	2003
H312	8037	9138	1761
H321	10202	9514	827
H322	8462	8982	215
H323	10042	7867	457

(b)	$U_{11}$	$U_{22}$	$U_{33}$	$U_{12}$	$U_{13}$	$U_{23}$
Cd	468(4)	399(4)	523(4)	- 5(2)	132(3)	15(2)
I1	425(3)	735(5)	451(4)	- 78(2)	18(2)	51(2)
I2	621(4)	487(5)	694(4)	- 132(3)	88(3)	121(3)
P	396(8)	381(1)	456(9)	- 15(7)	70(7)	- 27(7)
C11	654(56)	567(68)	576(49)	63(47)	- 51(42)	- 79(43)
C12	731(75)	780(106)	1007(98)	195(76)	- 29(66)	- 14(80)
C21	680(58)	716(74)	475(41)	- 5(51)	243(40)	- 128(44)
C22	847(73)	639(77)	532(48)	- 227(62)	107(46)	24(46)
C31	595(48)	481(54)	600(48)	- 159(41)	114(39)	- 40(40)
C32	1023(104)	673(88)	675(61)	- 267(78)	82(62)	210(58)

Table A.1.7

Final positional (a) and thermal (b) parameters for



(a)	$\underline{x}$	$\underline{y}$	$\underline{z}$
Cd1	2753(1)	140(1)	9158(1)
Cl(11)	2592(2)	- 99(1)	9249(2)
Cl(12)	2592(3)	1842(2)	7951(1)
P1	4347(2)	2107(1)	10100(1)
Cl11	5118(9)	2382(5)	9564(5)
Cl12	5435(10)	1617(6)	9271(7)
Cl13	5917(13)	1856(8)	8735(9)
Cl14	6824(13)	2411(9)	9074(8)
Cl15	6527(10)	3152(8)	9385(6)
Cl16	6023(9)	2939(6)	9925(5)
Cl21	5163(9)	1495(6)	10892(5)
Cl22	4563(11)	899(6)	11143(6)
Cl23	5249(13)	365(6)	11768(6)
Cl24	5959(12)	877(8)	12392(6)
Cl25	6605(10)	1443(8)	12145(6)
Cl26	5921(8)	1996(6)	11538(5)
Cl31	4052(8)	3074(5)	10447(5)
Cl32	3451(9)	3640(4)	9812(5)
Cl33	3250(11)	4465(6)	10096(6)
Cl34	2690(11)	4354(7)	10602(7)
Cl35	3245(9)	3770(7)	11217(6)
Cl36	3443(9)	2955(6)	10928(5)
Cd2	646(1)	135(1)	9284(1)
Cl(21)	1037(2)	1632(1)	9250(2)
Cl(22)	1183(2)	- 489(2)	10509(1)

	<u>x</u>	<u>y</u>	<u>z</u>
P2	- 321(2)	- 675(1)	8115(1)
C211	- 1682(8)	- 346(6)	7746(5)
C212	- 1752(10)	561(7)	7564(7)
C213	- 2869(18)	853(14)	7411(11)
C214	- 3675(14)	335(17)	6844(9)
C215	- 3544(12)	- 565(13)	7050(9)
C216	- 2444(11)	- 838(11)	7160(7)
C221	226(9)	- 682(5)	7415(5)
C222	- 251(10)	- 1276(6)	6789(5)
C223	343(12)	- 1311(8)	6301(7)
C224	597(15)	- 541(9)	6085(8)
C225	1080(9)	51(6)	6708(5)
C226	455(11)	114(7)	7186(6)
C231	- 301(8)	- 1748(5)	8638(5)
C232	- 748(8)	- 1858(5)	8951(5)
C233	- 715(9)	- 2746(6)	9175(6)
C234	382(10)	- 3085(6)	9455(5)
C235	827(10)	- 2968(6)	8875(7)
C236	798(10)	- 2079(6)	8646(6)
H1	4605	2750	9119
H2	5982	1270	9717
H3	4759	1252	8989
H4	5345	2160	8271
H5	6167	1370	8553
H6	7088	2601	8655
H7	7435	2090	9502
H8	7212	3506	9674
H9	5993	3510	8941

	<u>x</u>	<u>y</u>	<u>z</u>
H10	5752	3493	10002
H11	6581	2650	10407
H12	5644	1139	10694
H13	4027	1237	11328
H14	4087	512	10690
H15	5700	- 15	11562
H16	4793	- 15	11970
H17	5516	1221	12631
H18	6485	477	12802
H19	7084	1092	11943
H20	7084	1810	12604
H21	5491	2393	11748
H22	6405	2358	11347
H23	4782	3348	10780
H24	3877	3732	9470
H25	2719	3359	9493
H26	2794	4845	9639
H27	3983	4754	10394
H28	2637	4940	10833
H29	1925	4125	10289
H30	3974	4032	11567
H31	2779	3668	11530
H32	3875	2564	11383
H33	2713	2673	10607
H34	- 1952	- 439	8180
H35	- 1208	896	8021
H36	- 1588	664	7083
H37	- 2954	1485	7246
H38	- 2988	790	7915
H39	- 4428	545	6785

	<u>x</u>	<u>y</u>	<u>z</u>
H40	- 3588	411	6331
H41	- 4105	- 920	6619
H42	- 3656	- 650	7553
H43	- 2342	- 766	6651
H44	- 2327	- 1468	7328
H45	981	- 926	7734
H46	- 274	- 1872	7013
H47	- 1024	- 1080	6456
H48	- 81	- 1664	5818
H49	1074	- 1613	6607
H50	1111	- 622	5806
H51	- 119	- 280	5711
H52	1115	648	6490
H53	1850	- 154	7041
H54	- 261	421	6875
H55	887	466	7670
H56	- 772	- 2099	7894
H57	- 1531	- 1639	8738
H58	- 289	- 1504	9427
H59	- 993	- 2791	9609
H60	1210	- 3096	8708
H61	369	- 3726	9574
H62	866	- 2766	9946
H63	1616	- 3174	9085
H64	375	- 3325	8400
H65	1079	- 2023	8214
H66	1277	- 1724	9114

(b)

	$U_{11}$	$U_{22}$	$U_{33}$	$U_{12}$	$U_{13}$	$U_{23}$
Cd1	506(4)	508(4)	468(3)	- 76(3)	198(3)	- 51(3)
C1(11)	546(17)	464(12)	807(16)	37(11)	301(13)	- 30(11)
C1(12)	1002(26)	955(21)	433(13)	- 198(18)	207(14)	51(13)
P1	434(14)	416(11)	394(11)	- 9(9)	167(10)	- 29(9)
C111	590(71)	442(49)	577(51)	28(44)	346(48)	1(40)
C112	695(80)	578(55)	832(71)	21(48)	501(62)	- 135(49)
C113	475(126)	826(82)	1073(115)	- 46(77)	717(102)	- 143(78)
C114	942(117)	1004(95)	941(92)	8(79)	710(88)	67(74)
C115	541(76)	897(87)	698(62)	- 27(61)	357(54)	120(59)
C116	680(66)	562(56)	658(53)	- 71(47)	389(47)	40(43)
C121	652(70)	499(50)	420(46)	55(46)	246(45)	51(40)
C122	879(95)	480(53)	620(61)	- 124(52)	259(61)	- 5(44)
C123	1211(130)	589(57)	749(71)	95(63)	551(81)	136(51)
C124	1100(125)	870(79)	465(61)	150(76)	311(70)	147(56)
C125	683(82)	1002(81)	584(66)	261(65)	158(57)	114(60)
C126	454(65)	660(59)	394(45)	- 63(47)	34(42)	- 79(40)
C131	501(63)	457(46)	415(43)	95(40)	128(40)	2(35)
C132	560(68)	645(59)	458(51)	201(51)	85(45)	3(46)
C133	883(101)	488(58)	788(65)	135(58)	440(65)	17(48)
C134	770(97)	619(63)	996(81)	98(58)	513(73)	- 158(56)
C135	560(76)	754(67)	667(62)	- 87(52)	375(56)	- 294(53)
C136	572(68)	589(55)	545(48)	47(46)	350(46)	40(40)
Cd2	489(5)	440(3)	429(3)	- 58(3)	213(3)	- 32(3)
C1(21)	690(19)	417(12)	1021(20)	23(11)	510(16)	- 46(12)
C1(22)	571(16)	733(14)	416(11)	124(11)	220(10)	26(10)
P2	410(13)	453(11)	351(10)	- 20(9)	162(9)	- 30(8)
C211	421(60)	796(66)	480(50)	134(45)	143(41)	56(44)
C212	647(86)	945(79)	683(68)	409(65)	202(60)	348(60)

	$U_{11}$	$U_{22}$	$U_{33}$	$U_{12}$	$U_{13}$	$U_{23}$
C213	1158(193)	1655(190)	1155(151)	754(160)	531(147)	539(145)
C214	931(120)	2922(314)	833(88)	1054(150)	320(79)	415(131)
C215	452(100)	2101(182)	824(97)	- 29(103)	61(75)	- 448(109)
C216	552(86)	1439(129)	634(75)	8(79)	75(61)	- 333(60)
C221	835(76)	460(45)	516(48)	- 174(44)	454(49)	- 108(36)
C222	762(83)	673(61)	485(50)	- 226(54)	430(53)	- 128(45)
C223	1177(116)	1029(91)	741(68)	- 511(82)	613(74)	- 466(67)
C224	1592(155)	1164(99)	786(84)	- 508(96)	825(97)	- 159(72)
C225	616(73)	628(59)	560(52)	- 222(50)	220(48)	32(44)
C226	793(89)	617(59)	628(62)	- 147(58)	251(59)	- 114(50)
C231	488(62)	416(44)	500(44)	- 38(39)	242(42)	- 78(36)
C232	571(64)	519(49)	574(53)	- 24(41)	317(46)	67(40)
C233	662(75)	621(56)	560(57)	- 80(49)	253(51)	10(45)
C234	873(88)	549(58)	509(54)	- 119(55)	184(53)	146(44)
C235	685(88)	493(51)	820(75)	120(50)	259(65)	94(49)
C236	564(74)	596(58)	631(57)	- 4(49)	257(51)	6(46)

# Appendix A.2 Tables of observed and calculated structure factors.

OBSERVED AND CALCULATED STRUCTURE FACTORS FOR UPRN320G02

M	N	L	FO	FC	M	N	L	FO	FC	M	N	L	FO	FC	M	N	L	FO	FC	M	N	L	FO	FC	M	N	L	FO	FC																					
1	1	0	107	157	1	1	0	51	51	1	1	4	202	245	-2	1	0	86	-89	4	1	0	1	87	-86	-1	1	0	100	-112	-3	1	0	83	88	-3	1	0	14	-35	2	1	0	121	102	-8	1	0	81	-90
2	2	0	141	-155	2	2	0	56	61	-1	1	4	124	128	-1	1	0	64	-66	-3	1	0	1	87	-86	-1	1	0	100	-112	-3	1	0	83	88	-3	1	0	14	-35	2	1	0	121	102	-8	1	0	81	-90
3	3	0	177	-208	3	3	0	61	67	-2	1	4	168	173	-2	1	0	72	-74	-4	1	0	1	87	-86	-2	1	0	100	-112	-4	1	0	83	88	-4	1	0	14	-35	3	1	0	121	102	-9	1	0	81	-90
4	4	0	219	-277	4	4	0	66	73	-3	1	4	212	217	-3	1	0	84	-86	-5	1	0	1	87	-86	-3	1	0	100	-112	-5	1	0	83	88	-5	1	0	14	-35	4	1	0	121	102	-10	1	0	81	-90
5	5	0	267	-340	5	5	0	71	79	-4	1	4	256	261	-4	1	0	96	-98	-6	1	0	1	87	-86	-4	1	0	100	-112	-6	1	0	83	88	-6	1	0	14	-35	5	1	0	121	102	-11	1	0	81	-90
6	6	0	321	-417	6	6	0	76	85	-5	1	4	300	305	-5	1	0	112	-114	-7	1	0	1	87	-86	-5	1	0	100	-112	-7	1	0	83	88	-7	1	0	14	-35	6	1	0	121	102	-12	1	0	81	-90
7	7	0	381	-500	7	7	0	81	91	-6	1	4	344	349	-6	1	0	128	-130	-8	1	0	1	87	-86	-6	1	0	100	-112	-8	1	0	83	88	-8	1	0	14	-35	7	1	0	121	102	-13	1	0	81	-90
8	8	0	447	-645	8	8	0	86	97	-7	1	4	388	393	-7	1	0	144	-146	-9	1	0	1	87	-86	-7	1	0	100	-112	-9	1	0	83	88	-9	1	0	14	-35	8	1	0	121	102	-14	1	0	81	-90
9	9	0	521	-800	9	9	0	91	103	-8	1	4	432	437	-8	1	0	160	-162	-10	1	0	1	87	-86	-8	1	0	100	-112	-10	1	0	83	88	-10	1	0	14	-35	9	1	0	121	102	-15	1	0	81	-90
10	10	0	603	-990	10	10	0	96	109	-9	1	4	476	481	-9	1	0	176	-178	-11	1	0	1	87	-86	-9	1	0	100	-112	-11	1	0	83	88	-11	1	0	14	-35	10	1	0	121	102	-16	1	0	81	-90
11	11	0	695	-1200	11	11	0	101	123	-10	1	4	520	525	-10	1	0	192	-194	-12	1	0	1	87	-86	-10	1	0	100	-112	-12	1	0	83	88	-12	1	0	14	-35	11	1	0	121	102	-17	1	0	81	-90
12	12	0	807	-1500	12	12	0	106	147	-11	1	4	564	569	-11	1	0	208	-210	-13	1	0	1	87	-86	-11	1	0	100	-112	-13	1	0	83	88	-13	1	0	14	-35	12	1	0	121	102	-18	1	0	81	-90
13	13	0	939	-1900	13	13	0	111	181	-12	1	4	608	613	-12	1	0	224	-226	-14	1	0	1	87	-86	-12	1	0	100	-112	-14	1	0	83	88	-14	1	0	14	-35	13	1	0	121	102	-19	1	0	81	-90
14	14	0	1091	-2500	14	14	0	116	225	-13	1	4	652	657	-13	1	0	240	-242	-15	1	0	1	87	-86	-13	1	0	100	-112	-15	1	0	83	88	-15	1	0	14	-35	14	1	0	121	102	-20	1	0	81	-90
15	15	0	1263	-3300	15	15	0	121	269	-14	1	4	696	701	-14	1	0	256	-258	-16	1	0	1	87	-86	-14	1	0	100	-112	-16	1	0	83	88	-16	1	0	14	-35	15	1	0	121	102	-21	1	0	81	-90
16	16	0	1455	-4400	16	16	0	126	313	-15	1	4	740	745	-15	1	0	272	-274	-17	1	0	1	87	-86	-15	1	0	100	-112	-17	1	0	83	88	-17	1	0	14	-35	16	1	0	121	102	-22	1	0	81	-90
17	17	0	1667	-5800	17	17	0	131	357	-16	1	4	784	789	-16	1	0	288	-290	-18	1	0	1	87	-86	-16	1	0	100	-112	-18	1	0	83	88	-18	1	0	14	-35	17	1	0	121	102	-23	1	0	81	-90
18	18	0	1909	-7600	18	18	0	136	401	-17	1	4	828	833	-17	1	0	304	-306	-19	1	0	1	87	-86	-17	1	0	100	-112	-19	1	0	83	88	-19	1	0	14	-35	18	1	0	121	102	-24	1	0	81	-90
19	19	0	2191	-10000	19	19	0	141	445	-18	1	4	872	877	-18	1	0	320	-322	-20	1	0	1	87	-86	-18	1	0	100	-112	-20	1	0	83	88	-20	1	0	14	-35	19	1	0	121	102	-25	1	0	81	-90
20	20	0	2523	-13000	20	20	0	146	489	-19	1	4	916	921	-19	1	0	336	-338	-21	1	0	1	87	-86	-19	1	0	100	-112	-21	1	0	83	88	-21	1	0	14	-35	20	1	0	121	102	-26	1	0	81	-90
21	21	0	2915	-17000	21	21	0	151	533	-20	1	4	960	965	-20	1	0	352	-354	-22	1	0	1	87	-86	-20	1	0	100	-112	-22	1	0	83	88	-22	1	0	14	-35	21	1	0	121	102	-27	1	0	81	-90
22	22	0	3367	-22000	22	22	0	156	577	-21	1	4	1004	1009	-21	1	0	368	-370	-23	1	0	1	87	-86	-21	1	0	100	-112	-23	1	0	83	88	-23	1	0	14	-35	22	1	0	121	102	-28	1	0	81	-90
23	23	0	3889	-28000	23	23	0	161	621	-22	1	4	1048	1053	-22	1	0	384	-386	-24	1	0	1	87	-86	-22	1	0	100	-112	-24	1	0	83	88	-24	1	0	14	-35	23	1	0	121	102	-29	1	0	81	-90
24	24	0	4491	-36000	24	24	0	166	665	-23	1	4	1092	1097	-23	1	0	400	-402	-25	1	0	1	87	-86	-23	1	0	100	-112	-25	1	0	83	88	-25	1	0	14	-35	24	1	0	121	102	-30	1	0	81	-90
25	25	0	5183	-47000	25	25	0	171	709	-24	1	4	1136	1141	-24	1	0	416	-418	-26	1	0	1	87	-86	-24	1	0	100	-112	-26	1	0	83	88	-26	1	0	14	-35	25	1	0	121	102	-31	1	0	81	-90
26	26	0	5975	-60000	26	26	0	176	753	-25	1	4	1180	1185	-25	1	0	432	-434	-27	1	0	1	87	-86	-25	1	0	100	-112	-27	1	0	83	88	-27	1	0	14	-35	26	1	0	121	102	-32	1	0	81	-90
27	27	0	6877	-75000	27	27	0	181	797	-26	1	4	1224	1229	-26	1	0	448	-450	-28	1	0	1	87	-86	-26	1	0	100	-112	-28	1	0	83	88	-28	1	0	14	-35	27	1	0	121	102	-33	1	0	81	-90
28	28	0	7909	-92000	28	28	0	186	841	-27	1	4	1268	1273	-27	1	0	464	-466	-29	1	0	1	87	-86	-27	1	0	100	-112	-29	1	0	83	88	-29	1	0	14	-35	28	1	0	121	102	-34	1	0	81	-90
29	29	0	9181	-112000	29	29	0	191	885	-28	1	4	1312	1317	-28	1	0	480	-482	-30	1	0	1	87	-86	-28	1	0	100	-112	-30	1	0	83	88	-30	1	0	14	-35	29	1	0	121	102	-35	1	0	81	-90
30	30	0	10613	-140000	30	30	0	196	929	-29	1	4	1356	1361	-29	1	0	496	-498	-31	1	0	1	87	-86	-29	1	0	100	-112	-31	1	0	83	88	-31	1	0	14	-35	30	1	0	121	102	-36	1	0	81	-90
31	31	0	12345	-170000	31	31	0	201	973	-30	1	4	1400	1405	-30	1	0	512	-514	-32	1	0	1	87	-86	-30	1	0	100	-112	-32	1	0	83	88	-32	1	0	14	-35	31	1	0	121	102	-37	1	0	81	-90
32	32	0	14387	-220000	32	32	0	206	1017	-31	1	4	1444	1449	-31	1	0	528	-530	-33	1	0	1	87	-86	-31	1	0	100	-112	-33	1	0	83	88	-33	1	0	14	-35	32	1	0	121	102	-38	1	0	81	-90
33	33	0	16749	-280000	33	33	0	211	1061	-32	1	4	1488	1493	-32	1	0	544	-546	-34	1	0	1	87	-86	-32	1	0	100	-112	-34	1	0	83	88	-34	1	0	14	-35	33	1	0	121	102	-39	1	0	81	-90
34	34	0	19441	-350000	34	34	0	216	1105	-33	1	4	1532	1537	-33	1	0	560	-562	-35	1	0	1	87	-86	-33	1	0	100	-112	-35	1	0	83	88	-35	1	0	14	-35	34	1	0	121	102	-40	1	0	81	-90
35																																																		





OPERATOR AND CALCULATOR CHECKS FOR 4 X 4 SET CALCULATIONS	
1	...
2	...
3	...
4	...
5	...
6	...
7	...
8	...
9	...
10	...
11	...
12	...
13	...
14	...
15	...
16	...
17	...
18	...
19	...
20	...
21	...
22	...
23	...
24	...
25	...
26	...
27	...
28	...
29	...
30	...
31	...
32	...
33	...
34	...
35	...
36	...
37	...
38	...
39	...
40	...
41	...
42	...
43	...
44	...
45	...
46	...
47	...
48	...
49	...
50	...
51	...
52	...
53	...
54	...
55	...
56	...
57	...
58	...
59	...
60	...
61	...
62	...
63	...
64	...
65	...
66	...
67	...
68	...
69	...
70	...
71	...
72	...
73	...
74	...
75	...
76	...
77	...
78	...
79	...
80	...
81	...
82	...
83	...
84	...
85	...
86	...
87	...
88	...
89	...
90	...
91	...
92	...
93	...
94	...
95	...
96	...
97	...
98	...
99	...
100	...





OBSERVED AND CALCULATED STRUCTURE FACTORS FOR		DEC	CRISTOPH
H	K	L	PC
0	0	0	100
0	0	1	100
0	0	2	100
0	0	3	100
0	0	4	100
0	0	5	100
0	0	6	100
0	0	7	100
0	0	8	100
0	0	9	100
0	0	10	100
0	0	11	100
0	0	12	100
0	0	13	100
0	0	14	100
0	0	15	100
0	0	16	100
0	0	17	100
0	0	18	100
0	0	19	100
0	0	20	100
0	0	21	100
0	0	22	100
0	0	23	100
0	0	24	100
0	0	25	100
0	0	26	100
0	0	27	100
0	0	28	100
0	0	29	100
0	0	30	100
0	0	31	100
0	0	32	100
0	0	33	100
0	0	34	100
0	0	35	100
0	0	36	100
0	0	37	100
0	0	38	100
0	0	39	100
0	0	40	100
0	0	41	100
0	0	42	100
0	0	43	100
0	0	44	100
0	0	45	100
0	0	46	100
0	0	47	100
0	0	48	100
0	0	49	100
0	0	50	100
0	0	51	100
0	0	52	100
0	0	53	100
0	0	54	100
0	0	55	100
0	0	56	100
0	0	57	100
0	0	58	100
0	0	59	100
0	0	60	100
0	0	61	100
0	0	62	100
0	0	63	100
0	0	64	100
0	0	65	100
0	0	66	100
0	0	67	100
0	0	68	100
0	0	69	100
0	0	70	100
0	0	71	100
0	0	72	100
0	0	73	100
0	0	74	100
0	0	75	100
0	0	76	100
0	0	77	100
0	0	78	100
0	0	79	100
0	0	80	100
0	0	81	100
0	0	82	100
0	0	83	100
0	0	84	100
0	0	85	100
0	0	86	100
0	0	87	100
0	0	88	100
0	0	89	100
0	0	90	100
0	0	91	100
0	0	92	100
0	0	93	100
0	0	94	100
0	0	95	100
0	0	96	100
0	0	97	100
0	0	98	100
0	0	99	100
0	0	100	100





### Appendix A.3

#### Equations of least squares planes

Equations of least squares planes referred to orthogonal axes with distances ( $\bar{A}$ ) of relevant atoms from the planes in square brackets and errors in parentheses.

(i) (Me<sub>2</sub>PhP)CdCl<sub>2</sub>

Plane 1 :- C11, C12, C13, C14, C15, C16.

$$0.4305X - 0.7171Y - 0.15481Z + 1.7301 = 0$$

$$\left[ \text{C11, } 0.0011(71); \text{ C12, } -0.0133(71); \text{ C13, } 0.0229(74); \right. \\ \left. \text{C14, } 0.0011(71); \text{ C15, } 0.03(71); \text{ C16, } 0.0018(58) \right]$$

Plane 2 :- Cd, C1(1), C1(2), P.

$$-0.7754X + 0.5889Y - 0.2279Z + 1.3771 = 0$$

$$\left[ \text{Cd, } 0.0281(10); \text{ C1(1), } -0.0097(14); \text{ C1(2), } -0.0084(19); \right. \\ \left. \text{P, } -0.0100(14) \right].$$

Plane 3 :- Cd, C1(2), C1(2'), Cd'

$$-0.3442 X - 0.918 Y - 0.1963 Z + 1.2998 = 0$$

#### Angles between planes :-

<u>Planes</u>	<u>Angle/°</u>	
1,2	51.9	
1,3	58.0	
2,3	89.8	213

(ii) (Me<sub>2</sub>PhP)CdBr<sub>2</sub>

Plane 1 :- C11, C12, C13, C14, C15, C16.

$$0.4218X - 0.7423Y - 0.5207Z + 3.6085 = 0$$

[C11, -0.015(149); C12, 0.0019(189); C13, 0.0105(225);  
C14, -0.0088(213); C15, -0.0053(191); 0.017(166)] .

Plane 2 :- Cd, Br1, Br2, P.

$$-0.7916X + 0.5742Y - 0.2089Z + 5.4479 = 0$$

Cd, 0.0197(10); Br1, -0.0065(14); Br2, -0.0060(26);  
P, -0.0072(37) .

Plane 3 :- Cd, Br2, Br2', Cd'

$$0.3245X + 0.1201Y - 0.9382Z + 5.0183 = 0$$

Angles between planes :-

<u>Planes</u>	<u>Angles/°</u>
1,2.	49.4
1,3	57.6
2,3	89.5

(iii) (Me<sub>2</sub>PhP)CdI<sub>2</sub>

Plane 1 :- C11, C12, C13, C14, C15, C16.

$$0.3827X - 0.7821Y - 0.4918Z + 5.1207 = 0$$

C11, -0.011(18); C12, -0.003(26); C13, 0.020(29);

C14, -0.023(30); C15, 0.008(27); C16, 0.009(26) .

Plane 2 :-

Cd, I1, I2, P.

$$-0.8215X + 0.5394Y - 0.1849Z + 2.4633 = 0$$

[Cd, -0.0026(17); I1, 0.0008(14); I2, 0.0008(13);  
P, 0.0010(58)].

Plane 3 :- Cd, I1, I1', Cd'

$$0.3070X + 0.1487Y - 0.9400Z + 6.4915 = 0$$

Angles between planes :-

<u>Planes</u>	<u>Angle/°</u>
1,2	49.8
1,3	62.4
2,3	89.9

(iv)  $\alpha$ -(Cy<sub>3</sub>P)CdCl<sub>2</sub>

Equations are of the form :-

$$aX + bY + z - d = 0$$

Plane	Atoms	a	b	c	d
1	Cd1, C1(11), C1(21), Cd2	-0.0505	-0.0338	-0.9982	16.3735
2	Cd2, C1(21), C1(22), P2	0.9700	-0.2407	+0.0352	-6.9005
3	Cd2, Cd2', C1(22'), C1(22)	0.0558	-0.7788	-0.6248	11.5338
4	C111, C112, C116	0.1574	0.4576	-0.8751	13.4896
5	C112, C113, C115, C116	-0.6694	0.4354	-0.6019	9.2251
6	C113, C114, C115	0.1112	0.4686	-0.8764	12.3375
7	C121, C112, C126	-0.6969	0.6997	-0.1570	-0.4831
8	C122, C123, C125, C126	0.6876	-0.3867	-0.6145	14.6766
9	C123, C124, C125	-0.6778	0.729	-0.2158	2.9263
10	C131, C132, C136	-0.2666	-0.7886	-0.5541	13.8360
11	C132, C133, C135, C136	-0.8724	-0.1490	-0.4655	6.6920
12	C133, C134, C135	-0.3210	-0.7595	-0.5658	14.8727
13	C211, C212, C216	0.8976	-0.1217	-0.4237	13.5257
14	C212, C213, C215, C216	0.2254	0.2213	-0.9488	14.7366
15	C213, C214, C215	0.8656	-0.1106	-0.4884	15.3142
16	C221, C222, C226	-0.9384	0.3211	-0.1275	-3.1156
17	C222, C223, C225, C226	-0.5088	0.4029	-0.7608	7.3209
18	C223, C224, C225	-0.9315	0.3382	-0.1339	-1.9084
19	C231, C232, C236	-0.2212	-0.8979	-0.3807	1.6637
20	C232, C233, C235, C236	-0.2497	-0.2415	-0.9377	12.5039
21	C233, C234, C235	-0.2229	-0.8925	-0.3921	0.6826

---

Plane Distances (Å) of relevant atoms from planes with errors in parentheses for  $\alpha$ -(Cy<sub>3</sub>P)CdCl<sub>2</sub>

---

1	Cd1,0.0355(7);Cl(11),-0.0322(27);Cl(21),-0.0351(31);Cd2,0.0318(5)
2	Cd2,0.0262(9);Cl(21),-0.0086(36);Cl(22),-0.0087(31);P2,-0.0090(28)
5	C112,-0.0090(13);C113,0.0091(177);C115,-0.0090(133);C116,0.0080(114)
8	C122,0.0029(132);C123,-0.0029(151);C125,0.0030(138);C126,-0.0029(109)
11	C132,-0.0002(124);C133,0.0020(157);C135,-0.0002(132);C136,0.0002(118)
14	C212,-0.0206(124);C213,0.0205(213);C215,-0.0207(168);C216,0.0207(133)
17	C222,-0.0110(110);C223,0.0111(142);C225,-0.0110(108);C226,0.0109(126)
20	C232,-0.0018(96);C233,0.0078(106);C235,-0.0018,(123);C236,0.0018(106)

---

Angles between Planes :-

Planes	Angle/°	Planes	Angle/°
1,2	89.6	13,14	54.7
4,5	51.6	14,15	50.6
5,6	48.9	13,15	4.1
4,6	2.9	16,17	45.2
7,8	49.2	17,18	44.5
8,9	52.7	16,18	1.1
7,9	3.5	19,20	51.0
10,11	52.5	20,21	50.2
11,12	48.9	19,21	0.7
10,12	3.6		

---

Torsion Angles  $\alpha$   $-(\text{Cy}_3\text{P})\text{CdCl}_2$  :-

<u>Atoms</u>	<u>Angle /<math>^\circ</math></u>	<u>Esd in parentheses</u>
C111 - C112 - C113 - C114	57.1	(1.6)
C112 - C113 - C114 - C115	-55.6	(1.7)
C113 - C114 - C115 - C116	53.9	(1.6)
C114 - C115 - C116 - C111	-54.8	(1.4)
C115 - C116 - C111 - C112	55.9	(1.3)
C116 - C111 - C112 - C113	-57.2	(1.3)
C121 - C122 - C123 - C124	55.4	(1.4)
C122 - C123 - C124 - C125	-58.1	(1.5)
C123 - C124 - C125 - C126	58.5	(1.5)
C124 - C125 - C126 - C121	-55.8	(1.3)
C125 - C126 - C121 - C122	54.3	(1.2)
C126 - C121 - C122 - C123	-53.7	(1.3)
C133 - C134 - C135 - C136	-54.3	(1.4)
C131 - C132 - C133 - C134	-56.4	(1.3)
C132 - C133 - C134 - C135	53.9	(1.4)
C134 - C135 - C136 - C131	56.6	(1.2)
C135 - C136 - C131 - C132	-58.1	(1.1)
C136 - C131 - C132 - C133	58.2	(1.1)
C211 - C212 - C213 - C214	-52.7	(2.0)
C212 - C213 - C214 - C215	54.7	(2.3)
C213 - C214 - C215 - C216	-56.6	(2.8)
C214 - C215 - C216 - C211	59.3	(1.8)
C215 - C216 - C211 - C212	-61.8	(1.5)
C216 - C211 - C212 - C213	57.4	(1.5)
C221 - C222 - C223 - C224	-48.0	(1.6)
C222 - C223 - C224 - C225	49.7	(1.8)
C223 - C224 - C225 - C226	-49.9	(1.7)

<u>Atoms</u>	<u>Angle /°</u>	<u>Esd in parentheses</u>
C224 - C225 - C226 - C221	50.5	(1.4)
C225 - C226 - C221 - C222	-51.3	(1.3)
C226 - C221 - C222 - C223	48.8	(1.3)
C231 - C232 - C233 - C234	56.80	(1.2)
C232 - C233 - C234 - C235	-55.8	(1.2)
C233 - C234 - C235 - C236	55.9	(1.3)
C234 - C235 - C236 - C231	-56.4	(1.3)
C235 - C236 - C231 - C232	55.9	(1.1)
C236 - C231 - C232 - C233	-56.6	(1.1)

(v)  $\alpha$ -(Cy<sub>3</sub>P)HgCl<sub>2</sub>Equations of the form:  $aX + bY + cZ - d = 0$ 

Plane	Atoms	a	b	c	d
1	Hg1,Hg1',C1(12),C1(12')	0.1702	0.8617	-0.4781	-2.5163
2	C111,C112,C116	0.9677	-0.1001	-0.2313	0.9247
3	C113,C114,C115	0.2268	0.2031	-0.9525	-2.3651
4	C112,C113,C115,C116	0.3685	-0.2948	-0.8816	3.3415
5	C121,C122,C126	-0.4744	-0.4207	-0.7733	-8.6650
6	C123,C124,C125	-0.4844	-0.4144	-0.7705	-9.7992
7	C122,C123,C125,C126	-0.9690	0.0156	-0.2467	-4.5734
8	C131,C132,C136	0.1167	0.7923	-0.5988	-0.0653
9	C133,C134,C135	0.1050	0.7971	-0.5947	1.0749
10	C132,C133,C135,C136	-0.6687	0.6984	-0.2552	-3.3983
11	Hg2,Hg2',C122, C122'	-0.1062	-0.4442	-0.8896	3.2464
12	C213,C214,C215	0.0512	-0.9070	-0.4181	1.0271
13	C211,C212,C216	0.0083	-0.9085	-0.4178	-1.8764
14	C212,C213,C215,C216	0.6676	-0.3920	-0.6330	-4.9770
15	C221,C222,C226	-0.0673	0.5544	-0.8295	3.3036
16	C223,C224,C225	-0.1382	0.5397	-0.83041	2.5752
17	C222,C223,C225,C226	0.4797	0.4550	-0.7502	1.2335
18	C231,C232,C236	-0.7286	0.4159	-0.5442	7.8906
19	C233,C234,C235	-0.9085	0.2006	-0.3666	7.7206
20	C232,C233,C235,C236	0.9361	-0.1454	-0.3202	-4.2379

Plane Distances of relevant atoms from planes in (Å)

estimated standard deviations in parentheses for  $\alpha$ -(Cy<sub>3</sub>P)HgCl<sub>2</sub>

4	C112 0.0184(133); C113 -0.0186(150); C115 0.0191(148); C116 -0.0189(133)
7	C122 -0.0080(148); C123 0.0080(189); C125 -0.0081(190); C126 0.0081(146)
10	C132 -0.0013(145); C133 0.0014(148); C135 -0.0014(149); C136 0.0013(135)
14	C212 -0.0087(129); C213 0.0088(143); C215 -0.0085(141); C216 0.0084(128)
17	C222 -0.0084(144); C223 0.0084(186); C225 -0.0085(169); C226 0.0086(203)
20	C232 -0.0114(190); C233 0.0115(243); C235 0.0115(197); C236 0.0115(156)

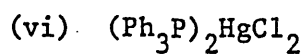
Angles between planes:-

<u>Planes</u>	<u>Angle/°</u>	<u>Plane</u>	<u>Angle/°</u>
2,3	65.2	12,13	2.4
3,4	30.7	12,14	49.1
2,4	87.2	13,14	51.2
5,6	0.7	15,16	4.1
5,7	49.9	16,17	36.6
6,7	49.2	15,17	32.6
8,9	0.7	18,19	19.1
9,10	50.3	18,20	55.4
8,10	51.1	19,20	40.4

Torsion angles  $\alpha$ -(Cy<sub>3</sub>P)HgCl<sub>2</sub>:-

<u>Atoms</u>	<u>Angle/°</u>	<u>E.s.d. in parentheses</u>
C111-C112-C113-C114	59.3	(1.6)
C112-C113-C114-C115	-56.1	(1.8)
C113-C114-C115-C116	54.0	(1.8)
C114-C115-C116-C111	-54.7	(1.5)
C115-C116-C111-C112	57.7	(1.3)
C116-C111-C112-C113	-51.2	(0.8)
C121-C122-C123-C124	53.3	(1.5)
C122-C123-C124-C125	-53.7	(1.7)
C123-C124-C125-C126	55.4	(1.7)
C124-C125-C126-C121	-54.5	(1.5)
C125-C126-C121-C122	55.0	(1.3)
C126-C121-C122-C123	-54.6	(1.4)
C131-C132-C133-C134	-57.8	(1.5)
C132-C133-C134-C135	-56.0	(1.4)
C133-C134-C135-C136	56.7	(1.5)
C134-C135-C136-C131	-56.0	(1.4)
C135-C136-C131-C132	55.26	(1.3)
C136-C131-C132-C133	-56.7	(1.4)
C211-C212-C213-C214	55.6	(1.4)
C212-C213-C214-C215	-54.4	(1.5)
C213-C214-C215-C216	55.1	(1.5)
C214-C215-C216-C211	-56.4	(1.3)
C215-C216-C211-C212	56.4	(1.2)
C216-C211-C212-C213	-56.1	(1.3)
C221-C222-C223-C224	40.8	(2.1)
C222-C223-C224-C225	-43.1	(2.3)
C223-C224-C225-C226	39.7	(2.3)

<u>Atoms</u>	<u>Angle/°</u>	<u>E.s.d. in parentheses</u>
C224-C225-C226-C221	-37.8	(2.3)
C225-C226-C221-C222	37.4	(2.3)
C226-C221-C222-C223	36.7	(2.0)
C231-C232-C233-C234	-56.9	(1.7)
C232-C233-C234-C235	56.6	(1.9)
C233-C234-C235-C236	-56.0	(1.8)
C234-C235-C236-C231	57.6	(1.7)
C235-C236-C231-C232	-59.9	(1.4)
C236-C231-C232-C233	61.1	(1.5)



Equations of the form

$$aX + bY + cZ - d = 0$$

<u>Plane</u>	<u>Atom names</u>	a	b	c	d
1	C11,C12,C13,C14,C15,C16	-0.7140	-0.6303	-0.3048	-2.5741
2	C21,C22,C23,C24,C25,C26	0.2295	0.1089	-0.9672	-3.7134
3	C31,C32,C33,C34,C35,C36	-0.5690	0.5876	-0.5753	-0.9127
4	C41,C42,C43,C44,C45,C46	-0.2521	-0.5306	-0.8093	-2.9692
5	C51,C52,C53,C54,C55,C56	-0.0489	0.8600	-0.5079	3.8784
6	C61,C62,C63,C64,C65,C66	0.9628	-0.0695	-0.1611	-3.1570

Plane    Distances of relevant atoms from planes in (Å) e.s.d.'s  
as indicated

- 1    C11 -0.0003; C12 0.0001; C13 0.0003; C14 -0.0004; C15 0.0003;  
C16 0.0001  
all errors (0.0342)
- 2    C21 -0.0001; C22 -0.0001; C23 0.0001; C24 -0.0001; C25 -0.0001;  
C26 0.0001  
all errors (0.0226)
- 3    C31 -0.0001; C32 0.0001; C33 -0.0001; C34 0.0002; C35 0.0003;  
C36 0.0003  
all errors (0.0225)
- 4    C41 -0.000; C42 -0.0002; C43 0.0003; C44 -0.0002; C45 -0.000;  
C46 0.0002  
all errors (0.0241)
- 5    C51 -0.0003; C52 0.0003; C53 -0.0003; C54 0.0003; C55 -0.0003;  
C56 0.0003  
all errors (0.0230)

Plane Distances of relevant atoms from planes in (Å)

6 C61 -0.0003; C62 0.0004; C63 -0.0002; C64 -0.0001; C65 0.0002;  
C66 -0.000  
all errors (0.0424)

Angles between planes

<u>Planes</u>	<u>Angle/°</u>
1,2	86.4
1,3	77.8
2-3	60.7
4-5	88.1
4-6	89.7
5-6	88.5

## Appendix A.4

### Point group, line group and factor group analyses

#### Definition of terms

Reduction formula:-

$$n_j = \frac{1}{h} \sum_R \chi_r(R) \cdot \chi_j(R) \quad (1)$$

Where:-  $n_j$  = number of times the  $j^{\text{th}}$  irreducible representation appears in the completely reducible representation;  
 $h$  = the order of the group (i.e. total number of operations);  
 $\chi_r(R)$  = the character in the reducible representation corresponding to operation  $R_j$ ;  
 $\chi_j(R)$  = the character in the  $j^{\text{th}}$  reducible representation corresponding to operation  $R$ .

$$\chi_r(R) = p(R) \cdot \chi'(R) \quad (2)$$

Where:-  $p(R)$  = the number of atoms unshifted by operation  $R_j$ ;  
 $\chi'(R)$  = factor representing the contribution to the character per unshifted atom.

The reduction formula (1) can thus be represented by:-

$$n_j = \frac{1}{h} \sum_R p(R) \cdot \chi'(R) \cdot \chi_j(R) \quad (3)$$

Characters in any representation under operations in the same class are identical, i.e.  $\chi_r(R)$  values are the same for all  $R$  in the same class.

Hence:-

$$n_j = \frac{1}{h} \sum_K g(K) \cdot p(K) \cdot \chi'_r(K) \cdot \chi_j(K) \quad (4)$$

where:-  $\chi_r(K)$  = the character in the reducible representation for operations in the  $K^{\text{th}}$  class;

$g(K)$  = number of operations of  $K^{\text{th}}$  class;

$p(K)$  = number of atoms unshifted by operations in  $K^{\text{th}}$  class;

$\chi'(K)$  = contribution to the character per unshifted atom for operations in the  $K^{\text{th}}$  class.

In all the derivations used in this Thesis, the organic ligands are treated as point masses.

### 1) Point group analysis of $(\text{Et}_3\text{P})\text{CdI}_2$

Calculation of total number of modes:-

$C_{2h}$	E	$C_2$	i	$\sigma_h$
$g(K)$	1	1	1	1
$p(K)$	8	2	0	6
$\chi'(K)$	3	-1	-3	1
$g(K) \cdot p(K) \cdot \chi'(K)$	24	-2	0	6
$A_g$	1	1	1	1
$B_g$	1	-1	1	-1
$A_u$	1	1	-1	-1
$B_u$	1	-1	-1	1

$$n_{A_g} = \frac{1}{4} (1)(24) + (1)(-2) + (0) + (1)(6) = 7$$

$$n_{B_g} = 5$$

$$n_{A_u} = 4$$

$$n_{B_u} = 8$$

$$\text{Hence:- } \Gamma_{\text{tot}} = 7A_g + 5B_g + 4A_u + 2B_u.$$

From the  $C_{2h}$  character table:-

$$\Gamma_{T+R} = A_g + 2B_g + A_u + 2B_u.$$

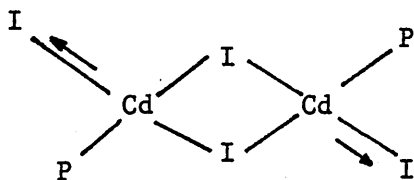
$$\text{Hence:- } \Gamma_{\text{vib}} = 6A_g(\text{Ra}) + 3B_g(\text{Ra}) + 3A_u(\text{I.R.}) + 6B_u(\text{I.R.}).$$

Prediction of  $\mathcal{N}(\text{Cd-P})$ ,  $\mathcal{N}(\text{Cd-I})_t$  and  $\mathcal{N}(\text{Cd-I})_b$  :-

These calculations are performed using internal displacement

co-ordinates. The term  $p(K)$  in the reduction formula (4) is then taken as equal to the number of internal displacement co-ordinates unshifted by an operation in the  $K^{\text{th}}$  class. Translation and rotation modes are not then included.

$\mathcal{N}(\text{Cd-I})_t$  :



$C_{2h}$	E	$C_2$	i	$\sigma_h$
$p(K)$	2	0	0	2
$g(K)$	1	1	1	1
$g(K) \cdot p(K)$	2	0	0	2

$$n_{A_g} = 1$$

$$n_{B_g} = 0$$

$$n_{A_u} = 1$$

$$n_{B_u} = 0$$

$$\text{Thus:- } \mathcal{N}(\text{Cd-I})_t = A_g(\text{Ra}) + B_u(\text{I.R.}).$$

Similarly:-

$$\Gamma(\text{Cd-P}) = A_g(\text{Ra}) + B_u(\text{I.R.})$$

$$\Gamma(\text{Cd-I})_b = A_g(\text{Ra}) + B_g(\text{Ra}) + A_u(\text{I.R.}) + B_u(\text{I.R.}).$$

2) Factor group analyses for  $(\text{Et}_3\text{P})\text{CdI}_2$ .

The structure consists of discrete dimers of  $C_i$  point group symmetry which crystallise in the monoclinic space group  $P2_1/c$  [ $C_{2h}^5$  Number 14, 2 dimers per unit cell].

The cadmium, iodine and phosphorus atoms all lie on general positions in the unit cell, with Wyckoff notation as 4e for all these atoms.

Adams and Newton [12] have computed various sets of 'Factor group and point group tables' which contain the contribution of each atom in a unit cell to a representation of a factor group. By use of their table (number 14) for  $P2_1c$  ( $C_{2h}$ ) the various modes can be predicted:-

Wyckoff	$A_g$	$B_g$	$A_u$	$B_u$
2A-D	0	0	0	0
4E	3	3	3	3

Thus the total number of modes is predicted as:-

Atom	Wyckoff site	$A_g$	$B_g$	$A_u$	$B_u$
Cd	4e	3	3	3	3
P	4e	3	3	3	3
I(1)	4e	3	3	3	3
I(2)	4e	3	3	3	3
		12	12	12	12

Hence:-  $\Gamma_{\text{tot}} = 12A_g + 12B_g + 12A_u + 12B_u$

The acoustic and optical translatory lattice modes ( $T_A + T_O$ ) are obtained by summing the rows in table 14 which correspond to the centres of gravity of the molecules (i.e. translatory independent atoms):-

$$\Gamma_{T_A + T} = 3A_u + 3B_u.$$

Rotatory lattice modes (R) are obtained by consideration of only polyatomic groups:-

$$\Gamma_R = 3A_g + 3B_g$$

$$\Gamma_{int} = 9A_g(Ra) + 9B_g(Ra) + 9A_u(I.R.) + 9B_u(I.R.).$$

Prediction of  $\mathcal{N}(\text{Cd-P})$ ,  $\mathcal{N}(\text{Cd-I})_t$  and  $\mathcal{N}(\text{Cd-I})_b$  modes:-

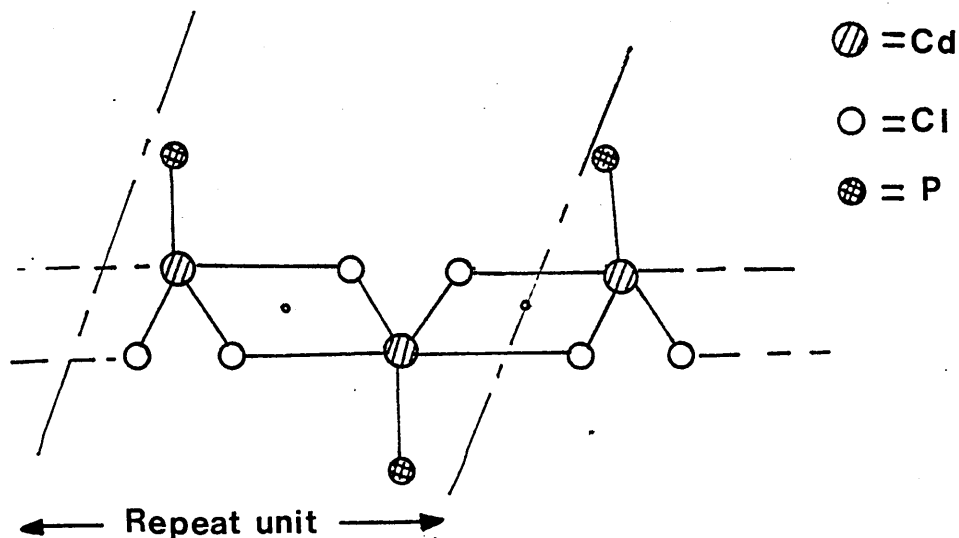
From vector tables:-

$$\mathcal{N}(\text{Cd-P}) = A_g(Ra) + B_g(Ra) + A_u(I.R.) + B_u(I.R.).$$

$$\mathcal{N}(\text{Cd-I})_t = A_g(Ra) + B_g(Ra) + A_u(I.R.) + B_u(I.R.).$$

$$\mathcal{N}(\text{Cd-I})_b = 2A_g(Ra) + 2B_g(Ra) + 2A_u(I.R.) + 2B_u(I.R.).$$

3) Line group analysis of  $(\text{Me}_2\text{PhP})\text{CdX}_2$  [ X = Cl, Br or I ] .



The three structures are similar and can be envisaged as consisting of polymeric chains belonging to  $C_i$  line group.

$C_i$	E	i
$A_g$	1	1
$A_u$	1	-1
p(K)	8	0
g(K)	1	1
$\chi'(K)$	3	-3
g(K).p(K). $\chi'(K)$	24	0

Hence:-  $\Gamma_{\text{tot}} = 12A_g + 12A_u.$

and  $\Gamma_{\text{T} + \text{R}} = 3A_g + A_u$

Thus  $\Gamma_{\text{vib}} = 9A_g(\text{Ra}) + 11A_u(\text{I.R.}).$

Prediction of  $\gamma(\text{Cd-P})$  and  $\gamma(\text{Cd-X})_b$  modes:-

$\gamma(\text{Cd-P})$ :-

$C_i$	E	i
$A_g$	1	1
$A_u$	1	-1
p(K)	2	0
g(K)	1	1
p(K).g(K).	2	0

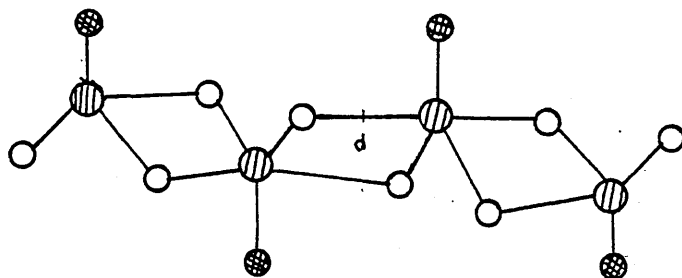
$\gamma(\text{Cd-P}) = A_g(\text{Ra}) + A_u(\text{I.R.}).$

$\nu(\text{Cd-X})_b :-$

$C_i$	E	i
$A_g$	1	1
$A_u$	1	-1
$p(K)$	8	0
$g(K)$	1	1
$p(K) \cdot g(K)$	8	0

$$\bar{\nu}(\text{Cd-X})_b = 4A_g(\text{Ra}) + 4A_u(\text{I.R.}).$$

4) Point group analysis of  $\alpha - (\text{Cy}_3\text{P})\text{CdCl}_2$



$\text{⊘} = \text{Cd}$

$\text{○} = \text{Cl}$

$\text{⊗} = \text{P}$

The structure consists of discrete tetrameric units belonging to  $C_i$  point group.

$C_i$	E	i
$A_g$	1	1
$A_u$	1	-1
$\chi'(K)$	3	-3
$p(K)$	16	0
$g(K)$	1	1
$p(K) \cdot g(K)$	16	0

$$\Gamma_{\text{tot}} = 24A_g + 24A_u$$

$$\Gamma_{R+T_A} = 3A_g + 3A_u$$

$$\Gamma_{\text{vib}} = 21A_g(\text{Ra}) + 21A_u(\text{I.R.}).$$

Calculation of  $\nu(\text{Cd-P})$ ,  $\nu(\text{Cd-Cl})_b$  and  $\nu(\text{Cd-Cl})_t$  modes:-

$\nu(\text{Cd-P})$ :-

$C_i$	E	i
$A_g$	1	1
$A_u$	1	-1
$p(K)$	4	0
$g(K)$	1	1
$p(K) \cdot g(K)$	4	0

$$\nu(\text{Cd-P}) = 2A_g(\text{Ra}) + 2A_u(\text{I.R.}).$$

$\nu(\text{Cd-Cl})_t$ :-

$C_i$	E	i
$g(K)$	2	0
$p(K)$	1	1
$p(K) \cdot g(K)$	2	0

$$\nu(\text{Cd-Cl})_t = A_g(\text{Ra}) + A_u(\text{I.R.})$$

$\sim(\text{Cd-Cl})_b :-$

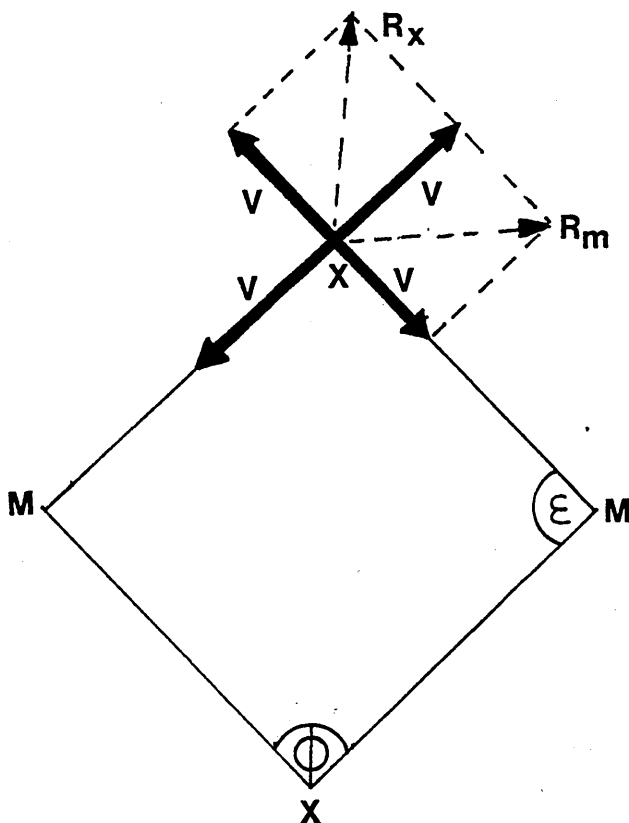
$C_i$	E	i
$p(K)$	12	0
$g(K)$	1	1
$p(K) \cdot g(K)$	12	0

$$\sqrt{\sim(\text{Cd-Cl})_b} = 6A_g(\text{Ra}) + 6A_u(\text{I.R.}).$$

Equations for predicting the positions of (MX) modes in planar four-membered ring systems

The behaviour of the bridge X in a planar and symmetric four membered ring  $M \begin{matrix} \diagup X \diagdown \\ \diagdown X \diagup \end{matrix} M$ , which is simultaneously influenced by both central M atoms, can be described by the superposition of two linear harmonic oscillators, each representing an isolated M-X bond.

The bridge vibrates along  $R_x$  and  $R_m$  as shown:

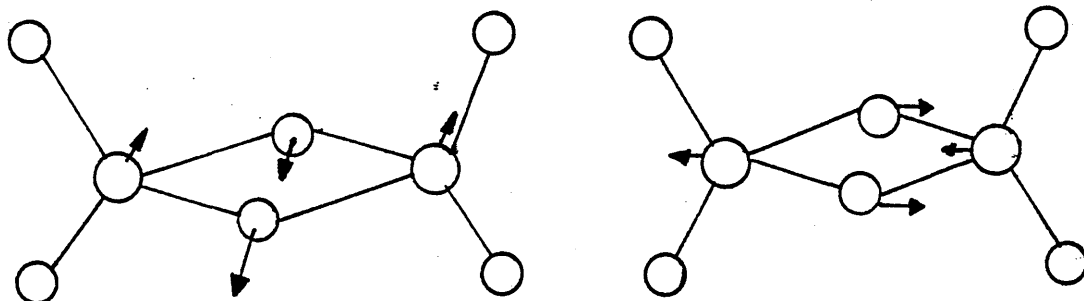


The form of such a figure depends upon the angle under which the central atoms influence the bridge. Using  $V$  as vector of the 'isolated' linear movement in the M-X direction then equations a and b describe the movement of the resulting components  $R_M$  and  $R_X$  in the direction M-M and X-X

$$R_m^2 = 2V^2(1 - \cos \phi) = 2V^2(1 + \cos \epsilon) \quad (a)$$

$$R_x^2 = 2V^2(1 - \cos \epsilon) = 2V^2(1 + \cos \phi) \quad (b)$$

If one considers the two IR-active in-plane modes of vibration associated with the ring, as shown:



along  $R_x$

along  $R_m$

These forms of motion can be compared with the resultant vectors

$R_x$  and  $R_m$ .

Baran called the ring vibrations in the X-X and M-M directions

$\nu_s$  and  $\nu_a$  respectively. Re-arrangement of equations (a) and (b)

gives:

$$P = R_x/R_m = \nu_s/\nu_a$$

The angles of the bridge entity:-

$$\cos \epsilon = \frac{1-P^2}{1+P^2} \quad \text{and} \quad \cos \phi = \frac{P^2-1}{P^2+1}$$

## Appendix A.5

### Experimental Techniques

#### a) Preparative methods

All tertiary phosphine ligands used were obtained from Maybridge Chemicals (Tintagel, Cornwall) or Fluorochem Ltd. (Glossop, Derbyshire). The majority of the tertiary phosphines are air sensitive substances and the containers were opened in a glove box. Subsequent handling was via nitrogen-flushed syringes.

#### (i) 1:1 Stoichiometric complexes of the type $(R_3P)CdX_2$

[X = Cl, Br or I ].

Table A.5.1 contains analytical data for all these complexes prepared. The approximate quantities of cadmium dihalides used in the preparative methods are:-

$CdCl_2 \cdot 2.5H_2O$  (1.00g, 0.0044 mole),  $CdBr_2 \cdot 4H_2O$  (1.38g, 0.0044 mole) and  $CdI_2$  (1.61g, 0.004 mole). The methods of preparation for each complex are designated A,B,C etc. as outlined below. Because the crystallographic investigations into these compounds needed good quality, high purity samples, no attempt was made to maximise yields so no percentage yields are quoted.

A Equimolar proportions of the ligand and (hydrated) cadmium dihalide were dissolved in minimal quantities of ethanol as previously suggested [77]. The mixtures were heated to aid dissolution of the solute. The solution of the ligand was added dropwise to the cadmium dihalide solution and the precipitate, which formed after cooling in the refrigerator at 0°C, was suction dried. The product was recrystallised from ethanol.

B This method is similar to method A, but in this case the ligand and cadmium dihalide were dissolved in ethanol at room temperature and then method A was followed.

C The complex was prepared by adding an equimolar proportion of cadmium dihalide in ethanol and the resulting solution treated as in A.

D The preparation of  $\alpha$ -( $\text{Cy}_3\text{P}$ ) $\text{CdCl}_2$ , was carried out as previously described [37]. Thus the  $\beta$ -form was obtained by the reaction of  $\text{Cy}_3\text{P}$  and  $\text{CdCl}_2$  in 1:1 stoichiometry using methanol/acetone as the solvent. The mixture was heated to  $60^\circ\text{C}$  for half an hour when the precipitated product was cooled to room temperature and filtered off.

E This method was similar to A except that anhydrous cadmium dihalide was used and dichloromethane used as the solvent.

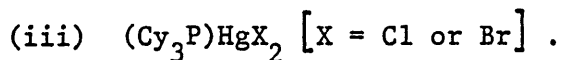
(ii) 2:1 Stoichiometric complexes of the type  $(\text{R}_3\text{P})\text{CdX}_2$   
[X = Cl, Br or I].

Table A.5.2 contains analytical data for all the 2:1 stoichiometric complexes prepared. The approximate cadmium dihalide quantities used were  $\text{CdCl}_2 \cdot 2.5\text{H}_2\text{O}$  (0.80g, 0.0022 mole),  $\text{CdBr}_2 \cdot 4\text{H}_2\text{O}$  (0.65g, 0.0022 mole) and  $\text{CdI}_2$  (0.80g, 0.0022 mole).

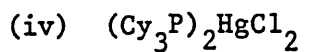
The various methods are given below:

F A solution of the ligand was added dropwise to a solution of the hydrated cadmium dihalide in 2:1 molar proportions, each in minimal quantities of ethanol. Following cooling to  $0^\circ\text{C}$ , the precipitate was collected, suction dried and recrystallised from ethanol.

G In this method, described by Mann et al. [77] ,  $R_3P$  and a solution of cadmium dihalide in a 2:1 stoichiometry were shaken together in 50 cm<sup>3</sup> of water. The crystalline precipitate was collected by filtration and recrystallised from ethanol.



H The complexes for which the analytical data are shown in Table A.5.3 were prepared by the addition of solid  $HgX_2$  to a solution of  $Cy_3P$  in  $CH_2Cl_2$  in equimolar proportions. A clear solution was obtained from which a white solid was recovered on slow evaporation at room temperature, and this was then recrystallised from ethanol.



J The complex was prepared by addition of solid  $HgCl_2$  to a solution of  $Cy_3P$  in  $CH_2Cl_2$  in 1:2 stoichiometric proportions. A clear solution was obtained from which a white solid was recovered on slow evaporation at room temperature and was recrystallised from ethanol. Analytical data are shown in Table A.5.3.

Table A.5.1

<u>Complex</u>	<u>Method of preparation</u>	<u>% C</u>		<u>% H</u>	
		<u>Calc.</u>	<u>Found</u>	<u>Calc.</u>	<u>Found</u>
(Me <sub>2</sub> PhP)CdCl <sub>2</sub>	A	29.89	30.01	3.45	3.38
(Me <sub>2</sub> PhP)CdBr <sub>2</sub>	A	23.40	23.58	2.70	2.57
(Me <sub>2</sub> PhP)CdI <sub>2</sub>	B	19.05	18.02	2.20	2.39
(MePh <sub>2</sub> P)CdCl <sub>2</sub>	A	40.70	40.74	3.40	3.25
(MePh <sub>2</sub> P)CdBr <sub>2</sub>	A	33.05	33.86	2.77	2.60
(Et <sub>3</sub> P)CdCl <sub>2</sub>	A	23.90	24.01	5.01	4.90
(Et <sub>3</sub> P)CdBr <sub>2</sub>	C	18.45	18.65	3.90	3.83
(Et <sub>3</sub> P)CdI <sub>2</sub>	A	14.90	15.10	3.10	2.99
(Bu <sup>t</sup> <sub>3</sub> P)CdCl <sub>2</sub>	E	37.40	37.61	7.03	7.19
(Bu <sup>t</sup> <sub>3</sub> P)CdBr <sub>2</sub>	E	30.38	30.85	5.70	5.92
(Bu <sup>t</sup> <sub>3</sub> P)CdI <sub>2</sub>	E	25.35	25.76	4.75	4.80
α-(Cy <sub>3</sub> P)CdCl <sub>2</sub>	D	46.62	46.81	7.17	6.82
(Cy <sub>3</sub> P)CdBr <sub>2</sub>	D	39.12	39.34	5.47	5.72
(Cy <sub>3</sub> P)CdI <sub>2</sub>	D	33.43	33.63	5.14	5.51

Table A.5.2

<u>Compound</u>	<u>Method of preparation</u>	<u>% C</u>		<u>% H</u>	
		<u>Calcu- lated</u>	<u>Found</u>	<u>Calcu- lated</u>	<u>Found</u>
$(\text{Ph}_3\text{P})_2\text{CdCl}_2$	G	61.08	60.90	4.27	4.43
$(\text{Ph}_3\text{P})_2\text{CdBr}_2$	G	54.27	54.43	3.79	4.08
$(\text{Ph}_3\text{P})_2\text{CdI}_2$	G	48.54	48.39	3.39	3.10
$(\text{MePh}_2\text{P})_2\text{CdBr}_2$	G	53.50	53.20	4.49	4.60
$(\text{MePh}_2\text{P})_2\text{CdBr}_2$	G	46.43	46.55	3.89	4.09
$(\text{MePh}_2\text{P})_2\text{CdI}_2$	G	40.71	40.60	3.42	3.53
$(\text{Et}_3\text{P})_2\text{CdCl}_2$	H	34.35	34.10	7.21	7.00
$(\text{Et}_3\text{P})_2\text{CdBr}_2$	H	28.34	28.37	5.95	5.91
$(\text{Et}_3\text{P})_2\text{CdI}_2$	H	23.92	23.65	5.02	5.60
$(\text{Cy}_3\text{P})_2\text{CdCl}_2$	F	53.32	53.61	8.10	8.65

Table 2.5.3

<u>Compound</u>	<u>Method of preparation</u>	<u>% C</u>		<u>% H</u>	
		<u>Calculated</u>	<u>Found</u>	<u>Calculated</u>	<u>Found</u>
$(\text{Cy}_3\text{P})\text{HgCl}_2$	H	39.20	39.30	6.03	5.44
$(\text{Cy}_3\text{P})\text{HgBr}_2$	H	33.73	34.58	5.19	5.40
$(\text{Cy}_3\text{P})_2\text{HgCl}_2$	J	51.95	51.36	7.27	8.36

b) Crystallographic methods

The general methods of structure solution and refinement used in this work are well documented elsewhere [81] and will not be given.

(i) Space group determination : Space group information was determined by initially examination of oscillation, Weissenberg and precession photographs for symmetry and systematic absences. Any space groups not fully defined by systematic absences were subsequently determined in the structure analysis. The oscillation, Weissenberg and precession photographs were taken using conventional methods and with Cu-K $\alpha$  and Mo-K $\alpha$  radiations.

(ii) Data collection: All data, with the exception of that for (Cy<sub>3</sub>P)HgCl<sub>2</sub> were collected using Mo-K $\alpha$  radiation ( $\lambda = 0.71069\text{\AA}$ ) with a Stöe Stadi-2 two circle diffractometer. This instrument uses a graphite monochromator, a Philips PW 1964/20/30 scintillation counter as detector, and a PDP8/f control unit. Data were collected using the background- $\omega$  scan - background technique. In all cases Lorentz and polarisation corrections have been made and absorption corrections where stated. The data were output on paper tape, which was subsequently converted into cards (via an IBM 1130 computer). It was then placed in a suitable format onto disc such that it could be processed with the SHELX system of computer programs [82]. Computation was carried out using an IBM 370/135 and 370/145 computers at Sheffield City Polytechnic and an IBM 370/165 computer at the SRC computing laboratory at Daresbury. The data for (Cy<sub>3</sub>P)HgCl<sub>2</sub> were collected on a

Enraf-Nonius Cad-4 diffractometer (at Rothamsted Experimental Station) using Mo-K $\alpha$  radiation,  $\lambda = 0.71069\text{\AA}$ . The reflections were collected using a moving crystal/moving detector method (omega/2-theta) scan. The value of the coupling ratio between the detector and crystal motion was chosen to allow the smallest aperture width but still collecting the total integrated intensity. An absorption correction was applied to the data using the EMPASS [83] program.

c) Spectroscopic techniques

The solid infrared spectra were obtained using a Beckman RIIC FS-720 interferometer. Raw data were output on paper tape in the form of interferograms. The latter were converted into spectra using an IBM 1130 computer and conventional Fourier transform computational methods [84]. All spectra were ratioed against an instrumental background. All the samples were prepared by grinding 7-10 mg of sample with high density polyethylene to make a total of 20 mg volume. The mixture was then pressed into a circular disc, suitable for mounting into the interferometer.

All solution phase infrared spectra were recorded on a Nicolet interferometer at the University of Bristol (Department of Chemistry). The Raman spectra were recorded using a Codberg T-800 triple monochromator spectrophotometer using Ar<sup>+</sup> (488.0 nm) laser excitation, at the University of Bristol. The samples were all powders mounted in a capillary tube in the spectrophotometer.

<sup>31</sup>P n.m.r. spectra were recorded on a JOEL FX 900 Fourier transform spectrophotometer at the University of Bristol. Samples were dissolved in CH<sub>2</sub>Cl<sub>2</sub>/CD<sub>2</sub>Cl<sub>2</sub> and spectra recorded on the solutions

in 10 mm tubes. The spectral width was 10 kHz,  $^1\text{H}$  noise decoupling was applied and  $\text{H}_3\text{PO}_4$  external standard was added to the samples.

## References

1. N.A. Bell, M. Goldstein, T. Jones and I.W. Nowell, Inorg. Chim. Acta., 43, 87, (1980).
2. N.A. Bell, M. Goldstein, T. Jones and I.W. Nowell, J.C.S. Chem. Comm., 1039, (1976).
3. N.A. Bell, M. Goldstein, T. Jones, L.A. March and I.W. Nowell, Private Communication.
4. N.A. Bell, M. Goldstein, T. Jones and I.W. Nowell, Inorg. Chim. Acta., 28, L169, (1978).
5. N.A. Bell, M. Goldstein, T. Jones and I.W. Nowell, Inorg. Chim. Acta., 48, 185, (1981).
6. L. Falth, Chem. Scripta, 9, 71, (1976).
7. N.A. Bell, T.D. Dee, P.L. Goggin, M. Goldstein, R.J. Goodfellow, T. Jones, K. Kessler, D.M. McEwan and I.W. Nowell, J. Chem. Res. (S), 2, (1981); J. Chem. Res. (M), 201, (1981).
8. N.A. Bell, M. Goldstein, T. Jones and I.W. Nowell, Private communication.
9. D.G. Tuck, Rev. Inorg. Chem., 209, (1979).
10. G. Davison, "Introductory Group Theory for Chemists", Elsevier, London, (1979).
11. A. Elliott, "Infrared spectra and structure of organic long-chain polymers", Arnold, London, (1969).
12. D.M. Adams and D.C. Newton, "Tables for factor group and point group analysis", Beckmann-RIIC Ltd., Croydon, (1970).
13. D. Grdenic, Quart. Rev., 19, (1965).
14. T. Jones, "PhD Thesis" (C.N.A.A.), Sheffield City Polytechnic, (1979).
15. R.M. Barr and M. Goldstein, J. Chem. Soc. Dalton, 1180, (1974).
16. R.M. Barr and M. Goldstein, J. Chem. Soc. Dalton, 1593, (1976).
17. P.L. Goggin, R.J. Goodfellow and K. Kessler, J. Chem. Soc. Dalton, 1914, (1977).
18. M. Nardelli, L. Coghi and G. Mazzoni, Gazz. Chim. Ital., 88, 235, (1958).
19. L.R. Nassimbeni and A.L. Rodgers, Acta Cryst., 32B, 257, (1976).

20. M.M. Rolies and C.J. De Ranter, Acta Cryst., 34B, 3216, (1978).
21. G. Sawitzki and H.G. von Schnering, Chem. Ber., 107, 3266, (1974).
22. A. Ciesti Villa, L. Coghi, A. Mangia, M. Nardelli, and G. Pelizzi, J. Cryst. Mol. Struct., 1, 291, (1971).
23. R. Zannetti, Gazz. Chim. Ital., 90, 1428, (1960).
24. H. Paulus, Z. Anorg. Chem., 369, 38, (1969).
25. R.J. Flook, H.C. Freeman, F. Huq and J.M. Rosalky, Acta Cryst., B29, 903, (1973).
26. C.H. MacGillavry and J.M. Bijvoet, Z. Krist., 94, 231, (1936).
27. M. Nardelli, L. Cavalca and G. Fava, Gazz. Chim. Ital., 87, 1232, (1957).
28. M. Nardelli and L. Coghi, Ric. Sci., 379, (1958).
29. L. Cavalca, M. Nardelli and G. Fava, Acta Cryst., 13, 594, (1960).
30. L. Cavalca, M. Nardelli and L. Coghi, Nuovo Cimento, VI, 278, (1957).
31. R. Weiss, A. Mitschler and J. Fischer, Bull. Soc. Chim., France, 1001, (1966).
32. M. Nardelli, L. Cavalca and A. Braibanti, Gazz. Chim. Ital., 87, 137, (1957).
33. A. Forbes Cameron and K.P. Forrest, J. Chem. Soc. A., 1286, (1971).
34. A.V. Ablov and T.I. Malinovskii, Doklady Akad.Nauk, S.S.S.R., 123, 336, (1960).
35. M. Goldstein and R.J. Hughes, Inorg. Chim. Acta , 37, 71, (1979).
36. R.G. Goel and W.O. Ogini, Inorg. Chem., 16, 1968, (1977).
37. F.G. Moers and J.P. Langhout, Rec. Trav. Chim., 92, 996, (1973).
38. M. Goldstein and W.D. Unsworth, J. Mol. Structure, 14, 451, (1972).
39. M. Goldstein and R.J. Hughes, Inorg. Chim. Acta , 40, 229, (1980).
40. G.B. Deacon, J.H.S. Green and D.J. Harrison, Spectrochim. Acta, 21A, 1921, (1968).
41. R.G. Goel, W.P. Henry and R.C. Srivastava, Inorg. Chem., 20, 1727, (1981)

42. 'International Tables of X-Ray Crystallography', Vol IV, Kynoch Press, Birmingham (1974).
43. J.J. Daly, J. Chem. Soc., 3799, (1964).
44. P.L. Oriolo and M. Ciampolini, J.C.S. Chem. Comm., 1280, (1972).
45. P.J.H.A.M. van de Leemput, J.A. Cras and J. Willemse, Rec. Trav. Chim., 96, 280, (1977).
46. G.W. Bushnell, Canad. J. Chem., 56, 1773, (1978).
47. G.G. Messmer and E.L. Amma, Inorg. Chem., 5, 1775, (1966).
48. M.L. Schneider and H.M.M. Shearer, J. Chem. Soc. Dalton, 354, (1973).
49. J.H.S. Green, Spectrochim. Acta, 24A, 137, (1968).
50. P.L. Goggin, R.J. Goodfellow and K. Kessler, J. Chem. Soc. Dalton, 1911, (1977).
51. V. Baran, J. Mol. Structure, 13, 1, (1972); 13, 10, (1972).
52. R. Forneris, J. Hiraishi and F.A. Miller, Spectrochim. Acta, 26A, 581, (1970).
53. I.R. Beattie, T. Gilson and P. Cocking, J. Chem. Soc. A, 702, (1967).
54. R.M. Barr, Ph.D. Thesis, University of London, (1973).
55. E.A. Allen and W. Wilkinson, Spectrochim. Acta, 30A, 1219, (1974).
56. W.A. Henderson and C.A. Struli, J. Amer. Chem. Soc., 82, 5791, (1960).
57. C.A. Tolman, Chem. Rev., 77, 313, (1977).
58. B.E. Mann, J. Chem. Soc. Perkin (II), 30, (1972).
59. M.J. Gallagher, D.P. Graddon and A.R. Sheikhi, Aust. J. Chem., 29, 759, (1976).
60. R.S. Nyholm, Proc. Chem. Soc., 273, (1961).
61. L.E. Orgel, J. Chem. Soc., 4186, (1958).
62. H. Schmidbaur and K.H. Rathlein, Chem. Ber., 106, 2491, (1973).
63. K. Kessler, Ph.D. Thesis, University of Bristol, (1977).

64. S.O. Grim, P.J. Lui and R.L. Keiter, Inorg. Chem., 13, 342, (1974).
65. A. Yamaski and E. Fluck, Z. Anorg. Chem., 396, 297, (1973).
66. P. Shah, Diss. Abstr. Int. B., 37, 2845, (1976).
67. D. Grdenic and I. Kristanovic, Arkiv. Kemi., 27, 143, (1955).
68. R.S. McEwen and G.A. Sim, J. Chem. Soc. (A), 1897, (1969).
69. H. Brusset and F. Madaule-Aubry, Bull. Soc. Chim. France, 10, 3122, (1966).
70. C. Chieh, Canad. J. Chem., 55, 1583, (1977).
71. F. Genet and J.C. Leguen, Acta. Cryst., 25B, 2029, (1969).
72. D.J. Brauer, Abstracts of papers IX<sup>th</sup> International Conference on Organometallic Chemistry, Dijon 359, (1979).
73. R.W. Kuntz and P.S. Pregosin, Private communication. - cited ref. 7.
74. F.A. Cotton and G. Wilkinson, "Advanced Inorganic Chemistry", 3rd Ed., Interscience, London, (1972).
75. G.E. Coates and A. Lauder, J. Chem. Soc., 1857, (1965).
76. F.G. Moers and J.P. Langhout, Rec. Trav. Chim., 92, 996, (1973).
77. R.C. Evans, F.G. Mann, H.S. Peiser and D. Purdie, J. Chem. Soc., 1209, (1940).
78. R.C. Cass, G.E. Coates and R.G. Hayter, J. Chem. Soc., 4007, (1955).
79. L Pauling, "The Nature of the Chemical Bond", 3rd ed., Cornell University Press, Ithaca, N.Y.; 88, (1960).
80. E.W. Neuman, J. Amer. Chem. Soc., 54, 2195, (1932);  
H.L. Riley and V. Gallafent, J. Chem. Soc., 514, (1932).
81. G.H. Stout and L.H. Jensen, "X-Ray Structure Determination: A Practical Guide", Collier-MacMillan, London, (1968).
82. D.T. Cromer and D. Libermann, J. Chem. Phys., 53, 1891, (1970).
83. Sheldrick, Orpen, Reicheut and Raithby, Abst. 4th European Crystallographic Meeting, 147, (1977).
84. R.J. Bell, "Introductory Fourier Transform Spectroscopy", Academic Press, New York, (1972).

### Details of programme of postgraduate study

The author has

- a) completed a series of lectures at Sheffield City Polytechnic on 'Vibrational Spectroscopy - Group Theory';
- b) attended a course of lectures on "Computer Programming" at Sheffield City Polytechnic;
- c) attended meetings of the Infrared and Raman Discussion Group at I.C.I. Welwyn Garden City and Kodak Ltd., Harrow;
- d) participated in departmental research colloquia, and presented a colloquium of his own work;
- e) completed the following reading study programmes
  - (i) 'Introductory Group theory for Chemists', G. Davidson, Elsevier, 1971.
  - (ii) 'Vibrational spectroscopy of solids'. P.M.A. Sherwood, C.U.P., 1972.
  - (iii) 'Chemical Infrared Fourier Transform Spectroscopy', P.R. Griffiths, Wiley, 1975.
  - (iv) 'Laser-Raman Spectroscopy', T.R. Gilson and P.J. Hendra, Wiley, 1970.
  - (v) 'Tables of Factor-Group Analysis', D.M. Adams and D.C. Newton, Beckman, 1970.
  - (vi) 'Crystal Structure Analysis', J.P. Glusker and K.N. Trueblood, Oxford University Press, 1972.
  - (vii) 'X-Ray Structure Determination, a Practical Guide', G.H. Stout, and L.H. Jenson, Macmillan, 1968.
  - (viii) 'The Chemistry of Mercury', C.A. McAuliffe (Ed.), Macmillan, 1977.

(ix) 'Use of X-Ray Diffraction in the Study of Protein and Nucleic Acid Structure', K.C. Holmes and D.M. Blow, Wiley, 1966.

(x) 'The Crystalline State, Volume III. The Determination of Crystal Structures', H. Lipson and W. Cochran, Cornell University Press, 1966.

## Solution and Solid State Studies of Tertiary Phosphine Complexes of Mercury(II) Salts with Stoichiometry $\text{HgX}_2(\text{phosphine})_2$

*J. Chem. Research (S)*,  
1981, 2-3  
*J. Chem. Research (M)*,  
1981, 0201-0242

NORMAN A. BELL,<sup>a</sup> TERRY D. DEE,<sup>a</sup> PETER L. GOGGIN,<sup>b,\*</sup>  
MICHAEL GOLDSTEIN,<sup>a</sup> ROBIN J. GOODFELLOW,<sup>b</sup> TERRY JONES,<sup>a</sup>  
KATERINA KESSLER,<sup>b</sup> DAVID M. McEWAN,<sup>b</sup> and IAN W. NOWELL<sup>a</sup>

<sup>a</sup>Department of Chemistry, Sheffield City Polytechnic, Pond Street, Sheffield S1 1WB, U.K.

<sup>b</sup>Department of Inorganic Chemistry, The University, Bristol BS8 1TS, U.K.

The crystal structures of complexes having the stoichiometry  $\text{HgCl}_2(\text{PR}_3)_2$  differ markedly according to the nature of the phosphine. The respective angles between the Hg—P bond and the shortest Hg—Cl bond are  $128.7(4)^\circ$  for  $\text{PPh}_3$ ,  $145.4(3)^\circ$  for  $\text{PEt}_3$ ,  $147.8(7)^\circ$  for  $\text{PBu}_3$ , and  $162.1(1)^\circ$  for  $\text{PMe}_3$ .<sup>2,3</sup> It appears likely that these variations are related to differences in the donor properties of the phosphines and cannot be attributed simply to packing effects in the crystal.

Here we consider complexes of the type  $[\text{HgX}_2(\text{PR}_3)_2]$  ( $\text{PR}_3 = \text{PPh}_3$ ,  $\text{PEt}_3$ ,  $\text{PBu}_3$ , or  $\text{PMe}_2\text{Et}$ ;  $\text{X} = \text{Cl}$ ,  $\text{Br}$ , or  $\text{I}$ ) in the solid state using X-ray crystallography and vibrational spectroscopy, and in solution on the basis of vibrational and n.m.r. ( $^{31}\text{P}$  and  $^{199}\text{Hg}$ ) parameters.

The crystal structure of  $[\text{HgCl}_2(\text{PEt}_3)_2]$  has been determined, and important features are illustrated in Figure 1. The complex retains its monomeric molecular

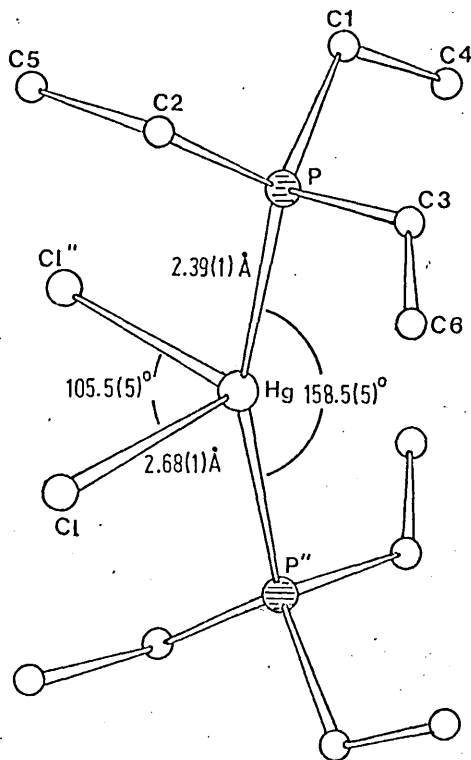


Figure 1 Molecular structure of  $[\text{HgCl}_2(\text{PEt}_3)_2]$

identity, the closest approach between two mercury atoms being 7.1 Å. The P—Hg—P angle is very wide and the Hg—Cl bond is unusually long for a terminal bond, being longer even than typical Hg—Cl bonds in Hg—Cl—Hg bridges.

Assignments of Hg—X stretching vibrations in the solid complexes have been sought on the basis of a  $\text{C}_{2v}$  molecular structure. Spectra obtained at low temperature were richer in detail than those measured

at ambient. Features arising from the bound phosphine are frequently quite intense, particularly in the Raman spectra, and are apt to complicate interpretation especially for the chloride complexes; furthermore such features are not necessarily invariant in appearance and wavenumber on changing the anionic ligand. The bands of the trialkylphosphine ligand are less confusing in spectra of solutions but now only a single Hg—X stretching band is observed in either the i.r. or the Raman spectrum. However, in most cases, there is significant difference between the two spectra in the position of the band maximum. Depolarisation ratio measurements show that the Hg—X stretching intensity observed in the Raman spectra arises largely from a totally symmetric mode. The Hg—X stretching assignments are summarised in Table 5, and if these are taken as a measure of relative bond strengths the Hg—X bonds are strongest in the  $\text{PPh}_3$  complexes and weakest in the  $\text{PMe}_2\text{Et}$  complexes.

Extensive n.m.r. studies have been undertaken for the trialkylphosphine complexes (including some temperature and solvent studies) and the most important parameters,  $^1J(\text{HgP})$ ,  $\delta(^{199}\text{Hg})$ , and  $^2J(\text{PP})$ , are listed in Table A. Measurement of the last of these required the use of a method based on  $^1\text{H}-\{^{31}\text{P}\}$  INDOR and was practicable only for the  $\text{PMe}_2\text{Et}$  and  $\text{PEt}_3$  systems. Taking account of published data,<sup>8,19</sup> the fractional decrease in  $^1J(\text{HgP})$  on changing X from Cl to a higher atomic number halide depends on the nature of the phosphine and follows the order  $\text{PMe}_2\text{Et} < \text{PBu}_3 \approx \text{PEt}_3 < \text{PPhBu}_3 < \text{PPh}_3$ . The  $^{199}\text{Hg}$  chemical shifts move to lower frequency on increasing the atomic number of the halide. The extent is greater for  $\text{PEt}_3$  or  $\text{PBu}_3$  complexes than for those of  $\text{PMe}_2\text{Et}$  and suggests that the halide participates less effectively in covalent bonding with the metal when  $\text{PMe}_2\text{Et}$  is the neutral ligand. Even for  $\text{PBu}_3$  complexes the substitution of two halides has only about the same effect as a single halide substitution in the linear  $[\text{Hg}(\text{CH}_3)\text{X}]$  compounds<sup>13</sup> (where X is opposite to the very high *trans* influence methyl group) and has only about half that found for the cations  $[\text{HgX}(\text{PMe}_3)]^+$ . These observations on  $\nu(\text{HgX})$ ,  $^1J(\text{HgP})$ , and  $\delta(^{199}\text{Hg})$  all indicate that the two trialkylphosphine ligands dominate the bonding about mercury, and that substitution of a methyl group for a longer chain n-alkyl group increases the dominance of the phosphine.

The P—P coupling constants for the  $\text{PEt}_3$  and  $\text{PMe}_2\text{Et}$  complexes of the mercury dihalide are all large and positive but less than in  $[\text{Hg}(\text{PR}_3)_2][\text{BF}_4]_2$  where we assume a linear cation to be present. If these are related to the  $\text{PHgP}$  angle [e.g.  $\propto -\cos(\text{PHgP})$ ] then for  $[\text{HgX}_2(\text{PMe}_2\text{Et})_2]$  the  $\text{PHgP}$  angle decreases with X in the order  $\text{OAc} > \text{Cl} > \text{Br} = \text{SCN} > \text{I} > \text{CN}$ . This trend appears to be similar to that observed in crystallographic studies of  $[\text{HgX}_2(\text{PPh}_3)_2]$  complexes where  $\text{PHgP}$  angles are for X =  $\text{ONO}_2$   $131.8^\circ$ ,<sup>21</sup>  $\text{SCN}$   $118.1^\circ$ ,<sup>21</sup>  $\text{I}$   $109^\circ$ ,<sup>4</sup>  $\text{CN}$   $108.9^\circ$ ,<sup>21</sup>  $\text{CF}_3$   $94.8^\circ$ ,<sup>20</sup> and the wider angles correspond to shorter Hg—P bonds. On the basis of the crystal structure and P—P coupling constants the  $\text{PHgP}$  angles appear to be considerably greater for the trialkyl-

\*Author to receive correspondence, and from whom copies of full text may be obtained.

Table 5 Hg—X stretching assignments ( $\nu/\text{cm}^{-1}$ ) in  $[\text{HgX}_2(\text{PR}_3)_2]$  complexes in the solid state and in solution

	Solid			$\text{CDCl}_3$ solution		
	$\text{HgX}_2$ sym.	$\text{HgX}_2$ asym.	average	$\text{HgX}_2$ sym.	$\text{HgX}_2$ asym.	average
$[\text{HgCl}_2(\text{PPh}_3)_2]$	237 <sup>a</sup>	223 <sup>a</sup>	230			
$[\text{HgCl}_2(\text{PBU}_3)_2]$	216 <sup>b</sup>	205 <sup>a</sup>	211	209 <sup>b</sup>	198 <sup>a</sup>	204
$[\text{HgCl}_2(\text{PET}_3)_2]$	189 <sup>a</sup>	176 <sup>a</sup>	183	209 <sup>b</sup>	198 <sup>a</sup>	204
$[\text{HgCl}_2(\text{PMe}_2\text{Et})_2]$	201 <sup>b?</sup>	~169 <sup>a?</sup>	185 <sup>?</sup>	200 <sup>b</sup>	193 <sup>a</sup>	197
$[\text{HgBr}_2(\text{PPh}_3)_2]$	155 <sup>b</sup>	164 <sup>a</sup>	160			
$[\text{HgBr}_2(\text{PBU}_3)_2]$	138 <sup>b</sup>	129 <sup>a</sup>	134	146 <sup>b</sup>	134 <sup>a</sup>	140
$[\text{HgBr}_2(\text{PET}_3)_2]$	152 <sup>b</sup>	132 <sup>a</sup>	142	146 <sup>b</sup>	130 <sup>a</sup>	138
$[\text{HgBr}_2(\text{PMe}_2\text{Et})_2]$	125 <sup>b</sup>	112 <sup>a</sup>	119	130 <sup>b</sup>	130 <sup>a</sup>	130
$[\text{HgI}_2(\text{PPh}_3)_2]$	129 <sup>b</sup>	137 <sup>a</sup>	133			
$[\text{HgI}_2(\text{PBU}_3)_2]$	105 <sup>b</sup>	107 <sup>a</sup>	106	122 <sup>b</sup>	112 <sup>a</sup>	117
$[\text{HgI}_2(\text{PET}_3)_2]$	110 <sup>b</sup>	109 <sup>a</sup>	110	118 <sup>b</sup>	112 <sup>a</sup>	115
$[\text{HgI}_2(\text{PMe}_2\text{Et})_2]$	100 <sup>b</sup>	94 <sup>a</sup>	97	114 <sup>b</sup>	112 <sup>a</sup>	113

<sup>a</sup>I.r. value. <sup>b</sup>Raman value.Table A N.m.r. parameters  $^1J(\text{HgP})$ ,  $^2J(\text{PP})$ ,<sup>a</sup> and  $\delta(^{199}\text{Hg})$ <sup>b</sup> of some complexes  $[\text{HgX}_2(\text{PR}_3)_2]$ 

Complex	Solvent	$\theta/^\circ\text{C}$	$^1J(\text{HgP})$	$^2J(\text{PP})$	$\delta(\text{Hg})$
$[\text{HgCl}_2(\text{PBU}_3)_2]$	$\text{CDCl}_3$	20	5125		-409
$[\text{HgBr}_2(\text{PBU}_3)_2]$	$\text{CDCl}_3$	20	4829		-476
$[\text{HgI}_2(\text{PBU}_3)_2]$	$\text{CDCl}_3$	20	4089		-722
$[\text{HgCl}_2(\text{PET}_3)_2]$	$\text{CH}_2\text{Cl}_2$	30	5067	+176	-409
$[\text{HgBr}_2(\text{PET}_3)_2]$	$\text{CH}_2\text{Cl}_2$	30	4788	+156	-470
$[\text{HgI}_2(\text{PET}_3)_2]$	$\text{CH}_2\text{Cl}_2$	30	4004		
$[\text{Hg}(\text{PET}_3)_2][\text{BF}_4]_2$	$(\text{CD}_3)_2\text{CO}$	30	4457	+219	-1145
	$\text{D}_2\text{O}$	30	4515	+212	-1020
$[\text{HgCl}_2(\text{PMe}_2\text{Et})_2]$	$\text{CDCl}_3$	-30	5606	+187	-497
	$\text{D}_2\text{O}^c$	30	5260	+221	-729
$[\text{HgBr}_2(\text{PMe}_2\text{Et})_2]$	$\text{CDCl}_3$	-30	5560	+170	-504
$[\text{HgI}_2(\text{PMe}_2\text{Et})_2]$	$\text{CDCl}_3$	-30	4778	+144	-555
$[\text{Hg}(\text{OAc})_2(\text{PMe}_2\text{Et})_2]$	$\text{CH}_2\text{Cl}_2$	-70	5932	+208	-769
$[\text{Hg}(\text{CN})_2(\text{PMe}_2\text{Et})_2]$	$\text{CDCl}_3$	-60	3225	+113	-250
$[\text{Hg}(\text{SCN})_2(\text{PMe}_2\text{Et})_2]$	$\text{CH}_2\text{Cl}_2$	-30	5084	+169	-439
$[\text{Hg}(\text{PMe}_2\text{Et})_2][\text{BF}_4]_2$	$(\text{CD}_3)_2\text{CO}$	30	4747	+249	-1243
	$\text{D}_2\text{O}$	30	4959	+237	-1085

<sup>a</sup>In Hz. <sup>b</sup>In p.p.m. to high frequency of neat  $\text{HgMe}_2$ . <sup>c</sup>0.68 mol  $\text{dm}^{-3}$ .

phosphine complexes, pointing to the basicity of the phosphine rather than its bulkiness as being the primary factor governing the angle. The same explanation can account for the P—Hg—Cl angles found in  $[\text{HgCl}_2(\text{PR}_3)_2]$  complexes.

Conductivity measurements on aqueous solutions of  $[\text{HgCl}_2(\text{PR}_3)_2]$  and  $[\text{Hg}(\text{PR}_3)_2][\text{BF}_4]_2$  ( $\text{PR}_3 = \text{PET}_3$  or  $\text{PMe}_2\text{Et}$ ) show that the chloride complexes undergo partial ionisation, and this is accompanied by an increase in the value of  $^2J(\text{PP})$  presumably as a result of a widening of the PHgP angle.

We conclude that where there are two types of ligand on mercury(II) in monomeric four-coordinate complexes  $[\text{HgA}_2\text{B}_2]$  the one which is the more effective  $\sigma$ -donor (A) tends to dominate the bonding about the metal at the expense of the other (B) and distorts the geometry towards one with a linear  $\text{HgA}_2$  unit.

Techniques used: Single crystal X-ray diffraction, i.r., Raman, n.m.r. [ $^1\text{H}$ ,  $^{31}\text{P}$ - $\{^1\text{H}\}$ ] and  $^{199}\text{Hg}$ - $\{^1\text{H}\}$  F.t.,  $^1\text{H}$ - $\{^{31}\text{P}\}$  and  $^1\text{H}$ - $\{^{199}\text{Hg}\}$  INDOR], conductivity.

References: 28

Figures 2–8: Infrared and Raman spectra of solid  $[\text{HgI}_2(\text{PMe}_2\text{Et})_2]$  (Figure 2), solid  $[\text{HgX}_2(\text{PBU}_3)_2]$ , X = Cl or Br (Figure 3),  $[\text{HgCl}_2(\text{PBU}_3)_2]$  in  $\text{CDCl}_3$  solution (Figure 4), solid  $[\text{HgCl}_2(\text{PET}_3)_2]$  (Figure 5),  $[\text{HgX}_2(\text{PMe}_2\text{Et})_2]$ , X = Cl, Br, or I in solution (Figure 6), solid  $[\text{HgX}_2(\text{PMe}_2\text{Et})_2]$ , X = Cl or Br (Figure 7), and solid  $[\text{HgX}_2(\text{PPh}_3)_2]$ , X = Cl, Br, or I (Figure 8)

Tables 1–2: N.m.r. parameters of some complexes  $[\text{HgX}_2(\text{PMe}_2\text{Et})_2]$  (Table 1) and  $[\text{HgX}_2(\text{PR}_3)_2]$ , R = Et or Bu<sup>n</sup> (Table 2)

Table 3: Estimates of P—Hg—P angles from values of  $^2J(\text{PP})$  in complexes  $[\text{HgX}_2(\text{PR}_3)_2]$

Table 4: N.m.r. parameters of  $[\text{HgX}_2(\text{PMe}_2\text{Et})_2]$  complexes (X = Cl or Br) in  $\text{D}_2\text{O}$

Table 6: Bond lengths and interbond angles in some crystalline  $[\text{HgX}_2(\text{PPh}_3)_2]$  complexes

Tables 7–11: Single crystal X-ray analysis of  $[\text{HgCl}_2(\text{PET}_3)_2]$ : crystal data and data collection (Table 7), atomic coordinates and isotropic temperature factors (Table 8), anisotropic thermal parameters (Table 9), bond distances and angles (Table 10), and measured and calculated structure factors (Table 11)

Paper: E/146/80

Received: 4th August 1980; final version received on 10th October 1980

References cited in this synopsis:

<sup>2</sup>N. A. Bell, M. Goldstein, T. Jones, and I. W. Nowell, *J. Chem. Soc., Chem. Commun.*, 1976, 1039.

<sup>3</sup>N. A. Bell, M. Goldstein, T. Jones and I. W. Nowell, *Inorg. Chim. Acta*, 1978, 28, L169.

<sup>4</sup>L. Fäilth, *Chem. Scripta*, 1976, 9, 71.

<sup>5</sup>A. Yamasaki and E. Fluck, *Z. anorg. Chem.*, 1973, 396, 297; S. O. Grim, P. J. Lui and R. L. Keiter, *Inorg. Chem.*, 1974, 13, 342.

<sup>13</sup>P. L. Goggin, R. J. Goodfellow, D. M. McEwan, A. J. Griffiths, and K. Kessler, *J. Chem. Research*, 1979, (S) 194, (M) 2315.

<sup>19</sup>E. C. Alyca, S. A. Dias, R. G. Goel, W. O. Ogini, P. Pilon, and D. W. Meek, *Inorg. Chem.*, 1978, 17, 1697.

<sup>20</sup>D. J. Brauer, Abstracts of papers. IXth International Conference on Organometallic Chemistry, Dijon 1979, 359.

<sup>21</sup>R. W. Kunz and P. S. Pregosin, unpublished work.

## A New Structural Type for 1:1 Complexes of Cadmium Dihalides with Unidentate Ligands: $\text{CdCl}_2(\text{PhMe}_2\text{P})$

NORMAN A. BELL, TERENCE D. DEE, MICHAEL GOLDSTEIN and IAN W. NOWELL\*

*Department of Chemistry, Sheffield City Polytechnic, Pond Street, Sheffield S1 1WB, U.K.*

Received May 21, 1979

*The crystal structure of dimethylphenylphosphine-cadmium(II) chloride has been determined from single-crystal X-ray diffraction data collected on a two-circle diffractometer. The analysis was carried out on 2820 reflections and refined by full-matrix least-squares calculations to a final R of 0.037. The crystals are monoclinic, space group  $P2_1/n$  with  $a = 7.057(5)$ ,  $b = 12.471(7)$ ,  $c = 12.905(8)$  Å,  $\beta = 93.08(5)^\circ$  and  $Z = 4$ . The structure is polymeric  $\text{CdCl}_2(\text{PhMe}_2\text{P})$  units are linked together by chlorine-bridges to give single chains running parallel to the  $a$ -axis. Each cadmium is pentaco-ordinate with one phosphorus and four chlorine atoms forming an elongated trigonal bipyramidal arrangement about the metal atom.*

### Introduction

The literature contains reports of a vast number of complexes of metal dihalides with unidentate ligands, but few attempts have been made to systematize, let alone rationalize, the structures adopted. In the case of  $\text{CdX}_2(\text{L})$  systems (L = unidentate ligand) the only structure which has been authenticated is a double-chain arrangement in which cadmium is octahedrally co-ordinated, as in  $\text{CdCl}_2(\text{MeNHCONH}_2)$  [1],  $\text{CdCl}_2(\text{imidazole})$  [2], and  $\text{CdCl}_2(\text{MeCSNH}_2)$  [3]. A dimeric halogen-bridged structure involving tetraco-ordinated cadmium atoms has often been suggested, but the evidence is unconvincing [4].

In our recent work on mercury(II) halide systems [5, 6] we have shown that the structure adopted by 1:1 complexes of type  $\text{HgX}_2(\text{R}_3\text{P})$  is critically dependent upon the nature of the phosphine donor, and some rationalization of the observed trends is possible. However, none of the structures determined appears to show any relationship to the double-strand chain structures found for the cadmium complexes referred to above [1–3], despite the fairly close relationships found with some (but not all) trihalogeno salts of these two metals,  $[\text{MX}_3]^-$  [7–9].

We have therefore undertaken a systematic study of the structures of  $\text{CdX}_2(\text{L})$  complexes. Our first result, the subject of the present paper, is noteworthy in that it establishes a new structural type which has not previously been considered by workers in this field.

### Experimental

Dimethylphenylphosphinecadmium(II) chloride was prepared as previously described [10], by the addition of an alcoholic solution of the phosphine to a hot alcoholic solution of hydrated cadmium chloride ( $\text{CdCl}_2 \cdot 2\frac{1}{2}\text{H}_2\text{O}$ ) in a 1:1 molar ratio. Recrystallisation from ethanol gave colourless needles suitable for single-crystal X-ray analysis.

### Crystal Data

$\text{CdC}_8\text{H}_{11}\text{Cl}_2\text{P}$ ,  $M_r = 321.5$ . Monoclinic,  $P2_1/n$ ,  $a = 7.057(5)$ ,  $b = 12.471(7)$ ,  $c = 12.905(8)$  Å,  $\beta = 93.08(5)^\circ$ ,  $U = 1134.0$  Å<sup>3</sup>,  $D_m$  (by flotation) = 1.90,  $D_c = 1.88$  g cm<sup>-3</sup>.  $Z = 4$ , Mo- $K\alpha$ ,  $\lambda = 0.7107$  Å,  $\mu(\text{Mo-}K\alpha) = 23.0$  cm<sup>-1</sup>,  $F(000) = 624$ .

### Intensity Measurements

A crystal of dimensions 0.10 × 0.10 × 0.48 mm was mounted with the  $a$ -axis coincident with the rotation ( $\omega$ ) axis of a Stöe Stadi 2 two-circle diffractometer. Using monochromated Mo- $K\alpha$  radiation and the background- $\omega$  scan-background technique, 3314 unique reflections were measured, of which 2820 had  $I > 3\sigma(I)$  and were considered to be observed [the net intensity  $I = T - B$ , where  $T$  = scan count,  $B$  = mean background count over the scan width;  $\sigma(I) = \sqrt{T + Bc/2t}$ , where  $c$  = scan time,  $t$  = time for background measurements at each end of the scan]. Corrections for Lorentz, polarisation and absorption effects were made.

### Structure Determination and Refinement

The cadmium atom position was determined from the three-dimensional Patterson function and the

TABLE I. Final Atomic Parameters. Estimated Standard Deviations for Non-Hydrogen Atoms are Given in Parentheses.

Fractional Co-ordinates ( $Cd \times 10^5$ ; remaining atoms $\times 10^4$ )			
	x	y	z
Cd	25383(5)	2221(2)	5148(2)
Cl(1)	4219(2)	936(1)	-978(1)
Cl(2)	648(2)	-1399(1)	-13(1)
P	2623(2)	850(1)	2405(1)
C11	1522(8)	-173(3)	3186(4)
C12	2384(10)	-601(6)	4081(5)
C13	1447(12)	-1397(6)	4612(5)
C14	-331(12)	-1707(6)	4313(5)
C15	-1202(10)	-1293(6)	3414(5)
C16	-263(8)	-515(5)	2864(4)
C2	1336(12)	2079(5)	2639(5)
C3	4952(11)	1097(6)	3002(6)
H12	3765	-321	4366
H13	2159	-1774	5279
H14	-1072	-2278	4773
H15	-2592	-1569	3143
H16	-948	-176	2171
H21	-96	2010	2306
H22	2038	2744	2286
H23	1299	2213	3465
H31	5838	402	2903
H32	4836	1252	3819
H33	5574	1784	2640

Anisotropic Thermal Parameters ( $\times 10^4$ ) of the Form:  $\exp[-2\pi^2 (U_{11}h^2a^{*2} + U_{22}k^2b^{*2} + U_{33}l^2c^{*2} + 2U_{12}hka^*b^* + 2U_{13}hla^*c^* + 2U_{23}klb^*c^*)]$

	$U_{11}$	$U_{22}$	$U_{33}$	$U_{12}$	$U_{13}$	$U_{23}$
Cd	290(2)	411(2)	337(2)	-23(1)	53(1)	-29(1)
Cl(1)	298(5)	450(5)	379(5)	24(4)	52(3)	83(4)
Cl(2)	310(5)	374(5)	675(7)	20(4)	-56(5)	-40(4)
P	375(6)	340(4)	337(5)	20(4)	29(4)	-20(4)
C11	383(24)	402(20)	310(18)	21(15)	22(16)	-35(14)
C12	504(33)	704(35)	457(26)	-72(27)	155(24)	88(25)
C13	721(48)	695(37)	480(28)	-96(33)	-93(28)	97(26)
C14	638(42)	640(33)	553(31)	-196(30)	92(27)	41(27)
C15	430(32)	750(37)	570(31)	-175(28)	20(24)	14(27)
C16	374(26)	516(24)	467(24)	-20(20)	-23(19)	-2(20)
C2	807(50)	440(25)	592(32)	191(28)	115(30)	-132(23)
C3	490(36)	654(33)	646(35)	-150(27)	-115(27)	-116(28)

remaining atoms were located from successive difference electron-density maps. Hydrogen atoms were included in positions calculated from the geometry of the molecule ( $C-H = 1.08 \text{ \AA}$ ). Common isotropic temperature factors were applied to methyl and phenyl hydrogens and refined to final values of  $U = 0.170(30)$  and  $0.057(10) \text{ \AA}^2$  respectively. Scattering factors were calculated [11] using an analytical approximation and the weighting scheme adopted was  $w = 1.0000/[\sigma^2(F_o) + 0.0086(F_o)^2]$ . Full matrix refinement with anisotropic temperature factors for all non-hydrogen atoms gave the final  $R = 0.037$  and

$R' = 0.047$ . The final difference map showed no peaks greater than  $0.24 e \text{ \AA}^{-3}$ . Final atomic parameters are listed in Table I, bond distances and angles in Table II. A list of observed and calculated structure factors is available from the Editor.

#### Calculations

All calculations, apart from preliminary data processing, were carried out on an IBM 370/165 computer at the SRC Computing Centre Daresbury, using the SHELX computing package [12].

TABLE II. Bond Lengths (Å) and Angles ( $^\circ$ ) with Estimated Standard Deviations in Parentheses.*Symmetry Code*

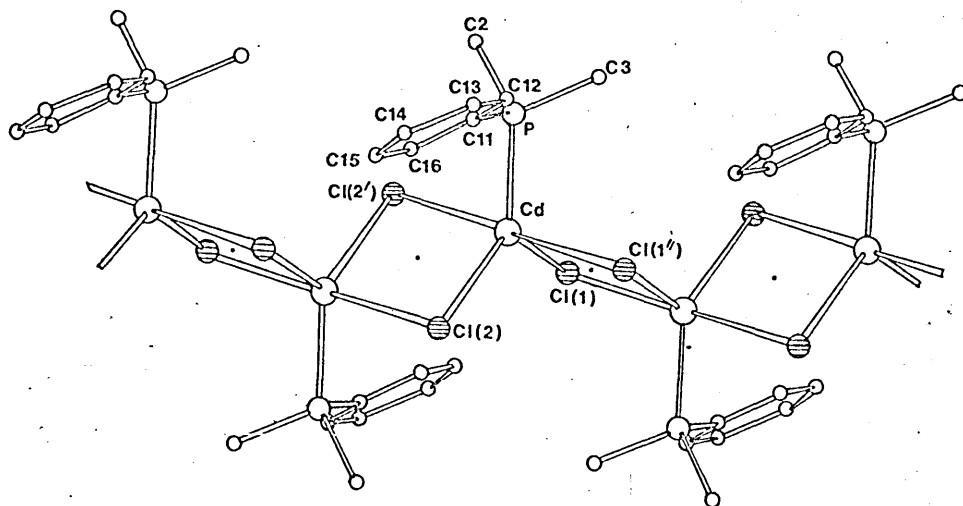
none	$x, y, z$
none	$-x, -y, -z$
none	$1-x, -y, -z$

*Bond Lengths (Å)*

Cd—Cl(1)	2.481(1)	P—C3	1.803(7)
Cd—Cl(2)	2.497(1)	C11—C12	1.384(7)
Cd—Cl(1'')	2.745(1)	C11—C16	1.373(7)
Cd—Cl(2')	2.734(1)	C12—C13	1.394(10)
Cd—P	2.560(1)	C13—C14	1.350(11)
P—C11	1.825(5)	C14—C15	1.384(10)
P—C2	1.815(6)	C15—C16	1.391(9)

*Bond Angles ( $^\circ$ )*

Cl(1)—Cd—Cl(2)	110.50(2)	Cd—P—C11	108.9(1)
Cl(1)—Cd—Cl(1'')	86.00(2)	Cd—P—C2	115.5(2)
Cl(1)—Cd—Cl(2')	92.60(2)	Cd—P—C3	115.7(3)
Cl(1)—Cd—P	130.00(4)	C11—P—C2	105.4(3)
Cl(2)—Cd—Cl(1'')	93.40(2)	C11—P—C3	106.8(3)
Cl(2)—Cd—Cl(2')	87.10(2)	C2—P—C3	103.7(4)
Cl(2)—Cd—P	119.50(3)	P—C11—C12	123.3(5)
Cl(1'')—Cd—Cl(2')	178.60(4)	P—C11—C16	117.4(4)
Cl(1'')—Cd—P	88.70(4)	C12—C11—C16	119.2(5)
Cl(2')—Cd—P	92.20(2)	C11—C12—C13	119.1(6)
		C12—C13—C14	121.4(6)
		C13—C14—C15	119.8(6)
		C14—C15—C16	119.1(6)
		C15—C16—C11	121.1(5)

Fig. 1. Single chain running parallel to the  $a$ -axis.**Results and Discussion**

Dimethylphenylphosphinecadmium(II) chloride adopts an unexpected polymeric structure in which cadmium is five co-ordinate (Fig. 1).  $\text{CdCl}_2(\text{PhMe}_2\text{P})$  units are linked together by chlorine-bridges to give

single chains running parallel to the  $a$ -axis. The resulting arrangement is quite different to the double-strand chains found [1–3] in other  $\text{CdCl}_2(\text{L})$  systems containing unidentate ligands [ $\text{L} = \text{MeNHCONH}_2$ , imidazole or  $\text{MeCSNH}_2$ ] and in which cadmium is octahedrally co-ordinated. Although the pyridine-N-

TABLE III. Equations of Least-Squares Planes Referred to Orthogonal Axes<sup>a</sup> with Distances (Å) of Relevant Atoms from the Planes in Square Brackets.

Plane A: Cd, Cl(1), Cl(2), P.

$$-0.7738X + 0.5899Y - 0.2307Z + 1.3725 = 0.0000$$

[Cd, 0.027; Cl(1), -0.009; Cl(2), -0.008; P, -0.010; Cl(1''), -2.707; Cl(2'), 2.753; Cl1, -0.347; C2, 1.542; C3, -1.242]

Plane B: C11, C12, C13, C14, C15, C16

$$0.4311X - 0.7177Y - 0.5468Z + 1.7311 = 0.0000$$

[C11, 0.001; C12, -0.014; C13, 0.023; C14, -0.020; C15, 0.007; C16, 0.002; P, -0.004]

<sup>a</sup>The orthogonalization matrix for the plane-equations is:

$$\begin{matrix} a & 0 & c\cos\beta \\ 0 & b & 0 \\ 0 & 0 & c\sin\beta \end{matrix}$$

oxide complex  $\text{CdI}_2(\text{C}_5\text{H}_5\text{NO})$  [13] contains single-strand chains, the involvement of both halogen and ligand atoms in the bridging is in contrast to the present chlorine-bridged structure.

The cadmium atom is essentially coplanar with P, Cl(1), Cl(2) (Table III), but the trigonal arrangement about the central atom is distorted with bond angles varying from 110.5 [Cl(2)-Cd-Cl(1)] to 130.0° [P-Cd-Cl(1)]. This angular distortion reflects the greater steric requirement of the phosphine ligand compared to that of the two chlorine atoms. While the Cd-Cl(1) and Cd-Cl(2) distances (mean 2.489 Å) are similar to those found [14] in monomeric  $\text{CdCl}_2(\text{Ph}_3\text{P})_2$  [2.504, 2.440(6) Å], they are significantly shorter than the Cd-Cl distances involving chlorine atoms bonded to two cadmium atoms found [1-3] in the polymeric  $\text{CdCl}_2(\text{L})$  complexes, L = MeNHCONH<sub>2</sub> [2.58, 2.62 Å], imidazole [2.604, 2.601(4) Å], or MeCSNH<sub>2</sub> [2.57, 2.66(2) Å]. Further chlorine atoms [Cl(2'), Cl(1'')] increase the co-ordination about cadmium to five, giving an elongated trigonal bipyramidal arrangement in which the Cl(1'')-Cd-Cl(2') grouping is almost linear (178.6°) and the (axial chlorine)-Cd-(equatorial atom) bond angles lie close to 90° (86.0-93.4°). The chlorine-bridges are very asymmetric; the Cd-Cl(1'') and Cd-Cl(2') distances (mean 2.740 Å) are substantially greater than the Cd-Cl(1) and Cd-Cl(2) values and are comparable with the distances found [2, 3] for chlorine atoms bonded to three cadmium atoms in the polymeric complexes  $\text{CdCl}_2$  (imidazole) (mean 2.711 Å) and  $\text{CdCl}_2(\text{MeCSNH}_2)$  (mean 2.760 Å).

The phosphine ligand is strongly co-ordinated to cadmium with the Cd-P distance of 2.560(1) Å being significantly less than that found [14] in  $\text{CdCl}_2(\text{Ph}_3\text{P})_2$  [2.635, 2.632(6) Å]. The bond lengths in

the phosphine ligand lie within expected ranges. Angular distortion about phosphorus, with the Cd-P-Cl1 bond angle (108.9°) for example being much smaller than the Cd-P-CH<sub>3</sub> values (mean 115.6°), can be attributed to the asymmetric nature of the phosphine ligand. The phenyl ring is twisted out of the Cd, P, Cl(1), Cl(2) mean plane by 50.9°, presumably to minimise steric interactions within the chain.

The single-chain structure with pentaco-ordinate metal atoms, which characterises the present complex, is similar to that found in  $\text{HgCl}_2(\text{Et}_3\text{P})$  [5]. In the phosphine complexes  $\text{HgCl}_2(\text{R}_3\text{P})$  (R = Me, Et, Bu or Ph) we have found [5, 6] that the size of the phosphine ligand plays an important role in determining the type of structure adopted. While small ligands (R = Me, Et) give rise to polymers, the more bulky tributyl- and triphenylphosphines form tetrameric and dimeric structures respectively. Such size effects appear to be less critical for the analogous cadmium complexes. Thus examination of the far-infrared spectra of the  $\text{CdX}_2(\text{L})$  complexes (X = Cl or Br; L = Ph<sub>2</sub>MeP, PhMe<sub>2</sub>P or Et<sub>3</sub>P) suggests that despite the differing steric requirements of the phosphine ligands, the complexes are isostructural. While the structural effect of ligand size may be less important for such cadmium complexes, the nature of the halogen does appear to play a significant structural role. Thus  $\text{CdI}_2(\text{Et}_3\text{P})$  appears from its far-infrared spectrum to have a different type of structure to that found for  $\text{CdCl}_2(\text{PhMe}_2\text{P})$ .

#### Acknowledgements

We thank the SRC for a Research Studentship (to TDD), an equipment grant and computing facilities.

#### References

- 1 M. Nardelli, L. Coghi and G. Azzoni, *Gazz. Chim. Ital.*, **88**, 235 (1958).
- 2 L. R. Nassimbeni and A. L. Rodgers, *Acta Cryst.*, **32B**, 257 (1976).
- 3 M. M. Roies and C. J. De Ranter, *Acta Cryst.*, **34B**, 3216 (1978).
- 4 R. C. Evans, F. G. Mann, H. S. Peiser and D. Purdie, *J. Chem. Soc.*, 1209 (1940); G. E. Coates and D. Ridley, *J. Chem. Soc.*, 166 (1964); R. G. Goel and W. O. Ogini, *Inorg. Chem.*, **16**, 1968 (1977).
- 5 N. A. Bell, M. Goldstein, T. Jones and I. W. Nowell, *Chem. Comm.*, 1039 (1976).
- 6 N. A. Bell, M. Goldstein, T. Jones and I. W. Nowell, *Inorg. Chim. Acta*, **28**, L169 (1978).
- 7 R. M. Barr and M. Goldstein, *J. Chem. Soc. Dalton*, 1180 (1974).
- 8 R. M. Barr and M. Goldstein, *J. Chem. Soc. Dalton*, 1593 (1976).

- 9 P. L. Goggin, R. J. Goodfellow and K. Kessler, *J. Chem. Soc. Dalton*, 1914 (1977).
- 10 R. C. Cass, G. E. Coates and R. G. Hayter, *J. Chem. Soc.*, 4007 (1955).
- 11 'International Tables for X-Ray Crystallography', Vol. IV, Kynoch Press, Birmingham (1974).
- 12 G. M. Sheldrick, SHELX. Programs for crystal structure determination. Univ. of Cambridge, England.
- 13 G. Sawitzki and M. G. von Schnering, *Chem. Ber.*, 107, 3266 (1974).
- 14 A. Forbes Cameron, K. P. Forrest and G. Ferguson, *J. Chem. Soc. A*, 1286 (1971).